Universidad Nacional Autónoma de México
Programa de Maestría y Doctorado en Ingeniería
Ingeniería Civil – Estructuras

Seismic Resilience Assessment of Urban Buildings

T E S I S

QUE PARA OPTAR POR EL GRADO DE:
DOCTOR EN INGENIERÍA

PRESENTA:
JUAN JESÚS GUTIÉRREZ TREJO

TUTOR PRINCIPAL:
DR. A. GUSTAVO AYALA MILIÁN, INSTITUTO DE INGENIERÍA

COMITÉ TUTOR:
DR. OSCAR ALBERTO LÓPEZ BÁTIZ, FACULTAD DE INGENIERÍA-UNAM
DR. ORLANDO JAVIER DÍAZ LÓPEZ, INSTITUTO DE INGENIERÍA-UNAM
DR. SAÚL ESTEBAN LÓPEZ RÍOS, FES-ACATLÁN-UNAM
DR. JESÚS MIGUEL BAIRÁN GARCÍA, UNIVERSIDAD POLITÉCNICA DE CATALUÑA

CIUDAD DE MÉXICO, NOVIEMBRE 2021

JURADO ASIGNADO:

Presidente: Dr. López Bátiz Oscar Alberto

Secretario: Dr. Díaz López Orlando Javier

1er Vocal: Dr. Ayala Milián Amado Gustavo

2do Vocal: Dr. López Ríos Saúl Esteban

3er Vocal: Dr. Bairán García Jesús Miguel

Lugar donde se realizó la tesis: Instituto de Ingeniería, UNAM, CDMX

TUTOR DE TESIS:

DR. GUSTAVO AYALA MILIÁN

_____

FIRMA

To my wife Mónica, and my little son, Jared Emilio.

To my parents, Esther and Guillermo, and my sister, Dalia Karina.

"If you thought that science was certain – well, that is just an error on your part."

"The language of probability allows us to speak quantitatively about some situation which may be highly variable, but which does have some consistent average behavior. Our most precise description of nature must be in terms of probabilities."

–Richard P. Feynman

"The most exciting phrase to hear in science, the one that heralds the most discoveries, is not "Eureka!" (I found it!), but That's funny..."

–Isaac Asimov

Acknowledgments

First of all, I would like to thank my parents, Esther and Guillermo, and my sister, Dalia Karina, for their unconditional support and love throughout my life. I would like also to thank my parents for the principles and values they have instilled in me, and for fostering discipline in me, as this is one of the principal means by which goals are achieved. I would thank especially to my wife, Mónica, for the love, patience and support she has shown me over the years. I dedicate this work to my little son, Jared Emilio, who at his early age shows a subtle curiosity for the things that surround him.

I would like to express my most sincere gratitude to Prof. Gustavo Ayala Milián for giving me the opportunity to carry out my doctoral research under his supervision and for proposing this research topic to me. I would like also to thank Prof. Ayala for having shared his wisdom and patience during these years, and for the advices given to me not as a disciple, but as a friend, which have allowed me to grow academically, but also as a human being.

I thank the members of my tutorial committee, Dr. Orlando Díaz López, Dr. Oscar López Bátiz, and Dr. Saúl López Ríos, for reviewing this research work and for their comments and suggestions, which undoubtedly enriched it significantly. I also thank Professors Humberto Varum, from the University of Porto, and Mario De Stefano, from the University of Florence, for their discussions and critical comments on my work during their academic visits to the Engineering Institute–UNAM.

I would like especially to thank Dr. Jesús Miguel Bairán García, of the Polytechnic University of Catalonia, for having accepted me as a visiting doctoral student at the Department of Civil and Environmental Engineering, School of Civil Engineering of Barcelona. I would like also to express my sincere thanks to Prof. Bairán for the suggestions and critical comments made during the development of this research work.

I am grateful to Dr. José Guadalupe Rangel Ramírez, of The Department of the Built Environment, Aalborg University, Denmark, for sharing his knowledge and making an important contribution to the initial stage of this research work.

I express my gratitude to my colleagues at the Wind Tunnel of the UNAM, Dr. Marco Antonio Escamilla García, Dr. Francisco Hector Bañuelos García, Dr. César Paniagua Lovera, Dr. Otoniel Palacios Hernández, Dr. Enrique Arcos, and M. Eng. Abraham Lagunas Muñoz, for the academic discussions and pleasant conversations in the moments of leisure, as well as the espresso coffee mornings, afternoons and evenings. I would like

especially to thank Dr. Héctor Rodrigo Amezcua Rivera and Dr. Pablo David Quinde Martínez for sharing their knowledge, which undoubtedly enriched this doctoral thesis.

I am deeply grateful to Ing. Ignacio Martínez Ortíz for having shared his vast wisdom with me and for having taught me that self-education is, without doubt, the only type of education that exists. I also want to thank "Inge Nacho", as he is better known, for having instilled in me the habit of questioning the basic aspects of science and engineering, which we take for granted; however, if we analyze in detail many of them, we can find gaps that give rise to new ideas in order to better understand the world around us. Thanks to his teachings and advices, I have been able to look forward, even though sometimes, I could not see the light. I dedicate this research work to the memory of "Inge Nacho". "*Until victory always*"– Ernesto "Che" Guevara.

I thank the *Programa de Maestría y Doctorado en Ingeniería* of the *National Autonomous University of Mexico* (**UNAM**) and the *Engineering Institute* (**II**) for the opportunity given to me to carry out my doctoral studies. To the *National Council of Science and Technology* (**CONACYT**) for the financial support given during the period of my studies at this institution. Additionally, I would like also to thank for the partial sponsorship of this research to the *Dirección General de Asuntos del Personal Académico* (**DGAPA-UNAM**) through the project titled **"Desarrollo e implementación de una metodología para la evaluación y diseño sísmico de edificios de concreto reforzado basado en resiliencia y control de daño"-PAPIIT IN104821**, and to the *Mexico City Institute for Construction Safety* (**ISC**) through the project number **1536**, titled **"Evaluación de la resiliencia sísmica de edificios de concreto reforzado de mediana altura diseñados con las normas técnicas complementarias-diseño por sismo 2017"**.

Contents

List of Figures

List of Tables

Abstract

In this thesis, a probabilistic methodology to evaluate the seismic resilience of new or existing individual buildings is presented. The methodology is formulated according to the theoretical concepts proposed by MCEER to define the seismic resilience of communities. The methodology proposed is introduced in the seismic performance evaluation scheme developed by PEER, which is divided into four steps: (1) seismic hazard analysis, (2) structural analysis, (3) damage analysis, and (4) consequence analysis. The approach to evaluate seismic resilience proposed in this study is introduced in the 3rd and 4th steps of the PEER scheme. As a result, decision variables (DVs) expressed in terms of vulnerability functions are obtained approximately using the bootstrap technique. These functions are (1) loss and recovery of functionality, measured as the percentage of non-usable area, (2) repair time, (3) recovery time, (4) repair costs, (5) indirect economic losses, (6) number of workers required to perform the repair work, (7) number of fatalities and number of people injured, and (8) equivalent economic value associated with the number of injured occupants and the number of casualties. The vulnerability functions of DVs are an important tool for both engineers and decision makers.

The proposed methodology allows estimating the probability that the building is tagged as usable, restricted use or unoccupiable, according to the post-seismic inspection of the structural, non-structural and furniture-type elements. The formulation of this methodology is based on the post-seismic inspection criteria proposed by the ATC-20 (1989). Likewise, this approach is an extension of the methodology proposed by Mitrani-Reiser (2007), which only considers the evaluation of the structural components, obtaining only the lower limit of the probability of the post-seismic inspection. With the improvement proposed in this research, the upper limit of such probabilities is obtained. With this tool it is demonstrated that the loss of functionality is mainly caused by the damage experienced by non-structural and furniture-type elements when the building in question is designed with a modern seismic design code.

Based on the combination of the severity of damage that can be experienced by structural, non-structural and furniture-type elements, a set of six limit states of functionality is developed: LS_0 fully functional, safe building, LS_1 partially functional and structurally safe, LS_2 restricted use, non-functional and structurally safe, LS_3 restricted entry, non-functional and structurally safe, LS_4 unsafe building, unoccupied, but repairable, LS_5 unsafe, irreparable building and LS_6 structural collapse. In turn, according to the damage characteristics of each functional limit state, a generic sequence of functional recovery is

prescribed for each of them.

To exemplify the proposed methodology, the evaluation of the seismic resilience of a seven-story reinforced concrete building with unreinforced masonry walls and designed in accordance with the Building Construction Guidelines of Mexico City (GCDMX, 2020), that is, with a modern seismic design code, is presented. The results show that the building is structurally safe, which corroborates the good behavior of the building with respect to the seismic demands used; however, from the point of view of non-structural and furniture performance, it is shown that the building loses functionality at seismic intensities lower than those that cause structural damage, including collapse prevention. The results also show that indirect economic losses and those equivalent to the number of injuries and fatalities can contribute significantly to the total financial losses.

Resumen

En esta tesis se presenta una metodología probabilista para evaluar la resiliencia sísmica de instalaciones individuales nuevas o existentes. La metodología está formulada de acuerdo a los conceptos teóricos propuestos por el MCEER para definir la resiliencia sísmica de comunidades. La metodología propuesta se introduce en el esquema de evaluación del desempeño sísmico desarrollado por el PEER, el cual se divide en cuatro etapas: (1) análisis de peligro sísmico, (2) análisis estructural, (3) análisis de daño y (4) análisis de consecuencias. La aproximación para evaluar la resiliencia sísmica propuesta en este documento se introduce en las etapas 3ra y 4ta del esquema PEER. Como resultado, se obtienen las variables de decisión expresadas en términos de funciones de vulnerabilidad, aproximadas con le técnica bootstrap: (1) pérdida y recuperación de la funcionalidad medida como el porcentaje de área no-usable, (2) tiempo de reparación, (3) tiempo de recuperación, (4) costos de reparación (5) pérdidas económicas indirectas, (6) número de trabajadores necesarios para realizar los trabajos de reparación, (7) número de víctimas mortales y número de personas lesionadas y (8) valor económico equivalente asociado al número de ocupantes lesionados y del que pierde la vida. Asimismo, las funciones de vulnerabilidad de las variables de decisión pueden ser una herramienta importante tanto para los ingenieros como los tomadores de decisiones.

La metodología propuesta permite estimar tanto la probabilidad de que la instalación sea etiquetada como usable, de uso restringido o no ocupable, de acuerdo a la inspección post-sísmica de los elementos estructurales, no estructurales y mobiliario. La formulación de dicha metodología está basada en el criterio de inspección post-sísmica propuesta por el ATC-20 (1989). Asimismo, dicha aproximación constituye una extensión de la metodología propuesta por Mitrani-Reiser (2007), quien únicamente considera la evaluación de los componentes estructurales, obteniéndose únicamente el límite inferior de la probabilidad de la inspección post-sísmica. Con la mejora propuesta en este documento se tiene como resultado el límite superior de dichas probabilidades. Con esta herramienta se demuestra que la pérdida de funcionalidad es originada principalmente por el daño que experimentan los elementos no estructurales y mobiliario cuando la instalación en cuestión es diseñada con un reglamento de diseño sísmico moderno.

Con base en la combinación de la severidad del daño que pueden experimentar los elementos estructurales, no estructurales y de mobiliario, se desarrolla un conjunto de seis estados límite de funcionalidad: LS_0 completamente funcional, edificio seguro, LS_1 parcialmente funcional, edificio seguro, LS_2 uso restringido, no funcional y estructuralmente seguro,

LS_3 entrada restringida, no funcional y estructuralmente seguro, LS_4 edificio inseguro, no ocupable pero reparable, LS_5 edificio inseguro, irreparable y LS_6 colapso estructural. A su vez, de acuerdo a las características del daño de cada estado límite de funcionalidad se prescribe para cada uno de ellos una secuencia genérica de recuperación de la funcionalidad.

Para ejemplificar la metodología propuesta se presenta la evaluación de la resiliencia sísmica de un edificio de concreto reforzado de siete pisos considerando muros de mampostería no reforzada, diseñado con el Reglamento de Construcciones de la Ciudad de México (GCDMX, 2020), esto es, con un reglamento moderno de diseño sísmico. Los resultados demuestran que la instalación es estructuralmente segura, lo cual corrobora el buen comportamiento de la instalación respecto al las demandas sísmicas empleadas; sin embargo, desde el punto de vista del desempeño no-estructural y de mobiliario, se demuestra que la instalación pierde funcionalidad ante intensidades sísmicas menores que las que causan el daño estructural, incluida la de prevención al colapso. Los resultados también demuestran que las pérdidas económicas indirectas y las equivalentes al número de lesionados y víctimas mortales pueden contribuir de forma significativa a las pérdidas financieras totales.

Chapter 1

Introduction

Historically seismic events have been one of the natural phenomena that have caused the most significant social and economic disruptions of communities. This is mainly due to the damage caused by these events on the physical buildings which are fundamental for the functioning of a city. The most important consequences are the loss of human lives and the economic losses. The latter are caused by the economic cost associated with the repairs and the interruption of business during the time that the damaged buildings are repaired and restored to the level of operation they had before a disruptive event occurs. In recent decades, emphasis has been placed on the importance of the impact of these losses on society in order to create contingency and risk mitigation plans for future events.

Toyoda (2008) conducted a comparative study of the direct and indirect financial losses to the commercial sector caused by the Mw 6.9 magnitude earthquake in Kobe, Japan, in 1995. The conclusion was that the indirect financial losses, *i.e.*, those resulting from business interruption, were accumulated over a 10-year interval and reached the quantity of $125 billion US dollars (double the direct financial losses, associated only with repair costs). Loss of functionality of buildings is the main factor in indirect economic losses and is mainly due to damage to architectural finishes, non-structural elements, contents, furniture, electronic equipment, although it can also be caused, to a lesser extent, by damage to structural components.

The February 2011 Christchurch, New Zealand earthquake of magnitude M_w 6.2 is an excellent example where the seismic intensities that affected the buildings can be considered similar to those used for their seismic design, and at the same time to avoid loss of life. This event occurred only 6.7 km from the city of Christchurch, so although it was not a large event, the proximity of the epicenter to the city in combination with the seismic intensities experienced by the buildings caused a large number of them to develop significant structural damage. In addition, a important number of these buildings had to be demolished even though they had been designed in accordance with the in-force seismic design code. As a consequence, the Central Business District (CBD) of Christchurch had to be cordoned off for a period of 2 years, and furthermore, reconstruction work did not start until three years after the seismic event occurred. As a result, many businesses had

to be relocated to another site, causing substantial indirect economic losses due to the time that the CBD remained inactive. The conclusion of many engineers in this regard was that the damaged buildings performed well from the point of view of the seismic design code used because the buildings did not collapse at the seismic intensity used in their structural design. In other words, the lives of the occupants were preserved in the face of the design seismic event. However, from the point of view of the affected users and owners, this event was not a success because they did not expect their buildings to experience significant damage because their buildings were designed with a modern seismic design code.

The earthquake of magnitude M_w 8.8 that occurred on February 27, 2010 on the coast of the Bío-Bío Region of Chile (present-day Ñuble Region) affected the city of Santiago. This earthquake caused minimal amounts of light damage in structural components to a large number of buildings; however, there was substantial severe damage to non-structural components, causing the closure of the affected buildings for a significant length of time and, as a consequence, large financial economic losses were generated (Miranda *et al.*, 2012).

In Mexico, an earthquake of magnitude M_w 7.1 recently occurred in the locality of Axochiapán, in the state of Morelos, at a distance of approximately 120 km from Mexico City, causing the collapse of 44 buildings (Galvis *et al.*, 2017) and a large amount of significant damage to medium-rise buildings, especially those constructed of reinforced concrete with reinforced and non-reinforced masonry infills (Weiser *et al.*, 2018). The federal government estimated that the cost of rebuilding the damaged buildings would be approximately $1.9 billion US dollars (El Economista, 2017).

From these few examples, it can be concluded that the most modern seismic design codes fulfill their main objective, which is to avoid structural collapse in seismic events whose intensities are similar to those used in the structural design. This also achieves the objective of safeguarding the lives of the occupants of the affected buildings. However, it is also shown that the guidelines are not conceived to prevent the loss of functionality of the buildings, nor to reduce direct economic losses, caused mainly by non-structural damage, or indirect losses associated with loss of functionality. That is, the design codes are not focused on making the structures resilient, therefore the main objective for which these buildings were conceived, which is to be functional for one or several particular causes, was not accomplished. Therefore, what should be done is to create mitigation plans to quickly reduce the negative consequences of potentially destructive events on the infrastructure, and therefore on the society and economy of the affected cities.

1.1 Motivation

The property that determines the recovery capacity of a community affected by a natural event, such as an earthquake, is known as resilience. In 2003, the Multidisciplinary Center for Earthquake Engineering Research (MCEER) developed a scheme to quantify it (Bruneau *et al.*, 2003). In this scheme, the evaluation of the resilience of a community can

be divided into two stages: the first consists in estimating the loss of functionality and the second in quantifying its recovery. This framework assumes that the loss of functionality is present immediately after the seismic event occurs. The second stage, corresponding to the recovery of functionality, depends mainly on the strategy adopted for recovery, *e.g.*, mitigation activities, activation of insurance policies, etc.

Currently, the most comprehensive and robust tool for evaluating the seismic performance of individual buildings is the scheme developed by the Pacific Earthquake Engineering Research Center, PEER, (Cornell and Krawinkler, 2000; Moehle and Deierlein, 2004; Mitrani-Reiser, 2007; Günay and Mosalam, 2013). This evaluation scheme is divided into four probabilistic processes: (1) seismic hazard analysis, (2) structural analysis, (3) damage analysis, (4) consequence analysis. The main objective of this methodology is to estimate the consequences of damage in terms of decision variables, *e.g.*, average annual exceedance rate of repair cost.

The evaluation scheme developed by PEER was adopted by FEMA P-58-1 in 2012 as a standard for evaluating the seismic performance of individual buildings. In this approach, important advances have been implemented to estimate the seismic risk of vulnerable buildings. For example, it is possible to estimate the probability that a building will be tagged as restricted use according to the ATC-20 (1989) post-seismic inspection criterion. It is also possible to estimate in probabilistic terms the costs and repair times, as well as the number of fatalities generated by structural collapse. However, factors such as loss of functionality due to damage to non-structural and furniture-type elements, number of injured persons, equivalent economic value associated with fatalities and non-fatalities, indirect economic losses and factors that prevent the initiation of repairs are not considered in the methodology proposed by the FEMA P-58-1 (2012a). These factors are of great relevance in evaluating the seismic resilience of buildings from a holistic perspective.

1.2 Objective

The general objective of this research work is to develop a methodology to evaluate the seismic resilience of new or existing buildings. The DVs that integrate the methodology proposed in this thesis used to explain the seismic resilience of buildings are: (1) loss of functionality due to structural and non-structural damage; (2) recovery of functionality; (3) repair time; (4) time in which to delay the start of repairs; (5) recovery time; (6) number of workers required to perform repair work; (7) repair costs of structural, non-structural and furniture-type elements; (8) indirect economic losses associated with business interruption; (9) number of fatalities and non-fatalities and their equivalent economic value; (10) indirect economic losses, associated with business interruption; and (11) total economic losses. In order to achieve the general objective of this research the following specific tasks were set:

1. Implement a methodology to simulate seismic record sets associated with various

seismic intensities, which are able to account for record to record variability, frequency content and duration in the intense phase.

2. Implement a probabilistic methodology to infer the damage experienced by each structural element (*e.g.*, columns and column-column connections) and non-structural element (*e.g.*, unreinforced masonry walls and stairs).

3. Develop a procedure for inferring damage to furniture-type elements, *e.g.*, overturning of bookcases and shelves, typical of an office building.

4. Develop a methodology to estimate the costs and repair times associated with structural, non-structural and furniture-type elements, as well as the number of workers required to perform the repair work.

5. Develop a procedure to simulate the evaluation of post-seismic structural safety, and develop a similar procedure to infer the safety of the usable floor plan areas of a hypothetical building when non-structural and furniture damage is experienced.

6. Define and implement functionality limit states, based mainly on the combination of the possible levels of damage that can be suffered by structural, non-structural and furniture-type elements.

7. Based on the previous task, develop for each proposed functionality limit state a series of generic events associated with the recovery of system functionality.

8. Adapt an existing methodology to estimate the probable number of people who may lose their lives due to seismic damage to a building.

9. Develop a procedure to estimate the number of people who may be injured by seismic damage to a building.

10. Develop a method to approximate the equivalent economic value associated with the number of fatalities and injuries caused by damage/collapse to a building.

11. Implement a methodology based on intensive random resampling calculations to approximate the vulnerability function associated with each DV indicated above.

To achieve these goals the general framework of seismic resilience proposed by Bruneau *et al.* (2003) in conjunction with the general aspects of the formulation developed by Cimellaro *et al.* (2006; 2010a) to assess the resilience of individual buildings are used, and they are introduced in the PEER-PBEE scheme. Therefore, the methodology proposed in this study can be considered as a complement to the PEER-PBEE and FEMA-P58-1 (2012a) frameworks to quantify the seismic resilience metrics in a rigorous probabilistic manner.

1.3 Organization of the thesis

In this thesis, a methodology to evaluate the seismic resilience of existing and future buildings is proposed. The contents of each chapter of this document are described below.

- Chapter 2. The scheme developed by MCEER to assess the resilience of a community that has been affected by a natural hazard and an adaptation of this scheme to assess the resilience of individual buildings affected by a seismic event proposed by Cimellaro *et al.* (2006, 2010a) are presented. This chapter also presents the framework for evaluating the seismic performance of buildings developed by PEER. Finally, the existing criteria for evaluating the seismic performance of buildings are described.

- Chapter 3. The general aspects and assumptions used for the formulation of the methodology to evaluate the seismic resilience of buildings proposed in this research work are described.

- Chapter 4. This chapter presents the considerations made to define the seismic demand to be used in the validation of the proposed methodology. It also presents the conditions used for the selection and definition of the number of simulated seismic records.

- Chapter 5. The criteria used by existing methodologies to estimate the maximum response in time history of structural and non-structural elements are described. A criterion is presented to approximate the individual maximum response of structural, non-structural and furniture-type elements when the analyzed structure corresponds to a three-dimensional model.

- Chapter 6. The criteria used to infer the damage that may be experienced by structural and non-structural elements are presented for each element individually. In this chapter, a procedure is proposed to infer the damage in furniture-type elements, *e.g.*, bookcases and shelves, by means of the rigid body dynamics theory.

- Chapter 7. The post-seismic evaluation criteria developed by the ATC-20 (1989) is presented. A methodology to estimate the probability that a building damaged by an earthquake will be tagged as safe, restricted use or unsafe, according to the level of structural damage developed is presented. With a similar criterion to the previous one, a methodology to estimate the probability that the building will be tagged as not usable, restricted use or usable according to the level of damage developed by the non-structural and furniture-type elements, is proposed. In this chapter, six limit states of functionality, LS, are proposed, in which the results of the post-seismic inspection of the structural, non-structural, and furniture-type elements are combined. In addition, for each limit state, a generic functionality recovery sequence is proposed.

- Chapter 8. A recursive method to estimate the loss and recovery of the functionality of individual buildings is proposed. This methodology estimates repair costs, repair times, time associated with events that delay the start of repairs, and recovery time, as well as the number of workers required to perform such activities. This chapter also presents a proposal for estimating indirect economic losses associated with business interruption, derived mainly from the loss of functionality of a building.

- Chapter 9. A methodology for estimating the number of occupants who are injured and the number of people who lose their lives as a result of damage to structural, non-structural and furniture-type elements, as well as those resulting from structural collapse, is presented. A procedure for estimating the equivalent economic value associated with fatalities and non-fatalities is also presented.

- Chapter 10. The general aspects of the bootstrap technique developed to perform statistical inference of complex problems such as the one corresponding to this research work are described. A procedure to approximate the vulnerability functions of the DVs with this technique, *e.g.*, repair time, number of fatalities, etc., is also presented.

- Chapter 11. The evaluation of the seismic resilience of a hypothetical seven-story reinforced concrete building with unreinforced masonry infill walls for office use is presented considering seven levels of seismic intensity, each associated with a specific return period.

- Chapter 12. A summary of the proposed methodology and the general conclusions of this research work, as well as its scope and limitations, are presented.

Chapter 2

Literature review

2.1 Resilience framework for assessing a community

Although the concept of resilience in several disciplines has taken great relevance in recent years, it was not until the 1960s that it began to be used in the area of psychology to define the level of capacity that a person has to adapt satisfactorily to adverse situations (Waller, 2001). In the 1970s the concept resilience began to be modified and adapted to be used in other fields of knowledge, *e.g.*, sociology, environmental engineering and economics, just to mention a few. In physics its interpretation was adapted to the study of the elastic properties of materials, specifically to define the capacity to recover its original shape after an external force was applied. Nowadays, in the most general sense, the concept resilience is used to describe the ability of any system to absorb and reduce the abrupt impacts caused by a disruptive event and recover its normal condition rapidly. In fact, the word *resilience* means *to jump back*, and comes from of the Latin word *resiliens*. This word is composed by two words. The first one is *re*, meaning *back* or *to return*, and the second one is *saliens*, from the present participle of the verb *salire*, meaning *to jump*. Putting the two words together forms the word *resaliens*, and changing the vowel *a* to *i* by apophonia, we have the word *resiliens*, *i.e.*, *to jump back*.

In the earthquake engineering field, Bruneau *et al.* (2003) was the first research group to adapt the concept of resilience to reduce the vulnerability of the communities and enhance its seismic performance. They define the seismic resilience as the property that determines the capacity of a community to minimize social disruptions caused by the major earthquakes and carry out recovery strategies to mitigate them in the shortest possible time, taking into account the enhancement of the seismic capacity of the affected systems to reduce and mitigate in a more effective way the effects of possible future earthquakes, keeping in mind that the principal objective of the improvement of the resilience is minimize the loss of life, number of injuries, economic losses, and in general, any reduction in quality of life due to the effects of the earthquakes. In this context, this research group have suggested that the resilience of any system can be explained through four basic properties: *robustness, redundancy, resourcefulness and rapidity.* Textually, these properties

are described as follows:

- **Robustness**: strength, or the ability of elements, systems, and other units of analysis to withstand a given level of stress or demand without suffering degradation or loss of function.
- **Redundancy**: the extent to which elements, systems, or other units of analysis exist that are substitutable, *i.e.*, capable of satisfying functional requirements in the event of disruption, degradation, or loss of functionality.
- **Resourcefulness**: the capacity to identify problems, establish priorities, and mobilize resources when conditions exist that threaten to disrupt some element, system, or other unit of analysis. Resourcefulness can be further conceptualized as consisting of the ability to apply materials (*i.e.*, monetary, physical, technological, and informational) and human resources to meet established priorities and achieve goals.
- **Rapidity**: is the capacity to meet priorities and achieve goals in a timely manner in order to contain losses and avoid future disruption.

Moreover Bruneau *et al.* (2003), further describes four global interrelated *dimensions* by which the main idea of resilience can be understood from a more general point of view: *technical, organizational, social* and *economic*, and is referred to by the acronym TOSE:

- **Technical**: it refers to the adequate performance of the physical components that integrate a set of buildings, *i.e.*, a community, when they are subject to seismic demands.
- **Organizational**: refers to the capacity of social organizations and their interaction to respond adequately to the emergency and carry out the necessary activities to mitigate the negative consequences in a rapid and timely manner.
- **Social**: refers to the ability of society and government jurisdictions to cope with the negative social consequences caused by the loss of critical services as consequences of the major earthquakes.
- **Economic**: refers to the capacity of social organizations to reduce and deal with direct and indirect economic losses caused by destructive seismic events.

The dimensions of resilience and its basic properties are related in a very complex way and difficult to study in its entirety due to the fact that the repair of damaged systems involves various agents and their own interests, *e.g.*, inspectors, engineers, insurers, owners of the affected properties, tenants, and that they are also usually strongly influenced by the policies and resources imposed by the government. For example, the technical dimension of resilience can be related to robustness and redundancy as physical characteristics that are provided not only to a building, but also to a set of systems located in a spatially

distributed manner in a community and inevitably inter-related. For instance, consider a hypothetical community in which there is a hospital, a school, an electric power system, drinking and waste water distribution and transportation systems. Suppose that an earthquake causes the failure of the electrical power system and the partial collapse of some buildings. These undesired events can easily generate the *cascade effect*, which is characterized by cause disruptions in a set of sub-systems, which depends on the damage system with the highest hierarchy or even indirectly affect the functionality of systems that did not experience damage. For this case, suppose that the hospital and the school were affected shortly after the earthquake occurred; however, despite the fact that the vital service is indispensable for the entire population, the principal system affected for this illustrative example is the hospital because this building will be necessary to provide the medical services to the injured people, including the one who was already receiving medical service at that time. These two subsystems are affected from the social, health and economic point of view. At the same time, it will be necessary to activate a contingency and mitigation plan (organizational dimension) to repair the damaged systems that form the electrical power system (technical) in the fastest (rapidity) and most effective way (resourcefulness).

Now suppose that also the system affected was the water distribution system. In order to adequately carry out the technical aspect of repairing the both affected system, in addition to the availability of human and economic resources, a specialized agent (*e.g.*, government department) is needed to coordinate them and manage economic resources available. If the damage experienced by the water distribution system is scattered over a considerable area, the speed with which the system is repaired may be affected due to the shortage of specialized personnel to carry out this type of works, and may be necessary to wait longer while technical and economic resources are again available, if they are not previously designated to perform the unexpected tasks. This hypothetical example demonstrates the complexity of the interaction of the dimensions of resilience with its basic properties.

2.2 Resilience framework for assessing individual buildings

The pioneer work presented by Bruneau *et al.* (2003) has been innovative in giving a new and general perspective of the philosophy of seismic resilience, *i.e.*, reduction of: (1) the probabilities of failures, (2) the consequences from failures and (3) the recovery time, by considering a holistic framework that introduce concepts that encompass the socio–economic functioning of modern society, *i.e.*, technical, organizational, social and economic aspects, by means of quantifiable units, *i.e.*, robustness and rapidity, and enhanced by increasing redundancy and using effectively resourcefulness. Nevertheless, this work did not offer an analytical methodology by which the main elements to the characterization to the seismic resilience of different units of analysis (*e.g.*, individual buildings and organizational systems) could be quantified. This fact is not surprising because the expe-

rience and the data needed to propose a robust methodology to assess seismic resilience at that time were limited, even simply because the problem was not fully understanded due to the very complexities and interactions that characterize it (as shown in the example above). Even today, despite the fact that in the last two decades the negative technical–organizational–social–economic consequences of some seismic events have been more extensively and objectively documented, *e.g.*, Northridge (Seligson *et al.*, 2006), 1994; Chile, 2010 (Miranda *et al.*, 2012) and Christchurch, 2011 (Almufti and Willford, 2014), and some numerical models and methodologies have been developed to simulate the components of the resilience of physical systems and social organizations, the problem is still open for study.

2.2.1 General resilience metrics

Based on the fundamental scheme proposed by Bruneau *et al.* (2003), Cimellaro *et al.* (2006; 2010a) extended this pioneer work to an analytical framework that incorporates the four basic dimensions in a unified terminology to quantify the seismic resilience of individual structures, *e.g.*, buildings, bridges, lifelines networks, etc. They define the resilience as a normalized function indicating capability to sustain a level of functionality or performance for a given building over a period of time defined as the recovery time. The latter is the period of time necessary to return the damaged building to a level of operation and comfort equal or better than that offered before it was affected by the disruptive event.

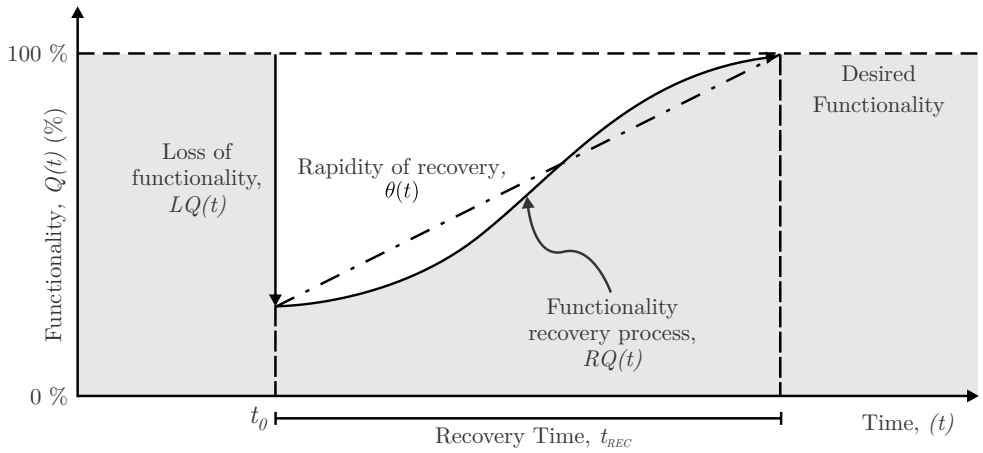

Figure 2.1: Schematic representation of the resilience of a building proposed by Bruneau *et al.* (2003) and extended by Cimellaro *et al.* (2006; 2010a).

Under these conditions this research group propose as generic index of resilience $R(t)$ of a building the area under the recovery curve $RQ(t)$ normalized by the recovery time t_{REC}, as shown in the following equation:

$$R(t) = \int_{t_0}^{t_0+t_{REC}} \frac{RQ(t)}{t_{REC}} dt \tag{2.1}$$

where t_0 corresponds to the instant of time when a potentially destructive earthquake occurs. From the four global properties, theoretically only robustness and rapidity can be calculated directly, as is shown in Fig. 2.1. Redundancy and resourcefulness are the means by which robustness and rapidity are modified to enhance the seismic resilience of a building. In this scheme, robustness is defined as the residual of the loss of functionality, and is described by the following equation:

$$S(t) = 100\% - LQ(t) \tag{2.2}$$

and the rapidity is mathematically defined as the mean rate of the recovery of functionality:

$$\theta(t) = \frac{LQ(t)}{t_{REC}} \tag{2.3}$$

Using the above definition of resilience adapted to the structural performance, it can be concluded that robustness and redundancy are two properties well defined that depend on the inherent geometrical configuration of the structural elements that conform the buildings and on the resistance of the materials used. These properties can be improved by using damage control elements, *e.g.*, energy dissipation devices, buckling restrained braces, adding columns or using innovative materials. The enhancement of the structural performance can help to the non-structural elements, contents and furniture to withstand important seismic demands, *e.g.*, reducing inter-story drifts or floor accelerations, without suffering important levels of damage. In effect, the damage experienced by these latter elements is the principal cause of loss of functionality, even when the seismic demands are below those used in seismic design, as discussed by Miranda *et al.* (2012), Filitrault and Sullivan (2014).

The enhancement of robustness and redundancy is carried out in the most general sense by means of the basic property of the resourcefulness, either before or after a damageable seismic event occurs. However, the implications of both scenarios are very different. For the first scenario, it is possible that resilience improvement will be less complicated organizationally, less costly, and faster to implement. Conversely, if the structure has experienced significant damage, the repair tasks, and in general, the activities required to restore the functionality of the system will be of a very different and complex nature. For example, in the latter case it will be necessary to first perform a post-seismic inspection to determine if the building is safe to be occupied by the users, and/or to conduct a bidding process to determine who is more competent to perform the repair works. In general, resourcefulness, as mentioned above, depends of the ability to employ the human, economic, physical, technological and informational resources to create contingency plans and execute recovery strategies that allow the damaged system returns to the condition for which it was originally designed. Finally, in this context, the rapidity can be understood

as the property that depends on all resources available to carry out the recovery process and the ability to use them in the most efficient way.

Seismic resilience is not only composed of the loss and recovery of functionality. For this property to be understood in a global context, it must be studied in conjunction with another series of variables, called decision variables DVs: (1) direct economic losses, (2) indirect economic losses, (3) number of lives lost, (4) number of people injured and (5) recovery time. Direct economic losses correspond to the costs of repair or replacement of structural, non-structural (contents and furniture) elements, and can be considered that occur during the seismic event. Indirect economic losses result primarily from business interruption, and depend strongly on the recovery time needed to repair the building. This category includes economic losses due to the relocation of businesses to other buildings, losses of financial income, etc. Direct economic losses are generally expressed as a fraction of the replacement cost of the entire building, so despite the large uncertainties involved in assessing these type of losses, it has been relatively easy to develop probabilistic methodologies to evaluate them, as those proposed by Aslani and Miranda (2005), Mitrani-Reiser (2007) and Yang *et al.* (2009), just to name a few. On the other hand, indirect economic losses are even more difficult to express by a similar criteria, mainly because they are influenced by many factors affecting the recovery time, *e.g.*, owner of the building and stakeholders, who are in charge of obtaining financial resources (*e.g.*, by charging insurance against natural disasters or by means of a bank loan), the management of government permits to be able to start the repair work, etc., and not only by the structural engineers who are in charge of planning and executing the repair activities. Due to the complexity of approximating the value of these variables, they must also be estimated in probabilistic terms.

2.3 PBEE framework developed by PEER

Currently the most robust tool for assessing structural performance is the Performance-Based Earthquake Engineering (PBEE) probabilistic method originally proposed by Cornell and Krawinkler (2000), and subsequently enhanced by Porter (2003), Moehle and Deierlein (2004), Mitrani-Reiser (2007), Günay and Mosalam (2013), among others, and finally adopted by the FEMA P-58-1 (2012a) guidelines. The main objective of this methodology is to estimate the consequences in explicit terms due to the earthquake damage to individual buildings, *e.g.*, monetary losses, repair time, injuries, casualties and environmental impacts, for decision-making analysis. These consequences are better known within the analysis framework as DVs, and, in addition to being useful for engineers, they are convenient for the stakeholders.

Due to the aleatory nature that characterizes the occurrence of the earthquakes, to the response of the affected buildings and the disruptive consequences that they originate on the society and economy, the scheme of evaluation of the seismic performance developed by the PEER is of a rigorous probabilistic character (Yang *et al.*, 2009). The PEER-PBEE methodology is composed by four probabilistic analysis: (1) seismic hazard analysis, (2)

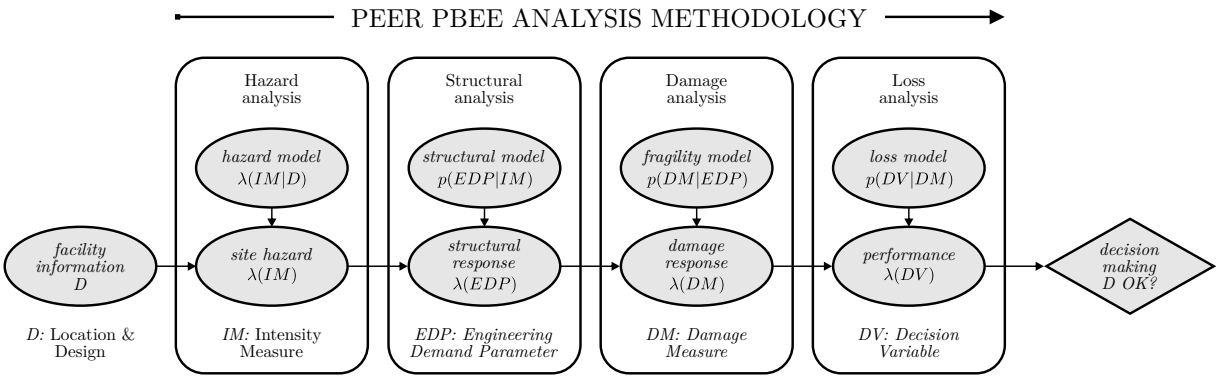

Figure 2.2: Flowchart of the framework for performance-based earthquake engineering (Porter, 2003).

structural analysis, (3) damage analysis and (4) loss analysis, as shown in the Fig. 2.2. The terms $p(X|Y)$ and $\lambda(X|Y)$ denote the probability density function (PDF) and the mean occurrence rate, respectively, of a random variable X conditioned on a random variable Y. The probability distributions resulting of these analyses are combined using the total probability theorem to obtain the expected value or the mean annual frequency of exceedance of the DVs of interest. The main characteristics of each analysis and the most relevant uncertainties that characterize them are described as follows.

2.3.1 Hazard analysis

The main objective of this analysis is to obtain the seismic hazard curve, which represents the level of seismic exposure of a particular building. The hazard curve is represented by means of a set of intensities conditioned to a various return periods, *e.g.*, peak ground acceleration PGA or spectral acceleration at the period associated with the first mode of vibration of the structure Sa(T1), and its mean annual rate of exceedance $\lambda(IM)$. The seismic hazard curve can be used to select a set of seismic records for each seismic intensity considered on the site of interest. These records are characterized by similar frequency content, intensity and duration (characteristics associated to the soil conditions where the structure is placed), and the influence exerted by the uncertainties of the fault mechanism and location, source-site distance, their magnitude-recurrence rates, level of attenuation, etc.

2.3.2 Structural analysis

This second step has two main objectives. The first is to determine the physical response not only of the structural elements, but also of the non-structural elements and contents, *i.e.*, of the elements that may experience some type of damage and therefore some type of consequence in terms of DVs. Within the PEER-PBEE methodology, the different types

of elements that integrate a building that are susceptible to experience damage are known as performance groups PGs and the physical response of these are called engineering demand parameters EDPs.

In general, the set of EDPs can be constituted by local physical variables, *e.g.*, forces and deformations, or global variables, *e.g.*, inter-story drifts and floor accelerations. The selection of the type of EDPs to be monitored depends on the type of PGs considered in the study and the level of refinement of the damage analysis. For example, in a column type element it is convenient to monitor the shear forces to infer the fragile failure (Krawinkler, 2005), while in a content type element, *e.g.*, a laboratory equipment, the physical parameter associated with its possible overturning is the maximum floor acceleration (Filitrault and Sullivan, 2014).

The second objective is to estimate the probabilities of collapse $Pr\left(C|IM\right)$ and survival $Pr\left(NC|IM\right)$ of the building given an IM. The collapse probability is calculated as the number of realizations that experienced the global collapse of the system divided by the total number of ground motions defined in an IM (Miranda and Aslani, 2003; Günay and Mosalam, 2013). The probability of survival of the structural system given an IM is obtained as $Pr\left(NC|IM\right) = 1 - Pr\left(C|IM\right)$.

The collapse probability of a building depends on its ductile capacity. Although a structure may collapse due to multiple failure mechanisms, three general criteria are highlighted in the specialized literature to determine the global collapse of a building: first component failure, side-sway collapse and gravity load collapse (Shoraka *et al.*, 2013).

The first criterion consists of determining whether at least one structural component loses its load-carrying capacity or exceeds a limit state of deformation, *e.g.*, shear strength or distortion in columns. This approach is frequently used to define collapse in structures that have low or no ductile capacity, and is consistent with the criterion proposed by ASCE (2006) for the limit state of collapse prevention. This criterion is easy to implement numerically; however, it does not take into account the redistribution of the internal forces developed by the structure during the seismic demand, so the probability of collapse associated with a intensity measure turns out to be conservative.

The lateral collapse criterion is suitable for structures that have the capacity to develop important ductilities, which in turn originate the presence of P-delta effects and reduction of lateral load capacity. In this approach, the collapse occurs when the structure develops dynamic instability, *i.e.*, when the interstory drifts increase rapidly while the seismic demand increases very little (Vamvatsikos and Cornell, 2002). This methodology takes into account the redistribution of the internal forces developed by the structural elements; however, it is possible that convergence problems may occur when the structure is close to dynamic instability.

The gravity load collapse mechanism occurs when the stiffness of the elements that transmit the vertical loads to the foundation begins to degrade until their capacity to support gravity loads is lost. This collapse mechanism begins to occur with the development of local failures in some elements, *e.g.*, columns, beams and connections, causing the vertical

loads to be distributed abruptly to the elements that still have the capacity to take both gravity and lateral loads. Nevertheless, the demand on these elements is of such magnitude that global collapse occurs when they lose their capacity to resist the total weight of the structure.

2.3.3 Damage analysis

The third step consists in relating the EDPs corresponding to the several types of elements, *i.e.*, structural, non-structural and contents, into a representative measure of discrete damage states DSs, *e.g.*, null, light, moderate and severe. Due to the uncertainty in the severity of damage that a PG may develop due to a seismic demand the way to infer the DS of each PG is using generic fragility functions (Goulet *et al.*, 2007; Yang *et al.*, 2009). These functions represent the probability distribution of the damage severity that the PGs can experience as a function of EDP by which the damage is related. An alternative way to interpret the meaning of a fragility function is the following: the probability of reaching or exceeding an undesirable event, *e.g.*, light cracking or shear failure (light and severe DSs, respectively) at a local level of analysis, or total collapse (severe DSs) at a global level of analysis. Additionally, the different DSs associated with each PG represent an indicator of the type of generic repair activities that need to be performed to restore the damaged components to their original operating state, and other consequences that will be discussed in the next chapter.

There are three ways to create fragility functions (Porter, 2000, 2019): (1) empirically, (2) analytically, and (3) from expert judgment and experience:

- The *empirical fragility function* is obtained by fitting the parameters of a probability distribution. For example, it is common in the field of earthquake engineering research to calibrate the parameters of the log-normal probability distribution function. The data used to calibrate the fragility functions is obtained in laboratory tests or from data collected from damages caused by real earthquakes.

- The *analytical fragility function* is obtained through numerical simulations of the behavior of individual elements (*e.g.*, drifts or reactions in a bridge column) or entire buildings models built to full size or scale (*e.g.*, maximum roof displacement).

- Fragility functions based on *expert judgment and experience* are obtained through experience gained from laboratory tests, from observing damage in damageable earthquakes and from performing numerical simulations. This means that this latter classification corresponds to a combination of the first two methods described above.

A common tool used for fitting the parameters of a fragility function (*e.g.*, the median and log-standard deviation in a log-normal distribution) is the maximum likelihood method (Shinozuka *et al.*, 2000; Backer, 2015).

2.3.4 Loss analysis

The last step of the methodology is to relate the DS experienced by the different PGs with the consequences, *i.e.*, DVs that are useful principally for the stakeholders, *e.g.*, investors, insurers, lenders, occupants, and in general for risk-based decision making for individual buildings. The result of this step is the quantification of probability distribution of the DVs: $p(DV|DM)$.

2.3.5 Combination of the analysis

There are several ways to express the DVs. The most common are in terms of the mean annual rate of exceedance or as a expected value of the DVs. Whatever the way of expressing the DVs, it is necessary to use the total probability theorem to combine the uncertainties associated with the results obtained in each of the probabilistic sub-analyses. The result of this process is the following canonical expression, first developed by Cornell and Krawinkler (2000):

$$\lambda(DV) = \int\int\int p(DV|DS)dp(DS|EDP)dp(EDP|IM)d\lambda(IM) \tag{2.4}$$

Naturally, this expression is a minimalist representation of a very complex problem (Moehle and Deierlein, 2004). Nevertheless, the components of this expression provide a clear perspective of the fields of research involved in the framework and also allows to have a panorama of the aspects that have to be improved.

The DVs commonly used nowadays by the PEER-PBEE methodology are: (1) repair costs, (2) repair times, (3) injuries, (4) deceases and (5) structural safety. In 2012 the FEMA P-58-1 (2012a) adopted this methodology to establish it as a standard guideline for evaluating the seismic performance of individual buildings. However, although this methodology represents an important step towards the quantification of the seismic risk of individual buildings, it is necessary a much broader and deeper interpretation of the seismic performance in individual buildings (Krawinkler and Deierlein, 2013), *i.e.*, it is necessary to take into account the resilience in an explicit way. There is a need to understand how the functionality of individual buildings is affected by the damage induced by moderate to high earthquakes intensities and what recovery strategies should be taken to return the buildings to its original/optimal functionality level, and what amount of human and economic resources are required to achieve it. In this context, a large number of engineers, researchers, politicians and sociologists have paid attention to the concept of *seismic resilience*, since through it it is possible to introduce socio-economic variables that are not considered in the standard methods for assessing natural risks.

2.3.6 General assumptions on the formulation of the PEER-PBEE methodology

It is convenient to mention that the combination of the processes that integrate the PEER-PBEE methodology can be done under the following hypotheses (Yang *et al.*, 2009):

1. There is statistical independence between the damage experienced DS and the IM, *i.e.*, the measure of damage DS only depends statistically on the magnitude of the physical response of the building, EDP: $p\left(DS|EDP, IM\right) = p\left(DS|EDP\right)$.

2. There is statistical independence between the DVs and the EDPs and the IM, *i.e.*, the consequences DV only depend on the magnitude of the damage experienced by the PGs: $p\left(DV|DS, EDP, IM\right) = p\left(DV|DS\right)$.

3. The building under study does not experience cumulative damage during the analysis process, *i.e.*, it is assumed that the building is restored to its undamaged condition after each non-linear dynamic analysis (NLDA) associated with each IM, and in general, from one IM to another.

2.4 Types of performance assessment

In general, there are three types of structural performance evaluation (ATC, 2011; NIST GCR 11-917-15, 2011; FEMA, 2012a): intensity, scenario and time/risk-based. The selection of one of these methods will depend on the type of evaluation to be carried out and the results to be obtained. A description of each one of them is presented below.

2.4.1 Intensity-based assessment

This type of evaluation is frequently used to review the seismic performance of a building with respect to the seismic demands used in the structural design; however, any type of target demand of interest can be used, *e.g.*, elastic response spectrum of accelerations, velocities or displacements. With the results obtained in the structural response, the damage and expected consequences are assessed. This corresponds to steps two to four of the PBEE-PEER methodology. The DVs obtained are expressed in terms of average values, these are, $(\overline{EDP}|IM)$, $(\overline{DM}|IM)$ and $(\overline{DV}|IM)$.

2.4.2 Scenario-based assessment

Scenario-based assessment is frequently used to estimate the seismic performance of a building with respect to a specific earthquake scenario, *i.e.*, an earthquake with a specific magnitude and location, relative to the site where the building in question is placed. This

type of evaluation is useful when it is desired to evaluate the performance of a building when a seismic event similar to one that occurred in the past is expected to occur again. To accomplish this, a set of accelerograms congruent with the dynamic soil properties of the site where the building in question is located must be selected and scaled to match to the IM of interest. The time histories can be real or numerically simulated by a suitable method. With the set of seismic records, the PEER-PBEER methodology is applied, *i.e.*, structural analysis, damage analysis and decision variable analysis. The result obtained with this type of assessment is the probability distribution of the DVs of interest, conditioned to a specific earthquake scenario.

2.4.3 Time/risk-based assessment

The time-based assessment (also known as seismic risk evaluation) is carried out taking into account several seismic intensities that can occur within a return period Tr with a probability of exceedance $Pr(IM > im)$ associated with a specific interval of time t, *e.g.*, life cycle of 50 or 100 years. This type of evaluation allows to consider the uncertainties associated to the magnitude, distance source-to-site, type of failure, seismic intensity, etc. This means that it is possible to consider, at least in probabilistic terms, all possible earthquakes that may occur in the period of time t and can affect a specific building. The DVs result of this type of assessment can be expressed in various ways, *e.g.*, rate of exceedance, probability distribution conditioned on seismic intensity, vulnerability function, etc. In fact, this type of evaluation corresponds to the general framework to evaluate the seismic performance of buildings developed by the PEER, explained previously.

Chapter 3

Overview of the proposed methodology

This chapter summarizes the methodology proposed to estimate the resilience of buildings damaged by the effects of earthquakes. The methodology is divided into three overall assessment processes: (1) loss of functionality, (2) stage of non-functional building and (3) recovery process of functionality, as shown in the Fig. 3.1. It has been shown that the stage associated with the delay time contributes significantly to the recovery time; however, in the scheme proposed by Cimellaro, unlike the one proposed in this research work, it is not taken into account. It has been shown that the stage associated with the delay time contributes significantly to the recovery time (Comerio, 2006); however, in the scheme proposed by Cimellaro *et al.* (2006), unlike the one proposed in this research work, it is not taken into account. In this regard, to evaluate the loss of functionality a process is simulated to determine the safety level of the damaged installation by means of the inspection criteria proposed by the ATC-20 (1989).

The objective of the numerical simulation of the inspection is to determine the probability that the structure is safe to be used by the occupants, restricted use, or unsafe for occupancy. It should be noted that in the numerical simulation of the post-seismic inspection, structural and non-structural components and furniture-type contents are considered. The post-seismic inspection simulation proposed in this document corresponds to an extension of the methodology originally proposed by Mitrani-Reiser (2007). The main difference is that this thesis considers not only structural inspection, but also non-structural and furniture inspection, which results in a clear explanation that the probability of the building losing functionality due to damage experienced by the latter two types of performance groups is higher than that associated with structural inspection.

With the results of the numerical evaluation of the post-seismic inspection, the events necessary to simulate the recovery of the damaged installation are determined. In general, the recovery process can be divided into two sub-processes. The first one corresponds to the events that impede the start of the repairs. Comerio (2006) called these events as *irrational factors* because it is not possible to determine a priori which factors will precede

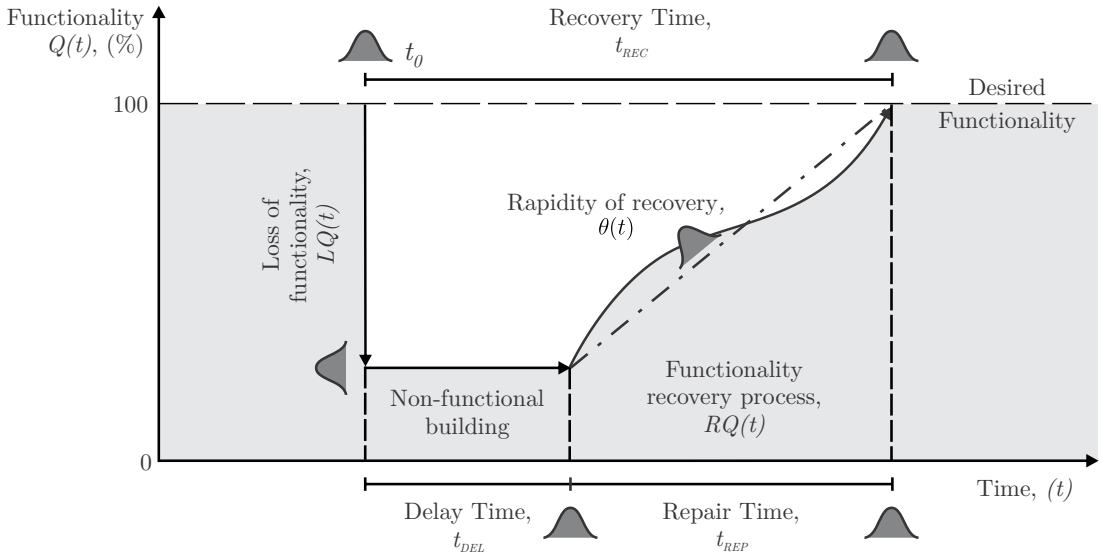

Figure 3.1: Schematic representation of the resilience of a building proposed in this study (adapted from Bruneau *et al.* (2003)).

the start of the repairs and the order in which they may occur. In this research work the irrational factors indicated in the flow chart shown of the Fig. 3.2a are considered. These factors can be considered the most representative, *i.e.*, those that contribute significantly to the recovery time of the damaged system: (1) structural, non-structural and contents inspection, (2) obtaining financing to perform the repair works, (3) structural redesign, (4) planning of repair activities and (5) management of government permits to initiate repairs. As a second overall recovery sub-process, repairs/replacement of structural, non-structural and furniture components are considered, as indicated in the flow chart in Fig. 3.2b.

Since the evaluation of damage involves great uncertainties, the overall configuration of damage that occurs from one realization to another is very different, this research study proposes six limit states of functionality LS. These limit states are determined by the severity of the damage experienced by structural, non-structural and furniture components. The result of the limit state assessment is the probability that the building will be: LS_0: fully functional, safe building; LS_1: partially functional and structurally safe; LS_2 restricted use, non-functional and structurally safe; LS_3 restricted entry, non-functional and structurally safe; LS_4 unsafe building, unoccupied, but repairable; LS_5: unsafe, irreparable building; and LS_6 structural collapse. These functionality limit states correspond to an extension of those proposed by Burton *et al.* (2016); however, from the point of view of the author of this work, they are presented here in a clearer and more concise way.

Because limit states provide an overview of the overall configuration of the damage experienced by an installation, it is necessary to use a quantifiable parameter as a measure of loss of functionality. In this thesis, the use of the percentage of non-usable area for each floor of the building as a measure of loss of functionality is proposed. This proposal is based on the fact that the repairs of the damaged PGs are performed by one or more

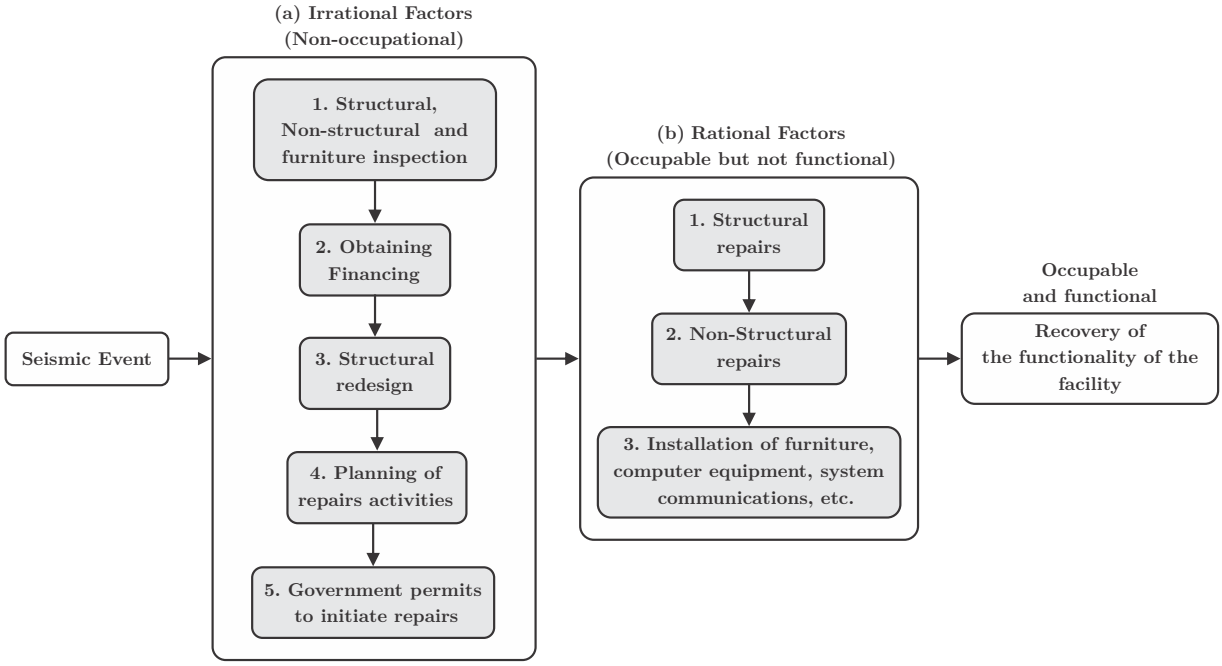

Figure 3.2: General sequence of recovery of the functionality.

crews, who need to move in certain areas within the building over a period of time. The process of reparation of the building is formulated within a recursive numerical scheme in which the times and costs of repair of the damaged components are considered, as well as the available human resources, to which a percentage of area is prescribed.

One of the most important aspects of seismic resilience is to reduce the number of fatalities and injured people. In this research work an adaptation of the criteria proposed by the FEMA P-58-1 (2012a) is proposed to estimate the number of fatalities, and with a similar criteria the number of people who are injured is estimated. Likewise, a procedure is proposed to estimate the equivalent economic value associated with the number of people who lose their lives and the corresponding number of injured users. The results obtained with this tool show that this type of consequences could generate significant economic losses.

This research work proposes an enrichment of the seismic performance evaluation methodology proposed by PEER in order to evaluate the seismic resilience of individual buildings. As explained in Chapter 2, the PEER-PBEE methodology is composed of four probabilistic analyses: (1) seismic hazard analysis, (2) structural analysis, (3) damage analysis, and (4) consequence analysis. The process of post-seismic inspection simulation corresponds to an improvement of the damage assessment (step 3), and the resilience assessment as an enrichment of the analysis of decision variables (step 4) by introducing not only the loss and recovery of functionality, but also the indirect economic losses, due to business interruption, and the equivalent cost of injuries and deaths. Finally, a combination of scenario-based and time/risk-based assessments will be used in this work. Details of the proposed methodology and considerations at each stage of the PEER-PBEE method are

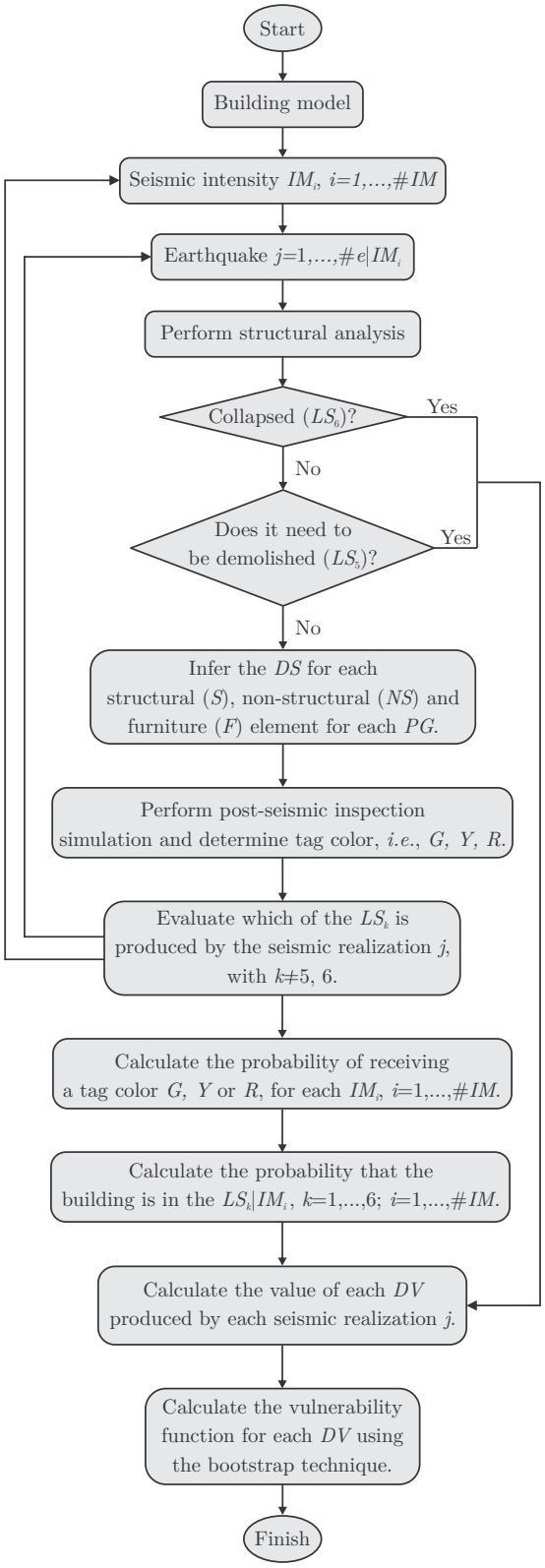

Figure 3.3: Flow chart of the proposed methodology.

presented in the following chapters.

The results of the DVs obtained with the proposed methodology are expressed through vulnerability functions. The uncertainty associated with the expected value of the sample mean of each DV at each IM is approximated by the bootstrap technique and expressed through the confidence interval for a 95% probability. The description of the proposed methodology is summarized in the flow chart in Fig. 3.3.

Chapter 4

Seismic demand definition: ground-motion simulation

In the field of probabilistic assessment of seismic performance of buildings it is convenient to have sets of seismic records that cover the seismic scenarios expected with the seismicity of the site where the building is located in order to obtain reliable static parameters of the structural response, the damage expected and its consequences, *i.e.*, the DVs. In this regard, usually for a specific seismically active site of interest there is an acceptable amount of accelerograms generated by low magnitude earthquakes. Unfortunately, there are few seismic records associated with moderate to high intensities. This fact has been a problem since the beginning of seismic risk studies until today.

To deal with this problem it is common to select a set of seismic records and modify their intensity through a linear scaling in its entire duration so that intensities are reached that generate structural damage. Seismic records should have similar properties with respect to frequency content, duration and intensity, at each level of seismic hazard considered in a specific study. One application of this type of scaling is used in the well known method Incremental Dynamic Analysis (IDA) developed by Vamvatsikos and Cornell (2002) to estimate structural performance under seismic demands. For example, by means of this technique it is possible to obtain the non-linear variation of the interstory drifts according to the linear variation of the spectral acceleration, or the calculation of the collapse probability, assuming that this occurs when the lateral displacements increase substantially when the seismic intensity experiences a small increase, *i.e.*, sidesway collapse. This methodology is easy to implement, so it has been widely used. However, its main disadvantage is that the duration of the records nor the frequency content is modified, so the structural performance can be over or under estimated, *e.g.*, is not considered an increase in the number of load cycles to which the structural is subjected, and therefore, fatigue damage is not properly taken into account. Consequently this methodology is not always the most appropriate (Jalayer, 2003; Quinde, 2019).

An alternative solution to overcome this limitation has been the development of methodologies to simulate synthetic seismic records, also known as seismological scaling. In

the specialized literature there is a great number of methodologies to simulate synthetic records; however, the most popular are those based on Empirical Green Functions (EGF) such as Joyner and Boore (1986), Wennerberg (1990), Ordaz *et al.* (1995) and Kohrs-Sansorny *et al.* (2005).

Joyner and Boore (1986) proposed a single-stage simulation scheme. This process consists of summing many identical seismic records of small intensity, called subevents, multiplied by a scaling factor, *i.e.*, stochastic summation. In this process it is assumed that the fault rupture has the same duration as the target event, that is, the seismic event of greater magnitude, of which it is desired to reproduce a record with similar characteristics. Likewise, the generation of the subevents is given in time intervals called rupture delay times, which, added together, result in the duration of the target event. In this regard, a uniform probability density function was used to generate these delays, which is why inconsistencies were produced with frequencies proportional to the corner frequency, resulting in synthetic records that were not representative with real accelerograms. Nevertheless, this aspect was fundamental for the development of more complex modeling, since this process allows in a very simplified way to simulate the irregular process of fault propagation. On the other hand, this research established some fundamental restrictions in the stochastic summation scheme and the need to implement a scaling factor to adjust the high and low frequencies.

Wennerberg (1990) showed that the single-stage process was not capable of simulating a complex source rupture process. Therefore, he proposed a two-stage simulation scheme. However, in this process, instead of using a uniform density function to characterize the rupture delay times, he used a probability density function consistent with the amplitude spectrum determined by the model w^2. Although this methodology gives better results, too many high frequencies appear in some regions of the amplitude spectrum. One of the advantages of this methodology is that it allows simulations of events of any size. Also, the two-stage process allows simulating the source complexity in a more approximate way.

Ordaz *et al.* (1995) proposed a probability density function that fits exactly with the w^2 model. This model was used with the single-stage approach, as proposed by Joyner and Boore (1986). As a result, the average of the response spectra of the simulated records fits adequately with the response spectrum of the target event record. Nevertheless, because the extended fault is assumed to be represented as a point source, the methodology does not take into account the directionality of the source, nor is it suitable for simulating records at sites close to the seismic source.

In this study the stochastic summation of small earthquakes method developed by Kohrs-Sansorny *et al.* (2005), referred as *Two-Stage Method*, is used. This method is a combination of the first three methodologies listed above. As its name indicates, composed of two stages. The first one consists in the simulation of the fault propagation process, which is modeled by a set of patches characterized by their random positions over the fault, and is assumed that this process occurs at a constant velocity. In the second stage, the energy released during the rupture process is modeled for each patch. It is accepted that the entire fault can be represented as a point source and as Green's empirical function a

single seismic record, produced by a small earthquake, can be used. Based on this type of fault the methodology requires the specification of only the seismic moment M_0 and the stress drop $\Delta\sigma$ of the target event. Finally, the seismic records associated to the simulated earthquake of greater magnitude are obtained, for each random realization, by multiplying them by a special scaling factor κ and summed together.

The main advantages of this method is that it takes into account the site effects, the variation in the frequency content and the duration of the seismic recorders simulated, producing more realistic and sufficiently different from each other. This approach is efficient when modeling earthquakes whose source-site distance of interest satisfies the far-field condition because the source-site distance is large enough to accept that the fault can be modeled as a point source. At the same time, this hypothesis is the main disadvantage of the method since it is inadequate to take into account directivity effects. Therefore, with this technique is not possible to model near-fault earthquakes.

The proposed methodology to evaluate the seismic resilience use 3D structural models to characterize the buildings and although earthquakes generate accelerations in three perpendicular directions, in this thesis only two horizontal synthetic seismic recorders are used. Likewise, although the Mexico City valley is affected by earthquakes of different nature, *e.g.*, intermediate depth and subduction earthquakes, in this study only the latter will be taken into account. Nonetheless, given the generality of the proposed approach to evaluate the seismic resilience, it can be applied to any number and type of seismic sources.

4.1 Considerations for selecting orthogonal pairs of synthetic horizontal ground motions

4.1.1 Condition I: Selection based on statistical independence between two pairs of seismic records

The selection of orthogonal horizontal pairs of synthetic time histories is not an easy task mainly due to its erratic nature. For this reason, the Seismic Task Group of ASCE Nuclear Structures and Material Committee, the American Society of Mechanical Engineers (ASME) and the Institute of Electrical and Electronics Engineers (IEEE) postulated the existence of *statistical independence* between both records as a selection criterion, and as a quantitative measure the correlation coefficient between both random variables was proposed. With all rigor, the statistical independence is satisfied only when the correlation coefficient ρ is zero. Nevertheless, this is not a realistic judgment because the two components associated with the same earthquake are not independent data; therefore the rational approach is to calculate the statistical properties of the correlation coefficients of the orthogonal ground motions.

One of the few studies carried out in this regard was conducted by Chen (1975). He

calculated the absolute value of the correlation coefficient of each pair of three sets of seismic records. The first of them from 104 pairs, the second from 12 pairs and the third from 13 pairs. These last two groups were used by Newmark *et al.* (1973) in a similar study. Finally, Chen (1975) proposed as an *upper limit value* the correlation coefficient of 0.16. This value was obtained as the mean of the averages of the absolute value of the correlation coefficient of the three groups of seismic records plus one standard deviation. Recently the ASCE (2000), ASCE (2005) and finally the NIST GCR 11-917-15 (2011) reached a consensus and proposed an upper limit of the correlation coefficient of 0.3 for two horizontal components of the ground motion. This limit value was justified by the results obtained by Hadjian (1981) and subsequently corroborated by Huang *et al.* (2010) using a larger set of seismic records. For practical purposes Hadjian (1981) recommends the use of the value 0.5 as a limit value for the correlation coefficient.

In this thesis, the assumption with 0.5 as correlation coefficient upper limit is used as the first condition to select the pairs of synthetic time histories for each random simulation, conditioned to an *IM*. The absolute value of the correlation coefficient is obtained by the following expression:

$$\rho = \left| \frac{\mathrm{E}\left[\{\ddot{x}_g(t) - \mu(\ddot{x}_g(t))\} \cdot \{\ddot{y}_g(t) - \mu(\ddot{y}_g(t))\}\right]}{\sigma\{\ddot{x}_g(t)\} \cdot \sigma\{\ddot{y}_g(t)\}} \right| \leq 0.3 \tag{4.1}$$

where E[·] is the mathematical expectation; $\mu(\cdot)$ and $\sigma(\cdot)$ are the mean and standard deviations of the two orthogonal synthetic time histories $\ddot{x}_g(t)$, $\ddot{y}_g(t)$, conditioned to the same return period.

4.1.2 Condition II: Geometric mean spectral acceleration interval given an *IM*

One of the most important results of the seismic hazard analysis is the determination of the seismic hazard curve for a specific structural period of interest Tr, which represents the mean annual rate of exceedance $\lambda(IM)$ of the expected IM in a specific site, *e.g.*, where a building of interest is located. A schematic illustration of a seismic hazard curve is shown in Fig. 4.1. This curve is constructed by using ground motion prediction equations, also known as attenuation relationships. These equations are functions that depend mainly of a set of seismic magnitudes of interest and their distance from the fault to a specific site, although parameters such as soil type and the directivity effects that cause the fault rupture can also be considered, depending on the degree of sophistication required (EERI Committee on Seismic Risk, 1989).

In the specialized literature a great number of attenuation relationship allows to predict different IMs, *e.g.*, the peak ground acceleration PGA, velocity V_g and displacement D_g. Nevertheless, those that enable the estimation of the spectral acceleration Sa(T1) are of special interest since these expressions are used to calculated the uniform hazard spectrum (UHS), an indispensable tool to construct the seismic design spectra. In this

respect, to take into account the two horizontal components of a seismic intensity, the attenuation relationship expresses the movement of the ground in terms of its natural logarithm $\log(IM)$. This is due to the natural logarithm of the geometric mean of both components is equivalent to the arithmetic mean of the logarithm of the two orthogonal components of intensity:

$$\log(\sqrt{IM_x \cdot IM_y}) \equiv \frac{\log(IM_x) + \log(IM_y)}{2} \tag{4.2}$$

Another reason why the geometric mean of the spectral acceleration is used is the fact that the orthogonal accelerations recorded at each instant of time are probably quite different from each other (NIST GCR 11-917-15, 2011). In fact, it is possible that the maximum intensity of the ground motion is presented in a different direction than that in which the accelerometer are oriented.

In the PBEE methodology the seismic hazard curve is of special interest because it is used as an artifice to select seismic records consistent with the seismicity of the site where the building in study is located (FEMA, 2012a). This artifice consists in constructing a set of intervals of intensities (IM_i^l, IM_i^u) around the expected value of each IM_i (consider the case shown in Fig. 4.1). There is no consensus on how to calculate these limits, but the following deterministic expressions can be used to obtain them:

For the lower limit:

$$IM_i^l = IM_i - \frac{IM_i - IM_{i-1}}{2} \tag{4.3}$$

For the upper limit:

$$IM_i^u = IM_i + \frac{IM_{i+1} - IM_i}{2} \tag{4.4}$$

Once the intensity intervals for each level of IM have been constructed, the seismic records whose intensity is within each interval are selected. This artifice, besides being useful to select accelerograms consistent with the seismicity of the site where the building of interest is located, also has the characteristic that it indirectly takes into account the uncertainties associated with the seismic demand, *i.e.*, the variability record-to-record inherent in recorded ground motions, and as a consequence, the variability in the structural response. Moreover, the selected seismic records in each interval of intensities have the quality, at least in statistical terms, that they are conditioned to a specific return period, which allows to carry out studies of the structural performance in a more consistent way.

In this thesis this artifice is used as a second condition to select the orthogonal horizontal pairs of individually simulated synthetic time histories with the approximation of Kohrs-Sansorny *et al.* (2005), conditioned to a specific return period. In reality the pairs of simulated records do not represent independent events, as mentioned in the previous

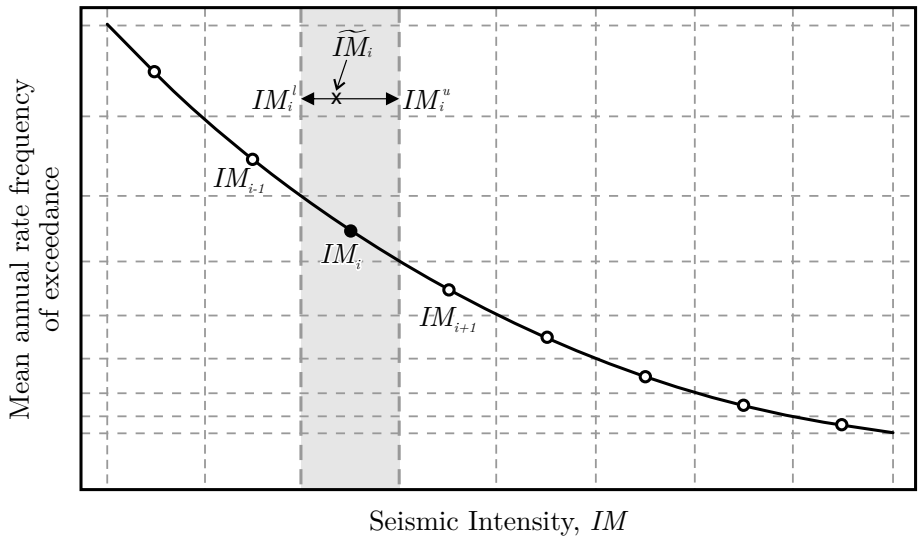

Figure 4.1: Schematic representation of a seismic hazard curve for a specific site. A discretization of intervals of IM corresponding to different return periods is also presented. A random realization of a spectral acceleration obtained by the geometric mean of two orthogonal components for a particular intensity is illustrated.

section. Therefore, as selection parameter, the geometric mean of the spectral acceleration $\widetilde{\mathrm{Sa}}(\mathrm{T})$, Eq. 4.5, as a function of the fundamental average period of vibration of the building $\mathrm{T} = (\mathrm{T}_x + \mathrm{T}_y)/2$, is used:

$$\widetilde{\mathrm{Sa}}(\mathrm{T}) = \sqrt{\mathrm{Sa}_x(\mathrm{T}) \cdot \mathrm{Sa}_y(\mathrm{T})} \tag{4.5}$$

T_x and T_y correspond to the fundamental periods of vibration of the structure in each orthogonal direction of analysis. This expression is valid as long as the first two vibration modes of translation are clearly identified; on the contrary, if only the first mode of vibration is identifiable, its period of vibration should be used (NIST GCR 11-917-15, 2011). This criterion of selection of orthogonal pairs of time histories is consistent with the functional form used by the attenuation relationship, as explained at the beginning of this section.

4.2 Number of synthetic earthquakes used in each *IM*

The number of NLDA to be performed in a seismic resilience study is a major aspect of statistical inference analysis since with this tool the data set obtained in the last step of the PBEE-PEER methodology is processed in order to assess the performance of a building in a holistic way, *i.e.*, to carry out the analysis of DVs as a whole. This information is the main way to answer questions such as:

- *How much should the owner of a building pay on average to insure it during a defined period of time, say one year?*
- *How long will at least a building be out of operation by accepting a certain amount and severity of damage?*
- *What is the confidence interval of the expected number of victims given a specific building design and a seismic intensity?*

The most important question that the seismic risk analyst must ask is what is the level of approximation that the results of a certain analysis have with respect to a proposed mathematical model. To try to solve this question statistical inference is a tool used to make decisions. Some of the results obtained in this stage are the expression of the variables of interest in terms of probability distributions, *e.g.*, fragility functions, or quantifying confidence intervals of a certain random variable.

It is by means of the theorem of Strong Law of Large Numbers and the Central Limit Theorem with which the size of the sample of a random variable is estimated to carry out a reliable statistical analysis (from the point of view of the theoretical model representing a given random phenomenon) of the mathematical expectation $\mu = \mathrm{E}[X]$ and the variance $\sigma^2 = \mathrm{Var}(X)$ of a random variable x (Soong, 2004; Rubinstein and Kroese, 2008). These two theorems are associated with the sum of independent random variables, and are described in the Appendix A in detail.

As demonstrated in section A.3 of Appendix A of this thesis, to perform an adequate statistical inference analysis with classical methods (*e.g.*, the maximum likelihood theory) according to Tchebycheff's inequality requires a number of 720 structural analyses when the building has a 10% probability of collapse and a 5% error in the estimation of this probability is accepted, when using the Bernoulli probability distribution as the approximation criterion. Performing this amount of three-dimensional NLDA to construct a sample of acceptable size of the probability densities of the physical response $\mathbf{EDP} \mid IM$, the damage $\mathbf{DS} \mid IM$, and the consequences $\mathbf{DV} \mid IM$, is an impractical job mainly because of the computational time demand.

4.2.1 Practical criteria for determining the number of ground motions

There is no general criteria that prescribes the minimum number of orthogonal ground motion pairs that must be used in three-dimensional NLDA to evaluate the performance of either a new or an existing structure. Moreover, the few criteria that exist differ from each other. This section describes some of the criteria proposed by various seismic design codes and evaluation standards to determine the minimum number of pairs of seismic records to be used in three-dimensional NLDA.

The ASCE (2010) recommends using at least seven pairs of seismic records simultaneously in the NLDA, and the resulting variables of interest are expressed by their arithmetic

average. In case of using less than seven pairs (but not less than three) it recommends to take the maximum value of the structural response of interest from the analyses performed. A similar criterion is proposed by the Eurocode 8 (2004), where it is established to perform at least seven non-linear time histories analyses, and to use the average of the response of the variable of interest as a design parameter.

The FEMA P-58-1 (2012a) recommends applying at least seven pairs of records if the pseudo-acceleration average spectrum fits reasonably well with the target spectrum, *e.g.*, design spectrum. Otherwise, at least eleven pairs of seismic records should be used. This last criterion was adopted from the study carried out by Huang *et al.* (2011). Likewise, in case at least one pair of seismic records applied simultaneously causes structural collapse, a number of pairs of ground motions should be used so that at least seven of them do not cause structural collapse at specific *IM*.

On the other hand, the NTC-DS (GCDMX, 2020) states that at least eight pairs of seismic records should be used if the period of vibration of the ground is less than 1 second, otherwise it suggests using twelve pairs. To perform NLDA a special arrangement between the accelerogram pairs must be made. This arrangement consists of applying the component with the highest intensity of spectral acceleration in the direction of the first translation mode of vibration, and the other component in the perpendicular direction of analysis. This design guideline recommends the selection of accelerogram pairs independent of each other; however, it does not define any criteria for determining independence as such. The NTC-DS (GCDMX, 2020) could use a criterion like the one used in this thesis, since after all, it is unlikely that two pairs of orthogonal seismic records are totally independent because they are generated by the same earthquake, even when they are created by numerical simulation. Because of this, a reasonably small limit value for the coefficient of variation between the pairs of seismic records can be established as a practical criteria.

Of all these criteria, the only one focused to evaluate DVs in terms of seismic risk, *e.g.*, economic losses, is the FEMA P-58-1 (2012a), the other criteria are focused to be used in the practice of structural seismic design, to be more concrete, in verifying the resistance and deformation of the structural elements of a given structural design. Also, none of the criteria described above specifies why they propose a certain minimum number of NLDA. It is possible that this is due, as discussed above, to the scarcity of seismic records generated by medium to high intensity earthquakes and the high computational cost of performing a large number of NLDA.

On the other hand, with respect to the techniques for estimating the parameters of a probability distribution, the method of moments and the method of maximum likelihood, require the assumption of a distribution function for the sample of a given phenomenon. The validity of the model building process using these techniques depends, therefore, on the justification of the hypothetical distribution and the amount of data used, as demonstrated in the Appendix A. However, if the hypothetical distribution does not agree with observed data, the resulting probability distribution function with parameters estimated by any procedure, as elegant as it is, would at best give a poor representation of the underlying phenomenon (Soong, 2004).

To address this two problems, this research work uses the aleatory resampling methodology better known as *bootstrap* technique, proposed by the statistician Bradley Efron in the late 1970s (Efron, 1979). This technique does not require a robust sample population to infer statistical parameters, and moreover, has the characteristic that it does not require the prescription of a specific probability distribution function and can therefore be considered to be of a general nature. It should be noted that the use of the bootstrap technique in the fields of resilience and seismic risk had not been done before, so it can be said that its use in this thesis represents a innovative application. In Chapter 10 the main characteristics of the bootstrap resampling technique will be discussed.

Having said this, the methodology to evaluate the seismic resilience of buildings proposed in this doctoral thesis will be validated with a small number of pairs of seismic records, *i.e.*, 20 pairs of simulated time histories for each of the seismic intensities considered in this study, mainly due to the high computational cost involved in performing a large number of NLDA and the lack of real seismic records of moderate to high intensity. Likewise, the way to express the variables that integrate the seismic resilience in a holistic way is achieved by means of vulnerability functions, *i.e.*, the *IM versus* the expected value of the DVs, and their respective confidence intervals. This way of expressing risk is similar to that proposed by Porter (2000), however, he uses two-dimensional structural models with elastic behavior.

Chapter 5

Assessment of the maximum response of the performance group components

The scheme proposed by PEER does not specify the type of structural analysis (linear or non-linear), nor the level of detail of the model geometry (*i.e.*, two-dimensional or three-dimensional). These aspects depend on the analyst's judgment, the level of precision with which the results are to be obtained and the importance of the building.

There are two fields of application of structural analysis. The first refers to earthquake engineering research, and the second to professional practice. In the field of earthquake engineering research, it is common to find works in which the structural response is approximated by two-dimensional models of representative building frames. On the contrary, in the area of practical engineering, nowadays, thanks to the capability of computers, it is common that engineers make more and more detailed models, *e.g.*, three-dimensional models.

However, currently the most powerful tools regarding seismic risk investigation are based on two-dimensional models (*e.g.*, Porter (2000), Goulet *et al.* (2007), Mitrani-Reiser (2007)). Regarding practice engineering, the seismic performance evaluation standard developed by FEMA P-58-1 (2012a) proposes a simplified scheme in which it is possible to take into account the three-dimensional behavior of the structural system. It should be noted that the FEMA P-58-1 (2012a) proposal could be considered as a derivation of the approaches proposed by Porter (2000) and Mitrani-Reiser (2007).

In the Assembly-Based Vulnerability of Buildings (ABV) methodology developed by Porter (2000), the three-dimensional response of the structural system is modeled in a simplified way through planar frames and its dynamic response is assumed to be linear elastic, even for intense seismic demands. In addition, each floor of the building is considered a unit of analysis and the PGs are grouped into each of these units. In this regard, an appropriate EDP is used to infer the damage that each performance group may experience. For

example, the physical response of columns with similar physical properties located on a particular floor or axis (*i.e.*, a particular unit) are monitored with a specific EDP, for example, the interstory drift. The maximum response captured during the time-history analysis is used to infer the potential damage that all elements belonging to a performance group and unit may develop. In other words, in order to simplify the structural and damage analysis, it is assumed that all elements of the same performance group belonging to the same unit experience the same EDP, and therefore it is assumed that all these elements develop the same level of DS. In the end, the numerical value of the DV that produces the DS experienced by a PG located in a unit is multiplied by the number of elements n_e belonging to the performance group and unit in study. This process is repeated the number of seismic realizations that conform a particular seismic intensity.

The methodology proposed by Mitrani-Reiser (2007) is similar to the one developed by Porter (2000). The main difference is that the former considers the non-linear behavior of the structural elements within the step-by-step dynamic analysis. From the inference of damage in each of the PGs, especially those corresponding to structural elements, the probability of the structure being tagged as safe, unsafe or restricted use is evaluated. In other words, the numerical simulation of the post-seismic inspection recommended by the ATC-20 (1989) is carried out to determine the structural safety of a building that has experienced a potentially destructive earthquake. This simulation process was named by Mitrani-Reiser (2007) as *virtual inspection*.

The approach proposed by FEMA P-58-1 (2012a) can be considered an extension of the methodologies developed by Porter (2000) and Mitrani-Reiser (2007). This methodology is implemented in the *Performance Assessment Calculation Tool* (PACT) computer program (FEMA, 2012a) so that it can be used in earthquake engineering practice. This approach takes into account the three-dimensional behavior of the structural system in a simplified form. The analyst performs the structural analyses according to the criteria considered appropriate. The absolute maximum structural response of each performance group, associated with each seismic realization s corresponding to a given IM, is stored in each row of the matrix $\mathbf{EDP} \mid IM$,

$$\mathbf{EDP} \mid IM = \begin{matrix} s_1 \rightarrow \\ s_2 \rightarrow \\ \vdots \\ s_k \rightarrow \end{matrix} \begin{bmatrix} \{(edp_1, edp_2, ..., edp_{n1})_{PG_1} ... (edp_1, edp_2, ..., edp_{nm})_{PG_m}\} \\ \{(edp_1, edp_2, ..., edp_{n1})_{PG_1} ... (edp_1, edp_2, ..., edp_{nm})_{PG_m}\} \\ \vdots \\ \{(edp_1, edp_2, ..., edp_{n1})_{PG_1} ... (edp_1, edp_2, ..., edp_{nm})_{PG_m}\} \end{bmatrix} \tag{5.1}$$

In this matrix, for example, the engineering demand parameter $(edp_2)_{PG_1}$, corresponds to the maximum structural response of the second unit (*i.e.*, the subscript of *edp* indicates the unit of analysis, which in this case corresponds to the second story) associated to the performance group PG_1, obtained in each structural analysis given a IM.

The maximum response edp_{max} associated with each performance group can be obtained in two ways. The first consists of performing the three-dimensional step-by-step analysis (linear or non-linear), and calculating the maximum response using the square root of the

sum of squares rule (SRSS) of each orthogonal horizontal component of the control point (*i.e.*, a node of the structural model) representative of each performance group associated with each unit,

$$edp_{max} = \max\left(\sqrt{edp_x(t)^2 + edp_y(t)^2}\right) \tag{5.2}$$

where the subscripts x and y refer to the two perpendicular horizontal directions of analysis. The second possibility is to perform two-dimensional structural analysis of the individual frames of the structural system in question. The maximum structural response is calculated, in the same way, with the SRSS rule criteria. That is, the criteria for estimating the maximum response is the same for both levels of structural analysis. The difference is that the maximum response obtained from a three-dimensional model will be correlated. If, on the other hand, the maximum response is obtained from the response of bidimensional structural models, the response will not be correlated. However, the main shortcoming with this second approach is that the dynamic response between the two criteria can vary significantly due to the simplification of the three-dimensional behavior to a two-dimensional one. Moreover, the structural response in the two-dimensional model does not capture the torsional behavior of the floors of the structural system, and therefore, the damage estimation in the elements (structural, non-structural and furniture) susceptible to torsional behavior is underestimated.

On the other hand, due to the high computational cost demanded by NLDA and the scarcity of real seismic records associated with medium to high intensity seismic demands, the methodology proposed by the FEMA P-58-1 (2012a) adopted the artificial structural response simulation technique developed by Yang *et al.* (2009). This approach assumes that the set of maximum responses comes from a joint lognormal distribution. The Monte Carlo method is used to generate the additional structural responses. In order to perform reliable statistical analysis of the losses, it is necessary to simulate a large number of synthetic responses, say in the order of hundreds or thousands, as shown in the Appendix A.

To generate the artificial structural responses consider the matrix arrangement of maximum responses associated with a seismic intensity, **EDP**, as described in Eq. 5.1. Because each seismic realization conditioned on a IM can be considered statistically independent of each other, the rows of this matrix represent independent and identically distributed observations. However, the values of each vector (*i.e.*, each row) $\mathbf{edp} = \{(edp_1, edp_2, ..., edp_{n1})_{PG_1} ....(edp_1, edp_2, ..., edp_{nm})_{PG_m}\}$, associated with a particular seismic record s, are, in general, correlated observations. Yang *et al.* (2009) assumes that the set of observations **EDP** are generated by a joint lognormal probability distribution. Therefore, it is possible to transform such observations to a lognormal scale,

$$\mathbf{Y} = \ln(\mathbf{EDP}) \tag{5.3}$$

Analogously to the maximum likelihood method, to infer the parameters of the joint

lognormal distribution of these independent and identically distributed observations, is calculated the mean $\mathbf{M_Y} = \mu_\mathbf{Y}$ and the standard deviation $\mathbf{D_Y} = \sigma_\mathbf{Y}$ from each $\mathbf{edp}_i$, *i.e.*, of the columns of the matrix **EDP**, and the correlation matrix, $\mathbf{R_{YY}} = \text{corr}_\mathbf{Y}$ is calculated. To generate an artificial structural response $\mathbf{z}$ in logarithmic scale with mean $\mathbf{M_Y}$ and covariance $\mathbf{S_Y} = \mathbf{D_Y R_{YY} D_Y}$, the following expression is used,

$$\mathbf{z} = \mathbf{D_Y} \cdot \mathbf{L_Y} \cdot \mathbf{U} + \mathbf{M_Y} \tag{5.4}$$

where $\mathbf{D_Y}$ is a diagonal matrix containing the standard deviation of the original structural response of each $\mathbf{edp}_i$; the matrix $\mathbf{L_Y}$ corresponds to the lower triangular decomposition of the correlation matrix $\mathbf{R_{YY}}$; $\mathbf{U}$ is a vector of random variables with mean 0 and standard deviation 1; and $\mathbf{M_y}$ is the vector containing the mean of the log-scale structural response. Because the additional vector of synthetic responses was generated on the lognormal scale, it is necessary to transform the response to normal scale, that is,

$$\mathbf{edp}^* = e^{\mathbf{z}} \tag{5.5}$$

To generate a large number of artificial responses, Eqs. 5.4 and 5.5 are evaluated a sufficient number of times such that the probability distribution of the artificial response satisfies the central limit theorem and the law of large numbers (*e.g.*, 10,000 times). The new matrix of additional structural responses can be written as follows,

$$\mathbf{EDP}^* = \begin{matrix} s_1^* \rightarrow \\ s_2^* \rightarrow \\ \vdots \\ s_l^* \rightarrow \end{matrix} \begin{bmatrix} \left\{(edp_1, edp_2, ..., edp_{n1})^*_{PG_1} ... (edp_1, edp_2, ..., edp_{nm})^*_{PG_m}\right\} \\ \left\{(edp_1, edp_2, ..., edp_{n1})^*_{PG_1} ... (edp_1, edp_2, ..., edp_{nm})^*_{PG_m}\right\} \\ \vdots \\ \left\{(edp_1, edp_2, ..., edp_{n1})^*_{PG_1} ... (edp_1, edp_2, ..., edp_{nm})^*_{PG_m}\right\} \end{bmatrix} \tag{5.6}$$

The symbol "*" is used to indicate that this is a randomly generated structural response and to differentiate it from the original sample. The subscript l indicates the number of additional synthetic responses. With the new set of maximum structural responses, the damage analysis and loss estimation for each IM is considered, as indicated in the following expression,

$$\mathbf{EDP}^* \rightarrow \mathbf{DM}^* \rightarrow \mathbf{DV}^* \tag{5.7}$$

This scheme is very attractive because it allows to generate any number of additional maximal responses at a relatively negligible computational cost compared to the computational demand required to perform the same number of linear or NLDA. However, the main problem with this technique is due to the assumption that the original sample of maximal responses is generated by a joint lognormal probability distribution. The only way to verify such an assumption is when the original sample size is sufficiently large such that the law of large numbers and the central limit theorem are satisfied. These theorems are presented in detail in the sections A.1 and A.2 of the Appendix A, respectively.

Again, due to the high computational cost of performing a large amount of NLDA, the bootstrap technique will be used to perform the statistical inference of the DVs, *i.e.*, the fourth stage of the PBEE-PEER framework. Its main quality is that it does not need the prescription of a probability distribution function F, as the methodology proposed by Yang *et al.* (2009), on the contrary, it works with the initial sample of data and therefore with the empirical probability distribution $\hat{F}$ of the underlying phenomenon. In this respect, the empirical probability distribution function has the quality of being transparent (Efron and Tibshirani, 1993).

On the other hand, in order for the methodology presented in this document to have a practical application, that is, that it can be applied to evaluate the inherent resilience of a structural design of a new or existing system, the methodology proposed in this thesis will be formulated based on the non-linear structural response of three-dimensional models. The maximum response of each element, *i.e.*, structural, non-structural and furniture components is approximated individually. For this purpose, the Eq. 5.2 is applied to each control point associated with each element. The matrix arrangement of the maximum responses **EDP** obtained with this criteria is similar to Eq. 5.1. The main difference is that in this case each element of the maximum responses matrix is associated with a specific element of each PG.

Chapter 6

Damage analysis

The loss of functionality $LQ(t)$ of a building that has experienced damage from a potentially destructive earthquake is mainly influenced by the damage experienced by the non-structural and contents components. Non-structural components can experience damage even at lower seismic intensities than the structural system was designed for, mainly because of their low capacity to deformation (Shoaf *et al.*, 2005; Almufti and Willford, 2014; Filitrault and Sullivan, 2014). Examples of vulnerable non-structural elements are partition masonry walls, steel door frames, windows, to name a few. Furniture type elements, or contents, *e.g.*, computers, are mainly affected by the translational and rotational accelerations of the slabs that compose the building (Taghavi and Miranda, 2004; Jaimes and Reinoso, 2013). This chapter describes the criteria to infer the damage experienced by structural, non-structural and furniture elements. Damage to the first two types of elements is inferred using a probabilistic criteria, while damage to furniture-type elements, *e.g.*, bookcases or shelves, is estimated deterministically.

6.1 Inference of the damage in structural and non-structural elements using fragility functions

The PBEE-PEER methodology does not establish a general criterion for determining whether damage is inferred by element or by group of elements. However, several researchers, for example, Mitrani-Reiser (2007), Goulet *et al.* (2007), Yang *et al.* (2009) and the guidelines proposed by FEMA P-58-1 (2012a), evaluate the damage by grouping a set of elements of the same PG assuming that they can experience the same level of physical response $EDP \mid IM$ and therefore the same level of damage $DS \mid IM$. To exemplify this, consider that on a given floor of a building, a set of buckling restrained braces are installed on the same axis. With this approach it is accepted that all these elements develop the same level of lateral displacement, and at any given time the same level of damage.

This criterion may be appropriate if the models used in the structural analysis are two-dimensional and also if it is demonstrated that the uncertainties associated with the me-

chanical properties of the elements in question and mass distribution are small enough to disregard their variability. However, the torsional effects in plant can cause differences in the EDPs associated with the elements in question and therefore the level of damage could be different. Moreover, as mentioned by Günay and Mosalam (2013), the damage level of an element shows variance, even for the same values of EDP due to the differences in the pattern and history of the structural response associated with the record-to-record variability. Therefore, the DS level for each element will be different due the maximum values of the set of EDPs conditioned to an IM also will be different.

In the methodology to evaluate the seismic resilience of buildings proposed in this thesis, three-dimensional structural models are used and both EDPs and DSs are evaluated individually, *i.e.*, element by element, so that each of them has its own probability distribution response $p(EDP|IM)$ and measure of damage $p(DS|EDP)$, and therefore, an individual DV for each element. The details of this point are explained in the next chapter.

In order to numerically assess the structural safety of a building that has been affected by an earthquake, it is necessary to evaluate the damage experienced by the different types of elements that integrate a building. In general, the components that can experience damage in an installation are referred to as performance groups, PGs. For example, a PG can be a group of buckling restrained braces with the same dimensions and mechanical properties that conform one floor axis. This process is carried out in steps two and three of the PBEE-PEER methodology, relating the structural response to a measure of damage representative of the PG that make up the building.

In order to take into account the uncertainty in the structural response and the main physical characteristics of the PG, *e.g*, variability of dimensions, mechanical properties, etc., several research groups, *e.g.*, Porter (2000) and Beck *et al.* (2002), have developed analytical and experimental procedures, through which they have obtained fragility functions representative of the damage pathology that the damageable components may experience. In general, the different PGs can be damaged in different ways, denominated, *discrete damage states, DS*. For example, a reinforced concrete column may experience a slight cracking when is affected by a moderate intensity demand, while when it is affected by a intense demand it may experience shear or axial failure. Due to the variability of the damage pathology the fragility functions are developed to capture various types of discrete damage states at a specific level of demand, EDP, *i.e.*, *sequential*, *simultaneous* and *mutually exclusive and collectively exhaustive* (MECE) damage states. For the first one, the damage pattern of the elements must be developed sequentially, experiencing damage state 1 first, then 2, and so on. For the second one, the elements can be in more than one damage state at the same time, and the order does not matter. For the last one, an element damaged can be in one and only one damage state, and the order does not matter.

The probability of reaching or exceeding a DS, conditioned to a EDP, is given by the following equations (Günay and Mosalam, 2013; Porter, 2019):

Sequential damage states:

$$Pr(DS|EDP) = \begin{cases} 1 - Pr(DS \geq 1|EDP) & ds = 0 \\ Pr(DS \geq ds|EDP) - Pr(DS \geq ds+1|EDP) & 1 < ds \leq N_{DS} \\ Pr(DS \geq ds|EDP) & ds = N_{DS} \end{cases} \tag{6.1}$$

Simultaneous damage states:

$$Pr(DS|EDP) = \begin{cases} 1 - Pr(DS \geq 1|EDP) & ds = 0 \\ Pr(DS \geq 1|EDP) \cdot Pr(DS = ds|DS \geq 1) & 1 < ds \leq N_{DS} \end{cases} \tag{6.2}$$

MECE damage states:

$$Pr(DS|EDP) = \begin{cases} 1 - Pr(DS \geq 1|EDP) & ds = 0 \\ Pr(DS \geq 1|EDP) \cdot Pr(DS = ds|DS \geq 1) & ds \in \{1, 2, ..., N_{DS}\} \end{cases} \tag{6.3}$$

These equations can be easily deduced from basic concepts of probability and set theory, or directly from the graphical representation of the fragility function of each discrete damage state that characterizes a specific performance group.

Using the total probability theorem, the probability that a component will reach or exceed a particular discrete damage state given that the building does not collapse, NC, at a specific seismic IM, is given by the following equation:

$$Pr(DS|NC, IM) = \int Pr(DS|EDP)p(EDP|NC, IM)dEDP \tag{6.4}$$

where $p(EDP|NC, IM)$ is the probability density function of the EDP, conditioned on the building not collapsing on a pre-established IM. The term $Pr(DS|EDP)$ is obtained from Eqs. 6.1 to 6.3, depending of the performance group used and its own pathology of damage.

In the methodology used in this study, the damage to a particular building is assessed element by element for each PG. In the methodology proposed by the FEMA P-58-1 (2012a), the damage is assessed for a group of elements of the same class with the same EDP, and therefore, all of those elements experiment the same damage state. This criterion offers conservative results, however, for the purpose of the evaluation of the functionality loss it is more convenient to evaluate the damage element by element, as will be shown in the next chapter. Likewise, with this criterion it is possible to determine, at least in terms of probability, the most vulnerable floor areas of the building.

To estimate the specific damage state experienced by an element e, the $edp_{i,j} \mid IM$ that characterizes its physical response and the inverse transform method $F^{-1}(u)$ are used. First, with the $edp_{i,j} \mid IM$ is calculated the range of probabilities of each $ds_i, i \in$

$1, 2, ..., N_{DS}$ that the e may experience. Subsequently, a random number with uniform distribution, $u(0, 1)$, is generated. The damage state of the element is determined from the range in which the random variable u lies. The probability of the DS corresponds to the range of probabilities $Pr(DS \mid EDP)$, *i.e.*, to the one obtained by one of Eqs. 6.1 to 6.3, depending on the type of damage that the PG may experience. This procedure is used to estimate the DS developed by each e of each PG.

6.2 Inference of the damage in furniture using the theory of rigid body dynamics

While most of the potentially destructive earthquakes affect buildings completely, there have been events that have caused damage mainly to non-structural elements and contents in large quantities. For example, the 27 February 2010 earthquake that affected the Bío-Bío Region in Chile caused a great deal of non-structural and contents damage in practically all types of buildings in the region, while some of the commercial, industrial, residential and office buildings suffered little structural damage (Miranda *et al.*, 2012). This earthquake showed that most modern seismic design codes are focused on preventing structural collapse in large earthquakes, and not on preventing damage to architectural elements, contents and furniture, which in addition to causing high economic losses, physical damage to occupants and disruption of quality of life, are the main cause of partial or total loss of functionality. These facts are of principal importance in essential buildings such as hospitals, transporting systems, drinking water and electricity distribution systems, just to mention a few, because they should remain in operation after a major earthquake since the loss of their functionality can have a significant impact on society and on the indirect economic losses caused by business interruption.

The methodology to evaluate the seismic performance in an integral way proposed by FEMA P-58-1 (2012a) adopted the procedure proposed in ASCE (2005) to estimate the dynamic behavior of the furniture assuming that it can be represented by the dynamic response experienced by a rigid block subjected to a history of accelerations at its base. The response of the block to horizontal excitation at its base can be classified in four types: rest, slide, rocking and overturning. The methodology proposed in FEMA P-58-1 (2012a) to determine if the rigid block experiences any of these four discrete damage states is using fragility functions, similarly to those used to evaluate damage in the PGs described in the previous section. Nonetheless, a comparative study between the prediction offered by the fragility functions proposed in ASCE (2005) and FEMA P-58-1 (2012a) with respect to a series of NLDA was presented in Dar *et al.* (2016). This research group concluded that the former offer unreliable, and in many cases non-conservative results. Due to this inconsistency in this thesis the theory of rigid block dynamics is used to estimate the performance of typical office furniture, *e.g.*, bookcases and shelves. The study of the dynamics of rigid bodies dates back to the pioneering work done by Housner (1963). The equation that describes the behavior of rectangular rigid bodies subject to a history of

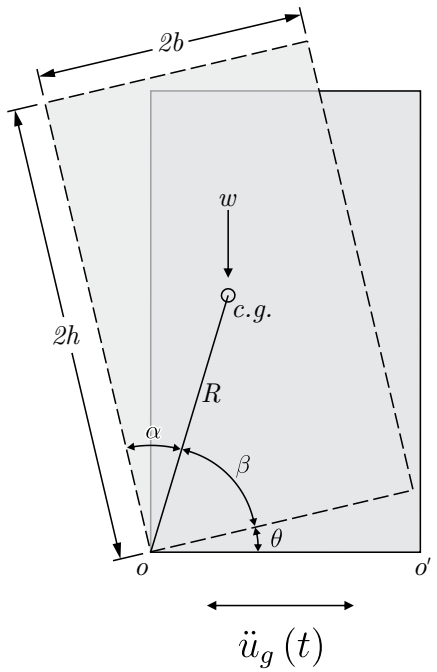

Figure 6.1: Schematic representation of a rigid block subjected to a history of accelerations at its base.

accelerations at their base is given by Eq. 6.5, which corresponds to a second order non-linear differential equation. In the derivation of this equation it is assumed that the coefficient of static friction between the block and the base, developed during the movement, is large enough in such way that the block does not slip and only experiences rocking and eventually overturning.

$$\ddot{\theta}(t) = p^2 \left\{ \sin[\alpha \cdot \mathrm{S}(\theta(t)) - \theta(t)] - \frac{\ddot{u}_b}{g} \cos[\alpha \cdot \mathrm{S}(\theta(t)) - \theta(t)] \right\} \tag{6.5}$$

In this equation $\ddot{\theta}(t)$ and $\theta(t)$ measure the angular acceleration and angular displacement, respectively, of the block base respect to the rotation point o (or o'); the term $p = \sqrt{3g/4R}$ corresponds to the oscillation frequency of the block base; the term R is the distance between the rotation point o (or o') and the gravity center $c.g.$ of the block; g is the gravity acceleration. $\mathrm{S}(\cdot)$ is the sign function and takes into account the direction of the rotation point during the movement, and $\ddot{u}_b$ corresponds to the acceleration imposed at the base. The coefficient of restitution proposed by Housner (1963), $r = 1 - \frac{3}{2}\sin^2\alpha$, is used to take into account the energy loss due to the impact between the block and the base. This is achieved through the velocity $\dot{\theta}_2$, which is calculated after the impact multiplying the pre-impact velocity $\dot{\theta}_1$ by the coefficient of restitution r.

In this work Eq. 6.5 is solved numerically by means of a space state scheme, which relates the variables of the differential equation in a system of equations such as that indicated in Eqs. 6.6 and 6.7. Under this scheme the 4th order Runge-Kutta method is used in

this work to solve the differential system equations, Eqs. 6.7. This technique for solving the equation of motion has been used by a large number of researchers, *e.g.*, Makris and Roussos (1998) and Dar *et al.* (2016), among other, and acceptable results have been reported.

$$\{y(t)\} = \begin{Bmatrix} \theta(t) \\ \dot{\theta}(t) \end{Bmatrix} \tag{6.6}$$

$$f(t) = \dot{y}(t) = \begin{Bmatrix} \dot{\theta}(t) \\ -p^2 \left[\sin\left(\alpha \cdot \mathrm{S}\left(\theta(t)\right) - \theta(t)\right) + \frac{\ddot{u}_b}{g} \cos\left(\alpha \cdot \mathrm{S}\left(\theta(t)\right) - \theta(t)\right) - \theta(t) \right] \end{Bmatrix} \tag{6.7}$$

Within the methodology presented in this work, it is possible to calculate the response of an indeterminate number of rigid blocks, *e.g.*, bookcases or shelves, located at any point on a given floor of the building under study, as indicated in the spatial distribution of the blocks representing the furniture in the example of the proposed methodology for assessing the seismic resilience of buildings, Chapter 11.

To determine the history of accelerations at the base of each block, a bilinear interpolation of the accelerations captured at the corners of the slab-forming panels was performed. To determine if the block under study experienced overturning, the maximum angular displacement of the rotation point the block was used as a EDP, with the limit displacement being $\theta_{max}(t) = 1.40$ rad ($\approx 80°$). For values of $\theta(t) > \theta_{max}(t)$ the numerical solution of Eqs. 6.7 diverges, being a clear indication that the block has been overturning. Also, since Eq. 6.5 does not represent the three-dimensional dynamic behavior of a rigid block, the differential equation was solved two times, one for each horizontal orthogonal direction of the building model, and finally the most unfavorable behavior of both analyses is used.

In mid-rise buildings, floor accelerations increase linearly from the first floor to the roof. Therefore, it is in the top floors where the highest intensity of floor accelerations is concentrated, and it is precisely in these floors where the content/furniture-type elements are more vulnerable to the effect of floor accelerations. This type of damage has been observed in recent seismic events, e.g., Chile 2010 and Mexico 2017 seismic events, to mention a few. In the application example (chapter 11), the proposed strategy adequately captured this phenomenon, so in general terms it can be concluded that this is adequate to simulate its dynamic behavior, and eventually the damage characterized by overturning .

The inference of damage state element by element, mainly of structural and non-structural components, can help to identify vulnerable areas and therefore susceptible to generate loss of functionality, and even the total or partial collapse of a building. At the same time, identifying the most vulnerable elements can be useful to propose structural retrofits to mitigate as much as possible the damage and therefore the loss of functionality.

Chapter 7

Assessment of the structural safety of a building using the inspection criteria proposed by ATC-20

After a potentially damaging earthquake has affected a community, there is the need to inspect buildings and facilities to assess the potential damage to determine if they are safe and can be occupied to continue in operation or, if not, they need to be repaired (Gutiérrez *et al.*, 2020). To restore the functionality of the damaged buildings, and consequently, the functionality of a city or community, the post-seismic inspection of all potential damaged buildings must done in the shortest possible time. Therefore, to reduce and optimize the inspection time, there must be a large number of specialized personnel to make the post-seismic evaluations. However, our experience from past destructive seismic events is that it is unlikely that the affected society will have a large number of qualified personnel to make this task due to the large number of buildings affected and their dispersed location within a city (Gallagher, 1989).

Due to this problem, the ATC-20 (1989) developed a methodology for inspecting conventional buildings (commercial, residential and office type), with the objective of optimizing the inspection time and issuing a report that defines the activities to mitigate the damage and to recover the functionality of the affected buildings. The methodology developed by ATC-20 (1989) is designed to be used by construction officials and structural engineers, and is divided into three levels of inspection: *rapid evaluation* (RE), *detailed evaluation* (DE), and *engineering evaluation* (EE). The first two assessments are visual inspections, while the third requires an engineering calculation process to determine the residual load capacity of the building of interest. The objective of the evaluation is to represent post-seismic structural safety using one of three types of tagging: *inspected, restrained entry*, or *unsafe*. These tags are identified by the *green* (G), *yellow* (Y), or *red* (R) colors, respectively. A fourth category involves the non-structural components inspection. Although they do not affect the stability of the structure due to the damage, they could fall inside and/or outside the building and cause injury to people. Examples of this type of elements

are ceilings, fire suppression systems, exterior windows, unreinforced masonry walls, contents and furniture. The tag assigned to these type of elements damaged is *area unsafe*, and a red tag color R_a is assigned to the building. The details of each type of evaluation are described below.

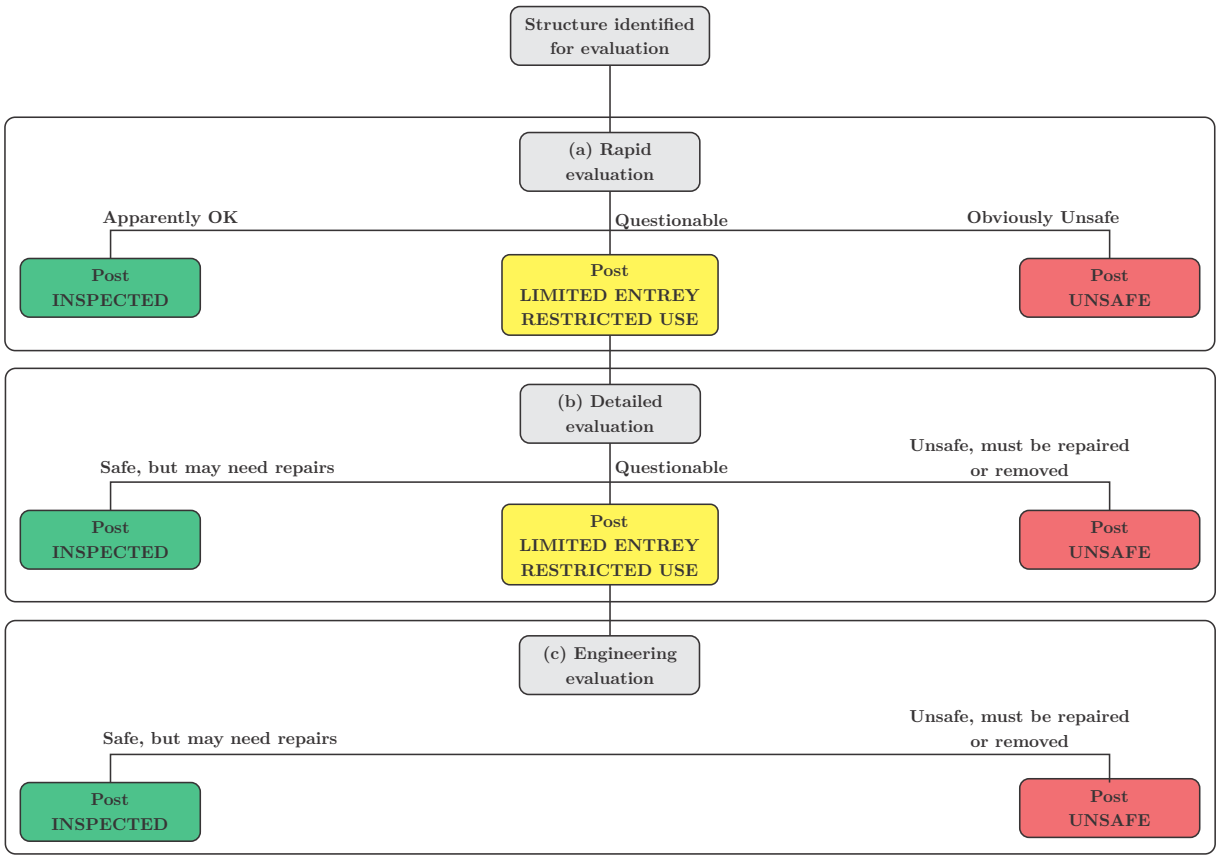

Figure 7.1: Flowchart of structural safety assessment proposed by ATC-20 (1989), reproduced from Gallagher (1989).

7.1 Rapid evaluation

The *RE* is performed at the exterior of the building with the objective of determining the amount and severity of structural damage by visual inspection, as illustrated in Fig. 7.1a. If severe structural damage is clearly present, then the building is posted as structurally unsafe and tagged with R color. If only severe non-structural damage is present, the posts assigned are structurally safe (G) and an area unsafe (R_a). This process may be completed from 10 to 20 minutes. If the severity of the structural and non-structural damage to the exterior building is not clear, and the inspector thinks that in the interior could exist any kind of damage, the building is posted as restrained entry (Y tag) and a *DE* of the interior of the building is required. If there is slight or no damage on the structural and

non-structural elements then the building receives a post inspected, *i.e.*, the building is safe (G tag).

7.2 Detailed evaluation

This type of evaluation aims to determine the safety of the building in situations where damage on the outside of the building may cause doubt of the structural safety. At least two structural engineers must make the DE of both exterior and interior of the structure. The main objective of this type inspection is to ensure that the structural elements, as well as the non-structural ones that are susceptible to falling, are safe enough for the building to be re-occupied, *i.e.*, inspected (G tag). If, on the other hand, moderate or severe damage to structural and/or non-structural elements occurs inside, then the building receives a restrained entry (Y tag) or unsafe post (R tag), as shown in Fig. 7.1b. This type of evaluation may be completed from 1 to 4 hours.

7.3 Engineering evaluation

Engineering evaluation is performed when the first two visual inspections are not sufficient to determine the structural safety of the building. This evaluation must be performed by a team of structural engineers. The result of this type of inspection is detailed maps of the structural and non-structural damage, which serve as support for performing structural analyses and numerically inferring the amount and severity of the damage. The possible outcomes of this evaluation are the post unsafe (R tag) or inspected (G tag), as shown in Fig. 7.1c. This type of assessment may be finished from 1 to 7 days, or even more, depending on the severity and quantity of the damage.

7.4 Numerical simulation of building safety using the ATC-20 inspection criteria

In 2007, Mitrani-Reiser (2007) developed a probabilistic methodology to estimate the post-seismic structural safety, *i.e.*, R, Y or G tags, based on the ATC-20 (1989) inspection criteria. This methodology, called *Virtual Inspector*, reproduces numerically the RE and DE process. For the first one, in case of obtaining a Y tag, *i.e.*, a restricted entry tag, the process of a DE is then simulated. Finally, the probabilities of each type of inspection are combined to obtain the probability that the building will be tagged as safe or unsafe given an IM. This methodology was adopted later by the FEMA P-58-1 (2012a) evaluation guide.

In this study, a methodology similar to the proposed by Mitrani-Reiser (2007) is introduced to assess the probability of a building being posted as unsafe, restricted entry or safe,

from structural, non-structural and furniture numerical inspect simulation, and with these results, six discrete states of functionality are inferred. The original methodology proposed by Mitrani-Reiser (2007) is modified in two aspects. The main difference is that in this work only the DE is simulated numerically, instead of doing the RE and DE virtual inspection because, as mentioned previously, the RE is performed due to the lack of a large quantity of personnel specialized to inspect many buildings potentially damaged in a short time. From the computational simulation viewpoint, it is not necessary to perform the two first numerical inspections since it is relatively simple to do using computer simulation. The second modification is that in the method proposed in this document, non-structural (NS) and furniture (F) components are explicitly evaluated in a similar way as it is done for structural elements. Although the presence of $NS-F$ damage combined with null structural damage is not a reason for post the building as structurally unsafe (R tag), it is a cause to consider a potential risk due to the possibility of the $NS-F$ falling (R_a tag), and naturally, induce injury to people and loss of functionality during the time interval in which their repair/replacement is carried out. The probability that the building is categorized in either R, Y or G tags is calculated with the following proposed equations:

$$\begin{aligned} Pr\left(TAG = R_T \mid PG_T, IM\right) &= Pr\left(S_D \mid IM, NC\right) \cdot Pr\left(NC \mid IM\right) + Pr\left(C \mid IM\right) \\ Pr\left(TAG = Y_T \mid PG_T, IM\right) &= Pr\left(M_D \mid IM, NC\right) \cdot Pr\left(NC \mid IM\right) \\ Pr\left(TAG = G_T \mid PG_T, IM\right) &= Pr\left(N_D, L_D \mid IM, NC\right) \cdot Pr\left(NC \mid IM\right) \end{aligned} \tag{7.1}$$

where the subscript T refers to the type of PG, *i.e.*, structural (S), non-structural (NS) or furniture (F) elements given an IM, product of a DE simulation, DE. The terms $Pr(S_D \mid IM, NC)$, $Pr(M_D \mid IM, NC)$ and $Pr(N_D, L_D \mid IM, NC)$, are the probability of experiencing severe (S_D), moderate (M_D), null or light (N_D, L_D) damage given that the building does not collapse (NC), and are calculated in the third step of the PBEE-PEER methodology. The term $Pr(C \mid IM)$ indicates the probability of collapse and $Pr(NC \mid IM) = 1 - Pr(C \mid IM)$ the probability of survival. Note that only the severe (overturning) and null (rest) damage states are considered in the evaluation corresponding to furniture, so for this case only the R and G tags are used, corresponding to the first and third of Eqs. 7.1.

The tagged probability of the post-seismic inspection obtained with the Virtual Inspector tool developed by Mitrani-Reiser (2007) only takes into account the damage experienced by the structural elements. This means that the tagged probability represents the lower limit of such probabilities because it does not consider the influence of damage experienced by non-structural and furniture-type elements (Gutiérrez *et al.*, 2020). The methodology proposed in this thesis explicitly takes into account the influence exerted by the latter components, so the probabilities associated with the virtual inspection correspond to an upper limit. In Chapter 11, where the application example is presented, it is shown that the probability of tagging associated with the unusable area (R_a tag), associated with

the inspection of non-structural elements and furnishings, is higher than the probability of tagging the building as unsafe (R tag) for the same IM. This suggests that the loss of functionality is governed by non-structural damage when the system is evaluated from a holistic point of view. Moreover, according to Shoaf *et al.* (2005), and Spence *et al.* (2011), among others, the damage experienced by non-structural elements is the main cause of light, moderate and severe injuries to occupants, and as will be discussed in Chapter 9, their respective equivalent economic value can represent a high percentage of total economic losses (Porter *et al.*, 2006).

The tagging that governs (G, Y, R color) the post-seismic inspection of the building in question is based on the prescription of hierarchy levels among the classes of PGs, the most important being that of the structural elements, followed by the non-structural elements and ending with the contents. Likewise, in each of these classes of PGs, a hierarchy is prescribed for the level of damage that can develop. This second hierarchy starts with severe damage, followed by moderate damage and ending with light damage. For example, if all three levels of damage are present in at least one element of the three PGs classes, the governing tag is red R, associated with structural damage.

7.5 Functionality limit states formulation

The notion of functionality limit state, LS, was introduced by Burton *et al.* (2016). These LSs explicitly relate a global damage configuration caused by an earthquake to a series of generic activities that must be performed to recover its functionality $RQ(t)$. In this work the idea proposed by Burton *et al.* (2016) is used, and, in order to achieve this, the configuration of each LS is derived from tagging of the post-seismic evaluation of structural safety, and from the evaluation of the unsafe areas, corresponding to the non-structural and furniture damage, as described in the previous section. Due to the great variability in the inference of the DSs that characterize the different PGs that integrate a building, the LSs allow to visualize generic configurations of the damage of structural, non-structural and furniture damage combination patterns for different seismic intensities. Likewise, since there are few real events that can be used as a basis for generating a robust and reliable recovery model, the only thing left to do is to propose generic recovery events $RQ(t)$ formulated using deduction by analogy, *i.e.*, from the perspective of heuristic reasoning (Polya, 1954).

The configuration of each LS and $RQ(t)$ is described below:

- LS_0*: Fully functional, safe building,* $TAG = G_S$. This state corresponds to an undamaged state, either structural (G_S), non-structural (G_{NS}) and furniture (G_F), so the building remains operational after the seismic event. However, it is possible that the owner may request an inspection to verify that there is no minor damage. In this case, the building could continue to provide service, if the owner decides, while the inspectors conduct the rapid assessment. Since no damage of any kind occurs, the integrity of the life of the occupants of the building is not compromised.

- LS_1: *Partially functional and structurally safe*, $TAG = G_S$. This state is composed by a combination of null structural damage (G_S) and light non-structural damage (G_{NS}), and/or by a severe furniture damage (R_F). Therefore, although the building is safe, a tag indicative that it is partially non-functional is assigned because some usable spaces cannot be occupiable by the users. This state could occur in buildings whose contents and furniture may experience accelerations of great magnitude causing them to fall. The generic recovery process for this limit state, $RQ_1(t)$, consist of the following events: (1) an inspection of the building due to the visual impact of the damage to the contents and furnishings, an after the completion of the inspection, the owner/stakeholders could apply for (2) an insurance to pay for the replacement of damaged elements, if the amount and severity require it. Likewise, in this limit state is possible that falling NS and F elements may cause injuries to the occupants.

- LS_2*: Restricted use, non-functional and structurally safe,* $TAG = G_S$. This limit state is characterized by the presence of non-structural moderate damage (Y_{NS}), null structural damage (G_S) and by any type of damage in the furniture (G_F, R_F). This limit state could occur in PGs with great capacity of deformation or by those composed by brittle materials, *e.g.*, interior partitions or interior/exterior windows. The process of recovery from this limit state, $RQ_2(t)$, is assumed to be composed of the following events: (1) post-seismic inspection, where it is determined that some areas of the building are not usable due to the presence of damage to NS and F elements; (2) an insurance to pay for the replacement/repair of damaged elements and (3) mobilization for repairs the PGs damaged. Similar to the damage that characterizes the LS_1, in this limit state, falling NS and F elements damaged can also cause injuries to the occupants.

- LS_3: *Restricted entry, non-functional and structurally safe* $TAG = Y_S$. This limit state occurs due to the presence of light structural damage (Y_S) and/or any type of discrete damage state in non-structural components (G_{NS}, Y_{NS}, R_{NS}) and furniture elements (G_F, R_F). The recovery path, $RQ_3(t)$, is assumed to be described of the following events: (1) Post-seismic inspection, where the building is declared restricted entry, that is, it receives a yellow tag; (2) obtaining the financing to pay for the repairs; (3) execution of the structural repairs. Once the structural repairs are completed the building is declared safety to be reoccupied, but with restrict use. The next step (4) is to repair/replace the NS and F elements. After this last process has been completed, the building has regained its ability to be functional. Finally, in this limit state, severe damage to NS and F elements can cause injury to users.

- LS_4: *Unsafe building, unoccupied, but repairable,* $TAG = R_S$. This condition is caused by the combination of severe S damage (R_S), and any state of non-structural damage (G_{NS}, Y_{NS}, R_{NS}) and/or furniture damage (G_F, R_F). The recovery process, $RQ_4(t)$, is assumed to be composed of the following events: (1) the post-seismic inspection is performed, in which it is determined that the building is unsafe, *i.e.*, it receives a red tag. Due to the quantity and sever of damage it is determined that the building can be repaired, *i.e.*, it did not experience significant residual drifts

and also the repair cost/time are acceptable to the stakeholders. After carrying out these activities, the building condition becomes restricted entry. During this state the building could be occupied by authorized personnel and the following events are performed: (2) obtain financial resources to pay for repairs, (3) repair process planning and (4) bidding process. Once the structural retrofit has been determined and the financing is obtained, (5) the structural repairs are carried out. After this step, the building is safe to be reoccupied, *i.e.*, with restricted use; however, in order to be fully functional, (6) the NS and F repairs and replacement must be done. Finally, in this limit state, severe damage to S and F elements and furniture can cause injuries to users.

- LS_5: *Unsafe, irreparable building,* $TAG = R_S$. This state corresponds to an unsafe building (R_S) as it experienced excessive residual deformations or local structural collapse, so it is determined that it must be demolished if the system is technically irreparable and/or the repair cost/time may be excessive. The recovery process, $RQ_5(t)$, is given by the demolition and reconstruction of the building. As in the previous case, in this limit state, severe damage to S, NS and F elements can cause injuries to users.

- LS_6: *Structural collapse,* $TAG = R_S$: This state corresponds to structural collapse, and its recovery process, $RQ_6(t)$, is given by the cleaning of debris and the reconstruction of the building. In this limit state it is considered, under a conservative judgment, that the number of fatalities is equal to the number of occupants who were in the building at the time of the seismic event.

Due to the complexity of the interaction of the events that define each LS, the basic concepts of probability and set theory are used to evaluate them. For example, the probability for the limit state LS_3 conditioned on an IM, is $Pr(LS_3 \mid IM) = Pr\{Y_S \cup [(G_{NS} \cap Y_{NS} \cap R_{NS}) \cup (G_F \cap R_F)] \mid IM\}$. The events between the brackets in this equation are obtained from the realizations that match with the events defined in the section 7.4, *i.e.*, in the structural, non-structural and furniture virtual inspection, according to the conditions pre-established in the ATC-20 (1989). The probability of the LS_3 is obtained recurring to the classic definition of probability, *i.e.*, the number of successful realizations divided by the total number of realizations, the latter being the total number of seismic recorders associated with a particular IM. In general, the probability for each functionality limit state $Pr(LS \mid IM)$ is calculated by the following expression:

$$Pr(LS \mid IM) = Pr(TAG_S \cup TAG_{NS} \cup TAG_F \mid IM) \tag{7.2}$$

These LSs are similar to those proposed by Burton *et al.* (2016). The main difference is that here they are deduced from the combination of the events associated with the ATC-20 (1989) virtual inspection corresponding to structural, non-structural and furniture elements and complemented under heuristic reasoning. This not only gives a logical character to the deduction of the limit states of functionality, but also allows to calculate

in a less ambiguous way the probability of each one of them. In other words, its numerical implementation is straightforward. Furthermore, given this consistency, it is possible to prescribe the events that integrate the recovery of the damaged system $RQ(t)$ for each of the LSs.

The assumption of the events that integrate the recovery of each of these limit states has been deduced from a heuristic reasoning. This means that the events contained in $RQ(t)$ can be refined and improved when more and better databases will become available of structural, non-structural and contents damage produced by potentially destructive seismic events in a wide range of buildings, and also of the activities involved in bringing the buildings back to their original operating level.

In general, the LSs can be interpreted as a series of combinations of discrete damage levels experienced by the various PGs that comprise a building. The tool presented in this thesis is intended to simulate such events in order to reduce and/or mitigate the negative social and economic consequences, whether for new or existing buildings, without having to actually experience them.

Chapter 8

Formulation of the model to quantify the loss and recovery of functionality of a building

8.1 Loss of functionality assessment in individual buildings: background

To estimate the loss of functionality of a building, one must first define the physical variables or processes that allow a building to be functional, as well as the use for which the design of the system itself was conceived. There are many different types of buildings, for example, bridges, hospitals, airports, hotels, etc. Although practically any type of building can experience loss of functionality due to damage caused by an earthquake, it is in the essential buildings where most of the research has been concentrated regarding the development of methods to quantify it. This is due to the fact that these types of buildings are indispensable to control and mitigate the damage caused not only by seismic events, but also by any potentially destructive event, *e.g.*, hurricanes, cyclones, floods, tsunamis, etc.

The type of essential building that has been most studied from the point of view of seismic resilience is the hospital. There are many definitions of loss of functionality in hospitals. However, because many of them are equivalent to each other, only the most relevant, but at the same time different from each other, are cited here. For example, Cimellaro *et al.* (2006) propose a global function of loss of functionality in terms of economic losses. This function considers structural and non-structural losses. The latter, in turn, considers (1) direct economic losses caused by damage to contents, (2) indirect economic losses (business interruption), (3) direct fatalities (caused by structural collapse) and (4) indirect fatalities (people requiring hospitalization). Each of these losses is expressed as the ratio of the number of damaged units to the total number of units, multiplied by its respective replacement cost. Total losses are obtained by adding each of the losses described above,

and multiplying by the probability of exceeding the seismic intensity that originated the destructive event.

Cimellaro *et al.* (2010a) define functionality in hospitals in terms of quality of service, waiting time and quality of life, measured as the percentage of the population in good health. In this regard, Yavari *et al.* (2010) and Jacques *et al.* (2014) define functionality in terms of the availability of services (*e.g.*, surgeries, intensive care, etc.) available in a hospital to attend people who are injured after an earthquake. Mitrani-Reiser *et al.* (2012) relate functionality to the amount of usable space in a hospital.

The FEMA P-58-1 (2012a) does not propose a quantitative measure of specific loss of functionality of conventional buildings. Like Mitrani-Reiser (2007), it uses the probability of structural safety tagging ATC-20 (1989). However, this approach takes into account many of the variables that make up seismic resilience: repair time, direct economic losses and probable number of fatalities. On the other hand, Burton *et al.* (2016) estimates the loss of functionality using the probability associated with each of the limit states of functionality proposed by them; however, they do not relate any physical measure as an indicator of loss of functionality. On the other hand, Burton *et al.* (2016) estimates the loss of functionality using the probability associated with each of the limit states of functionality proposed by them; however, they do not relate any physical measure as an indicator of loss of functionality.

It is easy to notice that for the same structural system the definition of loss of functionality varies from one author to another. This is because such definitions are formulated according to a specific problem. In a general context, Mieler and Mitrani-Reiser (2017) define the concept of functionality as the availability of a building for its intended use. Therefore, the loss of functionality occurs when its structural safety, serviceability and accessibility are compromised.

In this research work, the definition of functionality proposed by Mieler and Mitrani-Reiser (2017) will be used since it is closely related to the post-seismic inspection results of the ATC-20 (1989) criterion, and therefore to the LSs proposed above. As a measure of functionality it is proposed to use *the percentage of usable area*, PUA, of each floor of a building. Therefore, the loss of functionality is measured as *the percentage of non-usable area*, $PNUA$, produced by the damage experienced by the different PGs that integrate a building. Likewise, this dissertation studies the seismic resilience of buildings used for office purposes; however, the formulation to estimate the seismic resilience proposed here can be applied to a wider range of building types.

8.2 Quantification of loss of functionality: methodology proposed

In this thesis, the loss of functionality $LQ(t)$ is quantified using the minimum value of the set of mean values of the $PNUA$ of the group of floors n_f that conform a building.

To quantify the amount of non-usable area π in a specific floor induced by one seismic realization that does not cause demolition or collapse in a specific seismic intensity, *i.e.*, $LS \neq (LS_{5,6}) \mid IM$, considers that there is a set of elements $\mathbf{e}$, which can belong to any type of PG that have reached or exceeded a DS. To achieve the recovery of functionality of the floor f to its pre-earthquake functionality state, it is necessary that at least one crew, *i.e.*, a group of workers n_w, perform the repair works in a specific fraction of area of the floor f. Therefore, it can be established that the loss of functionality of a structural system $LQ(t)$, can be approximated as the ratio π between the total area a_{Rf} needed to perform the repairs in a given floor f by a least one crew, and the total area of the floor in study a_{Tf}. With this in mind the quantification of the area required to perform the repair activities at a specific floor f is given by the sum of the individual tributary area a_e of each component e damaged as the following equation indicates:

$$a_{Rf} = \sum_{i=1}^{ne} a_{e,i}(\mathbf{x}, PG) - \sum_{i=1}^{ne-1} \sum_{j=i+1}^{ne} a_{e,i}(\mathbf{x}, PG) \cap a_{e,j}(\mathbf{x}, PG) \tag{8.1}$$

where the first term quantify the sum of the individual tributary area $a_e(\mathbf{x}, PG)$ of all elements damaged n_e, of any performance group PG, located in a specific area on the floor f, and the second term quantify the overlap of the individual tributary areas $a_e(\mathbf{x}, PG)$. The term $\mathbf{x}$ refers to the spatial coordinates of each element e. The $PNUA$ of a specific floor f is obtained simply as the ratio of the non-usable area and the total usable area of a specific floor:

$$\pi = \frac{a_{Rf}}{a_{Tf}} \cdot 100\% \tag{8.2}$$

To illustrate this, Fig. 8.1 shows the plan view of a column, two beams and two masonry walls, which have experienced damage. The light gray color shows the tributary area pre-assigned to each element. This area is activated when the elements in question experience damage. Each of these areas is occupied by a different crew at the same or at a different time instant, depending on the type of performance group and its hierarchy, as will be explained later. The percentage of non-usable area for this hypothetical case is obtained by calculating the tributary area marked in light gray between the total area of the floor where these elements are located.

The physical metric π for measuring loss of functionality can be used to quantify not only the $PNUA$, but at the same time can be used to estimate the average number of components, n_{la}, that are no longer used within each floor f. Moreover, by simple comparison of the π on a specific floor f one can infer the level of comfort lost by the occupants of a building. For example, in a hospital, the number of beds that are no longer used on a given floor or space can be estimated by multiplying the total number of assets, n_a, by π. In fact, the method proposed by Cimellaro *et al.* (2010b) for estimating the number of beds lost in a hospital can be considered a particular case of the approach proposed in this document. In general, for the number of assets that lose their functionality

on a given floor in a seismic realization, regardless of the type of building, can be estimated by the following expression,

$$n_{la} = n_a \cdot \pi \tag{8.3}$$

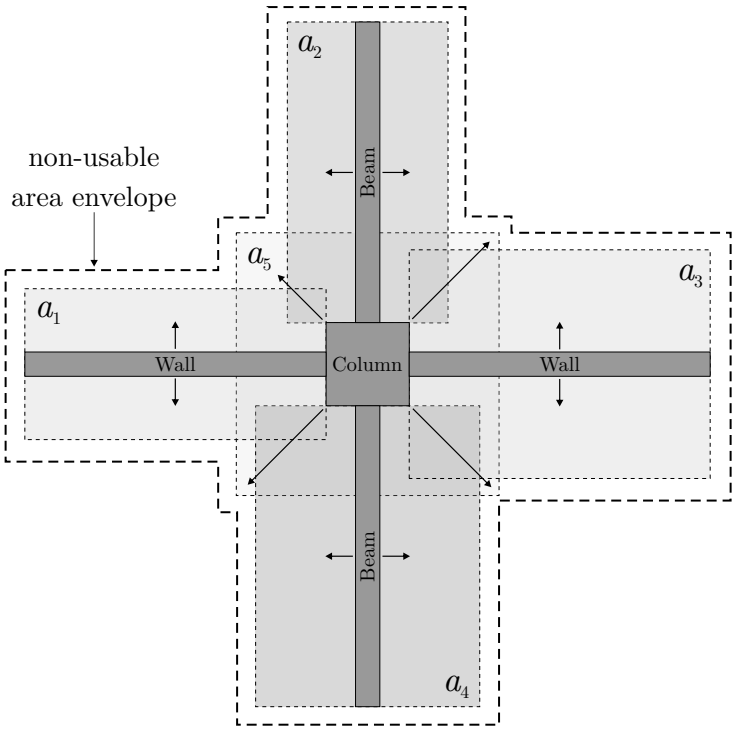

Figure 8.1: Illustration of the effective non-usable area (plan view) of a set of damaged elements.

Under a certain discrete damage level of an element, e, associated with a specific critical PG_c it is possible to lose 100% of the total usable area of a specific floor f or inclusive the entire building, even for relatively low quantities of elements damaged. Such is the case of the transportation and service systems into the building, *e.g.*, hallways, stairs and elevators, drinking water distribution systems, or HVAC systems. Naturally, the total loss of usable area under these conditions is highly dependent on the type of use of the building, the level of importance assigned to a fraction of a floor and the type of performance group. For example, in a hospital, it is very likely that if the contents of a surgery room are overturning, the functionality of the room will be completely lost during the seismic excitation or immediately after the earthquake occurs. By the contrary, if only some infill walls in the reception area suffers cosmetic damage, the building can continue in operation while a minimal number of workers perform the paint job in a short period of time. This condition is taken into account if one or more elements that are essential for the operation of the system reach or exceed a pre-established discrete damage state ds' located in a specific coordinate of a floor $\mathbf{x}'$:

$$\pi = 0\% \quad \text{if} \quad e \in PG_c \rightarrow (DS \geq ds' \mid EDP) \quad \text{and} \quad \mathbf{x}_e \in \mathbf{x}' \tag{8.4}$$

The effective percentage of non-usable area π^* in a floor is quantified by means of the mean value of the set of values associated to the seismic realizations that produce the configuration of a functionality limit state $(LS_0, ..., LS_4 \mid IM)$, and the loss of functionality of the entire building $PNUA$ is quantified as the minimum value of the set of expected values of the percentages of usable area of the group of floors that conform a building:

$$PNUA = \min(\pi_1^*, \pi_2^*, ..., \pi_{nf}^*) \tag{8.5}$$

This criterion is analogous to the case in which an affected region is cordoned off for a period of time. In this circumstance it is possible that a small percentage of the buildings in that area have collapsed or are in danger of collapse, and for the safety of bystanders and occupants of the buildings that did not experience major damage, access to the entire region in question is disabled. This is precisely what happened in the Central Business District (CBD) of Christchurch, New Zealand, as a result of the February 2011 M_w 6.3 magnitude earthquake. Because of this, the Central Business District (CBD) was cordoned off for a period of 2 years, and reconstruction work did not begin until three years after the seismic event occurred. Also, many companies had to relocate to another site, and many others never returned to their initial place of operation. This resulted in substantial indirect economic losses (Almufti and Willford, 2014).

It is difficult to establish the moment at which the loss of functionality occurs, especially when it is not easy to distinguish the level of damage experienced by the different components that integrate a building. If the amount and severity of damage experienced by a building is quite clear, it is certain that the building will cease to be functional immediately after the seismic event occurs (Cimellaro *et al.*, 2006). Since it is numerically difficult to establish the instant of time that the loss of functionality occurs, in this thesis it will be assumed that the percentage of non-usable area, estimated with Eq. 8.5, occurs immediately after the seismic event is presented. This is simply a consequence of the numerical model. However, despite the fact that Eq. 8.5 allows estimating the loss of functionality measured as the percentage of non-usable area, this value does not indicate if the system stops working completely, since for certain values of π it is possible that the building is still in operation. What makes it possible to identify whether the building continues in operation, or is declared as restricted use or not usable, are the functionality limit states. In other words, Eq. 8.5 allows the estimation of the average percentage of $PNUA$ of the entire building due to the seismic realizations conditioned to the LSs and its probability $Pr(LS \mid IM)$.

The assessment of the loss of functionality of a n-storey building is schematically illustrated in Fig. 8.2a (arrow with dotted line pointing downward at the instant the seismic event occurs). The gray lines perpendicular to the dotted line indicate the loss of functionality measured as the π on each of the n floors that conform a hypothetical building and a LS. Some of the components of various PGs located on the first three floors of the

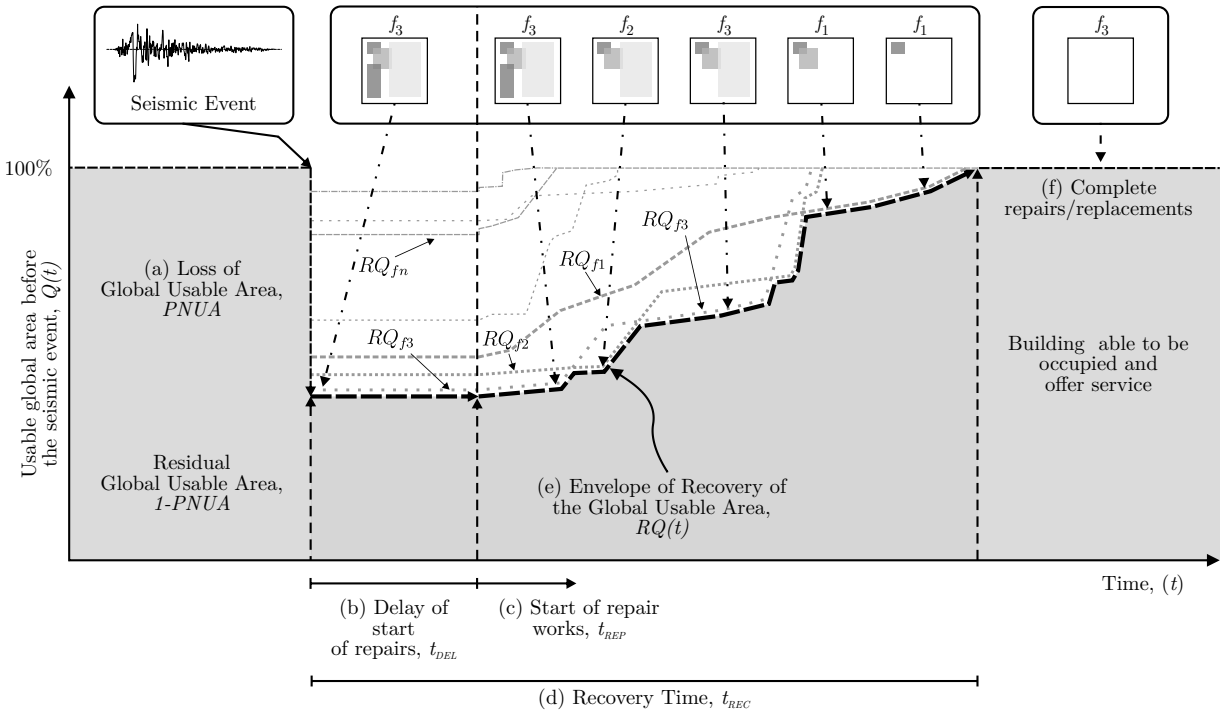

Figure 8.2: General scheme of the loss and recovery of functionality model proposed in this study.

hypothetical building contributed most to the loss of usable area. The minimum usable area of the building corresponds first to the third floor, then to the second and finally the first floor.

8.3 Recovery of functionality assessment: background

As well as there are few methodologies to estimate the loss of functionality in individual buildings, there are also few methodologies to approximate its recovery process. This is mainly due to the complexity of the interaction between the different sectors involved in recovery (*e.g.*, government agencies, insurance companies, banks, engineering and architectural firms, etc.) and to the limited information collected and systematized during past events that can be used to develop analytical models. Despite this, several research groups, *e.g.*, Bruneau *et al.* (2003); Miles and Chang (2006); Cimellaro *et al.* (2010a), FEMA P-58-1 (2012a), to name a few, have proposed approaches with various levels of refinement to estimate the recovery of functionality of both entire communities (*e.g.*, a city) and isolated systems (*e.g.*, a building).

In order to illustrate more clearly the recovery process of a community that has been or may be affected by catastrophic events, Bruneau *et al.* (2003) proposed a graphical scheme, as illustrated in Fig. 3.1 of section 2.2.1, where the recovery of functionality is expressed as a function of the recovery time. Also, Comerio (2006) showed that the recovery of the

functionality of a building depends on a large number of factors, mainly external to the building itself. For example, returning a damaged building to its original state of operation requires financial resources to perform the repair works. These resources may have to be obtained through a bank loan or the payment of an insurance policy, to mention a few possibilities. Recovery also depends on the strategy taken to achieve this objective, *e.g.*, planning the sequence in which repair activities are to be carried out. These facts clearly suggest that the recovery process is very complex because it is influenced by mutually interacting events in similar or different time periods.

Based on these ideas, Cimellaro *et al.* (2006, 2010a) identified three generic patterns of functionality recovery from a community: linear, exponential and trigonometric. These patterns are illustrated in Fig. 8.3. The linear recovery pattern can be used when there is neither a recovery strategy nor human or economic resources for such purposes. This could be the case in regions with scarce economic resources. The exponential recovery approach can be used when economic and social resources are available to initiate and drive the recovery of the affected community. However, as time progresses, the speed of recovery begins to decrease because resources are likely to begin to run out. Trigonometric recovery can be used to simulate a process in which initially there is neither a well-defined organization nor sufficient social and economic resources; however, at a certain moment it is possible that society will acquire the organizational capacity and financial resources to accelerate the recovery process. The linear, exponential and trigonometric recovery functions describing this behavior are indicated in Eq. 8.6.

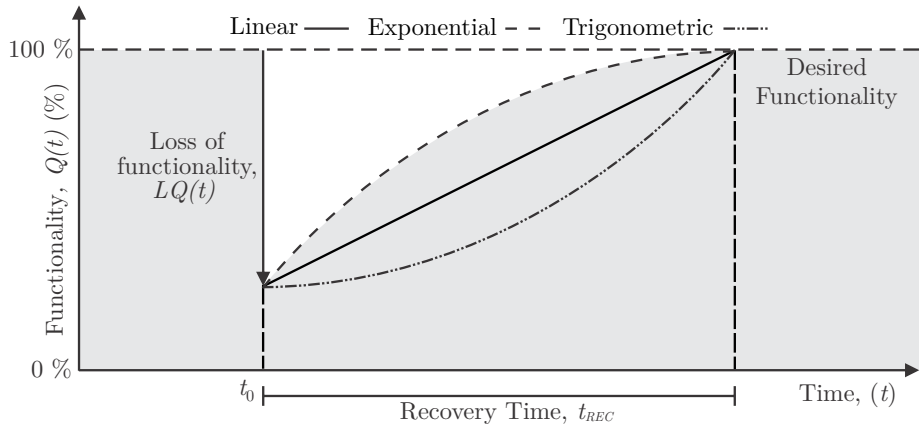

Figure 8.3: Schematic representation of the recovery functions proposed by Cimellaro *et al.* (2006, 2010a).

$$f_{REC}(t) = \begin{cases} a \cdot \left(\frac{t-t_0}{t_{REC}}\right) + b; \text{ linear} \\ a \cdot \exp\left(-\frac{b \cdot (t-t_0)}{t_{REC}}\right); \text{ exponential} \\ \frac{a}{2} \cdot \left\{1 + \cos\left(\frac{\pi \cdot b \cdot (t-t_{REC})}{t_{REC}}\right)\right\}; \text{ trigonometric} \end{cases} \tag{8.6}$$

where a and b are constant values that can be estimated only when the value of the time required for the system to recover its original operating state t_{REC} is known; t_0 is the instant of time at which the catastrophic event occurs.

On the other hand, Burton *et al.* (2016) propose a three-step recovery function for a shelter-in-place community (see Fig. 8.4). Three states of functionality are represented in each step: (1) the building is not safe for occupancy (NOcc); (2) the building is safe for occupancy but is not allowed to perform activities in the normal way (OccLoss); and (3) the building is safe and fully functional (OccFull). These three states are equivalent to the corresponding tagging possibilities according to the ATC-20 (1989), *i.e.*, green, yellow and red color tags. As described above, the recovery process is influenced by a large number of events, which contribute to a greater or lesser extent to the recovery time. These events can be associated to each of the recovery states proposed in this approach. For example, to the state in which the system is not occupiable t_{NOcc}, events such as planning repairs, obtaining economic resources and structural repairs can be assigned. The period of time in which the building is occupiable, but not usable t_{OccLoss}, non-structural repairs can be related. Finally, the state in which the building is declared as occupiable, t_{OccFull} can be linked with the time required for the installation of furniture, computer equipment and telecommunication services.

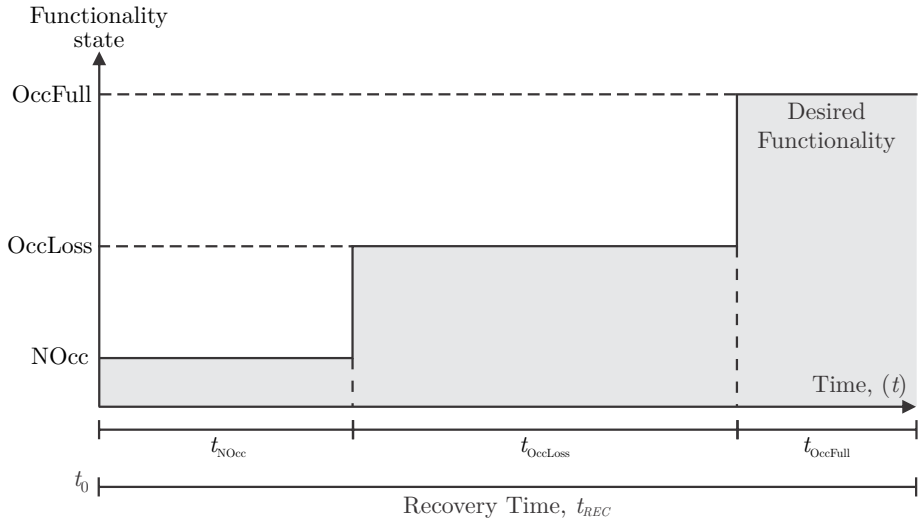

Figure 8.4: Schematic representation of the three step recovery function proposed by Burton *et al.* (2016).

The FEMA P-58-1 (2012a) guidelines to evaluate seismic performance proposes two strategies to assess the repair time of a building damaged by an earthquake. The first one correspond to a parallel repair sequence. This means that all elements damaged, regardless of which performance group belong to, are repaired simultaneously. The maximum repair time of the entire building corresponds to the element in which the repairs consumed a greater amount of time. The second scheme corresponds to a strategy in which the elements are repaired in series. The total repair time is calculated as the sum of the

repair time of each damaged element. The two schemes for quantification of the repair time presents inconsistencies because the time/cost repair probability distributions, described above, are calibrated to be executed by only one worker. Therefore, one worker per damaged element is required for the parallel repair scheme. However, after a destructive earthquake has affected a group of buildings located in the same region, it is likely that the specialized human resources to perform the reconstruction work will be limited (Gutiérrez *et al.*, 2019). Moreover, it is unrealistic to think that the number of workers obtained through this scheme can carry out the repair work at the same time because it is difficult to place a large number of workers in reduced spaces when the amount of damage is significant. With respect to the serial repair scheme, according to the condition in which the repair time/cost per element is obtained, the repair work is carried out by a single worker. Naturally, it is unlikely that a single worker will perform the repairs of all damaged components regardless of the type performance group in turn.

A methodology for resilience-based design purposes is proposed in the REDi^{TM} (2013). This methodology uses the results of the damage inference of each performance group generated by the PACT software (FEMA, 2012a). In this approach, a maximum number of workers $m_{w,\max}$ is proposed as a function of the total area of each floor of the building a_{Tf} (measured in square feet),

$$\begin{gathered} n_{w,\max} = 2.5 \times 10^{-4} \cdot a_{Tf} + 10 \\ 20 \leq n_{w,\max} \leq 260 \end{gathered} \tag{8.7}$$

In a real situation, construction and/or repair works are carried out by systematically organized tasks and performed by work crews in order to optimize the execution time and costs of the activities involved. Optimizing this type of task depends largely on the human and economic resources available and, as expected, it involves great uncertainties because many external factors have a major influence and are usually beyond the control of stakeholders and engineers. The activities associated with repairing buildings damaged by earthquakes become more complex by proper nature of the problem. Likewise, the number of professionals specialized in the subject is relatively reduced, both in the area of structural assessment and retrofit, and in the execution of repair activities. Furthermore, several buildings damaged by an earthquake may have to be repaired by the same company/organization, with the result that recovery time of more than one of the set of the buildings is prolonged by months or even years (Gutiérrez *et al.*, 2019).

8.4 Recovery of functionality: methodology proposed

In order to numerically simulate the repair time of a building damaged by an earthquake, the *Project Evaluation and Review Technique* (PERT) is used in this thesis. The PERT method is a technique of analysis, control and coordination of projects, and its main objective is to evaluate the duration of the tasks that make up a project. This method

was developed in 1958 for the Polaris project of the Office of Special Projects of the Navy of the Department of Defense of the United States (Richmond, 1968). By means of this method it was estimated that the Polaris project could be carried out in two years before what was predicted, as it actually occurred.

The PERT method can be represented by a network that graphically describes a sequence of activities. In the first instance, the project must be divided into specific tasks called *events* (E) whose logical sequence is completed by pre-established *activities* (A). It should be noted that a project can be composed of a few or even hundreds of events and activities. A flow chart based on the PERT method is schematically illustrated in Fig. 8.5. Each node of the diagram (depicted by a circle) represents an event, E. This in turn represents a time interval and is generally described as the beginning or end of some activity. The lines connecting the events represent activities, *i.e.*, the tasks that must be performed in order for the successor events to be executed, $A_{i\to j}$. Thus, an activity represents a period of time t_A within the flowchart. Each event is numbered in such a way that the arrows always indicate the preceding and the successors events. This relationship leads to the order of execution of the activities being inviolable; that is, all preceding activities common to an event must be completed before the event in question takes place, and none activity can begin until its predecessor events has executed. In addition, implicit in the quantification of the time associated to each event the human and economic resources allocated to each activity are taken into account.

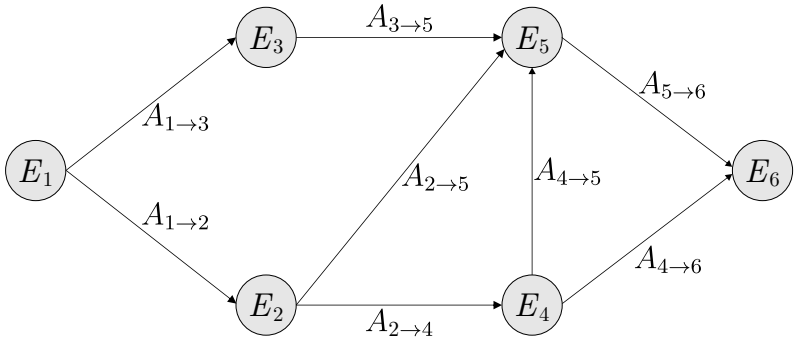

Figure 8.5: PERT diagram illustration (taken from Richmond (1968)).

8.5 Conditions to generate the repair activities within the recursive process of analysis

The following rules are used for constructing the activities and events that compose the general sequence of repair for every seismic realization that cause damage, conditioned to an IM, given that the structure does not have to be demolished or does not experience collapse, this is, not experience the LS_5 or LS_6, respectively:

1. Given an inventory of PGs, pre-establish a generic sequence in which repairs should

be executed, according to the hierarchy and importance of the damageable groups. For example, in a three-story building, if the stairs on the first floor experience severe and moderate damage, and there is also light damage to interior partitions on the third floor, by hierarchy we begin to repair the severe damage to the stairs and then the moderate damage. Finally, light damage to interior partitions is repaired.

By providing a generic sequence of repairs, it is recommended that decision makers know the pathology of the damage that may occur in the building of interest, and also, the possible alternatives to restore the building in the shortest time, avoiding to interrupt the functionality of the system as much as possible. In other words, it is desirable to have a mitigation recovery plan.

2. Infer the DS for each e that conform each PG, produced by a specific earthquake realization s, conditioned on an IM. This step corresponds to the methodology proposed in Chapter 6. Group the elements in a sets of equal severity of damage. Note that the damaged elements, belonging to the same PG, can be located on different floors.

3. Quantify the repair cost cr_e and time tr_e per element, defined within each PG. To achieve this it is necessary to establish a numerical relationship between th DSs that a particular element may experience and its respective repair activities. To do this, assume that a probability distribution function exists by which it is possible to estimate the probability that $Pr(CR_e \leq cr_e \mid DS)$ and $Pr(TR_e \leq tr_e \mid DS)$. Then, the inverse transform method to determine the numerical value of these two DVs for each damaged element, is used,

$$\begin{aligned} cr_e &= F_{CR_e}^{-1}\left(u_1 \mid \theta_{cr}\right) \\ tr_e &= F_{TR_e}^{-1}\left(u_2 \mid \theta_{tr}\right) \end{aligned} \tag{8.8}$$

where $u_{1,2}$ is a random variable uniformly distributed that takes values between 0 and 1, *i.e.*, $u_{1,2} \sim u\left(0,1\right)$, and θ is a vector that contains the parameters of the probability distribution of the DV. In this study, the unit repair cost/time probability distribution functions for the PGs proposed by the FEMA P-58-3 (2012b) are used. These probability distributions take into account debris clearance time, repair time and material transport time. Likewise, these probability distributions were calibrated considering that the repair activities for an element are performed by a single worker. Finally, the cost and repair time decision variables associated with the number of units u_e corresponding to a particular element, given a specific discrete damage state, is estimated as follows:

$$\widehat{dv_e} = dv_e \cdot u_e \cdot Pr(DS = ds \mid LS, IM) \tag{8.9}$$

4. Pre-establish a number of crews n_c, and the number of workers n_w, within each of them. This will depend on the number of damaged elements within a performance

group and the level of severity of the damage experienced by them, but also from the experience and the judgment of the analyst. Yoo (2016) interviewed a group of experts engineers in repairing buildings damaged by earthquakes and according to their experience they recommend use the following human resources to carry out the repairs:

- For light damaged state:

$$n_c = \begin{cases} 1 & \text{crew} \quad \text{if} \quad 1 \leq n_{DS_{\text{light}}} \leq 10 \\ 2 & \text{crews} \quad \text{if} \quad n_{DS_{\text{light}}} > 10 \end{cases} \tag{8.10}$$

- For moderate damage state or worst:

$$n_c = \begin{cases} 2 & \text{crews} \quad \text{if} \quad 1 \leq n_{DS \geq \text{moderate}} \leq 10 \\ 3 & \text{crews} \quad \text{if} \quad n_{DS \geq \text{moderate}} > 10 \end{cases} \tag{8.11}$$

- And the number of workers according to the severity of the damage:

$$\hat{n}_w = \begin{cases} 2 & \text{workers} \quad \text{if} \quad DS = \text{light} \\ 3 & \text{workers} \quad \text{if} \quad DS \geq \text{moderate} \end{cases} \tag{8.12}$$

Due to the lack of information associated with the human resources used for repair works in Mexico, in this study the number of crews and workers proposed by Yoo (2016) to simulate the repairs for each damaged group are used.

In this step it is assumed that the workers assigned to repair one performance group are different from those who repair another one. Therefore, the total number of workers is calculated as the sum of the number of workers repairing each damageable group:

$$n_w = \sum_{j=1}^{N_{PG}} \sum_{i=1}^{N_{DS}} \hat{n}_w(PG_j, DS_i) \tag{8.13}$$

5. Assign approximately in the same proportion the number of elements damaged in the same discrete damage state n_{DS_k} (estimated in step 2) to each crew n_c.

6. Define the repair activities. To do this, consider the following example: the crew c_k will repair the amount of elements of the set $\mathbf{e} = (e_1, e_2, ..., e_n)$, of which a subset $\hat{\mathbf{e}}_1$ is located on the floor r and the rest of the elements $\hat{\mathbf{e}}_2$ on the floor q, where $r \neq q$. Then, the activities to be performed by the crew c_k are $\mathbf{A}_i^r$ and $\mathbf{A}_{i+1}^q$. In this latter the subscript indicates the activity number and the superscript the number of the floor of the building that contains a specific performance group that will be repaired. These activities should be carried out sequentially by a specific crew c_k since the first activity contains the first elements $\hat{\mathbf{e}}_1$ to be repaired and the next crew, the following elements $\hat{\mathbf{e}}_2$ corresponding to the floors q and r, respectively.

With this in mind, the activities to be performed by a specific crew c_k are defined by the following expression:

$$\mathbf{A}_i^j \left(PG, DS, \hat{\mathbf{e}} \mid LS, IM\right) \rightarrow c_k \tag{8.14}$$

7. For all PGs, repairs begin with the activities whose elements belong to the most severely damaged state. Once these activities have been completed, the activities whose elements correspond to a state of less severe damage will continue, and so on.

8. It is possible to schedule activities in parallel, performed by two or more different crews, as long as these activities are defined by repairs of elements in the same DS and correspond to the same PG. For example, is possible that two different crews have to repair a set of elements that are located in a same floor and belong to the same PG. Likewise, it is considered that the repair time between elements is continuous; that is, there is no delay time between the beginning of the repair of an element and the completion of the repair of the previous element. The same criteria is adopted for the start/end repair for each activity $\mathbf{A}_i^j$.

9. In general, the execution time of the activity $\mathbf{A}_i^j$ is obtained by means of the following expression:

$$\widetilde{tr}(c_k) = \frac{1}{\hat{n}_w(c_k)} \sum_{\forall \mathbf{A}_i^j \in c_k} \widehat{tr}_e \left(\mathbf{A}_i^j \mid LS, IM\right) \tag{8.15}$$

   where the summation represents the sum of the repair time of each element in the same DS, corresponding to the same PG, repaired by a specific crew c_k, normalized by a number of workers $\hat{n}_w(c_k)$.

10. The start time $\tilde{t}_s$ of some of the activities depends on the completion of one or more predecessor activities. In this case the start time of that activity corresponds to the maximum repair time of the predecessor activities p:

$$\tilde{t}_s = \max \left\{ \widetilde{tr}_p(\mathbf{A})_1^{f1}, \widetilde{tr}_p(\mathbf{A})_2^{f1 \neq f2}, ..., \widetilde{tr}_p(\mathbf{A})_n^{f_{m-1} \neq f_m} \mid LS, IM \right\} \tag{8.16}$$

11. The completion time, $t_e(\mathbf{A}_i^j)$, of the activity $\mathbf{A}_i^j$ is calculated as the sum of the initial time, $\tilde{t}_s$, plus the repair time, $\widetilde{tr}(c_k)$. The maximum repair time for the entire repair project corresponds to the maximum completion time, and is obtained using the following expression:

$$t_{rep} = \max \left\{ t_e(\mathbf{A}_1^j), t_e(\mathbf{A}_2^j), ..., t_e(\mathbf{A}_n^j) \mid LS, IM \right\} \tag{8.17}$$

12. As well as the repair time spent by each crew was evaluated, it is possible to estimate the repair cost $\widetilde{cr}(c_k)$ associated with each activity $\mathbf{A}_i^j$ performed by a crew c_k. To achieve this, first it is necessary to evaluate the repair cost of each element for each

PG, according to the DS experienced. The repair cost of an activity is calculated with the following expression:

$$\widetilde{cr}(c_k) = \sum_{\forall \mathbf{A}_i^j \in c_k} \widehat{cr}(\mathbf{A}_i^j \mid LS, IM) \cdot [1 + n_w(c_k) \cdot \alpha] \tag{8.18}$$

where α is a factor that takes into account a percentage assigned to the crew c_k for the payment to the repair works of the activity $\mathbf{A}_i^j$ and $n_w(c_k)$ is the number of workers associated to the crew c_k. The total repair cost of the entire building is calculated by means of the addition of the all repair cost of each activity:

$$C_{REP} = \beta_1 \cdot \beta_2 \cdot \varphi \cdot \sum_{\forall \mathbf{A}_i^j} \widetilde{cr}(\mathbf{A}_i^j \mid LS, IM) \tag{8.19}$$

where $\varphi = (1 + \zeta)/(1 + \gamma)$ is a factor that take into account the depreciation ζ and discount annual rate γ applied to a range of t years, *e.g.*, life cycle, between the initial investment and the IM of interest; β_1 and β_2 are two factors that considers the local prices and the price increase of materials and labor after a major seismic event, respectively.

By means of the procedure described previously it is possible to take account not only the time and costs repairs, but also the human resources needed to perform the repair of a building damaged. In this regard, the space available to perform repairs is limited. This results in limiting the number of workers in the same period of time, which leads to slower repairs. The recursive method described above limits the number of workers in a natural way because (1) no more than two crews are allowed to perform activities on a floor at the same time (even considering that the number of workers increases when more than one performance group experiences severe damage) and (2) the number of crews and workers is prescribed based on the experience gained by engineers who have repaired buildings damaged by seismic events (Yoo, 2016). Moreover, the number of workers used in the methodology proposed in this thesis is within the limit prescribed by the REDi$^{\text{TM}}$ (2013) throughout the recovery process. By the contrary, the parallel repair scheme for estimating repair time proposed by the FEMA P-58-1 (2012a) does not prescribe a limit to restrict the maximum number of workers that can be on the same floor in the same period of time. The consequence of this is that the estimated number of workers can be very high, which would lead to congestion of workers in a same area of the building.

8.6 Estimation of recovery time

In real life, repair works do not start immediately after the occurrence of a seismic event. On the contrary, other events, called irrational factors, occur before repairs begin, because their nature involves great uncertainties and the sequence of their execution cannot be

established a priori. Comerio (2006) identified the irrational factors that have the major influence on the delay time for the start of repairs: (1) post-earthquake inspection, (2) structural review and possible redesign, (3) management of funding to finance the repairs, (4) bidding process, and (5) management of government permits to perform the repairs. The engineering firm Arup through the REDi^{TM} (2013) Rating System design guidance and criteria has calibrated a series of fragility functions representative of the time delay of irrational factors. These models consider, in a crude but practical way, the consequences of the severity of the damage experienced by structural and non-structural elements in the type of repairs:

- *Repair class* RC_1: There is minimal damage to the finishes of structural and non-structural elements. Therefore, this repair class corresponds to cosmetic repairs. This level of damage does not prevent the building from being reoccupied after the seismic event, so it can be considered that the building does not lose functionality.

- *Repair Class* RC_2: severe damage to non-structural components is presented. The life safety of the occupants is not at risk; however, users may be injured. It is not possible to reoccupy the building until repairs are completed. The building becomes re-occupiable and functional when all damaged components have been repaired.

- *Repair Class* RC_3: Severe damage in a significant number of structural and non-structural elements is presented. By definition, this level of damage puts life safety at risk, therefore, in order for the system to be reoccupied, repairs must first be completed.

The fragility functions characterizing the irrational factors are defined as a function of: (1) the repair class, (2) the type of structure (essential or non-essential), (3) height of the building (less than or greater than twenty stories), (4) the type of financing (insurance, private loans or backed loans). Each LS is associated with a generic recovery sequence $RQ(t)$, as described in Chapter 7. The two principal stages of the functionality recovery model proposed in this thesis are illustrated in Fig. 8.6[1]. The first stage (Fig. 8.6) corresponds to the evaluation of the factors that prevent the initiation of repairs. The sequence in which each irrational factor occurs and the interaction between these factors is very complex, for such reason in this document it is proposed to quantify the total delay time using a serial process. At the same time, it can be said that by taking into account the irrational factors within the resilience model, the interaction with dependencies external to the building is also being considered (in a very simple way). In this regard, the approach performed by the FEMA P-58-1 (2012a) does not take into account the time delay of the start of repairs, *i.e.*, this methodology considers only the time associated with repairs.

The second stage corresponds to the estimation of the repair of structural and non-structural elements, and installation time of the furniture (Fig. 8.6b). This second stage,

[1]This figure was presented in Chapter 3, however, for practical purposes in this section it is presented again.

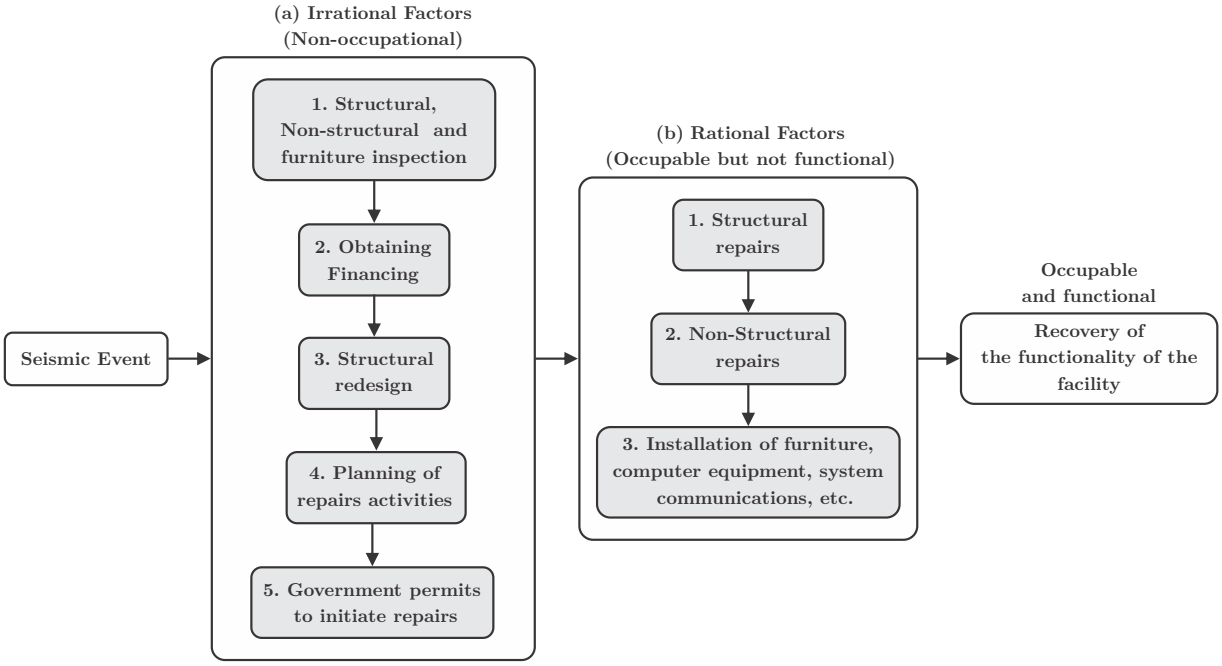

Figure 8.6: General sequence of recovery of the functionality.

as described above, is based on a recursive process, and in general, the repairs of the different PGs can be carried out by a combination of serial or parallel repairs.

In column 5 of Table 8.1, the sequence in which the irrational factors are presented for each of the LS, according to the recovery model proposed in this thesis. In the third column the repair class is indicated, and in the fourth column the tagging of the post-seismic inspection according to the criterion of the ATC-20 (1989). In this context, the fragility function of each irrational factor is defined by the repair class. To point this out, the irrational factors associated to the recovery states of functionality $RQ_3(t)$ and $RQ_4(t)$ are apparently the same; however, the repair class is different for each state, that is, the repair class RC_2 corresponds to the recovery state $RQ_3(t)$, and the class C_3 to the recovery state

Table 8.1: (1) Functionality limit state, (2) repair class based on the ATC-20 tagging (3), and (4) proposed sequence of irrational factors that delay the initiation of repairs.

(1) Functionality limit state LS	(2) Recovery state $RQ(t)$	(3) Repair class RC	(4) ATC-20 Tagging	(5) Irrational factors sequence
LS_0, LS_1	RQ_0, RQ_1	-	G_s	I
LS_2	RQ_2	RC_1	G_s	$I \rightarrow F \rightarrow M$
LS_3	RQ_3	RC_2	Y_s	$I \rightarrow F \rightarrow E/R \rightarrow M \rightarrow P$
LS_4	RQ_4	RC_3	R_s	$I \rightarrow F \rightarrow E/R \rightarrow M \rightarrow P$
LS_5	RQ_5	RC_3	R_s	$I \rightarrow F \rightarrow M \rightarrow P \rightarrow R$
LS_6	RQ_6	–	R_s	$D \rightarrow I \rightarrow R$

Notes: Post-seismic inspection (I), obtaining financing (F), evaluation or structural redesign (E/R), planning of repair activities (M), government permits to initiate repairs (P), debris removal (D) and reconstruction (R).

$RQ_4(t)$.

The total time preceding the start of repairs is determined by the sum of each of the irrational factors, for each seismic realization conditional on a repair class, to the LS and the IM,

$$t_{IF} = \left(\sum_{j=1}^{n_{IF}} \tilde{t}_{IF_j} \mid RC, LS, IM \right) \tag{8.20}$$

The numerical evaluation of each of the irrational factors is performed using the inverse transformation method, which has already been described above. Finally, the recovery time of the damaged building for a seismic realization is approximated by the sum of the delay time and the repair time for each seismic realization, conditioned to a functionality limit state, to a repair class and a seismic intensity,

$$t_{REC} = (t_{IF} + t_{REP} \mid RC, LS, IM) \tag{8.21}$$

This expression is consistent with the definition of functional recovery proposed by Almufti and Willford (2014). They define recovery of functionality as the time and resources required to restore the level of functioning (original or better) to a community or building affected by a destructive event.

Finally, the recovery of functionality is determined by the bi-univocal relationship between the recovery time accumulated at each instant of time $t_{REC}(t)$ according to the completion of the activities associated to the irrational factors IF, and the minimum average percentage value of usable area $\mathbf{A}_i^j$ (of the floors that have to be repaired) that is released as the repair work is completed over time, *i.e.*, $PUA(t)$. The functionality of the system is reached as soon as the re-installation of the damaged furniture is completed (see Fig. 8.2f).

8.6.1 Treatment of uncertainty in the functional recovery model

The classical formulation of the PERT method allows modeling the uncertainty in the duration time of a project by assuming that the duration of each activity is a random variable with Beta Unimodal probability distribution, with parameters (a, m, b). Likewise, the execution time of each activity is estimated using three probable values: conservative time t_c, most probable time t_m and pessimistic time t_b. The expected time for each activity t_a is evaluated by a combination of the above possibilities using the following expression (Richmond, 1968),

$$t_a = \frac{t_c + 4t_m + t_b}{6} \tag{8.22}$$

and the variance is given by,

$$\sigma^2 = \left(\frac{t_b - t_a}{6}\right)^2 \tag{8.23}$$

The methodology proposed in this document, conversely, uses only the general rules of the PERT method to construct the events, the activities and the sequence of execution of each one of them. The variation of the sequence of reparation product to the variability of activities are taken into account as a result that the number of damaged elements associated to each performance group also change because the damage configuration is different from one seismic realization to another, product to the record to record variability and the damage inference using the inverse transformation method, Eq. 8.8. Consequently, this also conducts to the critical path of repair for every realization changes, and therefore the method does not take into account only the variation in the inference of the damage and time/cost of repair and human resources, but also the repair time as a whole.

The expected value μ_{DV} and variance σ^2_{DV} of all DVs proposed in this dissertation will be estimated using the bootstrap technique. This technique is used to perform statistical inference, mainly when the underlying model of a process is very complex in such a way that it is not possible to derive closed equations, as in Fisherian inference (Efron and Tibshirani, 1993). This technique is classified within the modern methodologies of computational statistical inference, as is the case of artificial intelligence (Efron and Hastie, 2016). The corresponding uncertainty in the estimation of the expected value of the DVs will be expressed by its confidence interval, which will be calculated using the BC_a technique, which is part of the set of bootstrap techniques for estimating confidence intervals. Details of the implementation of this technique are presented in Chapter 10 of this work.

8.7 Quantification of economic losses due to business interruption

Indirect economic losses I_{EL} are originated by the loss of use of the building (Bruneau *et al.*, 2003; Cimellaro *et al.*, 2006; Comerio, 2006). These losses can affect not only the financial status of the owners of the building, but also the tenants of the building. Modeling this type of loss is very difficult because there can be a complex interaction between the tenants of each floor of the building with the building owner and, if applicable, with the conditions stipulated in the underwriting contract (Porter, 2003). On the other hand, I_{EL} may be reduced if the tenant decides to rent other offices. In this respect, the cost of moving generates extra economic losses. However, if business is reestablished in another building, the I_{EL} may be less than those resulting from the full recovery time of the damaged building.

These factors make it difficult to propose a detailed methodology to approximate such losses. Nevertheless, under certain assumptions it is possible to formulate a generic solution to the calculation of I_{EL}. In this thesis, indirect economic losses will be approximated by

assuming that the only financially disadvantaged person is the tenant of each floor. The I_{EL} for a seismic realization given an IM are estimated by the following linear function,

$$I_{EL} = \left(\sum_{i=1}^{n_f} I_{EL,f_i} \cdot t_{lu} \mid LS, IM \right) \tag{8.24}$$

where I_{EL,f_i} corresponds to the economic losses per unit of time, *i.e.*, per day, derived from the loss of business conducted on the f_i floor of the building; t_{lu} is the time in which the economic gains are lost; t_{lu} may be the recovery time t_{REC}, or less, in case the tenant leaves the damaged space and decides to rent another space. By definition, indirect economic losses can only occur in the limit states of functionality $LS_2, ..., LS_6$.

Chapter 9

Approximation of the number of injuries and casualties

The number of persons that could be injured during a seismic event does not only depend on the safety of the buildings, although this is obviously one of the most important aspects. The socio-economic level, demographic characteristics, population density, site conditions, behavior of people during the seismic event, among others, are some of the most relevant factors that contribute significantly to the number of fatal and non-fatal victims (Spence *et al.*, 2011).

Table 9.1 presents some of the seismic events over the past 70 years that have caused numerous casualties and injuries. This table was compiled from data published by Seligson and Shoaf (2003), Spence *et al.* (2011), which were obtained from a variety of sources, *e.g.*, official reports, newspaper reports, hospital records, among others. It should be noted that the data for earthquakes from 1995 to 2020 in this table were obtained by the author of this research work from newspaper reports and different electronic information sources, *e.g.*, El País newspaper, BBC News and Animal Político (Mexico). In this table it can be observed the lack of data, especially on the number of people who suffered serious and minor injuries.

This table shows that the number of fatalities does not obey a clear relationship with the magnitude of the seismic event. For example, the Tohoku earthquake (Japan, 2011) of M_w 9.0 produced a number, according to official reports, of 15,893 victims, while the earthquake in Haiti (Haiti, 2010) of magnitude M_w 7.0 caused an approximate number of 222,570 deaths. In this regard, the Aegean Sea earthquake (Turkey, 2020) of magnitude M_w 7.0 caused only 36 deaths. Something similar occurs with the number of severe injuries. The Tohoku earthquake caused approximately 6,152 people to suffer severe injuries, while the 7.4 magnitude Manjil-Rudbar earthquake (Iran, 1990) caused 710,000 people to experience severe injuries. In contrast, the M_w 8.0 Algarrobo earthquake (Chile, 1985) caused only 14 people to suffer severe injuries.

Although it is rare for the number of people suffering some type of minor injury to be recorded, as shown in the table, a similar comparative analysis can be made for this case

as well. For example, the Algarrobo earthquake (Chile, 1985) of magnitude M_w 8.0 caused 2,575 people to suffer some type of minor injury, while the Spitak earthquake (Armenia, 1988) of M_w 7.2 caused approximately 18,000 people to suffer minor injuries.

Table 9.1: Number of fatalities and non-fatalities of some of the earthquakes that have occurred in the last 70 years.

Year	Location	Magnitud M_w	Deaths	Serious Injuries	Minor Injuries
1952	Bakersfield (USA)	7.3	2	32	?
1970	Ancash (Peru)	7.9	67,000	?	?
1971	San Fernando (USA)	6.4	58	2,543	?
1972	Nicaragua	6.3	4,200 (3-6,000)	16,800	?
1976	Guatemala	7.5	22,778	76,506	?
1976	Tangshan (China)	7.5	240,000	160,000	?
1978	Tabas (Iran)	7.4	25,000	?	?
1980	Irpinia (Italy)	6.9	3,000	8,000	?
1985	Algarrobo (Chile)	8.0	180	14	2,575
1985	Michoacán (Mexico)	8.1	211	40,000	30,000
1987	Whittier Narrows (USA)	5.9	3	121	1,228
1988	Spitak (Armenia)	7.2	25,000	12,200	18,800
1989	Loma Prieta (USA)	6.9	62	3,757	?
1990	Manjil-Rudbar (Iran)	7.4	40,000	710,000	?
1990	Luzon (Philippines)	7.7	592	1,412	?
1993	Hokkaido (Japan)	7.8	231	?	?
1993	Guam	7.8	0	100	?
1994	Northridge (USA)	6.7	33	138	8-24,000
1995	Kobe (Japon)	6.9	1,800	6,434	?
2003	Bam (Iran)	6.6	27,000	268000	?
2010	Haití (Haití)	7	222,570	1,000	110,00
2010	Chile	8.8	525	?	?
2011	Christchurch (New Zeland)	6.2	185	164	2000
2011	Tohoku (Japon)	9	15,893	6,152	?
2017	Puebla (Mexico)	7.1	369	?	6,000
2020	Aegean Sea (Turkey)	7	36	1,607	?

Notes: This table was made from data reported by Seligson and Shoaf (2003), Spence *et al.* (2011), and the author of this research work.

Similarly, in Table 9.1 it can be seen that there is no proportional relationship between the number of people deceased and the corresponding number suffering some type of serious or minor injury. In some cases this ratio can reach a proportion of 60 to 1, as in the case of the Loma Prieta earthquake (USA, 1989) of magnitude 6.9, compared to the 17 to 1 ratio

of the Manjil-Rudbar earthquake (Iran, 1990) of magnitude 7.4. A similar situation occurs with respect to the number of people experiencing minor injuries relative to the number of fatalities. The Northridge earthquake (USA, 1994) of magnitude 6.7 caused 24,000 people to suffer minor injuries, while the number of fatalities amounted to 33, that is, there is a ratio of 727 to 1. The Spitak earthquake (Armenia, 1988) of M_w 7.2 caused approximately 18,000 people to suffer minor injuries, compared to the 25,000 people who lost their lives. This ratio is less than unity. These examples show that it is not appropriate to establish 3 to 1 or 4 to 1 ratios, as a criteria proposed on several occasions, as previously noted by Seligson and Shoaf (2003).

As mentioned above, while there is generally no consistent relationship between the number of deaths and the number of injuries, the Whittier Narrow (1987) of magnitude M_w 5.9, the Loma Prieta (1989) of magnitude M_w 6.9 and the Northridge (1994) of magnitude M_w 6.7, all occurring in California, USA, have revealed some interesting patterns. Shoaf *et al.* (2005) conducted a statistical study of the number of people injured by these three seismic events. This study was developed from a series of telephone surveys of residents of the affected communities by interviewers from the UCLA Institute for Social Science Research, Survey Research Center.

In these three cases, the highest percentage of non-fatal victims suffered some type of minor injury as a result of damage caused by falling non-structural elements and contents. Forty-five percent of those injured during the Loma Prieta earthquake and 83% associated with the Northridge earthquake suffered cuts, bruises and sprains. For the Whittier Narrow earthquake, 41% of respondents reported suffering minor head injuries, while 23% reported experiencing emotional damage. With respect to the Northridge earthquake, 32% of respondents reported experiencing emotional damage. On the other hand, for the Whittier Narrow earthquake, 50% of the injuries were caused by falling non-structural elements. Regarding the Loma Prieta earthquake, less than 10% of respondents reported having suffered some type of injury due to damage from non-structural elements, while 55% reported having experienced injuries due to falling objects. Fifty-five percent of respondents reported having experienced injuries due to falling objects. Likewise, 55% of those injured during the Northridge earthquake were affected by non-structural elements. Finally, one percent of the people surveyed reported some type of injury from a structural element. This is probably due to the fact that the earthquakes occurred within a region that has similar socio-economic, physical, construction and demographic characteristics, and site conditions. Table 9.2 summarizes the above percentages.

Shoaf *et al.* (2005) presented an interesting relationship between the percentage of injured personnel and the tagging of the post-seismic inspection of their home in relation to the 1994 Northridge earthquake. The home of 2.3% of the injured occupants did not experience structural damage of any nature. However, although it does not specify the cause of the injuries, it is possible that the injuries were due to falling objects (*e.g.*, furniture elements). Also, 27% of the injured persons indicated that their home received a G tag, while 45% and 28% indicated that their home received a Y and R tag, respectively.

It highlights the fact that the highest percentage of injured occupants is associated with

Table 9.2: Percentages of types of injuries and their causes for the earthquakes of Whittier Narrow (1987), Loma Prieta (1989) and Northridge (1994), in California, USA (Elaborated from data presented in Shoaf *et al.* (2005).

Type/Cause of injury	Whittier Narrow (1987) $M_w = 5.9$	Loma Prieta (1989) $M_w = 6.9$	Northridge (1994) $M_w = 6.7$
Cuts, bruises and sprains	83%	45%	-
Head injuries	40.5%	-	-
Emotional injuries	23%	-	32%
Falling of non-structural elements	50%	10%	55%
Damage in structural elements	1%	1%	1%

a home that received Y tag. According to the criteria described in Chapter 7, yellow tagging indicates that the building should have been inspected again; this time, reviewing the interior of the building with detailed criteria, and subsequently defining the level of post-seismic structural safety. In this regard, Shoaf *et al.* (2005) does not mention that such an update has been performed. Again, it is worth remembering that the tagging performed with the ATC-20 (1989) criterion only takes into account structural safety. So it is very likely that the high percentage of injuries was strongly influenced by the damage experienced by non-structural elements and contents, as reported in the study conducted by Shoaf *et al.* (2005). If this conjecture is correct, then it is convenient to establish a new classification in the post-seismic inspection criteria proposed by the ATC-20 (1989), in which the review of non-structural and contents elements is taken into account, as considered in this thesis.

This new criterion should be oriented to define the loss of functionality through a heuristic point of view, that is, taking into account not only the structural elements, but also the non-structural elements and contents. A large part of the economic and social consequences are caused by the damage suffered by this type of elements in earthquakes of moderate intensity. This is one of the main reasons why this thesis proposes to perform, at least in probabilistic terms, the virtual inspection of the performance of non-structural elements and furniture, in contrast to the methodology proposed by Mitrani-Reiser (2007), where only the inspection of structural elements is considered.

The research conducted by Shoaf *et al.* (2005) demonstrates the importance of collecting data with a systematized and objective criterion of the consequences of seismic events, not only from the point of view of the performance of the structural system, but also from the social and economic perspective. It highlights the relevance of recording the number of people who experienced certain types of injuries, since these data allow probabilistic models to estimate possible future injuries, and therefore, to reduce them as much as possible, as well as to establish measures to manage risk, *e.g.*, the creation of economic provisions to treat injuries derived not only from seismic events, but from any potentially destructive natural event. Unfortunately, this is precisely one of the major problems

encountered in the field of earthquake engineering. There is a sparse database regarding the number of people injured, the type of injury they experience, and the equivalent value this costs the affected society.

Despite this, and the scarcity of this type of data, some criteria and methodologies have been developed to estimate the percentage or number of people who may lose their lives during future seismic events. These methods are mainly based on the size of the building (*i.e.*, low, medium or high height), materials used in the construction (*e.g.*, reinforced concrete, wood, structural steel, etc.), age of the building, design criteria used (*e.g.*, ductile or non-ductile), type of collapse (*i.e.*, partial or total). Characteristics such as occupant age, gender, marital status and race are also factors that have been shown to influence the percentage of injured occupants and fatalities; however, these factors have not been considered in the current models developed to estimate the number of casualties, as is the case with the methodology developed by the FEMA P-58/BD-3.7.8 (2008).

On the other hand, most seismic design regulations are formulated to safeguard the lives of the occupants of a building when it is subjected to a seismic demand similar to that used in structural design. Despite this, few are the codes and design guides that explicitly accept the possibility of fatal and nonfatal casualties, and some others merely mention that their goal is to avoid such losses. For example, the FEMA 356 (2000) explicitly mentions the possibility of structural and non-structural damage leading to severe injuries in the presence of high intensity seismic intensities; however, it does not mention the possibility of injuries in the presence of moderate intensity earthquakes. The NTC-DS (GCDMX, 2020) as well as Vision 2000 (SEAOC, 1996), mention preventing loss of life as a design objective; however, they do not mention injury prevention as a performance objective, which, as mentioned above, is very likely to occur. The FEMA P-58-1 (2012a) through the FEMA P-58/BD-3.7.8 (2008), has been the first document to assess seismic performance to propose a systematized methodology, but at the same time simplified, to estimate the probable number of casualties inside a building. However, this assessment methodology does not allow estimating the probable number of people injured.

9.1 Criteria proposed by the FEMA P-58/BD-3.7.8 to estimate the number of fatalities

The FEMA P-58/BD-3.7.8 (2008) developed a set of criteria and empirical methodologies to estimate the peak number of people inside typical buildings (*e.g.*, hospitals, offices, hotels, etc.) as a function of daytime, day of the week, and month of the year, and the number of people who lose their lives due to total or partial collapse of a building caused by a seismic event. These approximations were developed by experts such as Murakami and Ohta (2004); Nichols and Beavers (2003); Shoaf *et al.* (2005) and Seligson *et al.* (2006), from an unrobust database of the number of fatalities caused by the Northridge (USA, 1994), Kobe (Japan, 1995) and Golcuk (Turkey, 1999) seismic events.

The FEMA P-58/BD-3.7.8 (2008) proposes two critera to estimate the number of fatalities

caused by a seismic event. The first approach consists of estimating the number of fatalities caused by the total or partial collapse of a building using the following equation,

$$n_d = \sum_{f=1}^{n_f} [P_f \cdot w_a \cdot w_b \cdot Pr(Cm_f) \mid IM] \tag{9.1}$$

where P_f corresponds to the peak population at floor f (occupants per $1,000$ ft^2) as a function of building usage; w_a considers the probability of collapse of floor f; w_b takes into account the fatality rate as a function of the type of building in question, *e.g.*, a hospital or a hotel; the term $Pr(Cm_f)$ corresponds to the probability of collapse of mode for the floor f, *e.g.*, pancake mode of failure for the second floor, and sidesway collapse mode of failure for the fifth floor; usually each floor of the building can have a failure mode, FEMA P-58-1 (2012a). Also, if all floors of the building are intended for the same use, the number of occupants also remains constant throughout the height of the building. In this first approximation, the peak number of occupants remains constant for each seismic realization, regardless of the seismic intensity of interest and the date of the seismic event.

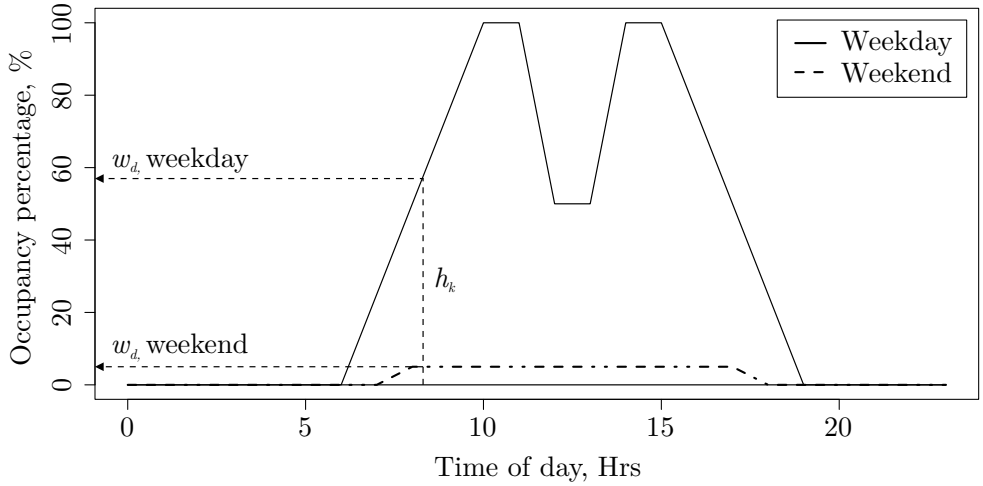

Figure 9.1: Generic model of percentage of weekday and weekend occupancy.

One of the key contributions of the methodology proposed by the FEMA P-58/BD-3.7.8 (2008) was the development of models representative of the number of peak occupants[1]. These models prescribe the percentage or average occupancy rate over time, *i.e.*, as a function of the time, day (weekday or weekend) and month in which a seismic event may occur. Fig. 9.1 illustrates the model corresponding to the expected occupancy percentage of the population of a building for office use as a function of the day of the week (see columns 1 and 2 of Table C.3). This figure shows the hours of the day when occupancy is maximum,

[1]Appendix C of this document presents a series of tables based on the type of use of the building indicating the fatality rate (Table C.1), peak population (Table C.2), occupancy percentage as a function of day of the week (Table C.3) and month of the year (Table C.4). These tables are taken from the FEMA P-58/BD-3.7.8 (2008) document.

the hours when it is null, and the hours when it is partial. The central concavity is due to the fact that during these hours a percentage of the personnel occupying the building go out to lunch. In this respect, if the building were for hospital use, the minimum occupancy percentage would be greater than zero and there would be no concavity. Likewise, the difference between the occupancy rate between weekdays and weekends would be very small.

To simulate the date when a seismic event occurs, first consider that the vectors $\mathbf{m} = (m_1, m_2, ..., m_{12})$, $\mathbf{d} = (d_1, d_2, ..., d_7)$ and $\mathbf{h} = (h_1, h_2, ..., h_{24})$, contain the months of the year, days of the week and hours of the day, respectively. Using the random sampling technique, the month m_i, the day d_j and the hour h_k in which a seismic event occurs are selected,

To estimate the daily occupancy percentage w_d as a function of the time of day h_k, it must be determined whether the sampled day d_j is a weekday or a weekend day. With the index h_k the occupancy percentage as a function of the time of day w_d is determined (see Fig. 9.1), and with the index m_i the expected peak percentage of the population w_m found at the building in the ith month is determined (see Table C.5). Note that the occupancy percentage for the month must also be determined from the day selected in the random sampling, *i.e.*, whether d_j falls on a weekday or weekend (see Tables C.5 and C.6 in Appendix C).

$$\begin{aligned} \mathbf{m} &\rightarrow m_i \rightarrow i\text{th month} \\ \mathbf{d} &\rightarrow d_j \rightarrow j\text{th day} \\ \mathbf{h} &\rightarrow h_k \rightarrow k\text{th hr} \end{aligned} \tag{9.2}$$

The second criteria proposed by the FEMA P-58/BD-3.7.8 (2008) to estimate the number of fatalities takes into account the variation of the peak population P as a function of the hour h_k, day d_j and month m_i of the year in which the seismic event occurs, and it is estimated with the following expression

$$n_d = \sum_{f=1}^{n_f} \left[\left(\frac{a_f}{\varphi} \cdot P_f \right) \cdot w_d \cdot w_m \cdot w_b \cdot w_a \mid IM \right] \tag{9.3}$$

where a_f corresponds to the area of the floor f measured in m^2, $\varphi = 92.9$ is a factor to convert $1,000$ ft^2 to m^2; P_f corresponds to the maximum peak population (occupants per 1,000 ft^2) as a function of building usage (see Table C.2, Appendix C); the factor w_d indicates the occupancy percentage as a function of the sampled d_j day; the factor w_m takes into account the occupancy percentage as a function of the randomly selected m_i month; the factors w_b and w_a were described above. The summation indicates the sum of fatalities resulting from the partial or total collapse at each floor of the building.

9.1.1 Criteria proposed to estimate the number of fatalities and injuries

In this thesis, a criteria similar to the approximation made with Eq. 9.3 to estimate the number of casualties is ised. The difference is that the approximation proposed here does not take into account the probability of each collapse mode, but simply assumes, under a conservative judgment, that the number of people occupying the building at the time of the seismic event that causes the structural collapse, *i.e.*, LS_6, causes the 100% loss of life. Also, to account for the fact that the maximum occupancy at each floor f may vary between 80 and 100 percent at the instant the seismic event occurs, a random factor $\delta_f \sim u(0.8, 1.0)$ with uniform probability distribution is used. In other words, although all floors have the same type of use, with the factor δ_f it is considered that each floor can have a different number of users. With these modifications Eq. 9.3 is written as follows:

$$n_d = \sum_{f=1}^{n_f} \left[\left(\frac{a_f}{\varphi} \cdot P_f \cdot \delta_f \right) \cdot w_d \cdot w_m \cdot w_b \mid LS_6, IM \right] \tag{9.4}$$

The approximations proposed by the FEMA P-58/BD-3.7.8 (2008) do not allow estimating the number of people who experience minor or severe injuries. This is because there is very little systematically documented information in past destructive earthquakes regarding the number of people experiencing any type of injury. However, the following expression is proposed in this work to estimate the number of people suffering any type of injury (whether minor, moderate, serious, severe or critical) given that at least one element of a prescribed performance group experiences severe damage,

$$n_i = \sum_{f=1}^{n_f} \left[\left(\frac{a_f}{\varphi} \cdot P_f \cdot \delta_f \right) \cdot w_d \cdot w_m \cdot (w_{e,f} \mid PG) \mid LS, IM \right] \tag{9.5}$$

In this equation, $w_{e,f}$ represents the fraction of elements located in plant f of a prescribed performance group PG that experience severe damage. Note that, for this case the fatality rate w_b is not considered. By definition, injured users can only occur in seismic realizations corresponding to the LS_1 to LS_5. This criterion is similar to the relationship studied by Shoaf *et al.* (2005) between the ATC-20 (1989) tagging and the percentage of people injured as a result of damage caused by the 1994 Northridge earthquake. The difference is that in this proposal the functionality limit states take into account the performance of the non-structural elements and contents, while in the data used by Shoaf *et al.* (2005) only the result of the structural inspection was used.

9.2 The economic equivalent value of injuries and deaths

The equivalent economic value associated with injuries and deaths caused by the damage induced by earthquakes on the buildings is one of the most important aspects of seismic resilience. In order to increase the recovery capacity of an injured person, that is, his or her resilience, it is first necessary to estimate the probable economic value of the medical treatment of the patient in question. Estimating this amount is of great importance in establishing policies to create economic funds for use in catastrophic events. Unfortunately, this is another problem that is poorly investigated in earthquake engineering, mainly because of the scarcity of this type of data.

In order to define regulatory actions and establish criteria to reduce risk, it is common for insurers and governmental entities to assign a monetary value to the type of injury and probable medical treatment that an injured person may receive. The US Department of Transportation through the Urban Institute (1991) conducted a statistical study in which they determined the economic value (in US dollars) that would be gained by avoiding an injury, whether fatal or non-fatal, regardless of the type of accident or event that caused it. In this context, injuries are referred to as statistical injuries, and are used to define the injury that an unknown person may suffer in the future. In this regard, the Association for the Advancement of Automotive Medicine (AAAM, 2001) developed a system to identify the type and level of severity of a statistical injury. This system was named the Abbreviated Injury Severity (AIS) code, and is comprised of a catalog of approximately 1,300 injury types.

Table 9.3: Federal values of statistical deaths and injuries avoided, in 1994 US$ (Porter *et al.*, 2006).

AIS scale	Level	Sample injuries (AAAM, 2001)	Treatment (FHWA, 1994)	Comprehensive Cost US dollars
1	Minor	Shoulder sprain, minor scalp laceration, scalp contusion	ST, OHTR, EDTR	$5,000
2	Moderate	Knee sprain; scalp laceration > 10 cm long and into subcutaneous tissue; head injury, unconscious < 1 hr	OHTR, EDTR, HNTC	$40,000
3	Serious	Femur fracture, open, displaced, or comminuted; head injury, 1-6 hr unconsciousness; scalp laceration, blood loss > 20% by volume	HNTC	$150,000
4	Severe	Carotid artery laceration, blood loss > 20% by volume; Lung laceration, with blood loss > 20% by volume	HTC	$490,000
5	Critical	Heart laceration, perforation; cervical spine cord laceration	HTC/DH	$1,980,000
6	Fatal	Injuries that immediately or ultimately result in death.	DH/DA	$2,600,000

Notes: Self treat (ST), Out of hospital treat and release (OHTR), Emergency department treat and release (EDTR), Hospitalized non-trauma cases (HNTC), Hospitalized trauma cases (HTC), Die in hospital (DH) and Dead on arrival (DA).

Table 9.3 (taken from the work done by Porter *et al.* (2006)) indicates the type of lesions most observed during the Whittier Narrow, Loma Prieta and Northridge earthquakes,

reported by Shoaf *et al.* (2005). These injuries were matched based on their level of severity with the classification established in the AIS. Also, the Federal Highway Administration (FHWA, 1994) established a generic criterion for assigning the type of medical treatment needed to treat some type of injury based on its severity, *i.e.*, the AIS classification. For example, suppose a person suffers a moderate injury (AIS2), say, a sprained knee. For this case there are three possible treatments: out of hospital treat, emergency department treat and hospitalized non-trauma. The medical intervention that a person should receive does not depend on the event causing the injury, but only of its severity. The type of treatment of an injured person is likely to receive is critical to establishing emergency protocols during these events. For example, identifying the number of beds available to treat severe or critical injuries in one or more hospitals near the disaster zone can be very useful in controlling and mitigating this type of risk. On the other hand, column 5 of Table 9.3 indicates the economic value assigned to cover the medical treatment of such injuries (Urban Institute, 1991). It should be noted that the equivalent values established by the Urban Institute (1991) were originally obtained for the purpose of quantifying the equivalent economic value of injuries caused by automobile accidents; however, these values have been used to assign the economic value to an injury regardless of the event that caused it.

In this context, one of the few studies relative to the equivalent cost associated with the fatal and non-fatal injuries registered, again, as a result of the 1994 Northridge earthquake was performed by Porter *et al.* (2006). The estimated economic value of the injuries caused by this earthquake was \$1.3 to 2.2 billion in 1994 US dollars. This amount is approximately 3-4% of the estimated \$50 billion in direct economic losses and business interruption. This means that if the economic value of an event with the characteristics of the 1994 Northridge earthquake had been previously estimated, an economic fund of at least \$2.2 billion dollars (taking a conservative criterion) would have been available, at least, from the U.S. government and insurance companies. It should be noted that the estimated cost associated with non-fatal injuries was 96%, mainly caused by non-structural elements, while 1% of the equivalent economic cost corresponds to injuries caused by structural elements. The 1994 Northridge earthquake is considered a moderate magnitude event, so this is an example of how earthquakes of this magnitude can be not only deadly, but also costly (Porter *et al.*, 2006).

9.2.1 Criteria proposed to quantifying the economic equivalent value of fatal and non fatal

To estimate the economic equivalent value caused by structural, non-structural or contents damage, the number of people who experience a fatal or non-fatal injury, estimated with Eqs. 9.4 and 9.5., will be related to one of the equivalent costs indicated in Table 9.3 through the level of severity of the injury suffered. The methodology proposed in this thesis does not allow to determine the type of statistical injury that an unknown person can suffer due to the damage experienced by a specific element that integrates a building,

so this will be determined by random sampling, that is, of the five possible levels of injury that a person can experience $\mathbf{l} = (l_1, ..., l_6)$, one will be selected at random sampling,

$$\mathbf{l} \rightarrow l_g \rightarrow g\text{th level of injury} \tag{9.6}$$

This criterion is analogous to that proposed by the FEMA P-58/BD-3.7.8 (2008) for estimating the date and time at which a seismic realization occurs. This random selection process must be repeated for each person who experiences an injury; therefore, the equivalent economic value of people injured is approximated by the following expression,

$$EEV_{INJ} = \sum_{f=1}^{n_f} \sum_{i=1}^{n_i} [\gamma \cdot v_{f,i} \cdot Pr(L = l_g) \mid LS, IM] \tag{9.7}$$

where $v_{f,i}(l_g)$ is the economic cost to treat the injury suffered by the ith individual on the f floor. The term γ is a factor that takes into account the inflation of the value of 1994 U.S. dollars to an equivalent value on the date the analysis is performed. The term $Pr(L = l_g)$ corresponds to the probability of selecting a lesson type among the six possibilities, *i.e.*, $Pr(L = l_g) = 0.167$ (1/6) for the LS_3 to LS_5 because in this conditions is probable that a user lose the life, and $Pr(L = l_g) = 0.20$ (1/5) for the LS_1 to LS_2 because in these conditions, by definition, the occupants only can suffer a lesion. Under this criterion it is possible to consider the option of a person losing his/her life without necessarily the building experiencing structural collapse. Again, by definition, the equivalent value of an injured person is associated only with seismic realizations corresponding to one of the $LS_1, ..., LS_5$. Eq. 9.7 is similar to the one used by Porter *et al.* (2006). The difference is that the expression proposed here takes into account the uncertainty associated with the random selection of a specific injury, whereas the deterministic expression used by Porter *et al.* (2006) used the number of people who lost their lives or suffered a fatal or nonfatal injury in a real seismic event.

The economic value equivalent to the number of human lives lost is estimated with the following expression, which is similar to Eq. 9.7,

$$EEV_{DEA} = \sum_{f=1}^{n_f} \sum_{d=1}^{n_d} [\gamma \cdot v_{f,d} \mid LS_6, IM] \tag{9.8}$$

Note that the seismic realizations that cause immediate loss of life are associated only with the collapse of the structural system, that is, with the LS_6.

The equivalent economic values proposed by the Urban Institute (1991) are deterministic, that is, they do not correspond to a probability distribution, so the approximation made by Eqs. 9.7 and 9.7 does not take into account the uncertainty associated with the cost assigned to each injury or loss of life. However, it is possible to take into account to some extent the uncertainty of the equivalent economic value. In the first instance the uncertainty originates from the estimate of the variable number of people experiencing a

type of injury in each seismic realization, conditional on the $LS_1, ..., LS_5$, and the number of people losing their lives in the LS_6. Then if the medical treatment selected for each injured person is performed by random sampling (Eq. 9.6), the equivalent cost will also be uncertain. Finally, the expected value and the total uncertainty, *i.e.*, the standard error, of the economic value associated with the potential number of fatal and nonfatal injuries will be approximated by means of the bootstrap technique, as will be described in Chapter 10.

9.3 Quantification of total economic losses

The total economic losses generated in each seismic realization s, conditioned to a LS and an IM, will be estimated as the algebraic sum of the random variables: (1) repair costs of structural, non-structural and furniture elements, (2) indirect economic losses, due to the loss of business during the time it takes for the building to recover its functionality, (3) economic value equivalent to the number of injuries and loss of life produced by the damage within the building:

$$EL_T = (C_{REP} + I_{EL} + EEV_{INJ} + EEV_{DEA} \mid LS, IM) \tag{9.9}$$

The expected value of the sample mean of total economic losses $\mathrm{E}[EL_T \mid IM]$ and its corresponding standard error will be estimated using the bootstrap technique, as will be described in the next chapter.

Chapter 10

The bootstrap technique

The way to express the DVs that compose the methodology to approximate the seismic resilience in a holistic way will be through the analytical construction of vulnerability functions, as shown in the Fig. 10.1. In general terms, a vulnerability function expresses the expected value of a given decision variable $E[DV \mid IM]$ as a function of a set of IMs:

$$V_f\left(IM, \mathrm{E}[DV \mid IM]\right) \tag{10.1}$$

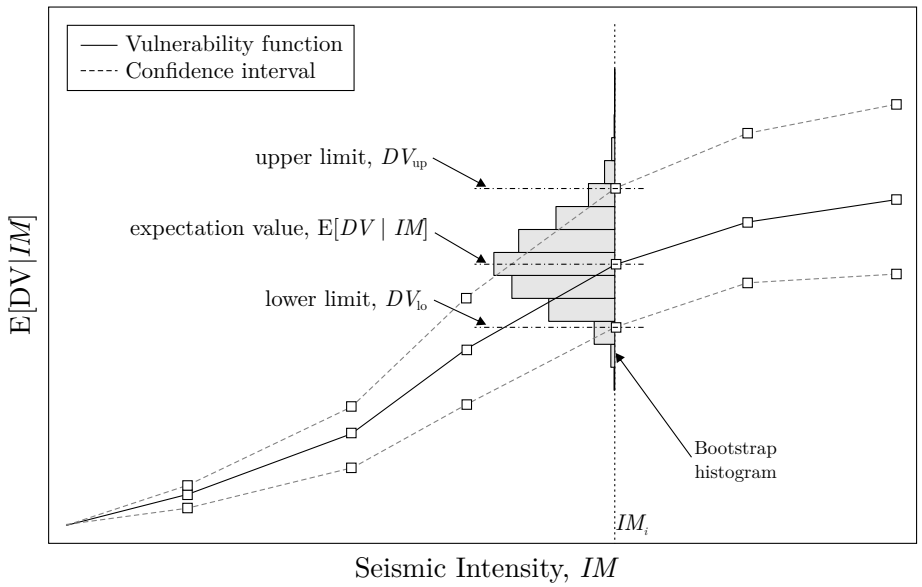

Figure 10.1: Schematic representation of the vulnerability function together with the confidence interval $(\hat{\theta}^*_{\mathrm{lo}}, \hat{\theta}^*_{\mathrm{up}}|IM)$.

To approximate the expected value of each DV associated to each IM, the statistical inference technique *bootstrap* will be used. This technique was developed by the American statistician Bradley Efron in 1979 in order to approximate the standard error $\widehat{\mathrm{se}} \approx \sigma$ underlying the estimation of the expected value $\hat{\theta}$ of a function of interest $s(\cdot)$ corresponding

to a random sample $\mathbf{x} = (x_1, x_2, ..., x_n)$ of size n, when n is small, that is, when the conditions characterizing the Central Limit Theorem and the Strong Law of Large numbers are not satisfied (see Appendix A).

The bootstrap technique is a special type of Monte Carlo simulation that distinguishes itself by not requiring a large amount of abstract and complex mathematical developments. On the contrary, it is a technique based entirely on relatively simple repetitive computational calculations. Moreover, this technique is of a general approach, so it is possible to apply it to almost any problem, regardless how complex it may be, as is the case of the research work of this thesis.

The term *bootstrap* was taken by Efron (1979) from the phrase *to pull oneself up by one's bootstrap* from the eighteenth-century stories entitled *The Adventures of the Baron of Munchausen* by the German writer and scientist Rudolph Erich Raspe. The use of this name is due to the fact that, although the sample size of the random variable is not large enough and the underlying problem appears to be very complex, and it is apparently not possible to perform reliable statistical inference, the bootstrap provides the necessary elements to make the data *come alive*, metaphorically speaking. That is, with the random resampling technique and special data processing it is possible to make statistical inferences reaching even better results than those that would be obtained with conventional techniques, for example, with the method of moments or the maximum likelihood method. In the next chapter this fact will be demonstrated with the application example of the methodology proposed in this thesis.

Although the bootstrap technique was initially conceived in order to better estimate the standard error $\widehat{\text{se}}$ associated with the computation of a parameter $\hat{\theta}$ underlying a random sample representative of a population, it is in the approximation of confidence intervals $\hat{\theta} \in (\hat{\theta}_{\text{lo}}, \hat{\theta}_{\text{up}})$ where this method is particularly powerful. This is because the maximum likelihood method (which is the method used by excellence in almost any practical and theoretical application of statistical inference) provides inaccurate results when the sample size n of a random variable is small.

Strictly speaking, the expected value $E[DV \mid IM]$ constitutes a random variable with large uncertainties, so it is not entirely convenient to express the results of the vulnerability functions only by means of the mean $\hat{\mu}_{DV}$ as a function of a set of IMs. A rational and objective way to express the vulnerability functions, independent of the sample size and the problem of interest, is to express the expected value together with its confidence interval, constrained to a specific probability. Confidence intervals provide more and better information than just the first two statistical moments. A vulnerability function and bootstrap confidence intervals of the expected value of a DV are illustrated in Fig. 10.1. In general terms, the confidence interval can be expressed by the following expression:

$$\text{E}[DV \mid IM] \in (DV_{\text{lo}}, DV_{\text{up}} \mid IM) \tag{10.2}$$

where DV_{lo} and DV_{lo} are the lower and upper limits of the confidence interval of the expected value $\text{E}[DV \mid IM]$. These limits are associated with a certain probability, which

makes them objective information, whereas expressing the vulnerability function using only the E$[DV \mid IM]$ gives it a subjective character because the inherent uncertainty is not specified.

In the following sections is described with detail the way to approximate the expected value $\hat{\theta} \approx \theta$ and its confidence interval $\theta \in (\hat{\theta}_{\text{lo}}, \hat{\theta}_{\text{up}})$ of any function $s(\cdot)$ or numerical process operating on a random sample $\mathbf{x}$ of size n of which its probability distribution F is unknown, *i.e.*, the only information available is the data $\mathbf{x}$ itself, as in most real-world statistics problems.

10.1 The empirical probability distribution of a bootstrap sample

The idea behind the synthetic construction of an empirical bootstrap probability distribution $\hat{F}^*$ of either a random sample $\mathbf{x}$ or a statistical parameter $s(\mathbf{x})$ is very simple. Consider a random sample of size n of a random variable $\mathbf{x} = (x_1, x_2, ..., x_n)$, whose elements are independently observed and have the characteristic of being identically distributed,

$$\hat{F} \rightarrow \mathbf{x} = (x_1, x_2, ..., x_n) \tag{10.3}$$

A bootstrap sample $\mathbf{x}^*$ is defined as a sample constructed from the random selection with replacement of n observations taken from the original sample $\mathbf{x} = (x_1, x_2, ..., x_n)$. That is, several of the values contained in $\mathbf{x}^*$ can be selected more than once from $\mathbf{x}$, or even not selected at all. This process is known as bootstrapping random resampling. The empirical probability distribution $\hat{F}^*$ underlying $\mathbf{x}^*$ is also a random distribution, generated from $\hat{F}$, and the set of samples $\mathbf{x}^*$ is the bootstrap sampling distribution. The symbol "*" indicates that the variable in question is data obtained from a bootstrap random resampling. The symbol "$\hat{}$" refers to the fact that the parameter or function under study is an approximation of a real parameter or function, say, the mean $\hat{\theta} \approx \mu$, or the variance $\hat{\theta} \approx \sigma^2$, for example.

To construct the bootstrap sampling probability distribution of $\mathbf{x}^*$ simply generate B times the random resampling process with replacement from the original sample $\mathbf{x}$, as indicated in the following expression:

$$\begin{array}{ccccc}
\hat{F}^{*1} & \rightarrow & \mathbf{x}^{*1} & = & \left(x^*_{i_1}, x^*_{i_2}, ..., x^*_{i_n} \mid \mathbf{x}\right) \\
\hat{F}^{*2} & \rightarrow & \mathbf{x}^{*2} & = & \left(x^*_{i_1}, x^*_{i_2}, ..., x^*_{i_n} \mid \mathbf{x}\right) \\
\vdots & & \vdots & & \vdots \\
\hat{F}^{*b} & \rightarrow & \mathbf{x}^{*b} & = & \left(x^*_{i_1}, x^*_{i_2}, ..., x^*_{i_n} \mid \mathbf{x}\right) \\
\vdots & & \vdots & & \vdots \\
\hat{F}^{*B} & \rightarrow & \mathbf{x}^{*B} & = & \left(x^*_{i_1}, x^*_{i_2}, ..., x^*_{i_n} \mid \mathbf{x}\right)
\end{array} \tag{10.4}$$

The set of bootstrap replicates B constitutes a set of independent and identically distributed samples. In the latter equation the subscripts $(i_1, i_2, ..., i_n)$ correspond to a set of n integers generated from a uniform probability distribution $i \sim u(a, b)$ (where $a = 1$ and $b = n$, are the parameters of the uniform distribution). Each of the integers i in this set indicates the observation to be selected from the original sample $\mathbf{x}$ to generate a bootstrap sample $\mathbf{x}^*$.

By definition, since the sample $\mathbf{x}$ is generated by the empirical probability distribution $\hat{F}$, the probability of observing the value x_i^* within each set of bootstrap replications is

$$Pr\left(x_i^* = x_j \mid \mathbf{x}\right) = \frac{1}{n};\ \forall\, i, j \in n \tag{10.5}$$

That is, each observation has the same probability of being selected. Likewise, the empirical probability distribution of a sample is defined as follows

$$Pr(A) = \frac{1}{n}\sum_{i=1}^{n} I\left(x_i \leq x\right) \tag{10.6}$$

where $I(\cdot)$ is a function that indicates the event of interest for which we wish to estimate the probability A.

The bootstrap sampling probability distribution of a sample is defined by the set B of bootstrap replicates of $\hat{F}^*$. However, although this result is very helpful, it is not precisely the determination of the set of $\hat{F}^*$ that allows us to make inferences about the set $\mathbf{x}$. What allows us to make statistical inferences are the characteristics of the set of bootstrap replicates $\mathbf{x}^*$ evaluated by means of the principle *plug-in*, $t(F)$.

10.2 The plug-in principle

One of the main goals of statistical inference is to determine representative characteristics of the population to perform decision making analysis. The plug-in principle allows to approximate these properties, and together with the bootstrap resampling technique it is possible to estimate in an easy and simple way the empirical probability distribution not only of the statistical parameters, but also of any kind of function or numerical process underlying F, no matter how complex it may be. The plug-in principle is defined by the following equation:

$$\theta = t(F) \tag{10.7}$$

In this expression $t(\cdot)$ is a function operating on the probability distribution F, and may represent, for example, the numerical process for estimating the mean, median, a special combination between two random variables (*e.g.*, correlation coefficient), or even something more complex, say the procedure for computing the eigenvalues and eigenvectors.

Note that the function $t(\cdot)$ works on the population distribution function, so the θ parameters underlying F are the actual parameters of the probability distribution. However, this principle can also be applied to problems where only the empirical probability distribution $\hat{F} \rightarrow \mathbf{x} = (x_1, x_2, ..., x_n)$ is known,

$$\hat{\theta} = t(\hat{F}) \tag{10.8}$$

Since $\hat{F}$ is an approximation of F, $\hat{\theta}$ is also an approximation of θ. The plug-in principle only allows approximations, but how accurate are the $\hat{\theta}$ estimates? To answer this question, it is necessary to approximate the value of the standard error $\widehat{\text{se}}$ and the $\widehat{\text{bias}}$ of the parameter estimated $\hat{\theta}$.

10.3 The bootstrap estimate of standard error

The standard error is one of the most common measures for expressing precision in estimating a statistic $s(\mathbf{x})$. The estimation of the standard error $\widehat{\text{se}}$ in the bootstrap technique is similar to the estimation of the standard deviation $\hat{\sigma}$ in classical statistical inference. The main difference lies in the fact that in the bootstrap world it is possible to infer the empirical probability distribution of the standard error itself of any statistical function of interest $\widehat{\text{se}}(s(\mathbf{x}^*))$, or in general, of the estimation any function $t(\hat{F}^*)$ that operates on the bootstrap sampling distribution, while in the estimation of the standard deviation $\hat{\sigma}$ only a random sample $\mathbf{x}$ of the population, or at best (although very difficult to achieve in practice) of the entire population, is used. Then, the standard error $\widehat{\text{se}}$ in the bootstrap technique is also treated as an independent and identically distributed random variable, instead of a fixed value, as is the case for the standard deviation $\hat{\sigma}$.

Suppose that a sample $\hat{F} \rightarrow \mathbf{x} = (x_1, x_2, ..., x_n)$ of size n of an independent and identically distributed random variable x_i of which its probability distribution F is unknown, and one wishes to estimate a parameter $\hat{\theta}$ that gives relevant information about that sample, that is,

$$\hat{\theta} = s(\mathbf{x}) \tag{10.9}$$

This expression emphasizes the estimation of the value of a statistic from a sample $\mathbf{x}$, while Eq. 10.8 is applied in a more general context, *i.e.*, $t(\cdot)$ operates on a probability distribution function F. However, from a practical point of view one can say that $s(\cdot)$ is equivalent to the plug-in principle, which is useful when the bootstrap technique is implemented in a computer language.

The standard error $\widehat{\text{se}}$ associated with the approximation of the value of a statistic $s(\mathbf{x}^*) = \hat{\theta}^*$ operating on each bootstrap replicate of $\mathbf{x}$, is given approximately by the following expression invented by Efron (1979):

$$\widehat{\text{se}} = \left\{ \frac{1}{B-1} \sum_{b=1}^{B} \left[\hat{\theta}^{*b} - \hat{\theta}^{*}(\cdot) \right]^2 \right\}^{\frac{1}{2}} \tag{10.10}$$

where

$$\hat{\theta}^{*}(\cdot) = \frac{1}{B} \sum_{b=1}^{B} s(\mathbf{x}^{*b}) = \frac{1}{B} \sum_{b=1}^{B} \hat{\theta}^{*b};\ b = 1, 2, ..., B \tag{10.11}$$

Eq. 10.10 is similar to the one used to estimate the standard deviation $\hat{\sigma}$ of the sample of a finite population $\mathbf{x} = (x_1, x_2, ..., x_n)$ from the set of independent and identically distributed observations x_i with arithmetic mean $\bar{x}$,

$$\hat{\sigma} = \left\{ \frac{1}{n-1} \sum_{i=1}^{n} [x_i - \bar{x}]^2 \right\}^{\frac{1}{2}} \tag{10.12}$$

The difference is that in the bootstrap technique, Eq. 10.10 estimates the standard error of the population mean of a statistic $s(\mathbf{x}^*)$. The sample population in this case is constructed numerically through the plug-in principle $\hat{\theta} = t(\hat{F})$ applied B times over the original sample,

$$\hat{\boldsymbol{\theta}}^{*} = (\hat{\theta}^{*1}, \hat{\theta}^{*2}, ..., \hat{\theta}^{*B}) = \left\{ s(\mathbf{x}^{*1}), s(\mathbf{x}^{*2}), ..., s(\mathbf{x}^{*B}) \right\} \tag{10.13}$$

Taking the limit of $\widehat{\text{se}}$ when B tends to infinity gives the ideal bootstrap estimate of the standard error $\widehat{\text{se}}_F(\hat{\theta})$

$$\lim_{B \to \infty} \widehat{\text{se}}_B = \sigma \tag{10.14}$$

In other words, the standard error approximation via bootstrap is improved when replicates are increased. This is because in most applications of the bootstrap technique, the parameter of interest θ can be expressed as the expected value conditional on the original sample $\mathbf{x}$, or equivalently, as an integral with respect to the sampling distribution (Hall, 1992). In practice, Efron (1981) found that it is sufficient to use an order quantity of 50 to 200 bootstrap replicates to estimate the associated statistical error in estimating a parameter of interest. Nevertheless, when the problem consists of estimating confidence intervals the number of bootstrap replicates needed to obtain reliable results can reach the order of 1,000, or even more (Efron, 1987; DiCiccio and Efron, 1996; Efron and Narasimhan, 2018).

10.4 The bootstrap estimate of expected value

The expected value of the bootstrap sample mean of a statistic $s(\mathbf{x}^*)$, or, in general, of a function $h(\mathbf{x}^*)$, is given by the following expression

$$\mathrm{E}[h(\mathbf{x}^*)] = \hat{\theta}(\cdot) = \frac{1}{B}\sum_{b=1}^{B} h(\mathbf{x}^{*b}) \tag{10.15}$$

Effectively, the estimate of the expected value of a function $h(\cdot)$ operating on each bootstrap random sample of $\mathbf{x}$ is contained in the process of calculating the standard error $\widehat{\mathrm{se}}$, *i.e.*, Eq. 10.15 is the same as that of the expression 10.11. The function associated with the plug-in principle that estimates the expected value of a random sample $\mathbf{x} = (x_1, x_2, ...x_n)$ coming from an unknown probability distribution function F, is given simply by the well-known arithmetic average,

$$h(\mathbf{x}^*) = \bar{x}^* = \frac{1}{n}\sum_{i=1}^{n} x_i^* \tag{10.16}$$

In this regard, it is known that the mean $\bar{x}$ of a random sample has expectation $\hat{\mu}$ and variance $\hat{\sigma}$. In other words, the expectation of $\bar{x}$ is equal to $\hat{\mu}$ and the variance of $\bar{x}$ is $1/n$ times the variance of $\mathbf{x}$. The estimation of the expected value $\mathrm{E}[DV \mid IM]$ of the sample mean of the DVs will therefore be approximated by the mean of the bootstrap sampling distribution of that statistic, after all, in practical applications what is of interest is the expected value and the coefficient of variation of the DVs corresponding to each IM of interest (Esteva *et al.*, 1988).

The coefficient of variation $\widehat{\mathrm{cv}}$ is calculated in an analogous way as it is done in the classical theory of statistics,

$$\widehat{\mathrm{cv}} = \frac{\widehat{\mathrm{se}}(s(\mathbf{x}^*))}{\mathrm{E}[s(\mathbf{x}^*)]} = \frac{\widehat{\mathrm{se}}_B(s(\mathbf{x}^*))}{\hat{\theta}(\cdot)} \tag{10.17}$$

10.5 The bootstrap estimate of bias

Another measure that allows us to estimate the precision of an estimator $\hat{\theta}$ is the numerical difference between the bootstrap expected value of a statistic $\mathrm{E}[s(\mathbf{x}^*)]$ and the value of the statistic as a function of the original random sample $s(\mathbf{x})$. This difference defines the bias bootstrap of an estimator $\hat{\theta}$,

$$\widehat{\mathrm{bias}} = \hat{\theta}^*(\cdot) - s(\mathbf{x}) \tag{10.18}$$

In this expression, $s(\mathbf{x})$ belongs to the original random sample statistic $\mathbf{x} = (x_1, x_2, ..., x_n)$ generated by an unknown probability distribution F, or lacking that, from a function $s(\cdot)$. Likewise, it is easy to observe that the estimate of $\widehat{\text{bias}}$ can be obtained directly from the bootstrap process of the standard error $\widehat{\text{se}}$ calculation.

As it is desirable that the standard error $\widehat{\text{se}}$ of an estimator $\hat{\theta}^*$ will be small, it is also desirable that the bootstrap estimate of the $\widehat{\text{bias}}$ will be small. When the bias of an estimator is small it provides scientific objectivity in the process of statistical inference (Efron and Tibshirani, 1993). The bootstrap bias is of primary importance in the estimation of bootstrap confidence intervals since this parameter is the cause of skewness at the extremes of the confidence interval with respect to the expected value of a parameter $\hat{\theta}$.

10.6 The number of sample size n and the number of bootstrap replications B

It is easy to question the veracity of the bootstrap technique when the original sample size n is small because it may not be representative of the population F. The reason for this is that the bootstrap resampling process tends to repeat observations in small samples, and therefore, the inference of the statistic $\hat{\theta}$ tends to differ from the true parameter θ. Nevertheless, the bootstrap technique has been shown to give good results for both relatively small and large sample sizes (Chernick and LaBudde, 2011). This is because it is quite large the number of samples with replacement that can be formed from a relatively small sample $\mathbf{x}$ when there are no repeated x_i observations in the original sample. This fact was demonstrated by Hall (1992), through the number of possible combinations that can be constructed from the set $\mathbf{x} = (x_1, x_2, ..., x_n)$,

$$\mathrm{C}_n^{2n-1} = \binom{2n-1}{n} = \frac{(2n-1)!}{n!(n-1)!} \tag{10.19}$$

For example, for a sample of size $n = 20$, the total number of combinations with replacement that can be formed from $\mathbf{x}$ is $68,923,264,410 = 6.89 \times 10^{10}$. This number is very large. Even the probability that the value of a statistic $\hat{\theta}$ is repeated in the total set of random samples of size n that can be constructed from $\mathbf{x}$ begins to decrease exponentially as the sample size n begins to increase. This probability is calculated as the quotient between the number of permutations $n!$ and the number of samples that can be formed from a set of independent and identically distributed observations $\mathbf{x} = (x_1, x_2, ..., x_n)$,

$$p_n = \frac{n \cdot (n-1) \cdot (n-1) \cdot ... \cdot 2 \cdot 1}{n \cdot n \cdot n \cdot ... \cdot n} = \frac{n!}{n^n} \tag{10.20}$$

In other words, the sample that is most likely to be resampled is the original sample, with probability $p_n = n!/n^n$. Figure 10.2a shows how quickly this probability decreases as n begins to increase. It can be seen that for $n = 10$, $p_n = 3.62 \times 10^{-4}$, and $p_n = 2.3 \times 10^{-8}$

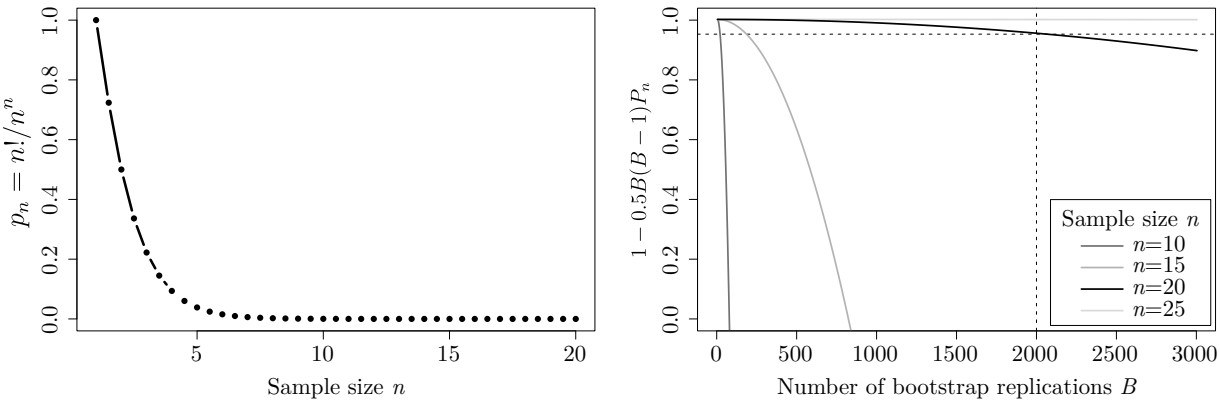

Figure 10.2: (a) Probability that the value of a statistic $\hat{\theta}$ associated each random sample that can be drawn from a sample $\mathbf{x}$ of size n is repeated considering that the observations x_i can be replaced. (b) Probability that no bootstrap random sample $\mathbf{x}^*$ is repeated, regardless of the order of the observations x_i^*, in the total set of bootstrap replicates B.

when $n = 20$. Such probabilities are practically negligible. It should be noted that this probability does not take into account the number of repeated replicates when the resampling is propagated with the bootstrap technique. If a number of B times the random resampling process is applied to the original sample $\mathbf{x}$, the probability that no sample $\mathbf{x}^*$ is repeated, regardless of the order of the observations x_i^*, is no greater than (Hall, 1992),

$$(1 - p_n)(1 - 2p_n)...[1 - (B-1)p_n] \geq 1 - \frac{1}{2}B(B-1)p_n;\ (B-1)p_n < 1 \qquad (10.21)$$

Figure 10.2b shows an application of Eq. 10.21 for $n = (10, 15, 20, 25)$ and $B = 1$ up to $B = 3,000$. It can be seen that for samples of size $n = 10$ and a small number of replicates B, the bootstrap technique fails. However, for $n = 15$ the probability that no bootstrap sample is replicated using $B = 500$ is greater than 0.6, and for $n = 20$, the probability that no bootstrap sample is replicated using $B = 2,000$ is greater than 0.9536. In other words, for the latter case, the probability that the same bootstrap sample is replicated is less than 0.0464. For $n = 30$ and $B = 2,000$, the probability that no bootstrap sample is replicated is approximately equal to 1. Therefore, it can be concluded that for $n \geq 20$ the bootstrap technique is reliable. This conclusion is very important because the number of times a bootstrap sample $\mathbf{x}^*$ is repeated is reflected in the bootstrap empirical probability distribution of a parameter of interest $\hat{\theta}^*$ and in the confidence interval approach. In general, the probability that one or more repetitions of the parameter $\hat{\theta}^*$ will occur tends to zero when $n \to \infty$.

10.7 Bootstrap confidence intervals

The bootstrap technique was developed in order to estimate the standard error $\widehat{\text{se}}$ with better precision when the available sample size is relatively small, giving very good results.

However, it is in estimating confidence intervals that the bootstrap technique has been most successful. As will be discussed below, this technique performs important corrections with respect to classical statistical approaches, and moreover, it does so automatically and without having to make any kind of theoretical modification for each new problem, no matter how complex it may be.

The conventional estimation of the confidence interval $(\hat{\theta}_{\text{lo}}, \hat{\theta}_{\text{up}})$ of a parameter $\hat{\theta}$ is based on the maximum likelihood theory developed by the English statistician and biologist Ronald A. Fisher in the 1920s. In order to use this approach it is necessary that the sample size n of the random variable in question must be large enough to satisfy the Central Limit Theorem and the Strong Law of Large Numbers. If these two conditions are met then each time the numerical model will be run the independent and identically distributed random variables x_i, it will be observed that $100 \cdot (1-\alpha)\%$ of the time the actual value of $\hat{\theta}$, no matter what the value of θ really is, will lie between the bounds of the confidence interval. If this condition is satisfied, then the bounds $(\hat{\theta}_{\text{lo}}, \hat{\theta}_{\text{up}})$ will be symmetric with respect to the expected value of $\hat{\theta}$, and the confidence interval can be expressed as follows,

$$\hat{\theta} \pm z^{(\alpha)} \cdot \hat{\sigma} \tag{10.22}$$

In this equation $\hat{\theta}$ is the maximum likelihood estimate of θ, $\hat{\sigma}$ is an estimate of the standard deviation, and $z^{(\alpha)}$ is the $100 \cdot \alpha$th percentile point of the standard normal distribution σ. For example, if one wishes to approximate the confidence intervals for a 95% probability, then $\alpha = 0.05$ and $z^{(0.05)} = -z^{(1-0.05)} = -1.645$. This results in

$$\theta \in (\hat{\theta} - 1.645 \cdot \hat{\sigma}, \hat{\theta} + 1.645 \cdot \hat{\sigma}) \tag{10.23}$$

It is easy to see that this confidence interval is symmetric. This approximation is widely used in practice because the values $\hat{\theta}$ and $\hat{\sigma}$ can be approximated with the point estimate of the arithmetic mean $\bar{x}$ and the standard deviation $\bar{\sigma}$, and the value of $z^{(\alpha)}$ can be easily obtained from the inverse function of the standard normal cumulative probability distribution $\Phi^{-1}(z)$ tabulated in most probability and statistics textbooks. The success of this approximation is due to the fact that under certain transformations and bias corrections it can be applied to any type of parametric distribution function. However, the confidence interval of Eq. 10.22 is far from providing reliable approximations because in practice it is difficult or economically costly to obtain a representative sample $\mathbf{x}$ of the population $\hat{F}$. As a consequence the confidence interval bounds are generally nonsymmetric, a product of the sample size $\mathbf{x}$ (DiCiccio and Efron, 1996).

The solution obtained from the maximum likelihood estimation is a first-order approximation. This can be easily seen in the following asymptotic expansion (Efron, 1987),

$$\hat{\theta} + \hat{\sigma} \cdot \left(z^{(\alpha)} + \frac{A_n^{(\alpha)}}{\sqrt{n}} + \frac{B_n^{(\alpha)}}{n} + \cdots \right) \tag{10.24}$$

where the higher order terms ($A_n^{(\alpha)}/\sqrt{n}+B_n^{(\alpha)}/n+\cdots$) are neglected by Eq. 10.22. In fact, the latter terms are those that consider the asymmetry of the bounds of the confidence intervals ($\hat{\theta}_{\text{lo}}, \hat{\theta}_{\text{up}}$) with respect to the expected value of $\hat{\theta}$, especially the second term since it exerts greater weight on the standard deviation $\hat{\sigma}$. Therefore, the intervals obtained using maximum likelihood theory should be considered as a first-order approximation, valid only when the sample size n is sufficiently large. As will be described later, the bootstrap technique allows to estimate confidence intervals with better precision.

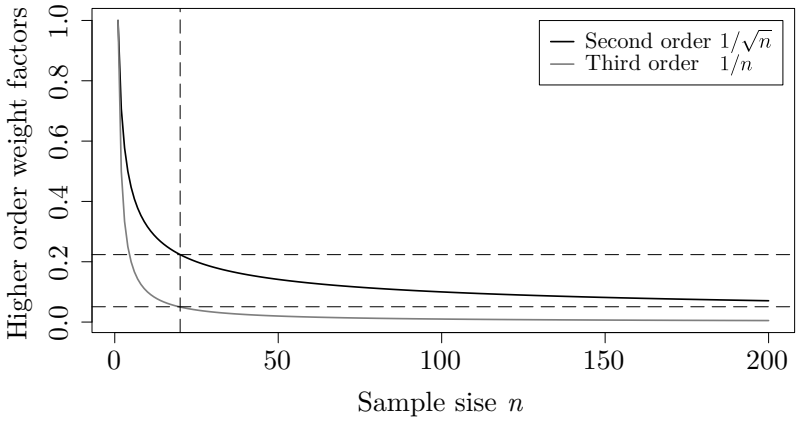

Figure 10.3: Weight factors associated with the second and third order terms ($A_n^{(\alpha)}/\sqrt{n}+B_n^{(\alpha)}/n+\cdots$) as a function of the size of an n sample of data that influence the estimation of confidence intervals ($\hat{\theta}_{\text{lo}}, \hat{\theta}_{\text{up}}$) of the expected value a $\hat{\theta}$ statistic.

Figure 10.3 illustrates the weight exerted by the second and third order terms as a function of the sample size n of an independently observed and identically distributed random variable x_i. It can be seen that in the estimation of the confidence intervals for a sample size $n = 20$ (dashed vertical line) a second order error of approximately 22% is present, while the third order error is 5%. Likewise, for samples of size $n < 20$ both errors start to increase exponentially, although the one associated with the third order term starts to become important when $n \leq 10$, that is, when the bootstrap technique is not reliable, as demonstrated in the previous section. In general, it can be concluded that for samples less than or equal to $n \leq 1,000$ a second-order correction is necessary (*i.e.*, $1/\sqrt{1,000} \approx 0.03$), and it can be assumed that for $n \geq 10,000$ the second-order correction can be omitted (*i.e.*, $1/\sqrt{10,000} \approx 0.01$). It can be concluded that for samples of size $n \geq 20$ the third-order correction can be neglected.

Using the bootstrap technique, it is possible to estimate not only better confidence intervals but also more precise ones (DiCiccio and Efron, 1996). Within this technique there are six variants to approximate such intervals: the standard normal method, the basic method, the studentized method, the percentile method, the BC_a method and the ABC method. In this research work, the BC_a method will be used because it is the one that offers the best results in practice (Efron, 1987; DiCiccio and Efron, 1996). The BC_a method makes two substantial improvements to the percentile method, the first being a bias correction and the second a correction to the standard error $\widehat{\text{se}}$. The BC_a method is able to automatically

perform a second-order approximation using only computational effort and non-complex equations.

10.7.1 Confidence intervals based on bootstrap percentiles

The BC_a approach has its basis in the percentile method, so it is convenient to describe it first. The percentile method is a computational algorithm that arises naturally from the empirical probability distribution bootstrap $\hat{G}^*$ of the estimation of the parameter $\hat{\theta}^{*b} = s(\mathbf{x}^{*b})$, $b = 1, 2, ..., B$. The bounds of the confidence interval of $\hat{\theta}^*$ are given by the $100 \cdot \alpha$ and $100 \cdot (1 - \alpha)$ percentiles of the empirical probability distribution $\hat{G}^*$ of the parameter $\hat{\theta}^*$, for the lower and upper bound, respectively. In other words, $(1 - 2\alpha)$ constitutes the empirical percentile interval of $\hat{G}^*(\hat{\theta}^*)$. Another way to obtain the lower and upper bounds is to select from the ordered set $\hat{\theta}^*$ the elements corresponding to the index $B \cdot \alpha$ and $B \cdot (1 - \alpha)$. Therefore, the percentile confidence interval of the expected value of the parameter $\hat{\theta}^*$ can be expressed as follows,

$$\left(\hat{\theta}_{\mathrm{lo}}, \hat{\theta}_{\mathrm{up}}\right) \approx \left(\hat{\theta}^*_{B \cdot \alpha}, \hat{\theta}^*_{B \cdot (1-\alpha)}\right)_{\mathrm{Per}} \tag{10.25}$$

The bootstrap distribution of $\hat{\theta}^*$ has the peculiar feature of performing a monotonic transformation $m(\cdot)$ automatically on the parameter of interest $\hat{\theta}^{*b}$ for each b (Efron, 1987; Hall, 1992), that is,

$$m(\theta) = \phi \therefore m(\hat{\theta}^*) = \hat{\phi}^* \tag{10.26}$$

This transformation, regardless of the shape of the empirical distribution of $\hat{F}$, leads to the bootstrap histogram of $\hat{\theta}^*$ acquiring the shape of the normal distribution with a high degree of approximation. This is known as *transformation-respecting*, and is equivalent to the transformation used by the maximum likelihood method to construct confidence intervals from a standard normal distribution and subsequently transform them to a parametric probability distribution that is non-normal. For example, $m(\cdot)$ is Fisher's z-transformation for the normal correlation coefficient, and for the Poisson distribution, $m(\theta) = \theta^{1/2}$ is used as the square root transformation. The monotonic transformation $m(\cdot)$ gives origin to the following expression,

$$\theta \in \left[m^{-1}(\hat{\phi} - z^{(1-\alpha)} \cdot c), m^{-1}(\hat{\phi} - z^{(\alpha)} \cdot c)\right] \tag{10.27}$$

where c is the standard deviation and $m(\cdot)^{-1}$ is the inverse transformation of $m(\cdot)$. Again, the $m(\cdot)$ transformation is performed automatically within the bootstrap computational algorithm through random resampling with replacement using the Monte Carlo technique and the computation of $\hat{\theta}^*$. This means that it is not necessary that the analyst explicitly knows the $m(\cdot)$ transformation because the bootstrap process performs the transformation by itself. Then the verification of the transformation $m(\hat{\theta}^*) = m^{-1}(\hat{\phi}^*)$ must necessarily

be through a comparison, *i.e.*, heuristically. For example, one way to test the capability of the percentile method is to compare the bounds obtained with it and those obtained using the standard intervals $\hat{\theta} \pm z^{(\alpha)} \cdot \hat{\sigma}$. Unfortunately, only in a very few special situations is it possible to obtain exact confidence intervals of a $\hat{\theta}$ parameter, and therefore, they can be used to compare the intervals obtained with the percentile method (DiCiccio and Efron, 1996).

It has been shown that the bootstrap percentile method provides good approximations when the parameter of interest is an unbiased parameter, *e.g.*, the mean; on the contrary, when it is a biased parameter the confidence interval bounds have to be shifted to the right or to the left, with respect to the expected value of $\hat{\theta}^*$. This discrepancy means that the percentile method does not produce an accurate coverage of the prescribed probability $(1-2\alpha)$ with which the calculation of the confidence interval is performed. This is, in effect, because $(1-2\alpha)$ constitutes a range of probabilities associated with a symmetric interval. It can then be concluded that the percentile method is a first-order approximation (Efron, 1987). The BC_a (bias-corrected and accelerated) approximation incorporates theoretical and practical changes to the percentile method, allowing second-order estimates of the confidence intervals of an estimator to be made automatically from a computational point of view.

10.7.2 Confidence intervals based on bootstrap BC_a method

The BC_a method, developed by Efron (1987) and DiCiccio and Efron (1996), also uses the percentiles of the bootstrap distribution of $\hat{\theta}^*$ to estimate its confidence interval; however, these percentiles do not have the same position as those used by the percentile method. This change is given by a constant $\hat{z}_0$ that corrects for bias and another constant $\hat{a}$ that considers the variation of the standard error in the estimation of $\hat{\theta}^*$. Like the percentile method, the confidence intervals can be obtained directly from the ordered set $\hat{\theta}^*$, by means of the elements corresponding to the indices $B \cdot \alpha_1$ and $B \cdot \alpha_2$, for the lower and upper bound, respectively. Then, the interval BC_a can be expressed as follows,

$$\left(\hat{\theta}_{\mathrm{lo}}, \hat{\theta}_{\mathrm{up}}\right) \approx \left(\hat{\theta}^*_{B\cdot\alpha_1}, \hat{\theta}^*_{B\cdot\alpha_2}\right)_{\mathrm{BC}_a} \tag{10.28}$$

The bootstrap percentiles α_1 and α_2 that approximate the probability interval $(1-2\alpha)$ are given by the following equation,

$$\alpha_{1,2} = \Phi\left(\hat{z}_0 + \frac{\hat{z}_0 + z^{(\beta)}}{1 - \hat{a} \cdot [\hat{z}_0 + z^{(\beta)}]}\right) \tag{10.29}$$

where $\beta = \alpha$ for the lower limit, and $\beta = 1-\alpha$ for the upper limit; $\Phi(\cdot)$ is the standard normal cumulative distribution function, $z^{(\beta)}$ is the classical percentile point of the standard normal distribution. The constant $\hat{z}_0$ is the responsible for correcting the bias by

the proportion of bootstrap values $\hat{\theta}^*$ smaller than $\hat{\theta}$. Roughly speaking, $\hat{z}_0$ measures the median of the bias of $\hat{\theta}^*$. Mathematically this ratio is calculated by the following equation,

$$\hat{z}_0 = \Phi^{-1}\left(\#\left\{\hat{\theta}^{*b} < \hat{\theta}\right\} \cdot B^{-1}\right) \tag{10.30}$$

where $\Phi^{-1}(\cdot)$ corresponds to the inverse function of the standard normal cumulative distribution. Note that $\hat{\theta}$ is calculated with the original sample $\mathbf{x} = (x_1, x_2, ..., x_n)$.

The acceleration constant $\hat{a}$ is so named because it refers to the rate of change of the standard error of $\hat{\theta}$ with respect to the true value of the parameter θ. In classical statistical theory the standard error $\widehat{\text{se}}$ remains constant for all θ. This constant is calculated as one-sixth of Pearson's skewness coefficient with respect to the mean of the original data sample $\mathbf{x}$, taking into account that this calculation is performed based on the jackknife technique[1], which is the predecessor of the bootstrap method. The constant $\hat{a}$ is calculated by the following approximation,

$$\hat{a} = \frac{1}{6} \cdot \frac{\sum_{i=1}^{n}\left[\hat{\theta}_{(\cdot)} - \hat{\theta}_{(i)}\right]^3}{\left\{\sum_{i=1}^{n}\left[\hat{\theta}_{(\cdot)} - \hat{\theta}_{(i)}\right]^2\right\}^{3/2}} \tag{10.31}$$

where

$$\hat{\theta}_{(\cdot)} = \frac{1}{n}\sum_{i=1}^{n}\hat{\theta}_{(i)} \tag{10.32}$$

In these summations the element x_i is removed from $\mathbf{x}$. In other words, the reduced jackknife data set is used,

$$\mathbf{x}_{i-1} = (x_i, x_2, ..., x_{i-1}, x_{i+1}, ..., x_n) \tag{10.33}$$

To this process corresponds the adaptation of Pearson's coefficient calculation to the jackknife technique, and the computation $[\hat{\theta}_{(\cdot)} - \hat{\theta}_{(i)}]$ are denoted as jackknife differences. Note that when $\hat{z}_0 = 0$ and $\hat{a} = 0$ the corrected percentiles of Eq. 10.29 reduce to those of the percentile method, *i.e.*, $\alpha_1 = \Phi\left(z^{(\alpha)}\right) = \alpha$ and $\alpha_2 = \Phi\left(z^{(1-\alpha)}\right) = 1 - \alpha$. In the practical problems $\hat{z}_0$ and $\hat{a}$ are nonzero, so the percentile method requires a second-order correction. Likewise, there are other ways to approximate the value of the acceleration constant $\hat{a}$; however, the criterion presented here is the one most commonly used in practice.

[1]The jackknife technique was developed by the British statistician Maurice Quenouille and the American statistician John W. Tukey to estimate the bias and standard error in the estimation of the value of a parameter θ. This technique is similar to the bootstrap in this respect; however, it has been shown that the latter gives better results in terms of bias and standard error estimation. Moreover, the bootstrap technique has been expanded to many fields of inferential statistics, for example, in regression problems, in the area of artificial intelligence (Efron and Hastie, 2016). There is even the Bayesian bootstrap version. Even to this day this technique continues refining and expanding.

To summarize, the BC_a method incorporates theoretical and practical advantages that make this method perform better than the classical methods. The first advantage refers to the fact that it respects the $\hat{F}$ transformation $m(\cdot)$ regardless of the type of function operating on the original sample $\mathbf{x}$. That is, the non-normality of the empirical distribution $\hat{F}$ is corrected by the bootstrap sampling distribution $\hat{G}^*$ by automatically recognizing the $m(\cdot)$ transformation during the bootstrap process. The second advantage of the BC_a method is that it covers with good accuracy the probability interval $(1-2\alpha)$. That is, being a second-order approximation, the probabilities that the value of θ lies between two extremes, say c_{lo} and c_{up}, $Pr(\theta > \hat{\theta}_{\text{lo}}) \approx \alpha + c_{\text{lo}}/\sqrt{n}$ and $Pr(\theta > \hat{\theta}_{\text{lo}}) \approx \alpha + c_{\text{lo}}/\sqrt{n}$ have a better approximation. In other words, this means that the error is reduced to zero with rate $1/n$ because this third order term is not taken into account by the BC_a approach. However, as described above, with the help of Fig. 10.3, this term can be neglected with respect to the effect exerted by the second-order term for samples of size $n \geq 20$.

The parametric and non-parametric bootstrap technique

There are two types of bootstrap inference, the parametric and the nonparametric. For the former the $\hat{\theta}$ parameters and the $\hat{F}$ probability distribution of the population are known. In contrast, in nonparametric inference the only information available to the analyst is the random sample $\mathbf{x}$, and hence, the empirical probability distribution $\hat{F}$, *i.e.*, we only know a portion of the total universe of observations of the underlying problem.

The bootstrap technique described until this point corresponds to the non-parametric technique. That is, any estimation performed during the process starts from the empirical probability distribution $\hat{F} \rightarrow \mathbf{x}$. The parametric bootstrap technique is not very different from the procedure presented above. The difference consist in that the bootstrap samples $\mathbf{x}^*$ are generated from a parametric probability distribution $f(\mathbf{x};\theta)$, rather than by randomly resampling with replacement of the elements of $\mathbf{x}$, where all are equally likely to be selected.

The problem with the parametric bootstrap is that the parameters defining the underlying probability distribution $\hat{\theta}$ must be known, a difficult task when the analyst has to make statistical inferences from small samples. The estimation of the parameters of a probability distribution is always accompanied by imposing biases or preconceptions, perhaps accurate, but also potentially misleading under certain circumstances (Efron and Tibshirani, 1993). In contrast, the empirical distribution is less biased and more transparent, and adapted to the bootstrap technique it is possible to estimate any kind of parameter $\hat{\theta}^* = t(\hat{F}^*)$ and its standard error $\widehat{\text{se}}$, no matter how complicated its numerical structure is, and moreover, without having to think about a particular probability distribution. The nonparametric version always has the same structure for any problem, while the parametric one differs from one application to another, resulting from the choice of the underlying probability distribution and the approximation of its parameters. Also, when the sample size n is large enough, and a probability distribution can be inferred to be used as the basis of the parametric bootstrap, the nonparametric bootstrap version gives similar or even better results than the parametric version (Efron, 1987; Efron and Narasimhan, 2018).

In this thesis, nonparametric bootstrap inference will be used to estimate the expected value E[$DV \mid IM$] of the DVs as well as their confidence interval $(\hat{\theta}^*_{\text{lo}}, \hat{\theta}^*_{\text{up}})$. This is because the nonparametric version is a general approach, while the parametric version requires information that the analyst may not be able to estimate, but only assume. In fact, the basis of the bootstrap technique was developed from nonparametric studies, demonstrating that in many cases, despite having the parameters of the distribution in question, it is better to assume that these are unknown because the conditions governing the parametric analysis often restrict the flexibility of the nonparametric technique, leading to inconsistent results.

The number of bootstrap replicates for estimating confidence intervals

In contrast to the number of bootstrap replicates needed to obtain standard errors with good approximation of the parameter $\hat{\theta}$, say 50 to 200, at least 1,000 bootstrap replicates with replacement are required to compute the confidence intervals $(\hat{\theta}_{\text{lo}}, \hat{\theta}_{\text{up}})$ to perform a second-order approximation (Efron, 1987). This difference is due to the fact that the α_1 and α_2 percentiles depend on the tails of the empirical probability distribution $\hat{G}^*$, where precisely fewer bootstrap observations of the parameter $\hat{\theta}^*$ are present. The bootstrap technique has the advantage of being an automatic algorithm, independent of the underlying problem, which allows estimating confidence intervals with greater precision, although it is 1,000 times computationally more expensive than the classical method (DiCiccio and Efron, 1996). To determine the number of bootstrap replicates needed to estimate the confidence intervals, the confidence interval limits $(\hat{\theta}^*_{\text{lo}}, \hat{\theta}^*_{\text{up}})$ of the sample mean $\hat{\theta}_{\mathbf{dv}}$ of each DV are used as a measure of stabilization. Then, the number B is estimated through an iterative scheme,

$$\left|\hat{\theta}^*_{\text{CI}_k}(B_i) - \hat{\theta}^*_{\text{CI}_k}(B_j)\right| \leq \varepsilon \rightarrow B_j;\ i < j \tag{10.34}$$

where ε is the error accepted as the convergence criterion, and the number of bootstrap replicates needed to perform the confidence interval analysis is B_j.

10.8 Approximation of the vulnerability function using the bootstrap method

The methodology to evaluate seismic performance in probabilistic terms proposed by PEER is composed of four large processes: (1) seismic hazard analysis, (2) structural analysis, (3) damage analysis and (4) decision variable analysis. The approximation of the seismic resilience of buildings damaged by the effect of potentially destructive earthquakes proposed in this thesis was introduced in the third and fourth stages of the PEER methodology, so it can be considered that the work presented in this thesis is an enrichment of the PEER methodology.

In summary, the methodology for assessing seismic rest (6) repair cost, (7) number of workers, (8) number of people injured, (9) number of casualties, (10) equivalent economic value associated with the number of injured persons, (11) equivalent economic value associated with the number of fatalities and (12) total economic losses. The DVs that produce the methodology proposed here comply with the definition of seismic resilience proposed by the MCEER (Bruneau *et al.*, 2003) and (Cimellaro *et al.*, 2006).

The bootstrap technique is applied to the sets of independent and identically distributed observations, $\mathbf{dv} = (dv_1, dv_2, ..., dv_{ns} \mid IM)$, obtained with the proposed methodology to approximate the seismic resilience of buildings, to approximate its inherent uncertainty. The uncertainty will be expressed by means of the bootstrap confidence interval BC_a, $\theta_{\mathbf{dv}} \in (\hat{\theta}^*_{\mathrm{lo}}, \hat{\theta}^*_{\mathrm{up}} | IM)$, of the expected value of each DV conditioned to an IM, $\mathrm{E}[s(\mathbf{dv}^*)|IM]$. For this purpose, it is assumed that the probability distribution F that generates such observations is unknown, that is, the only information available to the analyst is the random sample itself $\mathbf{dv}$ and its empirical probability distribution $\hat{F}$.

This assumption is very important in the proposed methodology because (1) the process that generates the DVs is very complex, and (2) the number of observations is not large enough to try to obtain a probability distribution of the DVs. As a consequence, trying to derive an analytical probability distribution function or exact confidence intervals for each of the DVs for each IM, can be a rather complex and laborious mathematical process, taking into account also that each DV has its own behavior. It is even possible that under these circumstances such probability distributions functions do not exist. This is why the bootstrap simulation scheme is very attractive. All the mathematical processing necessary to derive analytical expressions is delegated to the bootstrap simulation technique and the computer, leaving the stakeholder to analyze the results and make decisions. Moreover, although the number of bootstrap replications needed to obtain reliable confidence intervals can be large, the computational demand for calculating confidence intervals is far less than that needed to perform the same amount of NLDA.

10.8.1 Expected value approach of the decision variables conditioned to the functionality limit states *LS* and the seismic intensity *IM*

Consider the set of observations of a specific $(\mathbf{dv} \mid LS, IM)$, obtained using the seismic resilience simulation methodology proposed in this document,

$$\hat{F} \rightarrow \mathbf{dv} = (dv_1, dv_2, ..., dv_z \mid LS, IM) \tag{10.35}$$

The bootstrap sampling distribution $\hat{F}^*$ is obtained from the number of bootstrap replicates selected with replacement from the original sample of a particular $\mathbf{dv}$,

$$\hat{F}^* \rightarrow \mathbf{dv}^{*b} = \left(dv^*_{i_1}, dv^*_{i_2}, ..., dv^*_{i_z} \mid \mathbf{dv}, LS, IM\right); \quad b = 1, 2, ..., B \tag{10.36}$$

The expected value of the sample mean of a specific DV is approximated by Eq. 10.15. The plug-in principle in this case corresponds to the arithmetic average of the set of bootstrap replicates $\mathbf{dv}^*$ applied to the fourth stage of the PEER approximation. The vulnerability function $V_f(\cdot)$ is constructed from the bi-univocal relationship between each IM considered in the seismic resilience analysis, and the expected value of each DV, $\hat{\theta}^*_{\mathbf{dv}}(\cdot)$, conditioned to a LS and an IM,

$$V_f\left(IM, \left[\hat{\theta}^*_{\mathbf{dv}}(\cdot) \mid LS, IM\right]\right) \tag{10.37}$$

The results obtained with these expressions are useful when it is desired to know the seismic resilience associated to each LS, that is, the consequences derived from a specific configuration of the severity of the damage experienced by the structural, non-structural and furniture elements. The LSs help to identify the most probable damage patterns given an IM, keeping in mind that given the large uncertainties associated with each IM it is very likely that a great variety of configurations and damage levels (within a certain range) will be present. However, the effective vulnerability function is the one that takes into account the losses associated with each limit state $LS_1 \cap ... \cap LS_6$ together given an IM, that is, without distinguishing which LS produces them, but only which level of IM. In other words, the effective vulnerability function expresses the total losses as a function of seismic demand. In this respect, conventional risk analysis, *e.g.*, Porter (2000); Mitrani-Reiser (2007), FEMA P-58-1 (2012a), does not take into account any of these LSs explicitly, but only the consequences of a seismic demand.

10.8.2 The expected value and its confidence intervals of the decision variables conditioned to an *IM*

Since the LSs are mutually exclusive and collectively exhaustive events, the contribution of losses corresponding to each DV conditioned only to an IM can be quantified by the sum of the expected value of $\hat{\theta}^*_{\mathbf{dv}}(\cdot)$ obtained for each LS, conditioned to a specific IM. Then, the effective vulnerability function is defined by the following expression,

$$V_f\left(IM, \sum_{j=0}^{n_{ls}} \hat{\theta}^*_{\mathbf{dv}}(\cdot) | LS_j, IM\right) \tag{10.38}$$

Another way to obtain the effective vulnerability function is grouping the observations $\mathbf{dv}_j = (dv_1, dv_2, ..., dv_{z_i} | LS_j, IM)$ that conform each condition (LS_j, IM), $j = 0, 1, 2, ..., n_{ls}$, into a single set of observations,

$$\mathbf{dv} = (\mathbf{dv}_{1\times z_1}, \mathbf{dv}_{1\times z_2}, ..., \mathbf{dv}_{1\times z_n} | IM) \tag{10.39}$$

where z_n denotes the dimension of the vector $\mathbf{dv}_{1\times z_n}$, *i.e.*, the number of observations that produced the LS_j given an IM. In other words, each set of observations $\mathbf{dv}_{1\times z_n} | LS_j, IM$,

$j = 0, 1, ..., n_{ls}$, represents a partition of the total set of observations $\mathbf{dv}|IM$. The summation of the number of observations obtained at each LS corresponds to the number of NLDA performed at each IM. A schematic representation of the vulnerability function together with its confidence interval $(\hat{\theta}^*_{\text{lo}}, \hat{\theta}^*_{\text{up}}|IM)$ is illustrated in Fig. 10.4. A bootstrap histogram of the replicates $\hat{\theta}^*_{\mathbf{dv}}$ is also illustrated, in which it can be seen that the confidence interval bounds are not symmetric.

The vulnerability function expressed together with the confidence intervals of the sample mean is defined by the upper and lower bounds of a DV given an IM,

$$V_f \left(IM, \theta_{\mathbf{dv}} \in \left[\hat{\theta}^*_{\text{lo}}, \hat{\theta}^*_{\text{up}}|IM \right]_{\text{BC}_a} \right) \tag{10.40}$$

In this regard, in order to reduce the computational demand associated with the three-dimensional NLDA in the Chapter 4 the use of a small number of synthetic seismic record pairs was specified and justified. In particular, 20 pairs of seismic synthetic records are used in this work for each IM, and therefore, each DV has a set of 20 independent and identically distributed observations at each return period considered. Then, using Eq. 10.19, for $n = 20$, the number of distinct samples with replacement that can be formed is 68,923,264,410. The probability that a sample $\mathbf{dv}$ will be repeated within the number of possible combinations is $p_n = n!/n = 20!/20 = 2.3 \times 10^{-8}$ (calculated with Eq. 10.20). And the probability that no bootstrap sample $\mathbf{dv}^*$ repeats, for $B = 2,000$, regardless of order of the bootstrap observations, *i.e.*, yields the same value, is no greater than $1 - 0.5B(B-1)p_n = 1 - 0.5 \cdot 2,000 \cdot (2,000 - 1) \cdot 2.3 \times 10^{-8} = 0.9536$, calculated with Eq. 10.21.

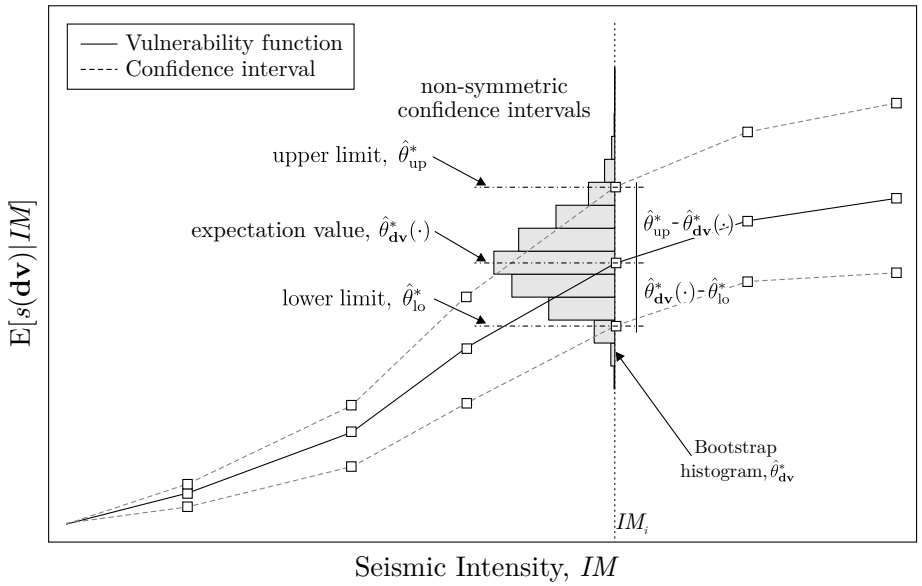

Figure 10.4: Schematic representation of the vulnerability function together with the confidence interval $(\hat{\theta}^*_{\text{lo}}, \hat{\theta}^*_{\text{up}}|IM)$.

Chapter 11

Numerical example

The September 19, 2017 earthquake of magnitude M_w 7.1 that occurred between the states of Puebla and Morelos at a depth of 57 km, and approximately 120 km from Mexico City (CDMX), caused in this the collapse of 44 low to medium height buildings, something that caused the loss of life of 228 people. Most of these buildings were between one and ten stories high, and were located in the transition zone of the Valley of Mexico. Sixty-four percent (28/44) of the collapsed buildings were 1 to 5 stories and 36% (16/44) were between 6 and 10 stories. Also, 20% (9/44) of these collapses were reinforced concrete (RC) and unreinforced masonry (URM) buildings and 9% (4/44) were confined masonry (CM) buildings. A significant number of the buildings that did not collapse, but were damaged, had construction characteristics similar to those of the buildings that experienced collapse (Galvis *et al.*, 2017).

A team of researchers and engineers from the Earthquake Engineering Research Institute (EERI), directed by Prof. Deborah Weiser, conducted a post-seismic evaluation of 713 buildings located around 13 accelerometer stations in the CDMX valley. The objective of this study was to correlate the level of damage observed [1] (null DS_0, slight DS_1, moderate DS_2 and severe DS_3, DS_4) with the different levels of recorded seismic intensity, duration of ground shaking, soil characteristics and construction characteristics of the evaluated buildings. For this purpose, buildings located within a 300 m radius of each accelerometer station considered in the study were inspected.

[1] In the post-seismic inspection performed by Weiser *et al.* (2018) the following convention was established to define the global damage states. DS_0-no observed earthquake-related damage. No repairs would be required. DS_1-minor (mostly cosmetic) damage. This damage typically involves minor cracks in masonry or concrete elements and/or minor damage to exterior non-structural components (ornamentation, facades, windows, etc.). Repairs would be localized and consist of patching/painting cracks and repairs to non-structural components. DS_2-moderate structural damage. This damage typically involves wider cracks and spalling in masonry or concrete elements. Cracks can be repaired in place by routing and repointing grout masonry walls, and patching/epoxy injecting cracks in concrete walls. DS_3-severe damage. This damage involves severe shear cracks in masonry and concrete elements. Residual drift of a story may be present. Repair of damaged elements in place may not be economical. DS_4-partial or complete collapse.

Of the 713 buildings inspected by Weiser *et al.* (2018), 553 were buildings constructed of RC with CM/URM infill walls. Seventy-four percent (110/553) of these buildings experienced no damage; however, 19 of the 553 (3%) experienced severe damage (DS_3) and 2% (15/553) experienced partial collapse, *i.e.*, DS_4. Also, of these 19 and 15 buildings, 13 (68%) and 13 (87%) of them, respectively, were built before the 1985 Michoacán earthquake of magnitude M_w 8.1. Then, 6 (32%) and 2 (13%) of the latter amounts, respectively, were built after this earthquake.

It is important to note that 26% (186/713) of the buildings between 1 and 9 stories inspected experienced one of the damage states DS_1-DS_4. The 80% of the 186 buildings (148/186) experienced minor and moderate damage, *i.e.*, DS_1 and DS_2, respectively. Of these 148 buildings, 60 (41%) were between 1 and 3 stories; while 88 buildings (59%) were between 7 and 9 stories. Twenty percent (38/186) suffered severe damage (DS_3) and partial collapse (DS_4). Of these 38 buildings, 29 (75%) were buildings between 4 and 9 stories in height. Of these buildings, 29% (11/38) were commercial and office buildings, while 61% (23/38) were residential. The remaining 10% (4/38) were government buildings. Also, 90% (34/38) of the buildings that experienced DS_3 and DS_4, were constructed of RC and URM infill walls. On the other hand, 30% (11/38) of the buildings that experienced severe damage and partial collapse were constructed after the 1985 Michoacán (Mexico) earthquake, and the remaining 70% (27/38) were constructed prior to this earthquake.

It is convenient to point out that after the 1985 earthquake, and before the earthquake of September 19, 2017, two updates[2] to the CDMX building regulations were issued, *i.e.*, the GDF (1987) and the NTC-DS (GCDMX, 2004a), in which the guidelines obtained from the technological advances developed during that period were presented. Although there were important damages and collapses of buildings designed with regulations subsequent to the 1985 earthquake, it was concluded that these collapses were caused by inadequate detailing of the reinforcement of structural elements and also due to deficiencies in the construction processes.

The events that occurred on September 19, 2017 described through the statistics shown above demonstrate that the most affected buildings (both, those that were damaged and those that collapsed) were those constructed of RC with URM/CM infill walls. Moreover, the largest percentage of these buildings are between 4 and 9 stories high, *i.e.*, 59% (60/148) of those that developed DS_1 and DS_2; and 76% (29/38) of those that experienced DS_3 and DS_4.

In order to exemplify the proposed methodology for estimating the seismic resilience of buildings and because of the facts described above, this chapter presents the seismic resilience assessment of a hypothetical seven-story RC with URM building for office use. Although the number of damaged buildings with these characteristics was not excessively large, the indirect economic losses resulting from these events were significant. Also, as will be seen below, the economic value derived from people being injured and/or losing their lives can be much more costly than thought. The following sections describe the

[2]The last update of the CDMX Building Code (GCDMX, 2017) was made in December 2017; however, this update was not made because of the earthquake of that same year, this fact was simply a coincidence.

building characteristics and the results of the seismic resilience assessment of the building in study.

11.1 Description of the building to be evaluated using the proposed methodology

For illustrative purposes, it is considered that the use of the hypothetical building is destined to offices. The distribution of spaces is shown in Fig. 11.1. The building has seven floors and three bays in each orthogonal direction. The height of each interstorey is 4.0 m, and the horizontal distance between columns is 6.5 m. The ground floor is composed of the reception, a lobby, a restaurant, a couple of toilets, and the stairs that give access to the upper floors. The rest of the floors are formed of six offices, two toilets and a meeting room. Fifteen *PG*s are used for the damage analysis: (1) columns, (2) beams, (3) column-beam connections, (4) exterior windows, (5) ceiling system, (6) sprinkler system, (7) gypsum interior partition, (8) unreinforced masonry exterior walls, (9) interior windows, (10) unreinforced masonry interior walls, (11) concrete stairs, (12) piping for cold and hot water system, (13) ducting HVAC (Heating, Ventilating and Air Conditioning) system, (14) central unit HVAC and (15) furniture (bookcases and shelves for typical use). In the Table 11.1 the parameters of the distribution of the probability of the *DS*s, and the corresponding parameters of the distribution of the probability of the unit costs and unit time of repair, are presented. These probability distributions were taken from the document FEMA P-58-1 (2012a), which were developed from experiments, expert judgment and experience, systematized inspections performed after actual seismic events, and numerical simulations (Beck *et al.*, 2002). Generic repair activities for the different *DS*s of the *PG*s used in this example are presented in Appendix B of this document. With respect to the furniture-type elements, an average replacement cost of $300 USD was assumed, and an average replacement time of 1 hr for each (10 hr for a 10 hr workday).

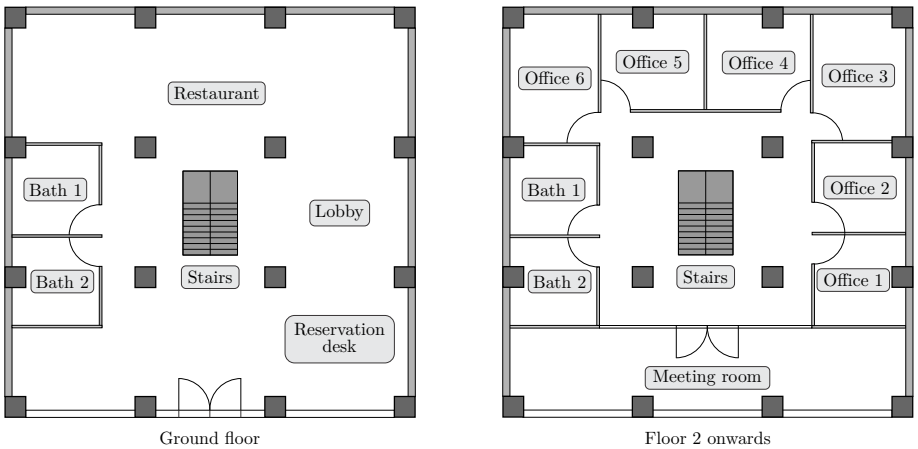

Figure 11.1: Space distribution of the usable areas in the building.

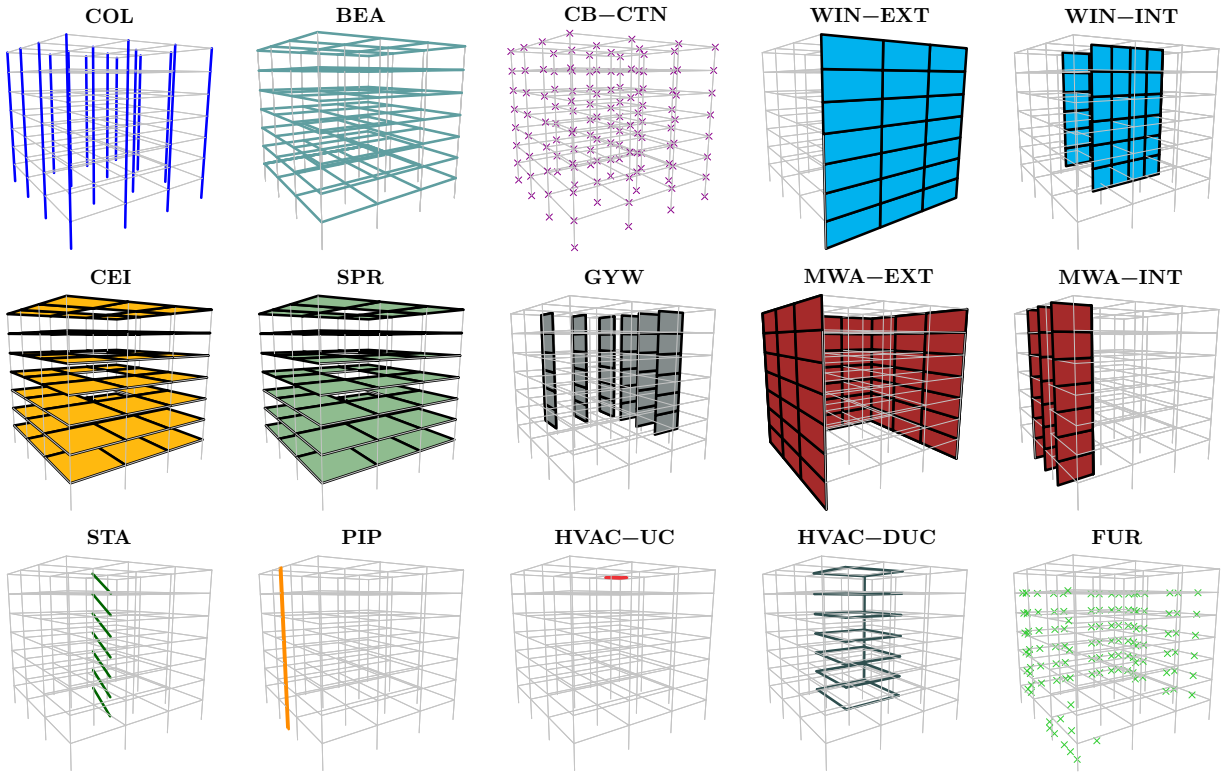

Figure 11.2: Localization of the *PG*s using in the case of study.

Also, all furniture-type components have dimensions of 2.0 m high, 1.3 m wide and 0.5 m deep. On the other hand, it was assumed that in each unit of the building, that is, each floor, there is a daily economic income of 1,000, 500, 700, 2,000, 300, 800 and 1,500 USD, respectively. These revenues are used to estimate the indirect economic losses caused by business interruption during the time that the building recovers its functionality. The spatial location of each component of the *PG*s is illustrated in Fig. 11.2.

11.1.1 Structural design and location of the building

The building was designed in accordance with Appendix A of the Complementary Technical Norms for Earthquake Design (NTC-DS) (GCDMX, 2004a). The concrete strength was taken equal to $f'_c = 25$ MPa with a modulus of elasticity of E_c=23,500 MPa. The tensile strength of longitudinal reinforcing steel was taken equal to f_y=410 MPa, while the transverse reinforcing steel was taken equal to f_{ys}=350 MPa; both materials are characterized by a modulus of elasticity $E_s = 206,000$ MPa. For the purposes of the NLDA, the compression strength of the masonry was considered to be f_m=9 MPa, and a modulus of elasticity E_m=4,850 MPa. A dead load w_d=5,400 Pa was used. Likewise, a maximum live load with value equal to w_m=2,450 Pa and an instantaneous live load of w_{lr}=1,765 Pa were considered. To take into account the cracking effect in columns and beams, their elastic stiffness was multiplied by the factors of 0.5 and 1.0, as recommended by the

Complementary Technical Norms for the Design and Construction of Concrete Structures (NTC-DCEC) (GCDMX, 2004b), to be taken into account in the limit state of collapse prevention. The basic loads and design combinations were obtained from Complementary Technical Norms on Criteria and Actions for the Structural Design of Buildings (NTC-CADEE) (GCDMX, 2004c).

It was assumed that the building is located at the seismological station of the Secretariat of Communications and Transportation (SCT), located in Zone IIIb (soft soil), according to the geotechnical zonation of the Mexico City. According to the structural characteristics of the building a seismic behavior factor of Q=2 was considered. The design of the structural components of the building are as follows. All columns have dimensions of 100×100 cm, a longitudinal reinforcement of 24 rods of No.10 (ϕ=31.7 mm) and stirrups of No.6 (ϕ=19.1 mm) located at each 10 cm. The beams have dimensions 90×70 cm, a longitudinal reinforcement of 18 rods of No.10 (ϕ = 31.7 mm), and stirrups of No.6 (ϕ=19.1 mm) located at each 10 cm. The thickness of each slab is 25 cm. With the proposed structural design, the fundamental period of the building is T1=0.61 s.

Although soil-structure interaction is an aspect that must be taken into account in short fundamental period structural systems such as the building studied in this application, for simplicity this physical aspect is not considered in this application.

11.1.2 Seismic hazard analysis

The application of the proposed methodology for estimating seismic resilience was performed using a combination of the time-based and scenario-based assessment, both described in the Chapter 4. For this example, only earthquakes generated by a subduction fault were considered. The evaluation was performed for seven levels of IM, with return periods of 50, 125, 250, 500, 1000, 1500 and 2500 years, with a probability of exceedance of 63, 33, 18, 10, 5, 3 and 2%, respectively, in an interval of 50 years. As a measure of IM the spectral acceleration Sa(T1) is used. The target mean spectral accelerations for each IM level used are: 0.15g, 0.22g, 0.29g, 0.36g, 0.47g, 0.54g and 0.63g, whose values were obtained from the seismic hazard curve shown in the Fig. 11.4[3], corresponding to the SCT site and a fundamental period of vibration of T1=0.6 s. To represent the variability of the seismic demand sets of 20 pairs of accelerograms were simulated for each return period using the model proposed by Kohrs-Sansorny *et al.* (2005) (described in the Chapter 4). As Green's empirical function the two horizontal components of the ground motion registered in the SCT accelerometer station generated by the April 25, 1989 earthquake M_w 6.9, with epicenter near the community of San Marcos, Guerrero, are used (see Fig. 11.3). For this event the magnitude of the seismic moment and the stress drop are $M_0 = 2.51 \times 10^{19}$ Nm (obtained with the expression proposed by Hanks and Kanamori (1979)) and $\Delta\sigma = 150$ bars (reported in Ordaz *et al.* (1995)), respectively. The distance between the source-site is approximately 311 Km, therefore, the far-field condition is accomplished

[3]The values to construct the seismic hazard curve were provided by Dr. Pablo Quinde Martínez, from the Engineering Institute of UNAM.

Table 11.1: Probability distributions of the damage states of the *PG*s used and their respective unit repair cost and repair time (FEMA, 2012a).

Performance Group, PG	Engineering Demand Parameter, EDP	Damage State, DS	Damage Probability Distribution Parameters			Unit	Damage Probability Distributions of the Unit Repair Cost, CR (USD) and Unit Repair Time, TR (days-worker)						Repair Dimensions (m)	
			D_{DS}	μ_{DS}	CV_{DS}		D_{CR}	μ_{CR}	CV_{CR}	D_{TR}	μ_{TR}	CV_{TR}	lx'	ly'
Column (COL) (B1041.003b)	ID	DS_1 (sec.)	LN	0.02	0.4	u	N	21,400	0.39	N	18.9	0.46	3.0	3.0
		DS_2 (sec.)	LN	0.0275	0.3		N	34,500	0.31	N	30.4	0.39		
		DS_3 (sec.)	LN	0.05	0.3		N	41,000	0.29	N	36.2	0.39		
		DS_4 (m.exc. DS_2 ,DS_4)	LN	0.05	0.3		N	34,500	0.31	N	30.4	0.39		
Beam (BEA) (B1042.021b)	R(rad)	DS_1 (sec.)	LN	0.0203	0.39	u	LN	10,600	0.52	LN	9.02	0.57	3.0	6.5
		DS_2 (sec.)	LN	0.0394	0.35		N	28,800	0.35	N	24.6	0.43		
		DS_3 (sec.)	LN	0.0602	1.0		N	43,600	0.37	N	37.2	0.44		
Column/Beam Connection (CB-CTN) (B1041.043b)	ID	DS_1 (sec.)	LN	0.015	0.4	u	N	21,400	0.39	N	18.9	0.46	3.0	3.0
		DS_2 (sec.)	LN	0.0175	0.4		N	34,500	0.31	N	30.40	0.39		
		DS_3 (sec.)	LN	0.02	0.4		N	41,000	0.29	N	36.20	0.39		
Exterior Windows (WIN-EXT) (B2022.021)	ID	DS_1 (sec.)	LN	0.0156	0.35	u	LN	1,970	0.12	LN	0.87	0.28	6.5	3.0
		DS_2 (sec.)	LN	0.0561	0.30		LN	1,970	0.12	LN	0.87	0.28		
Ceilings (CEI) (C3032.003b)	A(g)	DS_1 (sec.)	N	1.47	0.3	55 m^2	N	870	0.55	N	0.78	0.60	6.5	6.5
		DS_2 (sec.)	LN	1.88	0.3		LN	6,810	0.52	LN	6.18	0.58		
		DS_3 (sec.)	LN	2.03	0.3		LN	14,000	0.20	LN	12.8	0.32		
Sprinklers (SPR) (D4011.021a)	A(g)	DS_1 (sec.)	N	1.1	0.4	300 m	LN	350	0.65	LN	0.41	0.70	6.5	6.5
		DS_2 (sec.)	N	2.4	0.5		LN	2,650	0.41	LN	0.625	0.48		
Wall Partition of Gypsum (GYW) (C1011.001a)	ID	DS_1 (sec.)	LN	0.005	0.4	120 m^2	N	2,280	0.44	N	1.82	0.51	6.5	4.0
		DS_2 (sec.)	LN	0.01	0.3		LN	4,550	0.56	LN	3.51	0.61		
		DS_3 (sec.)	LN	0.021	0.2		LN	8,750	0.20	LN	6.76	0.32		
Int/Ext Masonry Wall (MWA-EXT) (B1051.013)	ID	DS_1 (sec.)	LN	0.0018	0.73	9 m^2	LN	600	0.36	LN	0.47	0.44	3.0	6.5
		DS_2 (sec.)	LN	0.0051	0.65		N	4,350	0.10	N	3.39	0.27		
		DS_3 (sec.)	LN	0.0086	0.56		N	7,630	0.14	N	5.95	0.29		
Interior Windows (WIN-INT) (B2022.034)	ID	DS_1 (sec.)	LN	0.0147	0.25	3 m^2	LN	1,970	0.12	LN	0.87	0.28	4.3	3.0
		DS_2 (sec.)	LN	0.0164	0.25		LN	1,970	0.12	LN	0.87	0.28		
Concrete Stairs (STA) (C2011.011b)	ID	DS_1 (sec.)	LN	0.005	0.60	u	LN	700	0.80	LN	0.772	0.84	6.5	6.5
		DS_2 (sec.)	LN	0.017	0.60		LN	3,700	0.57	LN	4.080	0.62		
		DS_3 (sec.)	LN	0.028	0.45		N	23,000	0.36	N	25.3	0.44		
Piping for hot/cold Drinking Water (PIP) (D2021.014a)	A(g)	DS_1 (sec.)	LN	2.25	0.4	300 m	LN	290	0.76	LN	0.31	0.80	3.0	3.0
		DS_2 (sec.)	LN	4.1	0.4		LN	2,650	0.41	LN	2.81	0.48		
Ducting HVAC (HVAC-DUC) (D3041.022c)	A(g)	DS_1 (sec.)	LN	3.75	0.4	300 m	LN	1,950	0.13	LN	2.15	0.28	11.5	3.0
		DS_2 (sec.)	LN	4.5	0.4		LN	21,500	0.14	LN	23.7	0.28		
Central Unit HVAC (HVAC-UC) (D3031.013b)	A(g)	DS_1 (−)	LN	0.72	0.2	u	LN	46,200	0.18	LN	9.51	0.31	6.0	6.0

Notes: ID: Interstory drift ratio, R: Rotation, A: Acceleration, LN: Lognormal distribution, N: Normal distribution, sec.: secuential, m.exc.: mutually exclusive.

in order to use the approach developed by Kohrs-Sansorny *et al.* (2005).

Figure 11.3: Location of the point source and the site of interest SCT (Secretary of Communications and Transport) accelerometer station in the Mexico City (map generated by © OpenStreetMap).

11.1.3 Structural analysis

The NLDA was performed in the Open System for Earthquake Engineering Simulation (OpenSees), developed in the Pacific Earthquake Engineering Research by Mazzoni *et al.* (2007). The columns and beams are modeled using bar elements with five integration points. Its inelastic behavior is modeled using fibers (Scapone *et al.*, 1996). The behavior of concrete is modeled using the constitutive model developed by Chang and Mander (1994), and of the longitudinal reinforcement steel with the model developed by Giuffrè and Pinto (1970). To take into account the stiffness contribution of the masonry infill walls, its behavior is modeled using the methodology proposed by Kadysiewski and Mosalam (2009), which takes into account the behavior within and perpendicular to the plane of the element. The parameters of the constitutive model for the masonry were calculated in accordance with the FEMA 356 (2000). In addition, P-Delta effects were considered for the NLDA. The fraction of the critical Rayleigh damping obtained from the modal analysis for the first three modes of vibration was 0.0498, 0.0495 and 0.0497. To solve the nonlinear dynamic equilibrium equation, the Newton Line Search algorithm was used in combination with the Newmark method with parameters $\beta = 0.25$ and $\gamma = 0.5$. The evaluation of the demolition limit state was done using the methodology developed by Ramirez and Miranda (2012).

Likewise, the building studied in this research work is characterized by being capable of de-

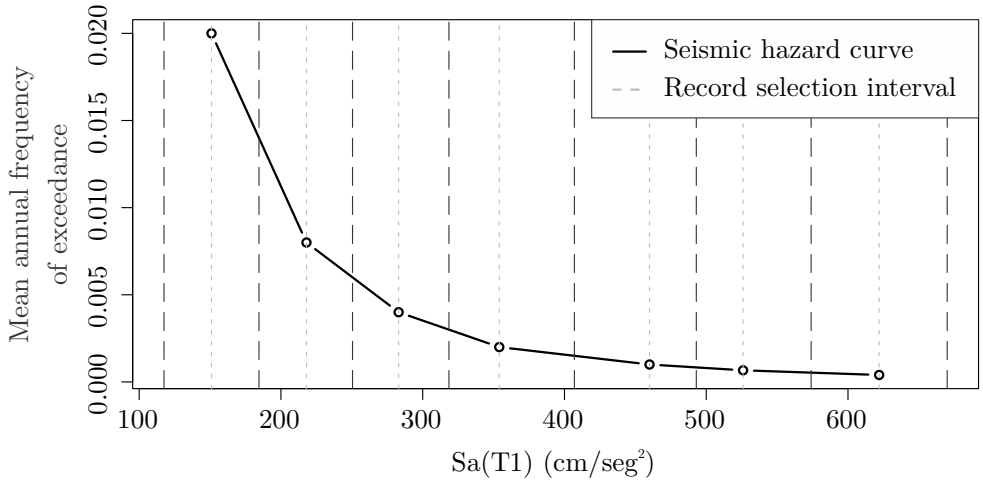

Figure 11.4: Seismic hazard curve for the SCT site and a fundamental period of vibration of T1=0.6 s.

veloping a limited ductility, so it is not appropriate to estimate the probability of collapse using IDA since this methodology is more suitable for buildings that may develop significant ductility demands (Shoraka *et al.*, 2013). Instead, structural collapse was determined when at least one building column exceeded a prescribed maximum drift (first component failure) in a seismic realization given a seismic intensity. This approach is consistent with the criterion proposed by ASCE (2006) for the limit state of collapse prevention. A value of 0.025 was used as the limiting collapse drift, as suggested by Xue *et al.* (2008) and Nazri (2018). The probability of collapse was estimated by dividing the number of times the structure collapsed by the total number of seismic realizations associated with a specific seismic hazard level.

11.2 Analysis of the results

The following sections present the resilience analysis of the hypothetical office building. The analysis is composed of (1) damage analysis of structural, non-structural and furniture-type elements; (2) probabilistic safety assessment according to the post-seismic inspection criterion of the ATC-20 (1989), and analysis of non-structural and furniture safety; (3) evaluation the probability of occurrence of one of the six limit states of functionality; (4) analysis of loss and recovery of functionality; (5) vulnerability analysis for each of the DVs proposed in this document.

For each of the seven seismic intensities considered in this application, a discrete sample of each DV associated with each LS is obtained. In other words, within the proposed methodology a number equal to $n_{IM} \times n_{LS}$ of possible configurations of loss and recovery of functionality is obtained, which in this case corresponds to 42 possibilities, and each of them contributes to a greater or lesser extent to the probability distribution at each IM. Also, by definition, the LSs in which the building has the ability to recover, *i.e.*, which

are resilient, are the LS_0 to LS_4. The LS_5 and LS_6, corresponding to the demolition and total collapse of the building, respectively, are not associated with a resilient condition of the building as it will not be able to recover for such level of damage. For simplicity, out of the 42 possibilities, the analysis of the loss and recovery of functionality of the events (LS_1, IM_1), (LS_3, IM_3) and (LS_4, IM_6) will be presented, which are the ones that contribute the most to the probability density of the seismic intensities IM_1 (Sa(T1)=0. 15g), IM_3 (Sa(T1)=0.29g) and IM_6 (Sa(T1)=0.54g), which correspond to recurrence periods of 50, 250 and 1,500 years, respectively.

The NTC-DS (GCDMX, 2004a) specify that the seismic intensity used in the design for the collapse prevention limit state corresponds to earthquakes whose return period is associated with 250 years. Therefore, the results of the analyses associated with this level of seismic hazard correspond to the evaluation of the seismic resilience of the building under study for the collapse prevention condition. Regarding the serviceability limit state, which corresponds to the immediate occupancy performance level, the NTC-DS (GCDMX, 2004a) do not specify to which seismic hazard level these intensities correspond, therefore, in this research work it is assumed that the seismic events associated to the 50-year return period seismic hazard level correspond to the demands of the serviceability limit state.

11.2.1 Damage analysis

The inference of the damage in structural and non-structural elements was performed using the probability criterion described in section 6.1, while the inference of the damage in furniture-type elements using the theory of rigid body dynamics, described in section 6.2.

Figure 11.5 illustrates the global damage configuration in terms of the DS developed by each element of each PG associated with a seismic realization corresponding to intensity IM_1 (Tr=50 yr, Sa(T1)=0.15g) and LS_1. In this image it can be seen that practically no performance group experienced damage, except for an interior masonry wall, located on the third floor, which experienced slight damage. This limit state, as described in section 7.5, generates a partial loss of functionality; however, the structural safety is not compromised, so it receives a G_S tag. The partial loss of functionality is due to the fact that the damage occurred in the bathroom area, that is, in a service area.

Figure 11.6 shows the damage configuration of each of the PGs corresponding to the LS_3 generated by an orthogonal pair of synthetic accelerograms associated to the IM_3 (Tr=250 years, Sa(T1)=0.29g). This figure shows that a partition wall, located on the third floor, experienced light damage, while some exterior masonry walls, located on the second, third and fourth floors, experienced light, moderate and severe damage. Likewise, some interior masonry walls, from the first to the fifth floors experienced light damage. Finally, the reinforced concrete stairways experienced light damage on the third and fourth floors. This LS corresponds to a restricted entry because several types of non-structural elements experienced light, moderate and severe damage, especially the stairs. Also, this LS is characterized by receiving a Y_S tag. Both the wall that experienced severe damage

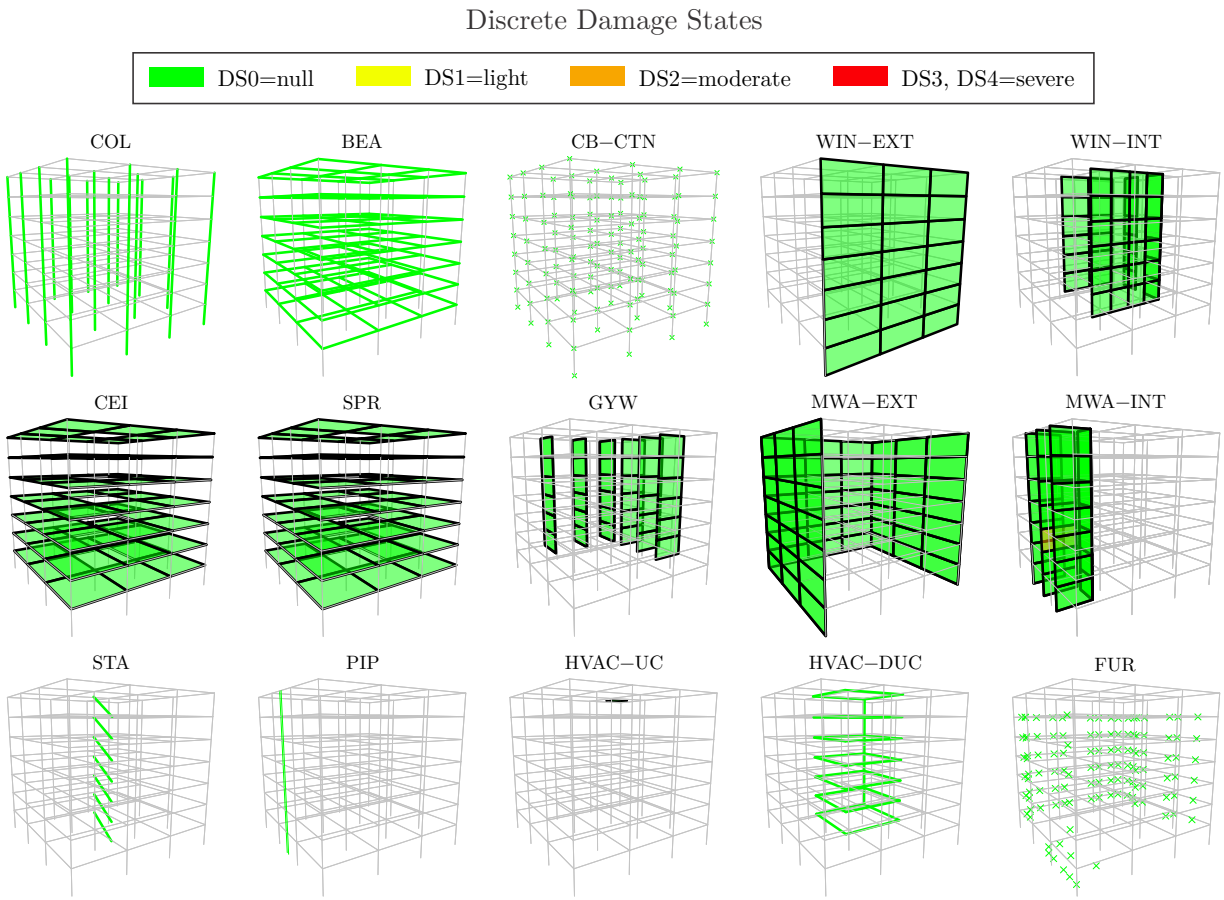

Figure 11.5: Discrete damage state developed for each element that conform every performance group of the building for a seismic realization for the case: LS_1, IM_1 (Tr=50 years, Sa(T1)=0.15g).

and the stairs that experienced light damage are key aspects of declaring the building restricted entry, non-functional but structurally safe.

Figure 11.7 shows the damage configuration of each of the PGs corresponding to the LS_4 generated by an orthogonal pair of synthetic accelerograms associated with IM_6 (Tr=1,500 years, Sa(T1)=0.54g). Contrary to the two previous cases, in this IM the structural elements experienced light, moderate and severe damage. It is observed that a significant number of columns of the first two floors experienced light damage, and one column, located on the second floor, experienced moderate damage. Likewise, a significant number of column-beam connections located in the first three levels experienced severe, moderate and light damage, a condition sufficient for the building to receive a R_S tag, indicating that the structural system is not safe. In this regard, the beam-type elements did not experience damage of any type. It can also be seen that a window of the facade experienced moderate damage, which, according to the pathology of the same would imply its fall, and possibly culminate in the cause of possible injuries on the users of the building, or on passersby. On the other hand, it can be observed that a large number of partition

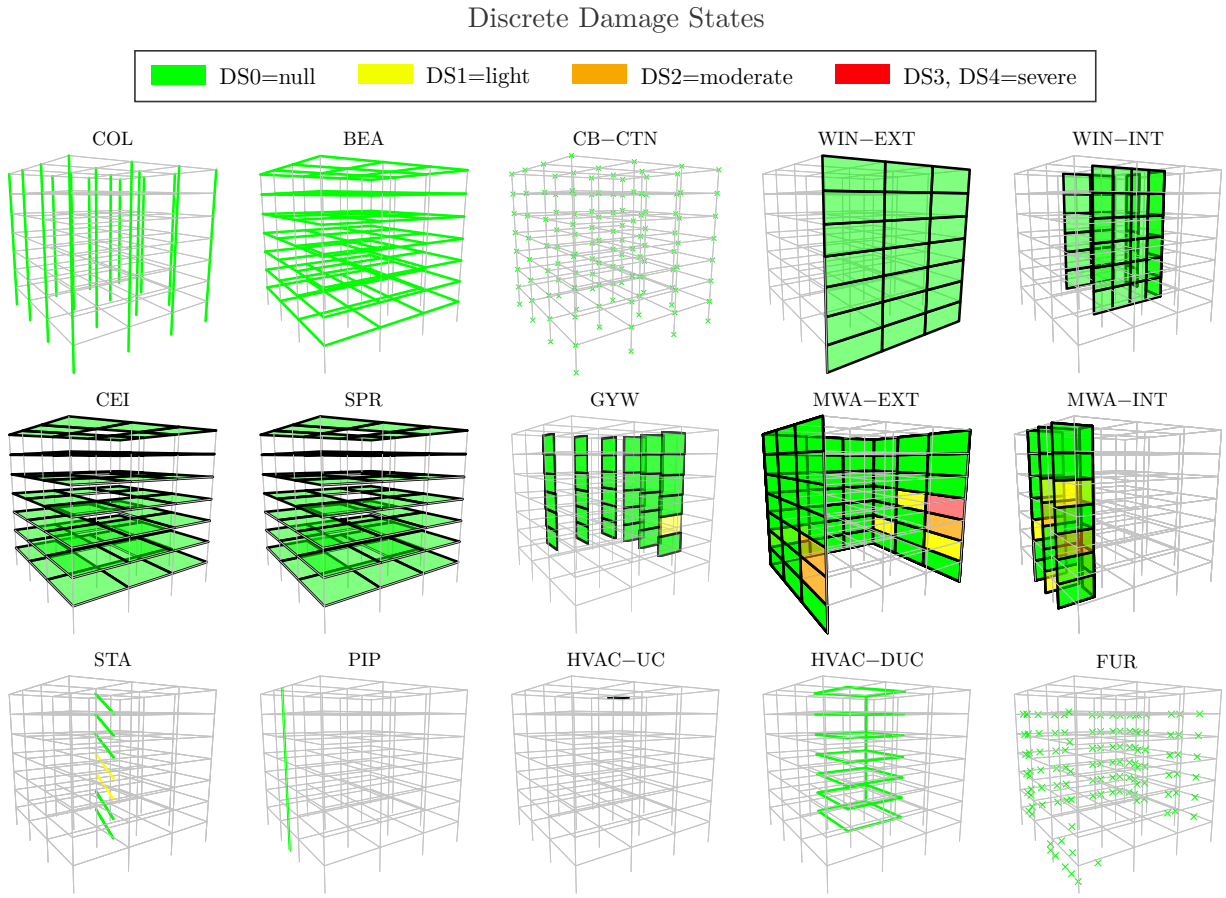

Figure 11.6: Discrete damage state developed for each element that conform every performance group of the building for a seismic realization for the case: LS_3, IM_3(Tr=250 years, Sa(T1)=0.29g).

wall elements experienced light and severe damage in most of the floors. It can also be observed that most of the interior and exterior masonry walls located in the first three floors experienced severe damage, while in the rest of the floors it is observed that this type of elements experienced light and moderate damage. The concentration of damage in this type of elements in the first three floors is a product of the demand of shear forces accumulated gradually from the top floor to the base of the building. In this case, the stairways also experienced damage on all floors, especially moderate and severe damage on the first and second floors. This condition automatically implies loss of functionality because these elements are the transportation routes within the building.

An interesting result is due to the performance of furniture-type elements. This figure shows that this type of element suffered severe damage, *i.e.*, overturning, in the last three floors of the building. This is due to the fact that the floor accelerations increase gradually from the base to the top floor of the building. This physical aspect is typical of short-period buildings, such as the one under analysis. It can also be observed that the periphery of the last three floors is where the greatest number of furniture-type elements that experienced

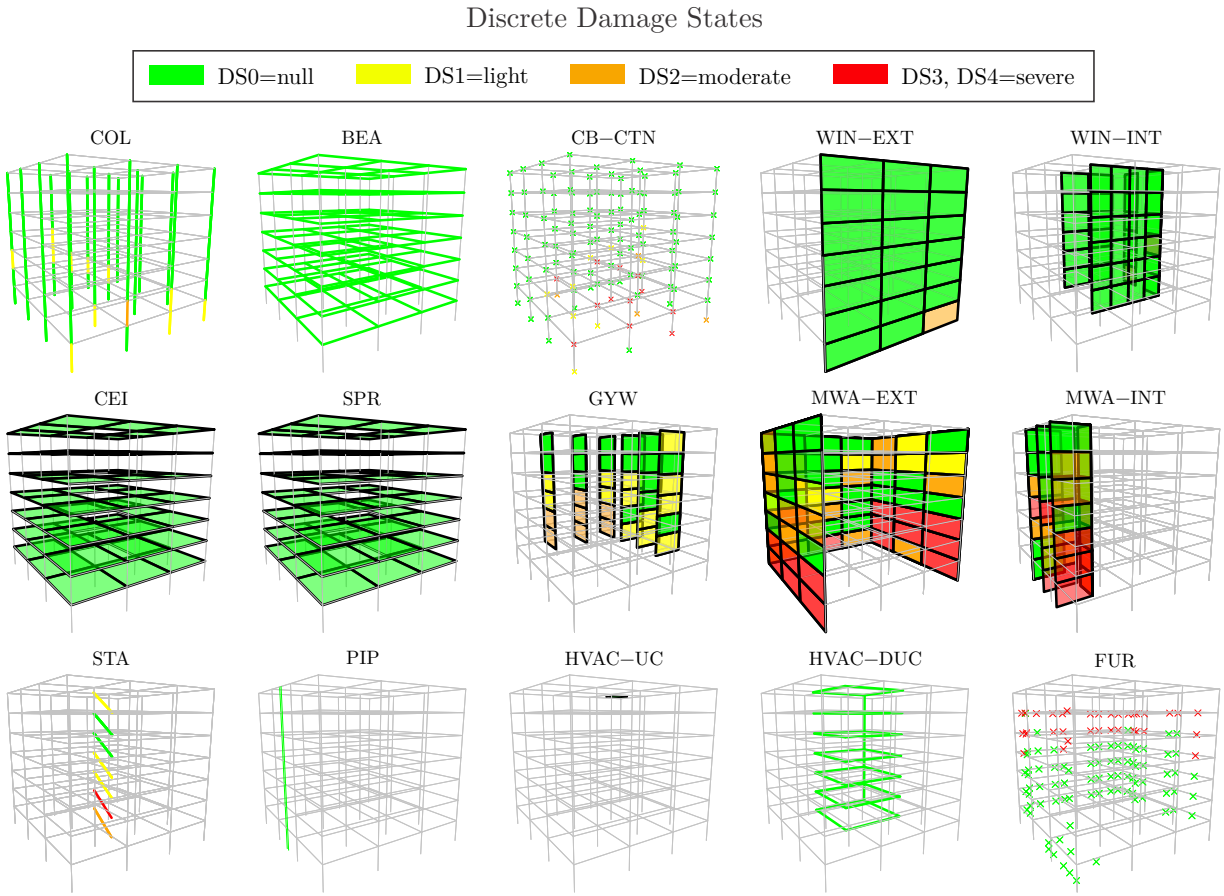

Figure 11.7: Discrete damage state developed for each element that conform every performance group of the building for a seismic realization for the case: LS_4, IM_6 (Tr=1,500 years, Sa(T1)=0.54g).

overturning are concentrated. This is due to the fact that the ends furthest from the center of mass of the building floors experienced a greater intensity of angular accelerations (see Fig. 11.8), as a result of the rotation of the vertical axis of the structure produced by the seismic demand imposed in each horizontal orthogonal direction of the three-dimensional NLDA.

11.2.2 Post-seismic evaluation analysis and limit states of functionality

A fundamental aspect of the methodology proposed in this thesis is the probabilistic evaluation of the post-seismic inspection, in which not only structural elements are taken into account, but also non-structural and furniture-type elements. This process is fundamental to determine which seismic realizations, associated to each IM, produce the damage configurations (as described in the previous section) of the LSs, and therefore the configuration of the events that allow estimating the recovery time of the building, as illustrated

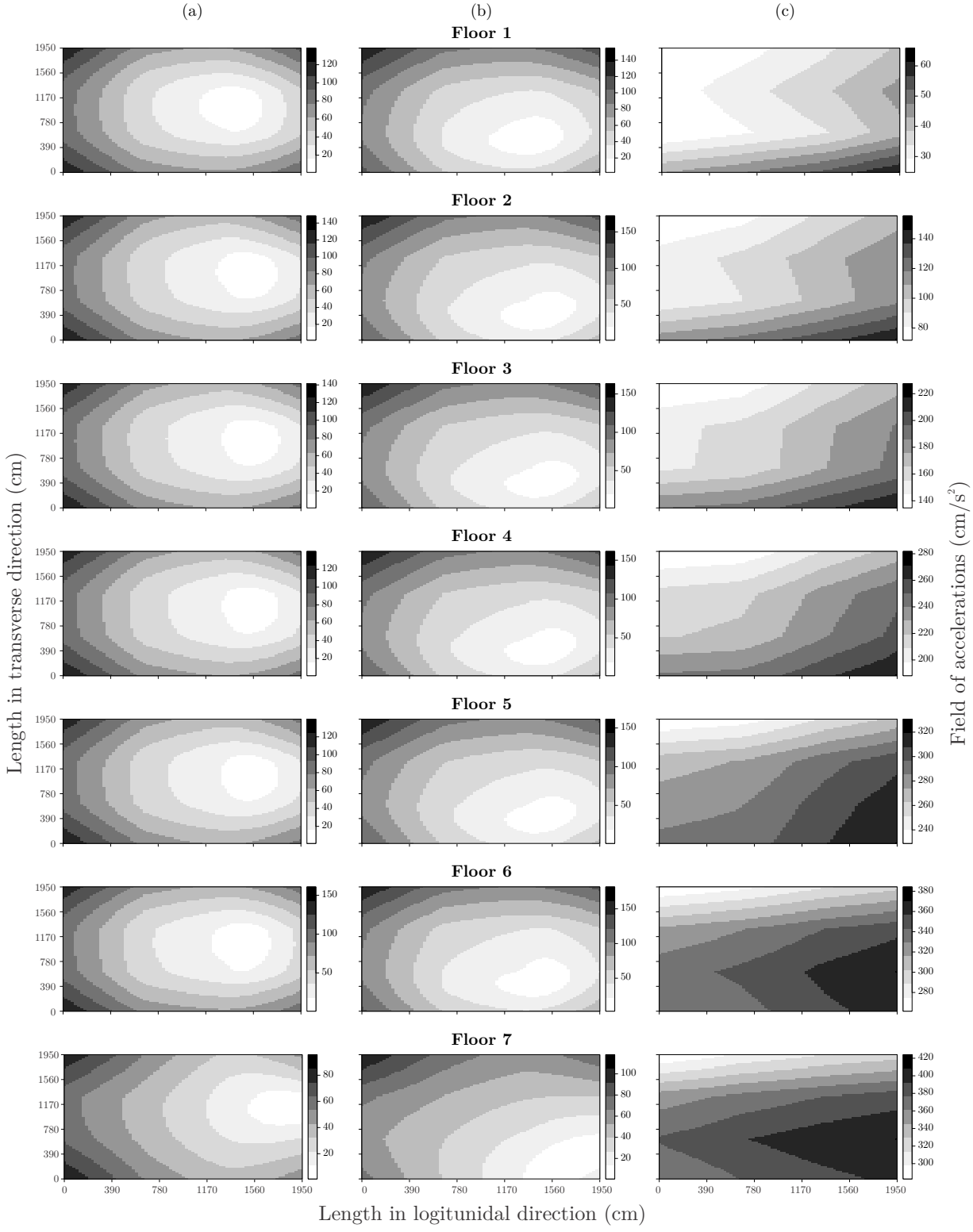

Figure 11.8: Field of accelerations of each floor of the building for the following conditions: (a) (LS_1, IM_1), (b) (LS_3, IM_3), and (c) (LS_4, IM_6), .

in the flowchart of Fig. 8.6.

Figure 11.9a shows the probability of tagging the post-seismic structural inspection for each IM considered in the study. This figure shows that the building is safe, from the structural point of view (green color line), from IM_1 (Tr=50 years, Sa(T1)=0.15g) up to IM_5 (Tr=1,000 years, Sa(T1)=0.47g), that is, the probability of the building receiving a G tag is $Pr(TAG = R_S \mid 0.47\text{g}) = 0.95$, and of being tagged with restricted use is $Pr(TAG = Y_S \mid 0.47\text{g}) = 0.05$, and of being tagged as unsafe is $Pr(TAG = R_S \mid 0.47\text{g}) = 0.0$. However, at intensity IM_6 (Tr=1,500 years, Sa(T1)=0.54g), the probability that the building is assigned a R tag is $Pr(TAG = R_S \mid 0.54\text{g}) = 0.5$. For this same level of IM, the probability of the structure being tagged with restricted use is $Pr(TAG = Y_S \mid 0.54\text{g}) = 0.35$, and of being tagged as safe $Pr(TAG = G_S \mid 0.54\text{g}) = 0.15$. For the IM with return period of 2,500 years the probability that the building is structurally unsafe is $Pr(TAG = R_S \mid 0.63\text{g}) = 1.0$.

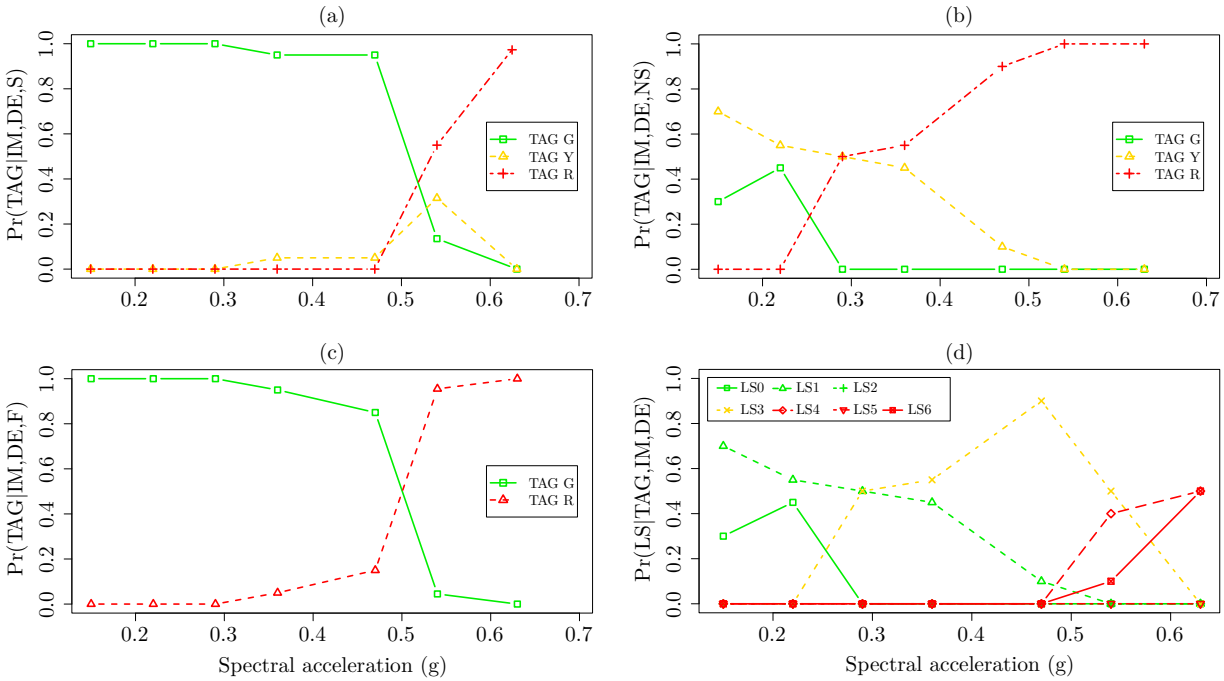

Figure 11.9: Probability of tagging of: (a) Structural, (b) Non-structural, (c) Furniture inspection, and (d) evaluation of LSs for each IM used.

These probabilities, and those to be described below, were approximated with Eqs. 7.1, developed in section 7.4, by using the classical definition of probability theory, *i.e.*, number of random realizations that result in success over the total number of realizations. For example, the previous section described the damage configuration resulting from a random seismic realization corresponding to each of the three events (LS_1, IM_1), (LS_3, IM_3) and (LS_4, IM_6).

Figure 11.9b presents the probability of tagging of non-structural safety, analogous to structural inspection; however, for this case the tagging refers to the safety of a certain

area of the building. For this case it is observed that the performance of the non-structural elements completely changes the picture not of the structural safety, but of the functionality itself. The red color line represents the probability that at least one element of the non-structural PGs will develop severe damage given a seismic intensity. It is observed that this probability starts to become relevant at IM_3 (Tr=250 years, Sa(T1)=0.29g), which corresponds to the design intensity according to NTC-DS (GCDMX, 2004a). This probability is $Pr(TAG = R_{NS} \mid 0.29\text{g}) = 0.5$. Comparing this probability with the one obtained for the same intensity but with respect to structural safety tagging, it can be observed that damage to non-structural elements controls the loss of functionality. This is a clear indication that the design regulations are not developed to take care of the integrity of the non-structural elements nor to avoid injury to users at the level of seismic demand of 250-year return period, but only in minimizing the damage that may be experienced by the structural elements in order to reduce the probability of collapse and avoid loss of life. However, as will be seen below, it is possible for non-structural elements to cause injury to occupants.

In Fig. 11.9c, which corresponds to the post-seismic inspection simulation of furniture-type elements, it can be seen that damage (*i.e.*, overturning) starts to occur at IM_4 (Tr=500 years, SA(T1)=0.36g). The probability that this type of element experiences severe damage at that IM level is $Pr(TAG = R_F \mid 0.36\text{g}) = 0.05$. For this same IM, the probability of the building being tagged as unsafe $Pr(TAG = R_S \mid 0.36\text{g}) = 0.0$. Again, this is a clear indication that loss of functionality is caused at seismic intensities lower than those that cause insecurity in the structural system, or even restricted use (according to the tagging criteria proposed by the ATC-20 (1989), in which only structural safety, but not functionality, is evaluated).

Figure 11.9d shows the probability of each LS as a function of each IM. This figure shows that for the immediate occupancy seismic demand IM_1 (Tr=50 years, Sa(T1)=0.15g) the limit state controlling the loss of functionality is LS_1, therefore, the building is structurally safe, as expected. However, for this case it is possible that some non-structural elements may develop slight damage, which can be repaired in a short period of time, without rendering the building non-functional, *i.e.*, only cosmetic repairs are required on a small number of elements.

Respect to the collapse prevention IM_3 (Tr=250 years, Sa(T1)=0.29g) it is observed that the LS_1 and LS_3 have the same probability, that is, $Pr(LS_1 \mid 0.29\text{g}) = Pr(LS_3 \mid 0.29\text{g}) = 0.5$. Taking a conservative approach for this case, it is concluded that the building has a high probability of being tagged with restricted use ($TAG = Y_S$). According to the shape of the probability curves $Pr(LS \mid IM)$ it is appreciated that such probabilities are governed by the performance of the non-structural elements (see Fig. 11.9b) up to intensity IM_5 (Tr=1,000 years, Sa(T1)=0.47g).

On the other hand, the probability that the LS_4 begins to be important up to IM_6=0.54g (Tr=1,500 years, Sa(T1)), with probability $Pr(LS_4 \mid 0.54\text{g}) = 0.4$. This LS reflects severe structural damage. It should also be noted that for this same level of IM the probability that the building will experience structural collapse is $Pr(LS_5 \mid 0.54\text{g}) = 0.1$, which is

an indication that the structural system is not safe at this level of intensities since this probability is not negligible according to seismic design standards against collapse.

For the IM_7 (Tr=2,500 years, Sa(T1)=0.63g) it is observed that the LSs that govern the performance of the system are LS_4 and LS_6, with probability $Pr(LS_4 \mid 0.63g) = 0.5$ and $Pr(LS_6 \mid 0.63g) = 0.5$, respectively. Taking a conservative criterion, that is, accepting that the governing limit state of functionality is LS_6, which corresponds to structural collapse, it is concluded that the building is not resilient to this level of seismic demand, since by definition, the limit states of functionality that allow the building to recover are $LS_0, ..., LS_4$. (The limit state LS_5 is also not resilient because this state corresponds to the probability that the system will have to be demolished; however, for this application example the probability that the building will have to be demolished is zero for all the seismic intensities considered in the study).

In general, it can be said that the building has the capacity to recover from seismic intensities less than or equal to Sa(T1)=0.47g, that is, with a recurrence period of approximately 1,000 years. However, as will be described below, resilience at these levels of seismic intensity can be costly not only from the point of view of structural, non-structural and furniture repairs, but also in terms of business interruption and the equivalent economic value associated with people being injured or losing their lives.

11.2.3 Analysis of loss and recovery of functionality

The first stage of seismic resilience corresponds to the loss of functionality. As described in section 8.2, this is approximated as the percentage of non-usable area inferred from the tributary area required to repair the number of elements that have experienced a given discrete damage state. It is assumed that over the tributary area assigned to each element the repair work will be performed by a number of workers during a given time interval. The last two columns of Table 11.1 indicate the dimensions lx' and ly' that define the tributary area of each element of each performance group. It is worth mentioning that these dimensions are independent of the severity of the damage experienced. In this context, what varies depending on the severity of the damage is the time and cost of repair and number of workers.

The second stage of seismic resilience of buildings as described in Fig. 8.6 of section 8.6 is composed of two major sub-stages. In the first sub-stage of this flowchart, the irrational factors, *i.e.*, the events that prevent the initiation of repairs, are presented. In this regard, in section 7.5 the LSs were presented and for each of them a generic recovery sequence was also formulated. Table 8.1 summarizes the sequence in which the irrational factors are presented depending on the LS in question.

To estimate the time corresponding to the irrational factors, the probability distribution functions proposed in the document REDi^{TM} (2013), Table 11.2, are used. These distributions are calibrated according to the repair class RC, which depends on the severity of the damage experienced by the building. Then, this generic sequence is the one that

feeds the recursive algorithm developed in section 8.5 to estimate the building repair time associated to each seismic realization of each LS.

The second sub-step presents the rational factors, *i.e.*, the events corresponding to the repair of the PGs. In section 8.5 the proposed methodology to approximate the repair time and cost, as well as the number of workers needed to repair each performance group was presented. This methodology is based on the CPM and PERT methods; therefore, this methodology is a recursive process. This last stage, then, is the one that corresponds to the simulation and optimization process of the sequence of rational factors (see Fig. 8.6b).

One of the essential conditions of this algorithm is the prescription of the sequence in which the PGs are to be repaired. Therefore, the analyst must have a general but clear idea of the sequence in which to repair the PGs that are susceptible to damage. To do this, it is necessary to have an inventory of the PGs and to establish hierarchies among them. For example, suppose that in a five-story building the staircase located on the second floor experiences severe damage and six partition walls located on the fifth floor develop light damage. Obviously, the staircase is the element that must be repaired first. In addition, this element is essential for workers to have access to the fifth floor and be able to perform the repair work on the partition walls. In summary, the process of repairing an earthquake-damaged building requires a damage mitigation plan, which must be consistent with the importance of the function of each performance group within the building.

Table 11.2: Probability distribution of the irrational factors that delay the initiation of repairs (REDi^{TM}, 2013)

Impeding Factor	Repair Class	Distr. Parameters	
		μ	σ
Post-seismic inspection	-	1 day	0.54
Obtaining financing	$C_{1,2}$	1 week	0.54
	C_3	6 weeks	1.11
Structural redesign	$C_{1,2}$	2 weeks	0.32
	C_3	4 weeks	0.54
Planning of repair activities	$C_{1,2}$	3 weeks	0.66
	C_3	7 weeks	0.35
Government permits to initiate repairs	$C_{1,2}$	1 week	0.86
	C_3	8 weeks	0.32

Note: All irrational factors correspond to a lognormal distribution.

For the example being described the following generic sequence will be used to repair the PGs: (1) stairs, (2) columns, (3) beams, (4) column-beam connections, (5) masonry exterior walls, (6) walls masonry interiors, (7) HVAC ducts, (8) HVAC central unit, (9) hydraulic drinking water system, (10) exterior windows, (11) fire protection system, (12) ceilings, (13) walls drywall interiors, (14) interior windows, and (15) furniture. The con-

ditions to generate the events and the repair activities are generated using the recursive algorithm proposed in section 8.5. Note that the first performance group to be repaired is the stairs, since these are the means of transportation for the workers to be able to repair the remaining PGs. Likewise, after performing this activity, the PGs to be repaired are those that give the system structural stability. Subsequently, the non-structural elements are repaired, and finally the furniture-type elements are reinstalled or replaced.

Continuing with the results of the resilience analysis of the seven-story RC building with URM, Figs. 11.10, 11.11 and 11.12 indicate the loss and recovery of functionality of each floor of the building, measured as the percentage of non-usable area $(PNUA \mid LS, IM)$, for events (LS_1, IM_1), (LS_3, IM_3) and (LS_4, IM_6), respectively. In these figures the loss of functionality is indicated at time instant $t = 0$ with a vertical red line, starting at 100%, and culminating at the percentage associated with the loss of usable area. At the same instant, $t = 0$, the percentage of usable area PUA of each floor is indicated with a vertical green line. The loss of functionality was estimated with Eq. 8.2 for each seismic realization contained the event (LS, IM). With the condition prescribed in Eq. 8.4, 100% of the usable area loss on each floor was quantified for the realizations in which an element of a performance group experienced a discrete damage state that automatically gives rise to total loss of PUA. The loss of functionality of each floor was estimated as the average of the loss of functionality associated with each seismic realization contained in the (LS, IM) events. This result can be appreciated with the gray colored lines, which start from the vertical axis at instant t_0. The blue color line indicates the trajectory of the non-usable area recovery, estimated as the average of the estimated trajectory in each seismic realization contained in each (LS, IM) condition. The black dashed vertical line indicates the time instant at which the building acquired 100% usable area, *i.e.*, the time at which the building can be used again, as it was before the seismic event caused it to lose functionality. The global loss of functionality of the system in study is calculated with Eq. 8.5, which approximates the envelope of the loss of functionality of each unit of analysis, *i.e.*, of each floor of the building. This process is exemplified in Fig. 8.2e.

Having said that, Fig. 11.10 presents the loss and recovery of functionality for each floor of the building under consideration for the (LS_1, IM_1) condition. The loss of functionality, starting from the first floor to the last floor resulted to be $(4, 3, 3, 2, 1, 1, 1, 2)$%, and the average recovery time for each floor of $t_{REC_f} = (1.3, 2.7, 1.7, 1.1, 0.9, 0, 0.3)$ days, respectively. The global resilience for this event is given in Fig. 11.13a. For this case the loss of functionality $(PNUA \mid LS_1, IM_1)$ was 4.0%, corresponding to the second floor, while the recovery time was $(t_{REC} \mid LS_1, IM_1) = 2.7$ days, corresponding to the second floor. For this case, despite having a recovery time greater than one day, this does not necessarily mean that the building stopped working since the $PNUA$ of each floor are practically negligible. This means that the amount of the elements that experienced damage was very few, and the severity of the damage relatively negligible, as illustrated in Fig. 11.5, and as explained in the numerical evaluation of the post-seismic inspection. In fact, the LS_1 is composed only of light non-structural damage and/or severe furniture damage, however, for the latter performance group, it did not experience damage in this analysis condition.

Note that although very few PGs experienced damage, the overall repair sequence pre-

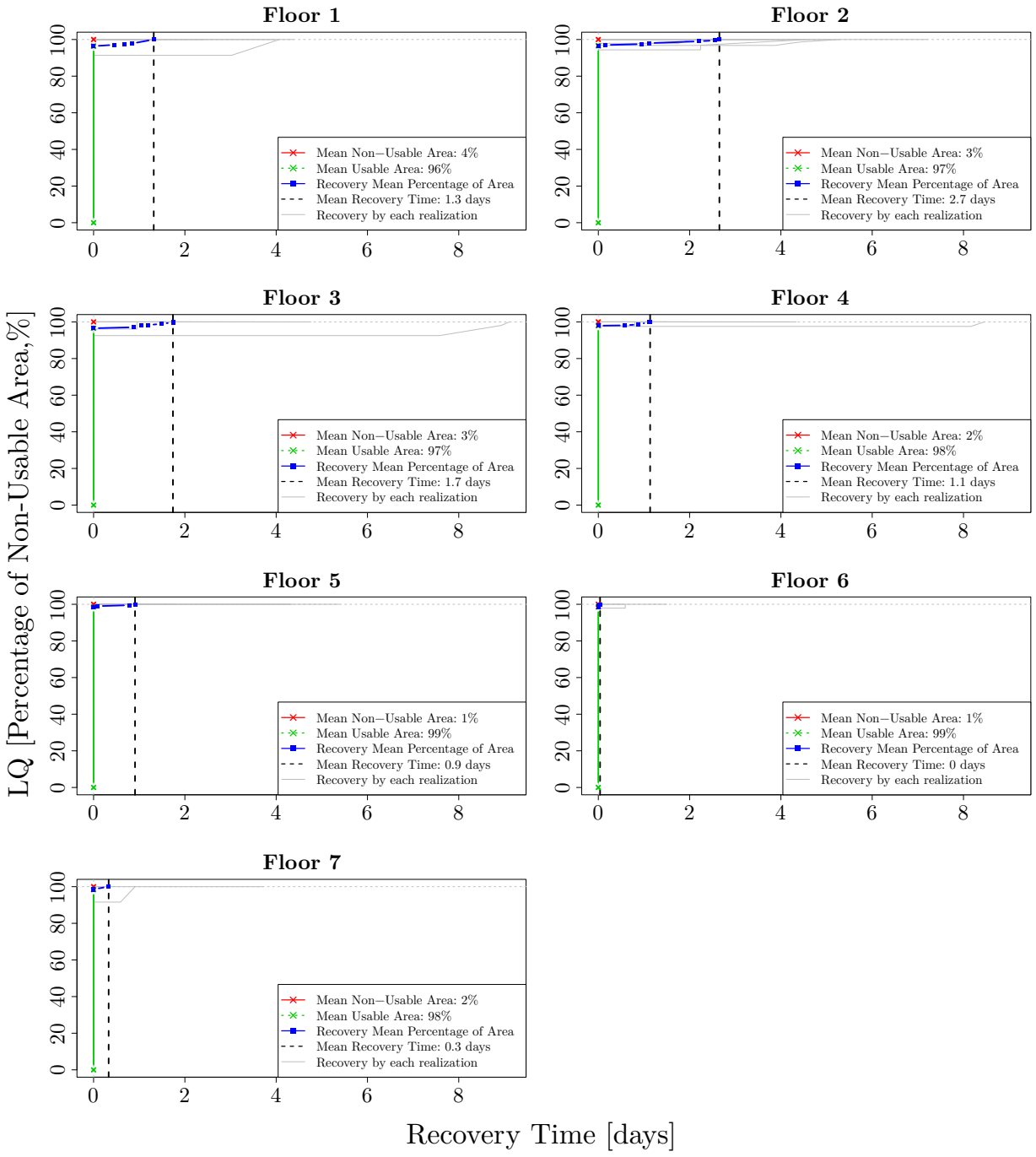

Figure 11.10: Recovery paths of usable area for the seven floors of the building for the resilience analysis case (LS_1, IM_1(Sa(T1)=0.15g)).

scribed for this example remains fixed, as the repair time and economic and human resources expended by the PGs that did not experience any damage are simply zero. In other words, the sequence of events that give rise to system recovery at the repair stage remains fixed for all LSs, and their participation depends only on they actually experiencing

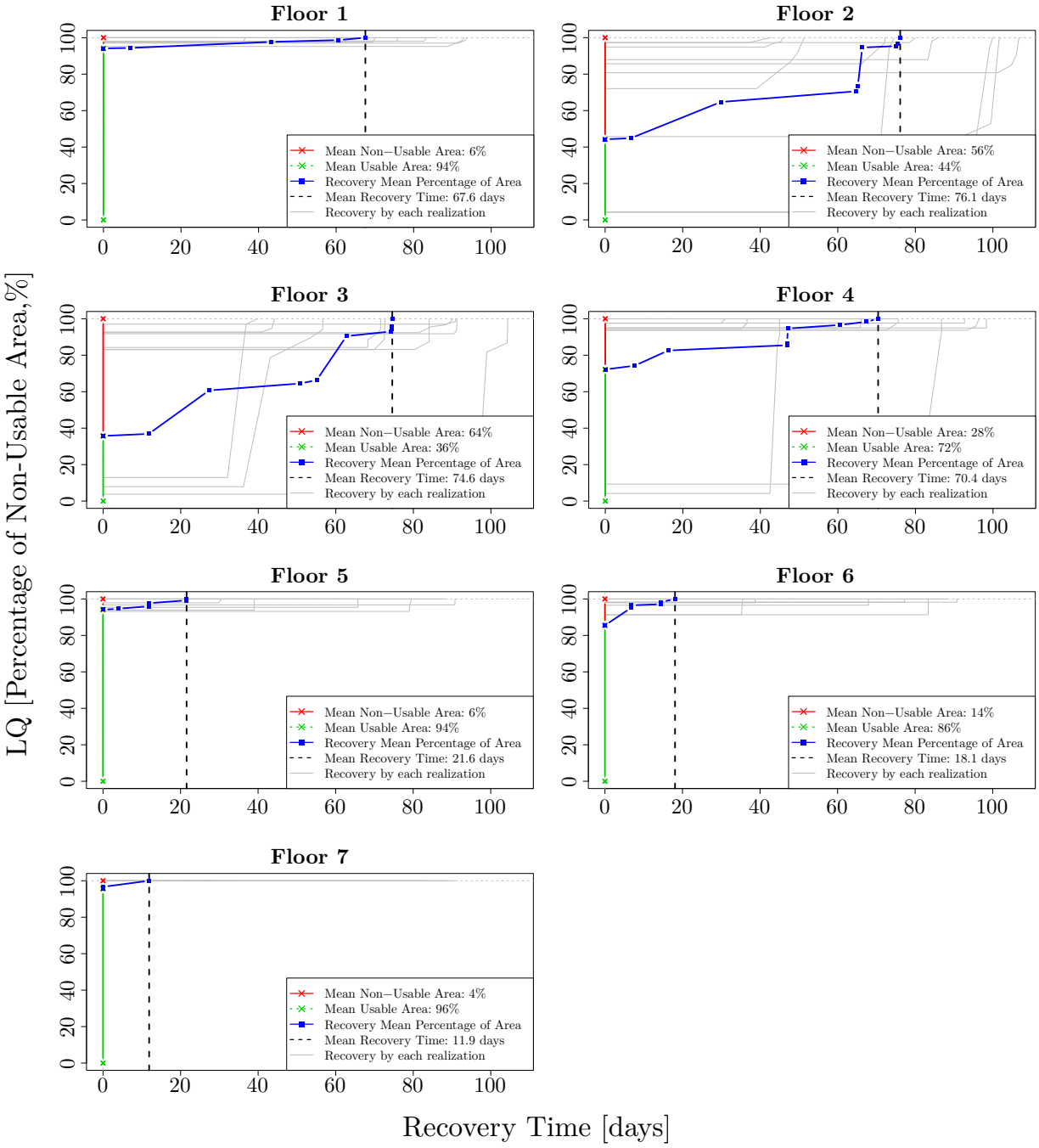

Figure 11.11: Recovery paths of usable area for the seven floors of the building for the resilience analysis case (LS_3, IM_3(Sa(T1)=0.29g)).

some discrete level of damage.

Figure 11.11 presents the loss and recovery of functionality for each floor of the building in question for the condition (LS_3, IM_3), which corresponds to restricted, non-functional but structurally safe entry, and is assigned a Y tag. The loss of functionality, starting from the

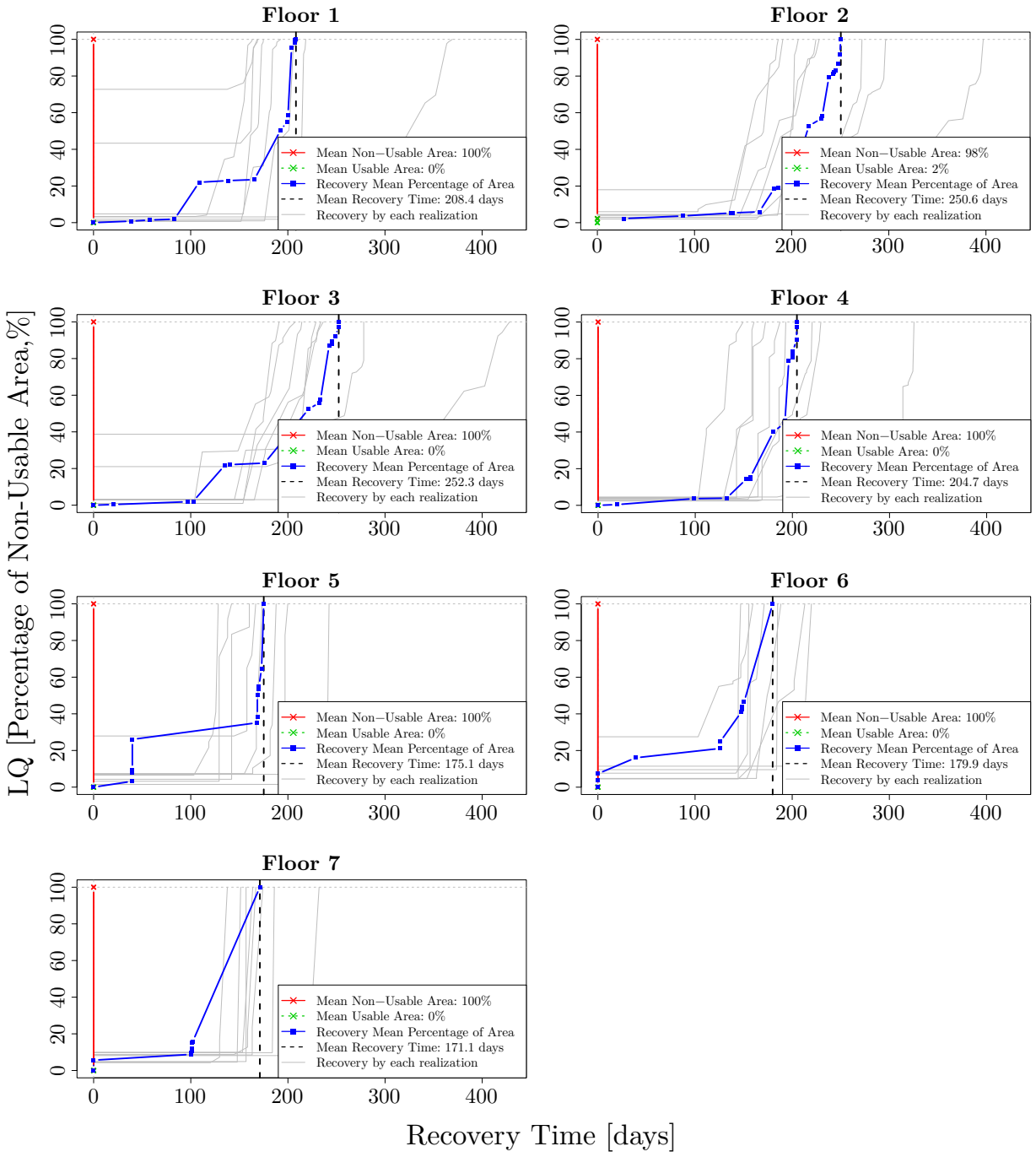

Figure 11.12: Recovery paths of usable area for the seven floors of the building for the resilience analysis case (LS_4, IM_6(Sa(T1)=0.54g)).

first floor to the last floor resulted to be $(PNUA \mid LS_3, IM_3) = (6, 56, 64, 28, 6, 14, 4)$ %, and the average recovery time for each floor of $t_{REC_f} = (67.6, 76.1, 74.6, 70.4, 21.6, 18.1, 11.9)$ days, respectively. The global resilience for this event, estimated with the envelope of the recovery of each plant, is shown in Fig. 11.13b. For this case the loss of functionality was

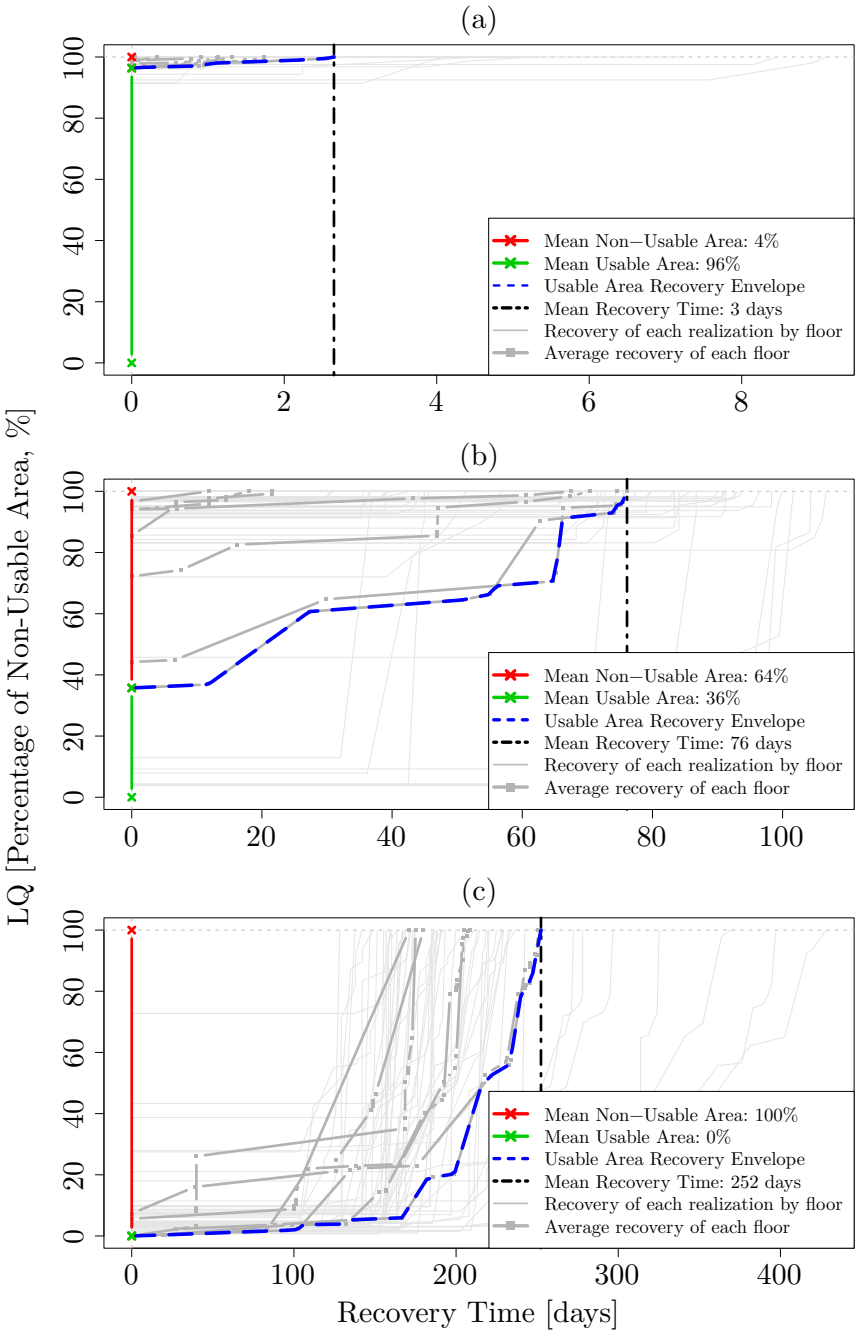

Figure 11.13: Recovery paths of the entire building for the resilience analysis: (a) (LS_1, IM_1), (b) (LS_3, IM_3) and (c) (LS_4, IM_6).

controlled by the third floor with 64%, while the total recovery time resulted in $t_{REC} =$ 76.1 days, corresponding to the second floor.

Likewise, for this second case, it is observed that the greatest loss of functionality is concentrated on the second, third, fourth and sixth floors, with 56, 64, 28 and 14% loss of usable area. This result suggests that the damage experienced by the non-structural

elements is concentrated on these floors, as shown in Fig. 11.6. The building is safe from the structural point of view; however, as mentioned in section 11.2.1, the main cause of the loss of functionality is the damage developed by the non-structural components, principally due to their low deformation capacity, as is the case of the reinforced concrete stairs and the unreinforced masonry walls. Indeed, some elements of the latter performance group experienced moderate and severe damage.

It should be recalled that the IM_3 (250 year return period) corresponds to the design intensity, as established by the NTC-DS (GCDMX, 2004a). Once again, this is an example that although design regulations have shown significant advances in terms of the life safety of the occupants in the event of intense earthquakes, they are not oriented towards limiting damage to non-structural elements. Of course, as Torroja (1960) literally pointed out: *Structures are not built to resist. They are built to be functional, having as an essential consequence that the construction maintains its form and condition over time. Their resistance is a fundamental condition, but, it is not the only purpose, not even the primary purpose.*

Figure 11.12 presents the loss and recovery of functionality for each floor of the building under consideration for the condition (LS_4, IM_6), which corresponds to an unsafe, unoccupiable, but repairable building ($TAG = R_S$), because this limit state of functionality is mainly controlled by the presence of severe structural damage. The result of the analysis suggests that the loss of functionality for all floors is 100%, while the average recovery time for each floor of is $(208, 251, 252, 205, 175, 178, 171)$, approximately. In Fig. 11.13c, the overall loss of functionality is indicated, which turns out to be 100%, and the recovery time is governed by the third floor, with t_{REC} =252 days.

Note that for light damage levels (*e.g.*, LS_1) the recovery time is close to the repair time. This means that recovery is not influenced by irrational factors; on the contrary, for excessive damage levels the recovery time is strongly influenced by irrational factors (*e.g.*, LS_3 and LS_4).

Another interesting aspect is the shape of the functional recovery curves of both the individual floors and the entire building. Moreover, in the three case studies shown in Figs. 11.10 to 11.12 it can be seen that the pattern of recovery is very similar, on a different scale, of course. The pattern being discussed is very similar to the trigonometric type recovery function proposed by Cimellaro *et al.* (2006, 2010a), and illustrated in Fig. 8.3. According to Cimellaro *et al.* (2006, 2010a), the initial, almost horizontal, slope of the trigonometric function is due to the fact that at the beginning of the recovery the society does not have the organization and financial resources to start the recovery process, *i.e.*, the loss of functionality remains constant during a time interval. When the society begins to have financial and human resources, and organizes them to start the recovery of functionality, the recovery curve begins to acquire the trigonometric recovery pattern mentioned above.

The trigonometric shape of the recovery of functionality curves obtained in this study is due to conditions different from those described by Cimellaro *et al.* (2006, 2010a). In the first instance, the slope parallel to the time axis that occurs at the initial stage of recovery

is due to factors that prevent the initiation of repairs, while the curve starts to gain slope at the moment when the first repair activity is completed, and so on. In Fig. 11.13a, it can be seen that the slope of the recovery curve is very small. This is because the building for the (LS_1, IM_1) event experienced an almost negligible amount of damage and severity. In Fig. 11.13b, where light to moderate damage to the non-structural components starts to become significant, it is seen that at the beginning of the recovery the slope of the recovery curve is slightly parallel to the horizontal axis. In this interval, activities such as structural inspection, financing process to pay for repairs, bidding process and repair planning are carried out. After this first stage, the slope increases substantially. This is because the number of structural elements that experienced damage associated with the event (LS_3, IM_3) was relatively small. In the next stage of the recovery curve, it can be seen that the slope of the recovery curve decreases significantly. The explanation is that the number of non-structural elements is much larger than that associated with structural elements; however, by definition the LS_3 is restricted use, non-functional, but it is safe from a structural point of view. Finally, for this case, a comparison can be made between the area above the curves corresponding to the loss of functionality of structural and non-structural elements. It can be seen that for the former, the area is much smaller than for the latter. Again, this is due to the fact that the density of elements that experienced a greater amount of damage is concentrated in the non-structural elements.

The recovery curve for the (LS_4, IM_6) event is illustrated in Fig. 11.13c. Again, for this case it can be seen that in the initial stage of recovery the slope has little slope. This stage corresponds to the factors that prevent the start of repairs, but unlike the previous case, in this case the corresponding time interval is much longer. After this stage, it is observed that the slope of the recovery curve begins to increase rapidly until the instant in which the recovery of 100% of the system operation is reached.

It can be concluded that the functionality recovery curves obtained with the methodology proposed in this work are a particular case of the trigonometric recovery function proposed by Cimellaro *et al.* (2006, 2010a). The conditions proposed by these authors correspond to a global system, *i.e.*, a system composed of a set of buildings, *e.g.*, a community or a city, while the conditions proposed in this work correspond to the recovery of an individual building. Also, effects external to the building are involved through irrational factors, which have been inferred from very little empirical information. As more information is systematically collected, it will be possible to consider more and better irrational factors.

11.2.4 Convergence analysis to determine the number of bootstrap replicates for statistical inference analysis

The statistical inference of the DVs was performed with the bootstrap technique described in Chapter 10, both for the $(\mathbf{dv} \mid LS, IM)$ condition and for the $(\mathbf{dv} \mid IM)$ condition, which corresponds to the vulnerability function, as described in section 10.8. To obtain the expected value of the sample mean of the DVs, their respective standard error $\widehat{\text{se}}$ and confidence interval BC_a, a convergence analysis was previously performed to determine

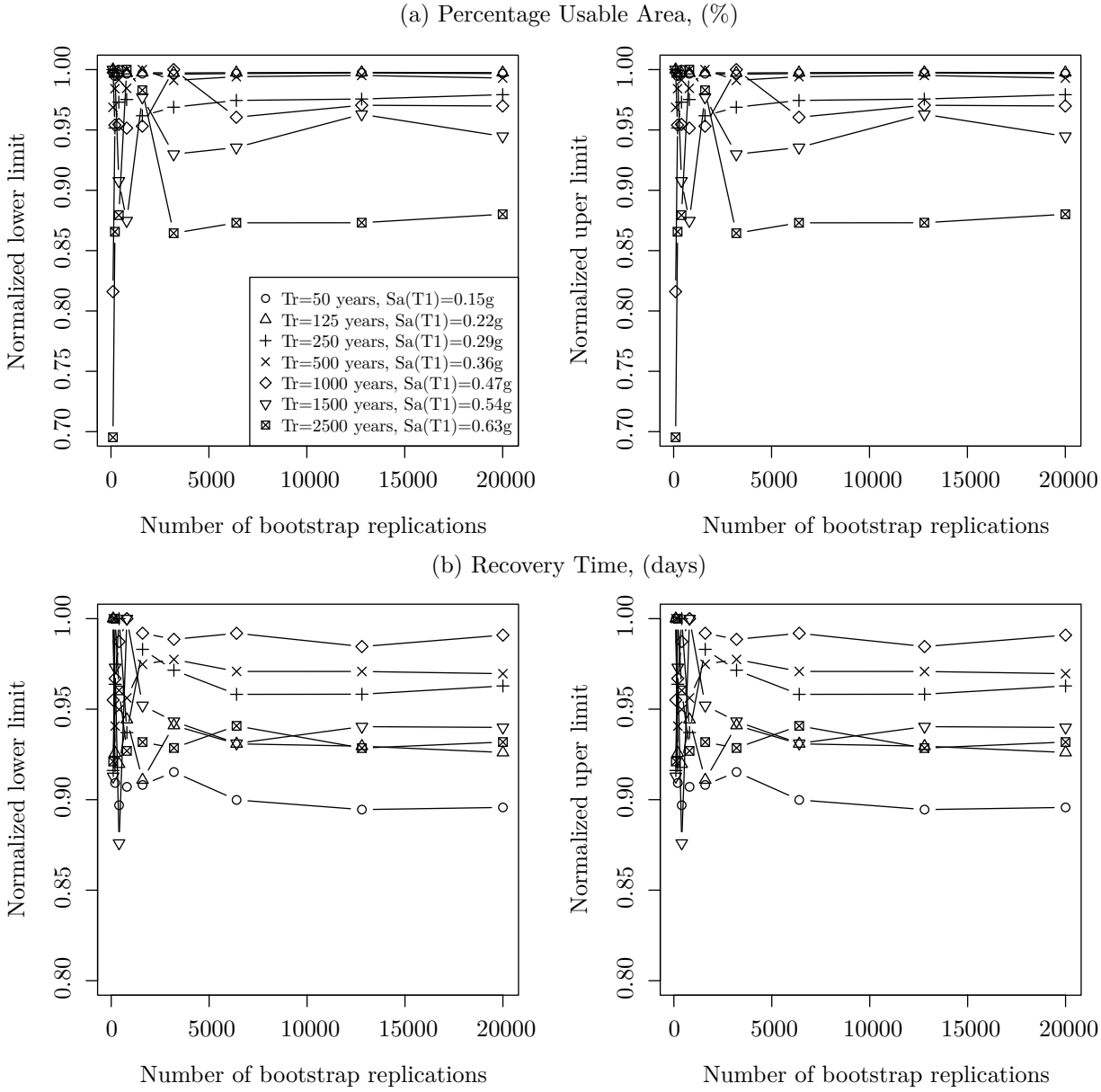

Figure 11.14: Number of bootstrap replications necessary to obtain an acceptable convergence in the calculation of the lower limit $\hat{\theta}^*_{\text{lo}}$ (left column) and upper limit $\hat{\theta}^*_{\text{up}}$ (right column) of the confidence interval BC_a, for the: (a) Percentage of Usable Area (PUA), and (b) Recovery Time (t_{REC}), for the seven seismic intensities considered in the study.

the number of bootstrap replicates B to be used. As described in section 10.7.2, it is known that with 200 bootstrap replicates is obtained an acceptable approximation of the standard error (Efron and Tibshirani, 1993). For approximating confidence intervals this number can be on the order of 1,000 or even much larger (DiCiccio and Efron, 1996); however, there is no general criterion for determining this number.

In this application the number of bootstrap replicates needed was determined with the

convergence criterion described in section 10.7.2. This criterion was applied to the confidence interval limits for a $(1-2\cdot\alpha) = 95\%$ probability of the expected value of the sample mean of each decision variable $\hat{\theta}^*_{\mathbf{dv}}(\cdot)$ and its respective standard error $\widehat{\text{se}}$, both normalized by the maximum value of each of them, obtained in each IM, considering the number of bootstrap replicates as a variable.

To exemplify this, the first column of Fig. 11.14a illustrates the convergence analysis for the lower bound $\hat{\theta}^*_{\text{lo}}$ of the confidence interval of the expected value of the sample mean of the percentage of usable area, and the second column presents the analysis for the upper bound $\hat{\theta}^*_{\text{up}}$, both for each IM considered in this application. Both figures show that the analysis stabilizes when approximately 6,000 bootstrap replicates are used. Using the same criterion, Fig. 11.14b presents the convergence analysis for the recovery time. In this second case it can be seen that for both statistical parameters to stabilize, approximately the same number of bootstrap replicates is required.

The convergence analysis was performed for each of the DVs and the number of bootstrap replicates for one of them at each IM was between 4,000 to 6,000 replicates. In order to establish a practical criterion, 10,000 bootstrap replicates were used to approximate (1) the expected value of the mean of each decision variable $\hat{\theta}^*_{\mathbf{dv}}$, (2) its respective standard error $\widehat{\text{se}}$ and (3) its confidence interval BC_a. It would seem that this quantity demands a lot of computational time. This is actually not the case. These computations are performed in a few minutes for the whole analysis, and compared to the time needed to perform the same amount of NLDA, the bootstrap statistical inference scheme is very attractive, and as will be seen below, it allows to obtain consistent results, at least from the point of view of statistical inference.

11.2.5 Statistical inference analysis using bootstrap technique

This section presents the statistical inference of the DVs used in this thesis to explain the seismic resilience of buildings for the (LS_1, IM_1), (LS_3, IM_3) and (LS_4, IM_6) events. In summary, the methodology proposed in this thesis allows to approximate the expected value of the sample mean of the following DVs:

1. Percentage of non-usable area $PNUA$ as a physical parameter representative of the loss of functionality $LQ(t)$.

2. Delay time $t_{IF}(t)$, corresponding to the factors that prevent the start of repairs.

3. Repair time of the PGs corresponding to structural, non-structural and furniture elements, $t_{REP}(t)$.

4. Recovery time $t_{REC}(t)$, corresponding to the sum of the delay time $t_{IF}(t)$ and the repair time $t_{REP}(t)$.

5. Rapidity of the recovery of functionality $\theta(t)$.

6. Indirect economic losses I_{EL} due to the loss of operability of the different units (floors) that make up the building.

7. Total repair costs C_{REP}, and its corresponding disaggregation, *i.e.*, those corresponding to structural elements $C_{REP,S}$, non-structural elements $C_{REP,NS}$ and furniture $C_{REP,F}$.

8. Number of workers n_w required to perform the repair work of the damage experienced by the various PGs comprising the building.

9. Number of injured occupants n_i generated by the damage experienced by the potentially damaging PGs.

10. Number of fatalities n_d generated by the damage experienced by the potentially damaging PGs and structural collapse.

11. Equivalent economic value associated with the number of injured EEV_{INJ}.

12. Equivalent economic value associated with the number of fatalities EEV_{DEA}.

13. Total economic losses EE_T, derived from repair costs, indirect economic losses I_{EL}, and the equivalent economic value associated with the injured EEV_{INJ} and fatalities EEV_{DEA}.

First, to illustrate the capability of the bootstrap technique consider the following example. The first column of Fig. 11.15 illustrates the histogram of the data obtained from the simulation of recovery time t_{REC} and percent usable area PUA for the (LS_3, IM_3) condition. The second column shows the histogram for the same cases but now obtained from the bootstrap random resampling of the sample mean of these DVs. In the first column, the blue dashed vertical lines located in the center of each histogram indicate the mean value, and the lines at the extremes their respective confidence interval estimated with the 2.5% and 97.5% percentiles of the seed sample. In the second column, the center lines indicate the sample mean, and the end lines indicate the confidence intervals approximated with the BC_a method. It can be seen that for both cases the histogram corresponding to the original data does not look good because the amount of data is very small. On the contrary, in the second column it can be seen that although the shape of the histogram is not normal, its appearance is much better. This is precisely one of the qualities of the bootstrap technique and the monotonic transformation $m(\cdot)$, described in section 10.7.1. This transformation is an intrinsic property of the percentile method, the basis of the BC_a method, and in many cases produces a histogram very close to one with normal distribution, regardless of the shape of the histogram of the seed sample $\mathbf{x}$, as seen in the second column of Fig. 11.15.

For event (LS_3, IM_3) the bootstrap expected value of the recovery time t_{REC} (see second column of Fig. 11.15b) was approximately 78 days. This value is very similar to that shown in Fig. 11.13a, obtained with the recursive algorithm for estimating the recovery of functionality, described in section 8.4. The same figure shows the extreme values of the

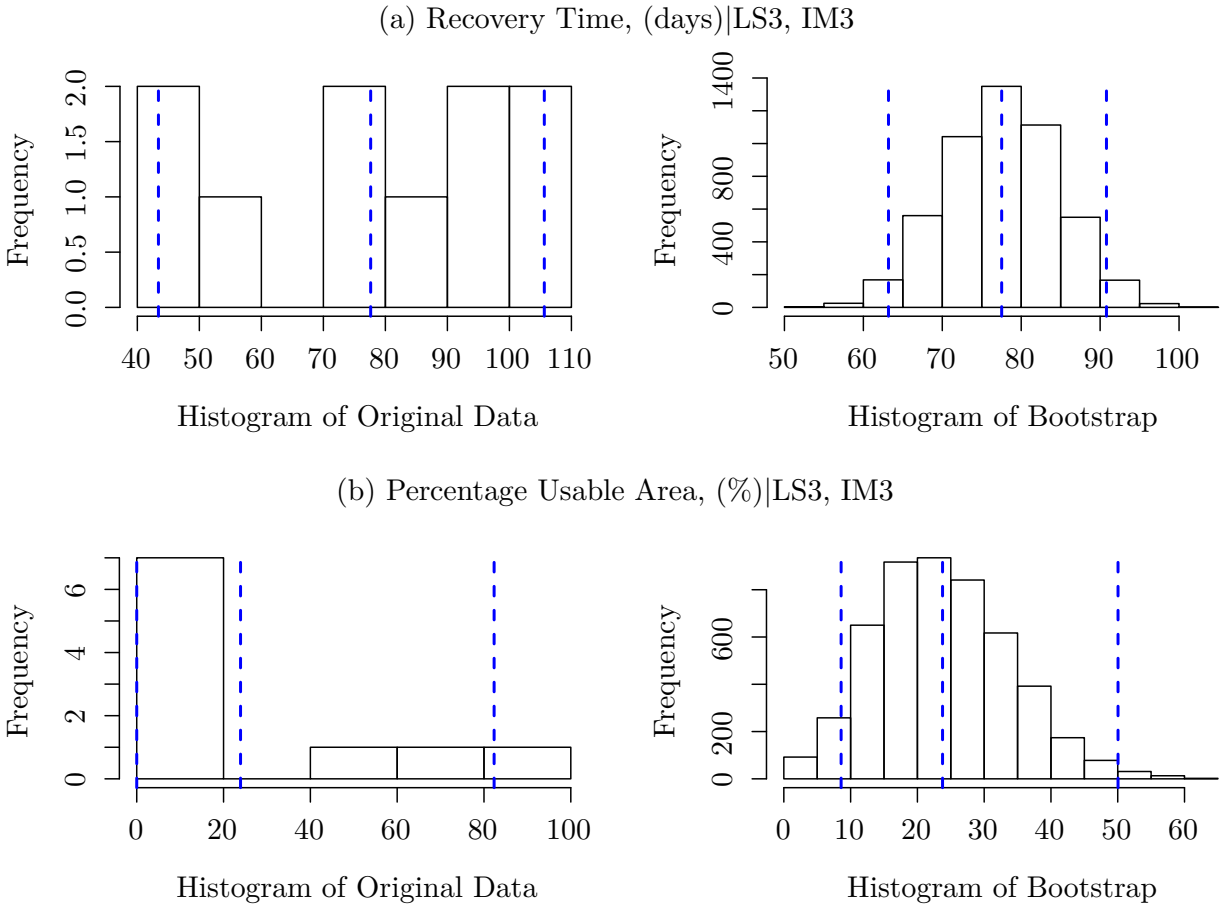

Figure 11.15: The first column shows the histogram of the seed data for recovery time t_{REC} and percent usable area PUA and the second column shows the histogram of the bootstrap replicates of the sample mean for the (LS_3, IM_3) event.

confidence interval estimated for a 95th percentile of probability. The lower limit obtained was $\hat{\theta}^*_{\text{lo}} = 63$ days, and the upper limit was $\hat{\theta}^*_{\text{up}} = 91$ days. It should be noted that the difference between the upper bound and the expected value of the mean is 46%, while the difference of the expected value of the mean and the lower bound is 53%. This difference is due to the non-normal shape of the histogram. If the histogram had a perfect normal shape both ratios would result in 50%. However, the BC_a method captures this difference and allows for a bias correction and a better approximation of the confidence interval, as described in the section 10.7.2.

In the second column of Fig. 11.15b, which corresponds to the percentage of usable area PUA, the histogram skewness is larger. For this case, the expected value of the sample mean is $\hat{\theta}^* = 24\%$, and the respective lower and upper limits of the confidence interval are 9% and 50%, respectively. The relative difference between these limits and the expected value of the sample mean is 63% and 36%, respectively. On the other hand, if for the latter case we had used to the classical methodology to estimate the confidence interval by means of the expression $\hat{\theta} \pm z^{(\alpha)} \cdot \hat{\sigma}$, the lower limit would have resulted in $24\% - 1.96 \times 33\% =$

-40.7%, while for the upper limit we have $24\% + 1.96 \times 33\% = +88.68\%$. Obviously the lower bound is physically inconsistent (this was performed for all the DVs studied and similar inconsistent results were obtained). For this case the standard deviation for the event $(PUA \mid LS_3, IM_3)$ turned out to be approximately 33%, while the standard error estimated with the bootstrap technique was 10%. For this reason, the bootstrap technique, and specifically the BC_a method, are powerful tools as they allow consistent and acceptable statistical inferences to be made in highly complex problems using only the power of computational calculation.

Table 11.3: Statistical inference of the DVs (1) for event (LS_1, IM_1) by bootstrap technique: expected value (3); confidence intervals (2, 4); standard error (5); bias (6); ratio of standard error to expected value (7); ratio of bias to standard error (8).

	DV (1)	$\hat{\theta}^*_{\mathrm{lo}}$ (2)	$\hat{\theta}^*_{\mathbf{dv}}$ (3)	$\hat{\theta}^*_{\mathrm{up}}$(4)	$\widehat{\mathrm{se}}$ (5)	$\widehat{\mathrm{bias}}$ (6)	$\widehat{\mathrm{se}}/\hat{\theta}^*_{\mathbf{dv}}$ (7)	$\mid \widehat{\mathrm{bias}}/\widehat{\mathrm{se}} \mid$ (8)
1	PUA	90	92	93	0.850	6.05E-03	0.009	6.60E-05
2	t_{IF}	1.3	1.9	2.6	0.326	-1.07E-03	0.171	5.59E-04
3	t_{REP}	1.7	2.7	3.7	0.486	4.12E-04	0.182	1.55E-04
4	t_{REC}	3.4	4.6	5.9	0.622	-6.54E-04	0.136	1.43E-04
5	I_{EL}	0	0	0	0	0	0	0
6	$C_{REP,T}$	0.0139	0.0208	0.03	0.004	-7.13E-06	0.182	3.43E-04
7	$C_{REP,S}$	0	0	0	0	0	0	0
8	$C_{REP,NS}$	0.0139	0.0208	0.03	0.004	-7.13E-06	0.182	3.43E-04
9	$C_{REP,F}$	0	0	0	0	0	0	0
10	n_w	10	14	16	1.36	-6.46E-03	0.098	4.66E-04
11	n_i	0	0	0	0	0	0	0
12	n_d	0	0	0	0	0	0	0
13	EEV_{INJ}	0	0	0	0	0	0	0
14	EEV_{DEA}	0	0	0	0	0	0	0

Note: The percentage of usable area is expressed as a percentage of the usable area; DVs associated with time in days; DVs associated with economic losses in MUSD; and the DVs associated with individuals in units.

Tables 11.3, 11.4 and 11.5 present the results of the statistical inference performed for each of the DVs studied for the events (LS_1, IM_1), (LS_3, IM_3) and (LS_4, IM_6), respectively. All statistical analysis presented in these tables is performed on the expected value $\hat{\theta}^*_{\mathbf{dv}}$ of the sample mean for the above events. In the third column the expected value of the mean of each DV is indicated, and in the second and fourth columns the lower and upper limit of the confidence interval $CI_{\mathrm{BC}_a 95}$, estimated with a 95% probability. The fifth column gives

the standard error and the sixth column gives the bias of the estimate of the expected value of the sample mean. The seventh column presents the ratio between the standard error and the expected value of the sample mean, *i.e.*, the coefficient of variation of the bootstrap estimate. Finally, the eighth column shows the ratio of the bias to the standard error.

For event (LS_1, IM_1), as already observed in Fig. 11.13a, the loss of functionality is practically zero, since the expected value of the percentage usable area PUA after the seismic event was 92% with an $CI_{\mathrm{BC}_a 95}$ of $(90, 93)\%$, while the recovery time t_{REC} is between 3.4 and approximately 5.9 days. For this case we have that the expected value of the inspection is 1.9 days, while the repair time is 2.7 days. Note that for the LS_1 it is not necessary for the building to close its spaces because the amount and severity of damage is negligible. That is, the repair of minor damage can be performed without affecting the operation of the building or the comfort of the occupants.

Table 11.4: Statistical inference of the DVs (1) for event (LS_3, IM_3) by bootstrap technique: expected value (3); confidence intervals (2, 4); standard error (5); bias (6); ratio of standard error to expected value (7); ratio of bias to standard error (8).

	DV (1)	$\hat{\theta}^*_{\mathrm{lo}}$ (2)	$\hat{\theta}^*_{\mathbf{dv}}$ (3)	$\hat{\theta}^*_{\mathrm{up}}$(4)	$\widehat{\mathrm{se}}$ (5)	$\widehat{\mathrm{bias}}$ (6)	$\widehat{\mathrm{se}}/\hat{\theta}^*_{\mathbf{dv}}$ (7)	$\mid \widehat{\mathrm{bias}}/\widehat{\mathrm{se}} \mid$ (8)
1	PUA	9	24	50	10.00	-1.49E-01	0.421	6.25E-03
2	t_{IF}	50.3	65.3	78	6.93	-8.87E-02	0.106	1.36E-03
3	t_{REP}	9.8	12.3	16	1.48	-1.33E-02	0.121	1.08E-03
4	t_{REC}	63	78	91	7.04	-1.02E-01	0.091	1.31E-03
5	I_{EL}	0.43	0.53	0.62	0.05	-6.93E-04	0.091	1.31E-03
6	$C_{REP,T}$	0.119	0.135	0.153	0.01	1.42E-05	0.063	1.05E-04
7	$C_{REP,S}$	0	0	0	0	0	0	0
8	$C_{REP,NS}$	0.119	0.135	0.153	0.01	1.42E-05	0.063	1.05E-04
9	$C_{REP,F}$	0	0	0	0	0	0	0
10	n_w	29	31	32	0.86	-9.12E-03	0.028	2.96E-04
11	n_i	0	1	1	0.17	1.52E-03	0.300	2.76E-03
12	n_d	0	0	0	0	0	0	0
13	EEV_{INJ}	0.013	0.080	0.255	0.05	1.70E-03	0.663	2.13E-02
14	EEV_{DEA}	0	0	0	0	0	0	0

Note: The percentage of usable area is expressed as a percentage of the usable area; DVs associated with time in days; DVs associated with economic losses in MUSD; and the DVs associated with individuals in units.

In column 7 of the Table 11.3 the bootstrap coefficient of variation $\widehat{\text{se}}/\widehat{\theta}^*_{\mathbf{dv}}$ is indicated. It can be seen that for all DVs this statistical parameter is small. This is because the damage experienced at this IM (Tr=50 years) was practically negligible, and therefore the dispersion generated on the DVs small. Also, column eight shows the ratio between the bias and the standard error of the analysis. It is observed that for all DVs this parameter resulted to be very small. As a rule of thumb, values less than or equal to 0.25 for this ratio can be said that the shape of the bootstrap histogram of the variable in study indicates that the mean squared error is no more than 3.1% larger than the standard error (Efron and Tibshirani, 1993).

For the event (LS_3, IM_3) (see Table 11.4), which corresponds to the design seismic intensity (Tr=250 years, 0.29g), it is observed that the expected value of the sample mean of the usable area PUA was 24% with an CI_{BC_a95} of $(9, 50)$%. The mean recovery time t_{REC} was 78 days, and its respective CI_{BC_a95} of $(63, 91)$ days. For this case note that the expected value of the mean value of the time preventing the start of repairs turned out to be approximately 65 days, while the repair time of approximately 12 days. This indicates that 84% of the delay in the recovery of functionality is due to irrational factors. Also, it should be noted that the repair time, estimated with the recursive process proposed in this thesis, is optimized by an average number of 31 workers. For this LS the building is declared as non-functional, hence, for this case the indirect economic loss due to the loss of revenue in each unit of the building was approximately 0.53 MUSD. Likewise, the expected repair cost was 0.135 MUSD. For this case the indirect economic losses turned out to be of greater magnitude than the direct economic losses. This is an aspect that should be taken into account by decision makers, since by making a long-term investment in the retrofitting of the building structure to improve its seismic performance at this level of seismic intensities it is feasible to reduce the indirect economic losses.

On the other hand, one person was injured in this event. The equivalent economic value of the injury was 0.080 MUSD, with an CI_{BC_a95} of $(0.013, 0.255)$ MUSD. This amount indicates that the injury experienced by the occupant was a severe injury. This result is consistent with data reported by Spence *et al.* (2011) and Porter *et al.* (2006), who argue that an important factor contributing to total economic losses is the equivalent value associated with nonfatal casualties.

For this event, it is observed that the standard error of the approximation of the expected value of the sample mean of some DVs increased significantly with respect to the previous case (see column seven of Table 11.4). This is directly reflected in the bootstrap coefficient of variation, a measure indicating the heterogeneity of the bootstrap sample $\mathbf{dv}^*$. The DVs that presented the greatest heterogeneity are the percentage of usable area, the number of workers, and the economic equivalent value of injured occupants, with 42%, 30%, and 66%, respectively. This is because in this event the severity and amount of damage experienced by the non-structural elements increased significantly, and therefore the dispersion of the values of the DVs also increased. This is also a consequence of the record to record variability of the accelerogram pairs corresponding to this seismic intensity.

About the ratio $\mid \widehat{\text{bias}}/\widehat{\text{se}} \mid$, was found to be less than 0.25; therefore, the mean squared

error is less than 3.1% of the standard error $\widehat{\text{se}}$. This suggests that there is no need to worry about the bias of the histogram of each DV obtained by random resampling, as in the bootstrap histogram of the recovery time in Fig. 11.15a. When the bias is negligible the shape of the histogram of bootstrap replicates of the statistic of interest $s(\cdot)$ acquires the shape of the normal distribution density.

Table 11.5 presents the results of statistical inference for event (LS_4, IM_6). For this event the loss of total functionality is evident, as can be seen in Fig. 11.7, where the amount and severity of damage experienced by each performance group speaks for itself. Therefore the result of the numerical simulation of the post-seismic inspection was that the building is unsafe ($TAG = R_S$), not occupiable, but repairable. For this event the building is not occupiable for a period between 225 and 334 days, with a mean of 259 days. Therefore, the indirect economic losses are substantially important, amounting to between 1.53 and 2.3 MUSD, with a sample mean of 1.8 MUSD. These losses can be reduced if the tenant of each floor decides to rent space in another building when the damaged building is safe to enter and relocate.

On the other hand, for this event the expected value of the sample mean of the direct economic losses was 1.10 MUSD with a confidence interval of $(0.92, 1.5)$ MUSD. On the other hand, note that 63.47% of the repair cost is associated with non-structural elements, while 35.86% with structural elements and finally 0.77% associated to the furniture-type elements. Also, for the building to be repaired in at least 106 days, 79 workers are required. Note that this amount corresponds to the sum of the workers repairing each performance group. Therefore, the workers repairing each performance group have their own specialization.

In the LS_4, by definition, due to the severity of the damage experienced mainly by the non-structural and furniture-type elements, it is likely that the users of the building will suffer some type of injury, whether light, moderate, severe or fatal. Indeed, for this event the model predicts that on average 3 people are injured, but it is possible that this number could be as high as 5 people, or at least one user could be injured. Assuming under a conservative criterion that 5 people are injured, the associated economic value would be 0.534 MUSD. Using the upper limit of the confidence interval and adding this last loss to the total losses (4.3 MUSD), 12.4% of the monetary losses are associated with the equivalent economic value of the injured. Again, as noted by Shoaf *et al.* (2005) and (Porter *et al.*, 2006), the economic cost associated with people injured as a result of damage to a building due to the effects of an earthquake can be very high.

Finally, it is observed that the bootstrap coefficient of variation $\widehat{\text{se}}/\hat{\theta}^*_{\mathbf{dv}}$ (column 7 of Table 11.5) increased for most DVs with respect to the (LS_3, IM_3) event analysis, especially for (1) percent usable area (46%), (2) repair time (49%), (3) total repair cost (93%), (4) cost of non-structural repairs (24%), (5) number of workers (85%), and (6) number of injured (18%). This increase in the coefficient of variation is a reflection of the increased uncertainty in the results of statistical inference. Column 6 of Table 11.5 shows that for all DVs the bias in the approximation of the expected value of the sample mean is relatively small. This means that the shape of the histogram of the bootstrap replicates of the

Table 11.5: Statistical inference of the DVs (1) for event (LS_4, IM_6) by bootstrap technique: expected value (3); confidence intervals (2, 4); standard error (5); bias (6); ratio of standard error to expected value (7); ratio of bias to standard error (8).

	DV (1)	$\hat{\theta}^*_{\text{lo}}$ (2)	$\hat{\theta}^*_{\mathbf{dv}}$ (3)	$\hat{\theta}^*_{\text{up}}$(4)	$\widehat{\text{se}}$ (5)	$\widehat{\text{bias}}$ (6)	$\widehat{\text{se}}/\hat{\theta}^*_{\mathbf{dv}}$ (7)	$\lvert \widehat{\text{bias}}/\widehat{\text{se}} \rvert$ (8)
1	PUA	0	1	2	0.44	6.96E-03	0.615	9.70E-03
2	t_{IF}	132.74	152.8	173.3	10.27	4.09E-02	0.067	2.67E-04
3	t_{REP}	76.83	106.3	157.3	19.25	-6.32E-01	0.181	5.95E-03
4	t_{REC}	225.20	259.1	334.0	24.79	-5.92E-01	0.096	2.28E-03
5	I_{EL}	1.53	1.8	2.3	0.17	-4.02E-03	0.096	2.28E-03
6	$C_{REP,T}$	0.9171	1.1038	1.5072	0.13	-3.83E-03	0.122	3.47E-03
7	$C_{REP,S}$	0.2591	0.3958	0.6775	0.10	-2.81E-03	0.248	7.09E-03
8	$C_{REP,NS}$	0.5984	0.6995	0.8080	0.05	-1.03E-03	0.078	1.47E-03
9	$C_{REP,F}$	0.0044	0.0085	0.0116	0.0018	1.06E-05	0.213	1.25E-03
10	n_w	72	79	88	4.15	-1.03E-01	0.052	1.30E-03
11	n_i	1	3	5	1.03	1.13E-02	0.353	3.87E-03
12	n_d	0	0	0	0	0	0	0
13	EEV_{INJ}	0.084	0.265	0.534	0.111	-2.36E-03	0.418	8.91E-03
14	EEV_{DEA}	0	0	0	0	0	0	0

Note: The percentage of usable area is expressed as a percentage of the usable area; DVs associated with time in days; DVs associated with economic losses in MUSD; and the DVs associated with individuals in units.

sample mean is approximately normal. Again, the quotient $\widehat{\text{bias}}/\widehat{\text{se}}$ is less than 0.25, so it can be said that the mean squared error is no more than 3.1% larger than the standard error $\widehat{\text{se}}$.

11.2.6 Vulnerability analysis of seismic resilience

Another way of expressing the variables that explain the seismic resilience of a building is in terms of vulnerability functions. That is, expressing the expected value of the sample mean of each decision variable and its respective confidence interval as a random variable of the intensity measure, as expressed in Eq. 10.40, written again here:

$$V_f\left(IM, \theta_{\mathbf{dv}} \in \left[\hat{\theta}^*_{\text{lo}}, \hat{\theta}^*_{\text{up}} | IM\right]_{\text{BC}_a}\right) \tag{11.1}$$

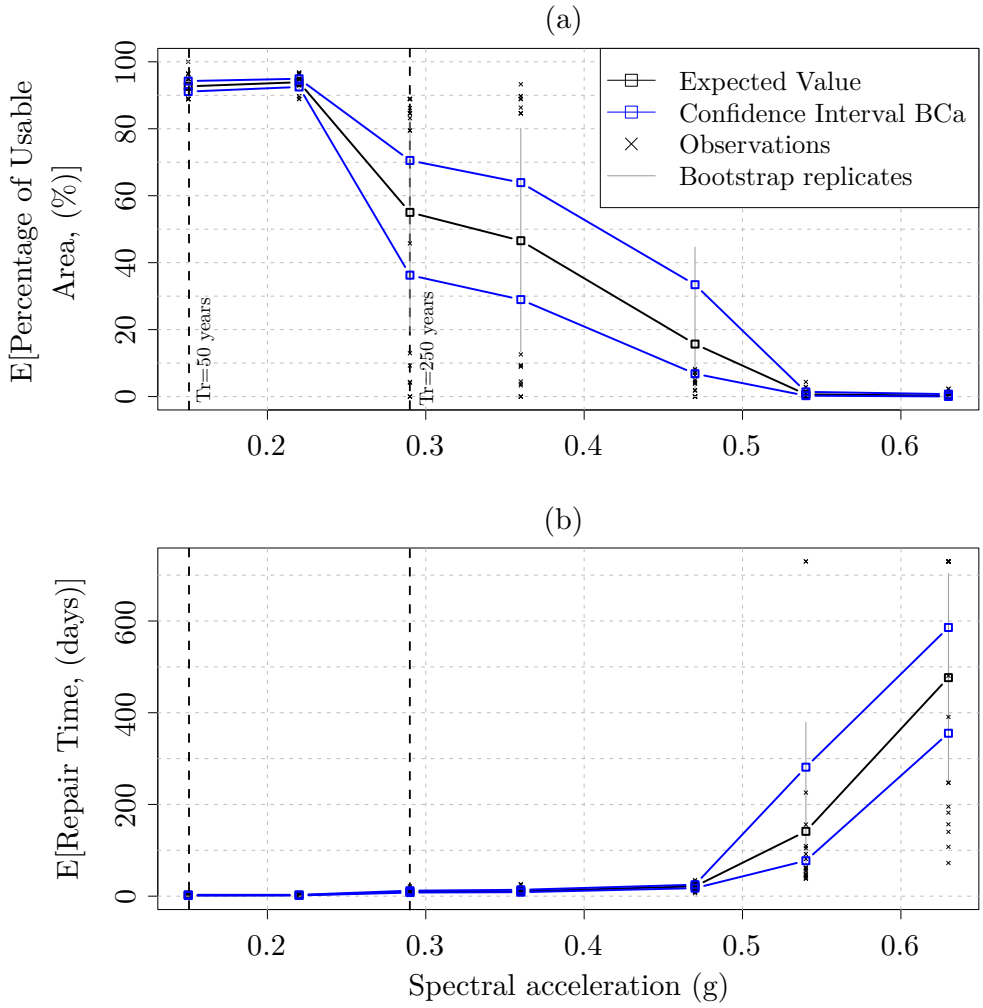

Figure 11.16: Expected value $\hat{\theta}^*_{\mathbf{dv}}$ and its confidence interval BC_a obtanied means the bootstrap method for the (a) Percentage of Usable Area PUA and (b) Repair Time t_{REP}.

For example, for the IM_3, the limit states of functionality that contributed to the probability distribution were LS_1 and LS_3, with 50% probability each (see Fig. 11.9d). This means that the observed data in each of these limit states of functionality $(\mathbf{dv} \mid LS_i, ..., LS_j, IM)$ are grouped into a single data set $(\mathbf{dv} \mid IM)$, for each DV, and processed using the bootstrap technique, in the same way as the data were processed in the previous section, but in this case the results of the resilience analysis are conditioned only to each IM. In this way, the vulnerability functions express the expected value of the total losses of each DV at each IM with their respective confidence interval. The vulnerability functions presented in this section were approximated with the methodology described in the section 10.8.2.

Figures 11.16 to 11.23 show the vulnerability function for each of the DVs studied in this thesis. The thick black lines indicate the expected value of the sample mean of the DV, while blue indicates the bootstrap confidence interval for a 95% probability. In this respect, by approximating the confidence interval of the estimate of the expected value

of the sample mean of the DVs we are also approximating the magnitude of the uncertainty of such approach. The symbol "×" indicates the original observations, *i.e.*, those obtained for the set of 20 orthogonal pairs of accelerograms associated with each IM. For visual convenience, the gray vertical lines represent the 10,000 sample mean observations obtained in the bootstrap analysis. The black vertical dotted lines indicate the IM associated with immediate occupation (Tr=50 years, left line) and collapse prevention (Tr=250 years, right line). These intensities correspond, as indicated above, to the design intensities specified by NTC-DS (GCDMX, 2004a).

In figure 11.16a it can be seen that the performance of the building from IM_1 (Tr=50 years, Sa(T1)=0.15g, immediate occupancy) to IM_2 (Tr=125 years, Sa(T1)=0. 22g) the building presents a good resilient capacity since it retains at least 91% ($\hat{\theta}^*_{\mathbf{dv}} = 93\%, CI_{\mathrm{BC}_a 95} \sim (91, 94)\%$) of its functionality in terms of percentage of usable area. For these two performance levels, the results suggest that the building practically recovers its functionality between 2 and 4 days. In this case, light damage occurs in very small quantities (mainly in non-structural elements), which must be repaired by approximately 7 to 13 workers. The total repair costs for this case are between 0.01 and 0.02 MUSD. These economic losses are controlled by the non-structural damage, *i.e.*, there were no losses derived from structural or furniture damage. For these two levels of seismic performance, there were no indirect economic losses due to business interruption, injuries or loss of life, therefore there were no equivalent economic losses for these two DVs.

For the IM_3 (Tr=250 years, Sa(T1)=0.29g) associated with life protection, the performance of the building is adequate from a structural point of view. However, it loses functionality in a substantial way mainly due to the severe, moderate and light damage experienced by the non-structural elements (*i.e.*, interior and exterior masonry walls, interior partition walls and stairs). The expected value of the sample mean usable area for this case was 55%, with an $CI_{\mathrm{BC}_a 95}$ of (36.71)%, while the expected value of the recovery time was 43 days, with an $CI_{\mathrm{BC}_a 95}$ of (26.60) days. To get the building back to its level of functionality requires an average of 28 workers with an $CI_{\mathrm{BC}_a 95}$ of $(26, 29)$ workers. In this regard, the mean time associated with factors that impede the start of repairs was 33 days. This means that while it is possible to optimize the repair time, it is more difficult to optimize the time associated with the irrational factors since they are beyond the control of the engineers. Regarding repair costs, their expected value from the sample mean was 0.09 MUSD with a confidence interval of $(0.08, 0.1)$ MUSD. Note that the direct costs for this event are controlled by the non-structural elements. For this level of performance neither the structural elements nor the furnishings were damaged.

In this seismic intensity, unlike the previous ones, there were already indirect economic losses caused by the interruption of business on the different floors of the building. The expected value of the sample mean was 0.29 MUSD ($CI_{\mathrm{BC}_a 95} \sim (0.18, 0.41)$ MUSD). Note that at this performance level the LSs contributing to the probability distribution were LS_1 and LS_3. While at LS_1, by definition, it loses functionality partially, operations within the building can continue; however, LS_3 by definition implies that the building is declared restricted use, and therefore non-functional. It is then to the limit state LS_3 that the indirect economic losses are attributed. This is an example of why the evaluation

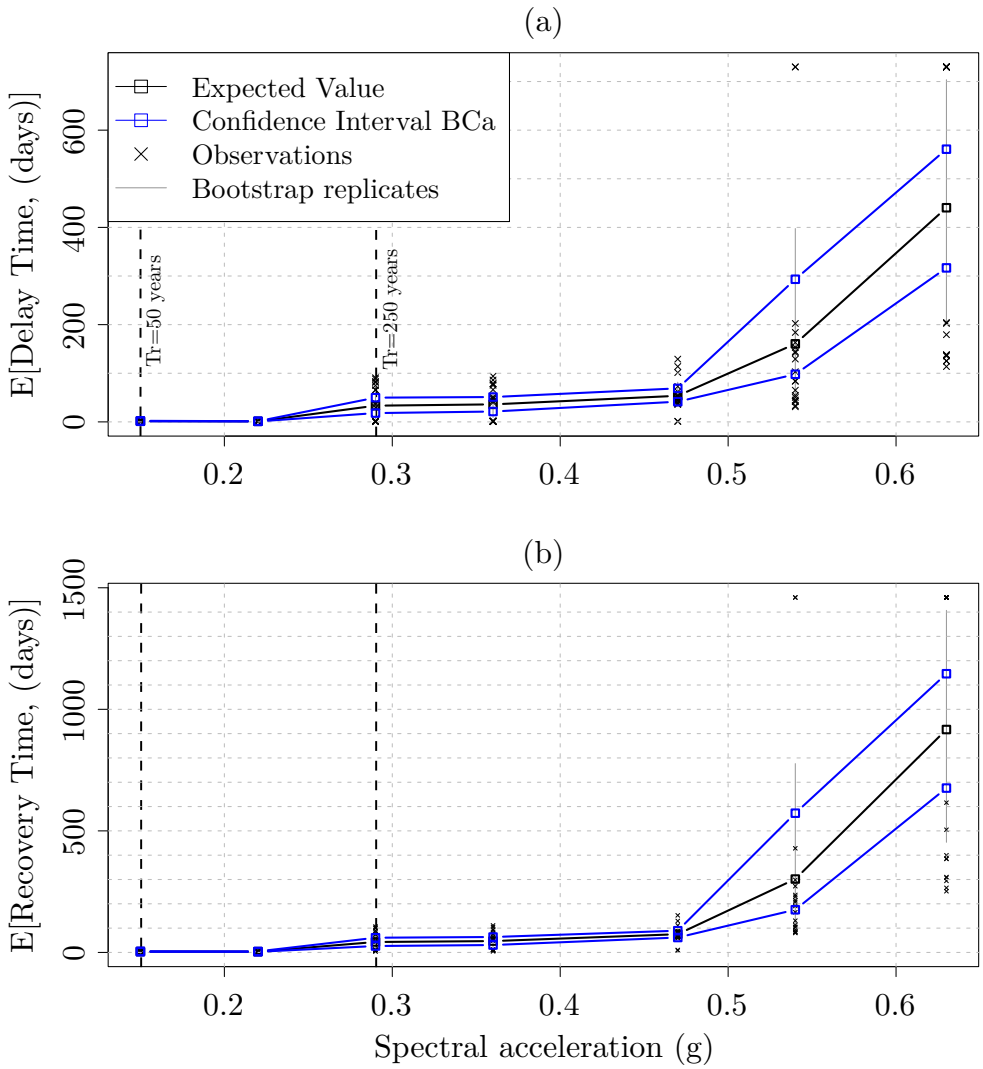

Figure 11.17: Expected value $\hat{\theta}^*_{\mathbf{dv}}$ and its confidence interval BC_a obtained means the bootstrap method for the (a) Delay Time t_{if} and (b) Recovery Time t_{REC}.

of functionality limit states is attractive, since they are useful to know the origin of the different losses. On the other hand, in this case there were no fatalities; however, one person experienced some type of injury. As a consequence, the equivalent economic value is 0.039 MUSD. Finally, the total economic losses associated with this level of performance were 0.43 MUSD, with an $CI_{\mathrm{BC}_a 95} \sim (0.28, 0.60)$ MUSD.

It can be concluded, for this performance level, which corresponds to the design seismic intensity, that the building is resilient because although it experienced damage to the non-structural elements (*i.e.*, interior and exterior masonry walls, interior partition walls and stairs), which caused the building to be unoccupiable for an interval of 26 to 60 days (*i.e.*, one to two months), and although one person was injured, the building has the capacity to recover. Furthermore, the building is structurally safe as none of the *PG*s of this type experienced any damage. While this condition is not the only one that should be taken

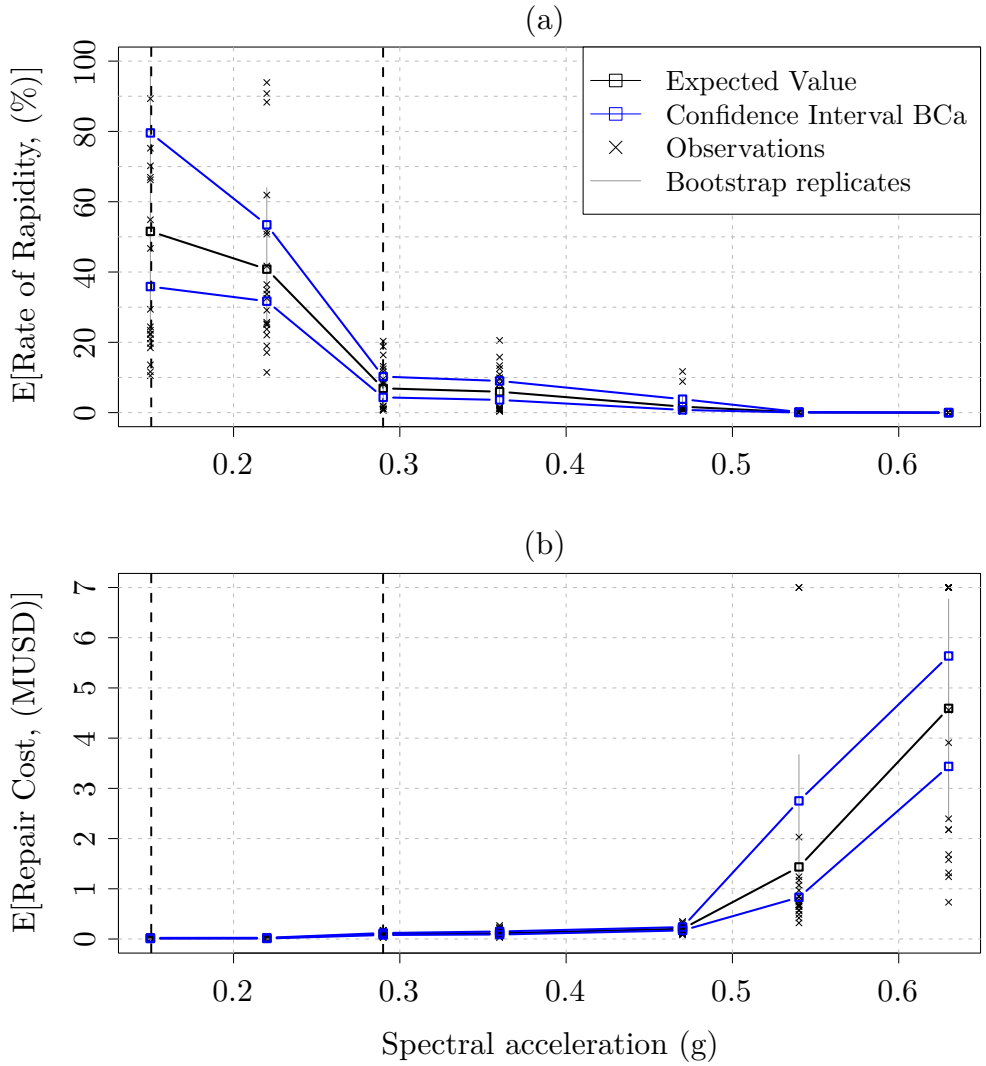

Figure 11.18: Expected value $\hat{\theta}^*_{\mathbf{dv}}$ and its confidence interval BC_a obtained means the bootstrap method for the (a) Rate of Rapidity of the Recovery and (b) Repair Cost C_{REP}.

into account in determining whether a building is resilient or not (*e.g.*, repair time and cost, and even indirect economic losses can be determining factors for decision makers), the structural stability of the building is an important factor, otherwise, if it does not collapse under a significant seismic intensity, it may have to be demolished, *e.g.*, because it experienced excessive residual distortions, *i.e.*, the LS_5.

For the fourth (Tr=500 yr, Sa(T1)=0.36g) and fifth (Tr=1000 yr, Sa(T1)=0.47g) seismic intensities, the overall percentage of usable area decreased from 55% to 45%, and from 55% to 15%, respectively; however, all other DVs remained approximately constant, as can be seen in Figs. 11.16 through 11.23.

For the IM_6 (Tr=1,500 yr, Sa(T1)=0.54g), the performance of the building changed drastically. The expected value of the sample mean of the percentage of usable area was 0.67%

and its respective confidence interval of $(0.26, 1.4)\%$, which means that the building is certainly no longer functional. At this IM the LSs that contributed to the probability distribution were LS_3, LS_4 and LS_6, with probability $Pr(LS_3, IM_6) = 0.5$, $Pr(LS_4, IM_6) = 0.4$ and $Pr(LS_6, IM_6) = 0.1$, respectively. By definition it is possible for the building in the LS_3 and LS_4 to be resilient; this is proven by their respective probabilities. However, the probability of collapse at this intensity is not negligible, $Pr(LS_6, IM_6) = 0.1$. This is an indication that the installation at this level of IM the structural elements experienced significant distortions in the 10% of the seismic realizations associated with this intensity.

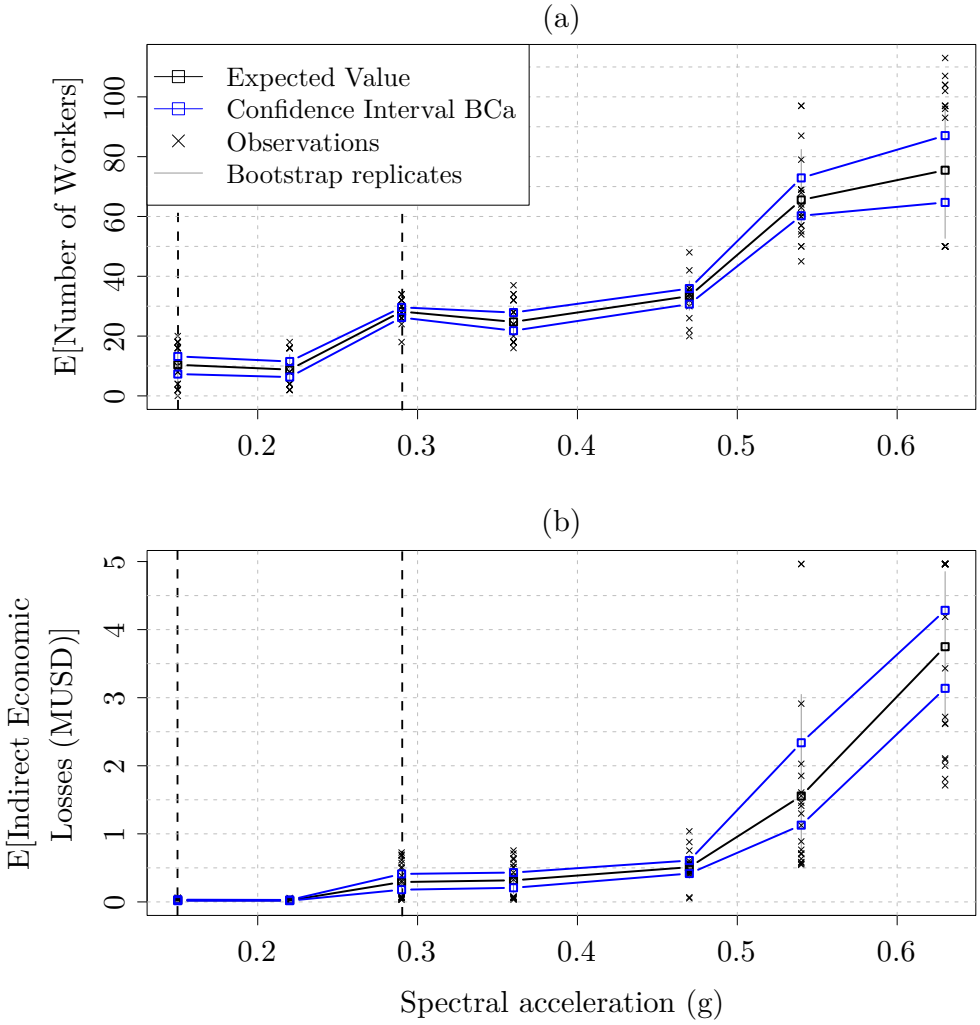

Figure 11.19: Expected value $\hat{\theta}^*_{\mathbf{dv}}$ and its confidence interval BC_a obtained means the bootstrap method for the (a) Number of Workers n_w and (b) Indirect Economic Losses I_{EL}.

For this level of IM the expected value of the sample mean recovery time was 301 days, with an $CI_{\mathrm{BC}_a 95}$ of $(175, 572)$ days. It should be noted that the time associated with the factors for this case was 160 days with an $CI_{\mathrm{BC}_a 95}$ of $(97, 293)$ days, while the repair time was 141 days with an $CI_{\mathrm{BC}_a 95}$ of $(77, 281)$ days. It can be noted that the factors

that prevent repairs from starting, again, contribute a high percentage to the recovery time. Unfortunately, engineers can do very little about this, as these factors are external to the building itself. Also, for the repair time to be of such magnitude, an average of 65 workers are required. On the other hand, the expected repair cost is 1.43 MUSD, of which 0.42 MUSD corresponds to structural elements, 0.93 MUSD to non-structural elements and 0.075 MUSD to furniture. Therefore, 65% of these losses are associated with non-structural elements and furniture. With respect to indirect economic losses caused by business interruption, the expected value of the sample mean was 1.55 MUSD ($CI_{\mathrm{BC}_a 95} \sim (1.13, 2.34)$ MUSD).

For this level of IM the damage experienced by the building caused between 2 and 4 people, with an average of 3, to suffer some type of injury. The mean equivalent economic value of these injuries was 0.29 MUSD, with an $CI_{\mathrm{BC}_a 95}$ of $(0.15, 0.51)$ MUSD. Regarding the number of fatalities, the analysis suggests that one person is expected to have lost his or her life; however, this number may increase to 3. The expected value of the sample mean of the respective economic cost was 1.14 MUSD, with an $CI_{\mathrm{BC}_a 95}$ of $(0, 3.43)$ MUSD.

Finally, for the seventh IM of study IM_7 (Tr=2,500 years, Sa(T1)=0.63g), the loss of functionality is imminent, only in this case it is less likely that the building will be resilient because the probability of collapse is 50%, *i.e.*, $Pr(LS_6, IM_7) = 50\%$. The remaining 50% corresponds to the LS_4. This means that the building has a 50% probability of recovery, of course, at a high social and economic cost. If the building did not collapse at this IM the recovery time for this case would be 916 days with a $CI_{\mathrm{BC}_a 95} \sim (676, 1146)$ days. The average repair time was 476 days, with a confidence interval of $(355, 585)$ days, and an average delay time of 440 days with an $CI_{\mathrm{BC}_a 95}$ of $(316, 560)$ days. Conservatively, for this level of performance the building would take at least 3 years to recover. The number of workers required to repair the damaged elements is between 65 and 87 workers, with an average of 75 workers.

On the other hand, the total repair cost was 4.6 MUSD with a $CI_{\mathrm{BC}_a 95}$ of $(3.45, 5.64)$ MUSD. In this case, the repair costs of the non-structural elements corresponds to 57% (2.6 MUSD) while the furniture corresponds to 0.7% (0.32 MUSD). Again, the cost associated with the non-structural elements controls the direct losses. Regarding indirect economic losses, the expected value of the sample mean was 3.74 MUSD with an $CI_{\mathrm{BC}_a 95}$ of $(3.13, 4.28)$ MUSD.

With respect to the number of occupants who suffered some type of injury, the average was 3 persons, with an $CI_{\mathrm{BC}_a 95}$ of $(1, 6)$ persons. The economic value equivalent to this type of damage amounted to 0.35 MUSD with an $CI_{\mathrm{BC}_a 95}$ of $(0.11, 0.76)$ MUSD. While the number of injured did not increase substantially from the IM of the previous case, the expected value of the number of fatalities increased significantly from 1 to 13 people, with an $CI_{\mathrm{BC}_a 95}$ of $(4, 28)$ people. This change is influenced by the LS_6, that is, by structural collapse. The equivalent economic value associated with the mortal victims was 30 MUSD with an $CI_{\mathrm{BC}_a 95}$ of $(9.9, 63.4)$ MUSD. Although, the probability of a large magnitude earthquake occurring is very small (2% probability of exceedance in 50 years), the consequences can be devastating.

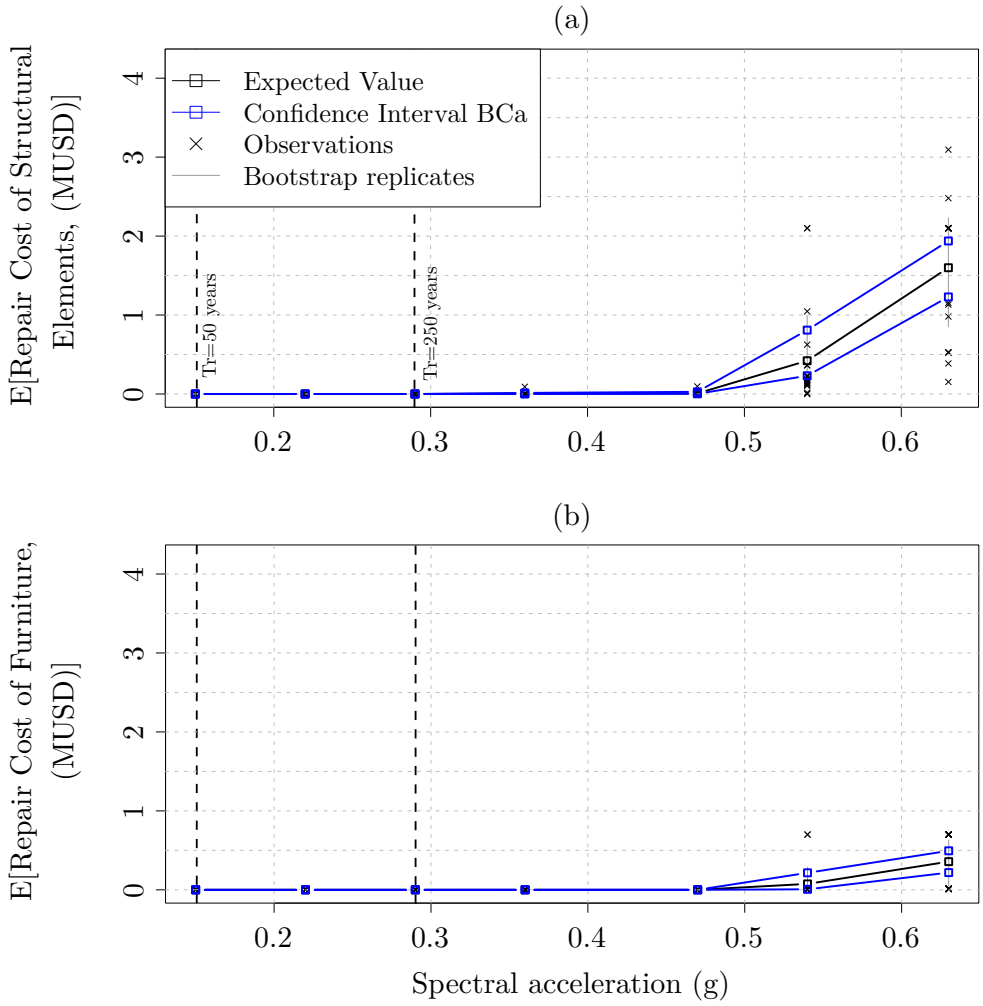

Figure 11.20: Expected value $\hat{\theta}^{*}_{\mathbf{dv}}$ and its confidence interval BC_a obtained means the bootstrap method for the (a) Repair Cost of Structural Elements $C_{REP,S}$ and (b) Repair Cost of Furniture $C_{REP,F}$.

In general terms, it can be concluded that the building designed with the NTC-DS (GCDMX, 2004a) and evaluated using the methodology proposed in this thesis is resilient to seismic intensities whose return period is between 50 years (Sa(T1)=0.15g) and 1,000 years (Sa(T1)=0.47g). Therefore, it is concluded that the building is resilient for the performance level for which it was designed. However, it should be noted that seismic intensities equal to or greater than the design intensities (Tr=250 years, Sa(T1)=0.29g), but less than Tr=1,000 years, although it is feasible for the building to recover its functionality despite having experienced damage, both direct and indirect economic losses can be high. This is mainly due to the damage experienced by the non-structural elements. For this example, the loss of functionality was dominated by interior and exterior masonry walls, interior drywall and stairs. For seismic intensities greater than those corresponding to return periods of 1,000 years, the building does not have the capacity to be resilient because the costs and repair times are very high. Likewise, the damage experienced by

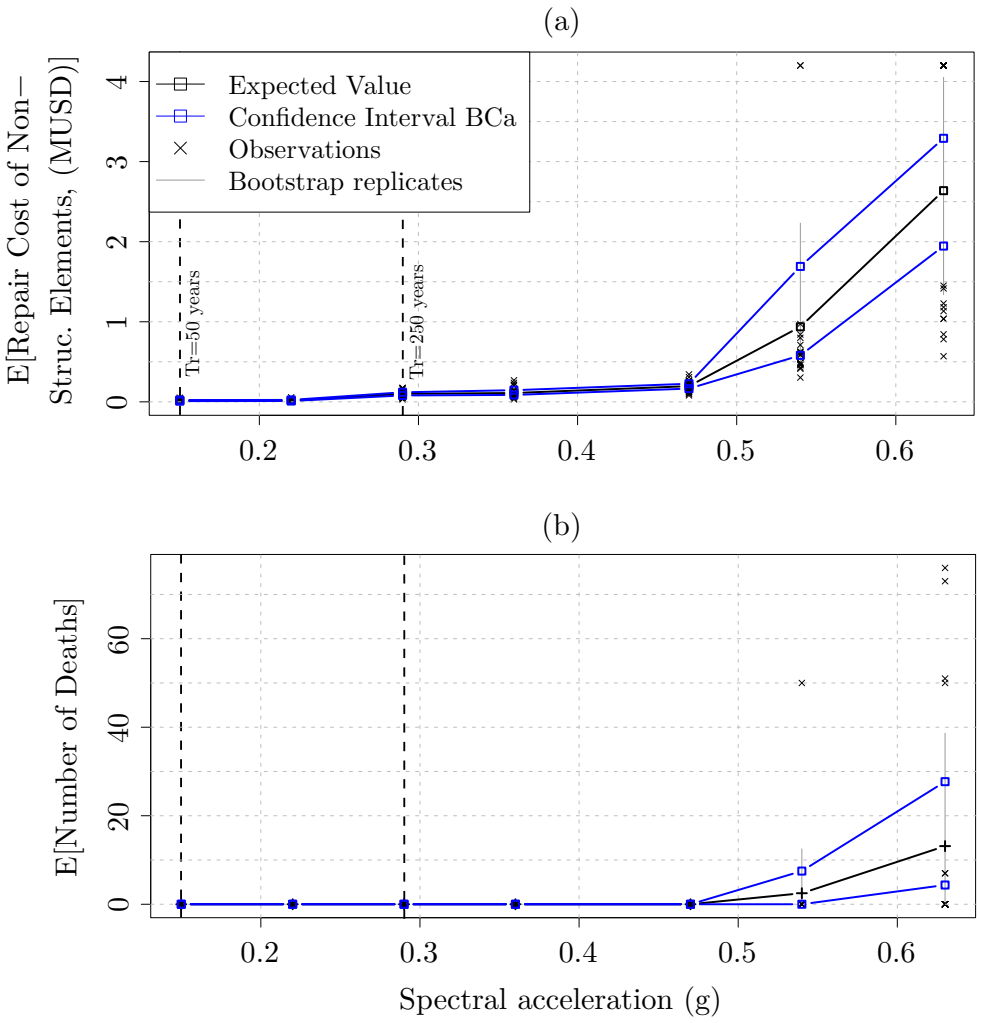

Figure 11.21: Expected value $\hat{\theta}^*_{\mathbf{dv}}$ and its confidence interval BC_a obtained means the bootstrap method for the (a) Repair Cost of Non-Structural Elements $C_{REP,NS}$ and (b) Number of Deaths n_d.

the non-structural and furniture-type elements causes the users to suffer injuries and may even lose their lives due to the total collapse of the building.

Finally, Fig. 11.23b presents the vulnerability function of the total economic losses EL_{TOT}, that is, the sum of (1) total repair costs C_{REP}, (2) indirect economic losses I_{EL}, (3) equivalent economic value associated with injuries EEV_{INJ} and (3) equivalent economic value associated with fatalities EEV_{DEA}. By simple comparison between these losses it is easy to deduce that for seismic intensities where the building is not resilient the most influential economic losses are those associated with non-fatal and fatalities.

It should be noted that the final conclusions deduced from the vulnerability analysis are consistent with the conclusions obtained from the probabilistic analysis of the post-seismic inspection simulation and the evaluation of the LSs performed in the section 11.2.2 of this

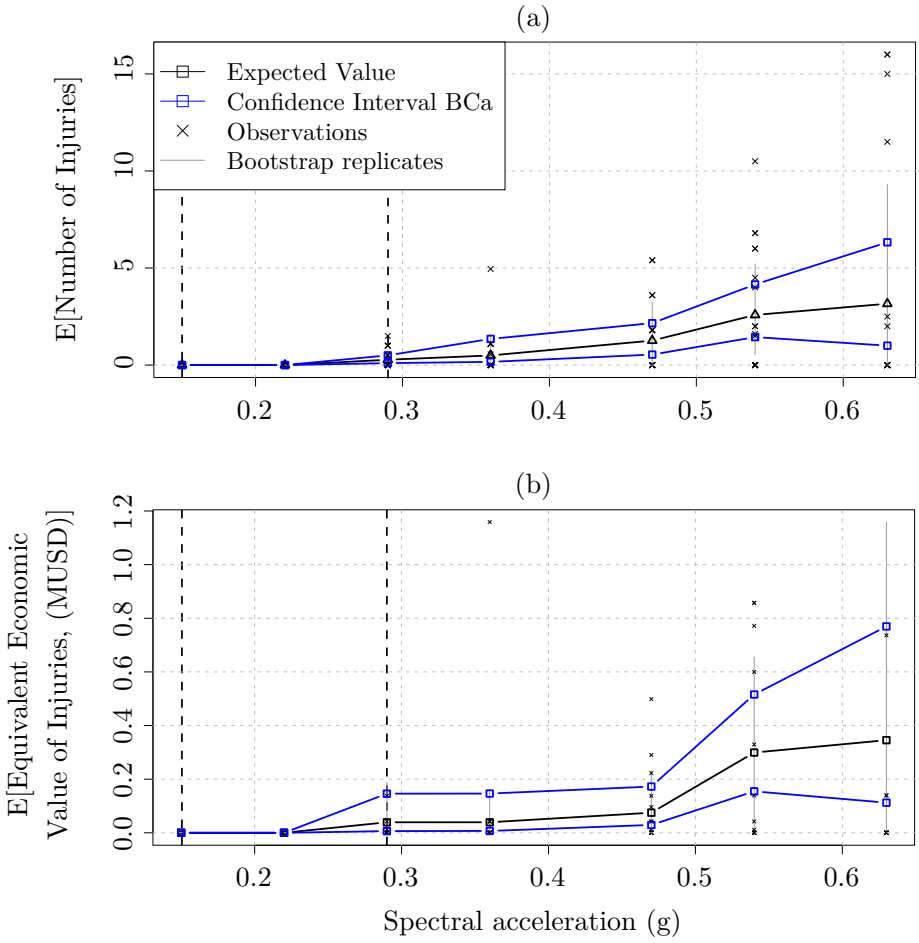

Figure 11.22: Expected value $\hat{\theta}^*_{\mathbf{dv}}$ and its confidence interval BC_a obtained means the bootstrap method for the (a) Number of Injuries n_i and (b) Equivalent Economic Value of Injuries EEV_{INJ}.

chapter. The difference is that with the analysis of the DVs one has the complete picture, at least from a statistical and probabilistic point of view, of the seismic resilience of the building in study.

Finally, it can be concluded that the numerical results associated with the damage inference and post-seismic inspection are consistent with the data reported by Weiser *et al.* (2018), indicated at the beginning of this chapter for the design seismic intensity (Tr=250 years, Sa(T1)=0.29g). Unfortunately, there is no information available to the general public regarding the direct and indirect economic losses, as well as the number of fatalities caused in particular by the damage experienced by each building. The lack of these data is one of the main drawbacks to validate methodologies such as the one proposed here. Therefore, in order to build reliable mathematical models to reduce and mitigate the negative consequences of earthquakes on buildings, it is desirable that these data be recorded systematically.

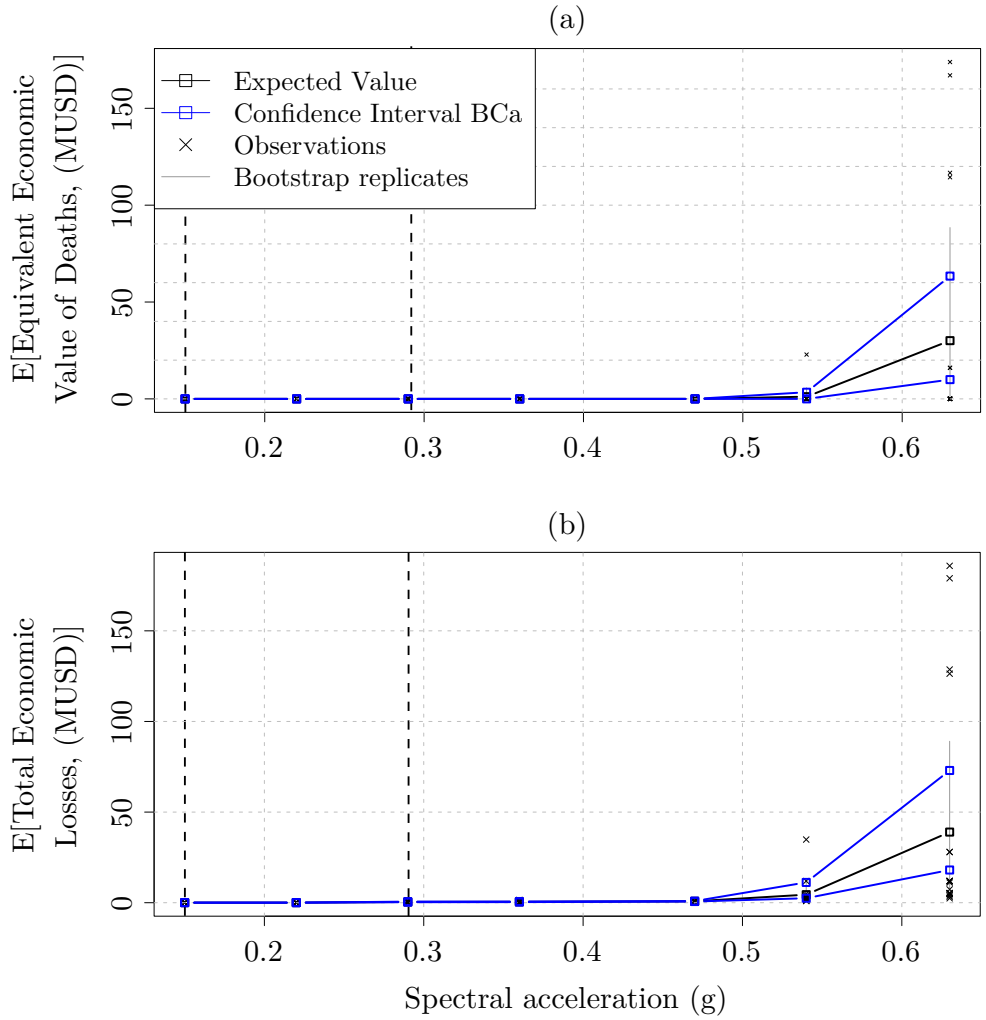

Figure 11.23: Expected value $\hat{\theta}^*_{\mathbf{dv}}$ and its confidence interval BC_a obtained means the bootstrap method for the (a) Equivalent Economic Value of Deaths EEV_{DEA} and (b) Total Economic Losses EL_{TOT}.

Chapter 12

Conclusions and recommendations

In this thesis, a methodology to evaluate the decision variables that explain the theory of seismic resilience of buildings developed by Cimellaro *et al.* (2006) was proposed. The DVs that characterize this theory are: loss and recovery of functionality, direct and indirect financial losses, loss of life and number of injured. These concepts are consistent with the general scheme developed by the MCEER (Bruneau *et al.*, 2003) to assess the resilience of communities to natural disasters. The methodology proposed in this research work was implemented in the probabilistic scheme for evaluating structural performance developed by PEER (Cornell and Krawinkler (2000); Moehle and Deierlein (2004); Günay and Mosalam (2013), among others). This scheme is integrated by four probabilistic analyses: (1) seismic hazard analysis, (2) structural analysis, (3) damage analysis, and (4) analysis of decision variables. The methodology developed in this study corresponds to an extension of steps three and four of the PEER probabilistic framework.

In summary, the proposed methodology is able to approximate the vulnerability functions of the following DVs: (1) percentage of non-usable area as a physical parameter representative of the loss of functionality; (2) delay time corresponding to the factors that prevent the start of repairs; (3) repair time of the PGs corresponding to structural, non-structural and furniture-type elements; (4) recovery time, corresponding to the sum of the delay time and the repair time; (5) speed of recovery of functionality; (6) indirect economic losses due to the business interruption of the different units (floors) of the building; (7) total repair costs, and its corresponding disaggregation, *i.e.*, those corresponding to the structural, non-structural and furniture-type elements; (8) number of workers required to perform the repair work of the damage experienced by the PGs comprising the building; (9) number of people injured by the damage experienced by the potentially damaging PGs; (10) number of fatalities caused by potentially damaging PGs and structural collapse; (11) equivalent economic value associated with the number of injuries and (12) number of fatalities; and (13) total economic losses, corresponding to the repair costs, indirect economic losses, and the equivalent economic value associated with the injured and fatalities.

The results obtained with the vulnerability functions of the DVs can be an important tool for both decision makers and engineers. For example, for decision makers this tool can be

useful to establish insurance policies, while engineers may use it to reduce the magnitude of the DVs associated with a given IM by implementing technologies to control the lateral displacements that induce the damage, *e.g.*, using buckling-restrained braces, base isolators, viscous dampers, tunned mass dampers, among others. Such decisions can be based on the information provided by the expected value of the sample mean of the DVs or with its respective confidence interval.

12.1 General conclusions

The following general conclusions have been obtained in this research work:

- A strategy was proposed and implemented to evaluate the damage experienced by structural and non-structural elements of three-dimensional structural models. The results of this analysis, in contrast to previous studies where the three-dimensional behavior of structures is evaluated by combining the response of plane frames, allow knowing which are the most vulnerable elements, and, therefore, which are the ones that cause the loss of functionality. This strategy may be of interest in the practice of structural engineering since this field is where three-dimensional structural models are used on a daily basis. Also, this information can be useful to create prevention and monitoring plans for the critical structural elements for the stability of the structures.

- A strategy was proposed and implemented to evaluate damage in furniture-type elements, *e.g.*, bookcases. In this case, such elements were idealized as rigid blocks, and their behavior was evaluated with the theory of rigid body dynamics. It was assumed that the blocks can only experience rest, rocking-rest and rocking-overturning. It was demonstrated that the implemented strategy, although simplified, adequately reproduces the physical phenomenon in general terms. For example, in medium-rise buildings such as the one studied in this research work, the floor accelerations increase linearly, from the base to the roof of the building. In real seismic events it has been observed that in this type of buildings the damage in contents is concentrated in the upper floors. This behavior was adequately reproduced with the proposed strategy. Moreover, the results indicated that the elements that were farthest from the centroid of the affected slabs were the ones that experienced overturning damage. This suggests that it was at these points of the slabs that the floor accelerations were concentrated, resulting from the rotation of the transverse axis of the slabs.

- A methodology was proposed and implemented to evaluate the probability of structural safety tagging according to the post-seismic inspection criteria developed by the ATC (1989). The methodology also considers the inspection of non-structural and furniture-type elements. The result of this last inspection is the probability of unsafe areas due to the risk generated by falling of this type. In general, this approach corresponds to an extension of the methodology developed by Mitrani-Reiser (2007)

(later adopted by FEMA P-58-1 (2012a)), where only structural elements are considered. The results show that although the damage experienced by non-structural components and contents does not compromise the stability of the structure, it is the main cause of the loss of functionality of the building. This is because the approximation proposed by Mitrani-Reiser (2007) gives the lower limit of probabilities of post-seismic safety tagging, while with the approximation proposed in this work the results correspond to the upper limit of such probabilities.

- Six limit states of functionality were proposed and implemented. These LSs correspond to an extension of those proposed by Burton *et al.* (2016) to evaluate the resilience of residential buildings. The LS proposed in this work correspond to an adaptation to evaluate the resilience of office-type buildings, and were formulated based on the probabilistic events that govern the ATC-20 (1989) post-seismic inspection, as well as heuristic criteria. Likewise, a generic sequence of recovery of the damaged building was defined in each LS. The results of this analysis provide insight into: (1) the most probable damage configuration (considering the structural, non-structural and furniture-type elements) at each seismic intensity considered in the study; (2) the probable causes of the loss of functionality, and (3) the general sequence of recovery of the building's functionality.

- A new parameter was proposed to quantify the loss of functionality. This parameter corresponds to the percentage of non-usable area, and is defined by the floor area that work crews need to perform repair work during a specific time interval. This parameter can also be used as a weight factor to estimate the average number of assets that lose functionality during a seismic event (*e.g.*, average number of unusable beds in a hospital room). In contrast to previous studies, given the generality of this factor, it can be used in the evaluation of the loss of functionality of any type of building.

- A recursive scheme was proposed and implemented to quantify the recovery of functionality. This scheme quantifies the costs and repair times, as well as the number of workers needed to perform the repair work. The FEMA P-58-1 (2012a) method proposes two strategies for repairing damaged elements. The first is to perform the repairs in series, and the second is to perform the repairs in parallel. Both strategies are inconsistent because the repair time and cost fragility functions proposed in FEMA P-58-1 (2012a) were calibrated using a single worker. Then, when the serial repair strategy is used, it is assumed that a single worker (per PG) performs the repair works. In the serial repair strategy it is accepted that each damaged component is repaired by one worker. This will obviously lead, on the one hand, to a congestion of workers when a large number of components are damaged, and on the other hand, it is not possible for the society to have a robust number of workers to repair all damaged buildings in a community. On the contrary, the strategy proposed in this research work is based on a hybrid scheme, which is formulated from the experience acquired in post-seismic rehabilitation works. In this scheme, a reasonable amount of elements that experienced a particular damage state is assigned to a number of

crews with a realistic number of workers. Likewise, the repair sequence of the PGs is given by their respective hierarchy relative to the stability and functionality of the structure.

- At this step, the recovery of functionality is also quantified, which is approximated as the percentage of area recovered per unit of time given that a certain number of damaged components are repaired. The results demonstrate that the conditions imposed in the recursive process give rise to trigonometric recovery curves, similar to the trigonometric recovery function proposed by Cimellaro *et al.* (2006). However, Cimellaro *et al.* (2006) argues that the trigonometric shape originates when society does not have a contingency plan to respond immediately after the seismic event, but at some moment it manages to organize itself and obtain the necessary resources to initiate the recovery process. The trigonometric shape that the curves obtained in this thesis acquire is due to the imposed recovery sequence. At the beginning of the recovery the slope of the curve is almost parallel to the horizontal axis. Irrational factors (post-seismic inspection, repair planning, etc.) are present at this stage, and their duration depends on the amount and severity of damage experienced by the PGs. After this stage is when repairs begin to be made and when the slope of the recovery curve begins to gradually increase until the repairs are completed. Also, it is assumed that immediately after the seismic event the irrational factors are presented, starting with the post-seismic inspection. Moreover, the pattern of these curves is presented in each of the event combinations (LS, IM), but at different scale.

- A procedure was proposed to estimate the number of users who are injured or lose their lives, as well as their respective equivalent economic value. This formulation corresponds to an extension of the methodology proposed by FEMA P-58-1 (2012a), where only the percentage of users who lose their lives is estimated in probabilistic terms. However, this methodology is not capable of estimating the number of people injured, nor the equivalent economic value. The results of the application example demonstrate that they are consistent with those reported in real seismic events. The results also prove that these types of financial losses can even be similar to repair costs in major earthquakes.

- A linear function was proposed to estimate the indirect economic losses. This function depends on the recovery time and the financial losses caused by the lack of income of the users of each floor of the building. Despite the limitations of this approximation, the results demonstrate that these types of financial losses can amount to large sums, even greater than the cost of repairing the building.

- With the results obtained from the methodology proposed in this thesis, vulnerability functions were constructed for each DV. This functions were created with the bootstrap technique, which proved to be adequate for statistical inference when the underlying problem is very complex and when the sample size of the variable in study is small. Likewise, the expected value of the sample mean was expressed together with its confidence interval. This way of expressing such functions is an innovative

aspect in the area of earthquake risk assessment, since it is common practice to use continuous probability distributions, *e.g.*, normal and lognormal. However, as demonstrated, to use these probability distributions the sample size of the variable of interest must be large enough to satisfy the Central Limit Theorem and the Strong Law of Large Numbers. However, this implies a problem because the amount of NLDA must be limited by the high computational cost. With the bootstrap technique this problem is almost always solved by random resampling, so relatively low computational effort is required.

12.2 Particular conclusions

The following particular conclusions have been obtained in this thesis:

- It was demonstrated that the minimum size of a sample of independent and identically distributed observations to be used in statistical inference with the bootstrap technique is 20. This suggests that the minimum number of NLDA given an IM that must be used in loss analysis is also 20. It was also found that in a sample of this size the error in estimating the confidence intervals of the expected value of the sample mean when using maximum likelihood theory is approximately 22%. This error is associated with the second order term of the asymptotic expansion. The error corresponding to the third order terms is 5%. With the bootstrap random resampling technique, the second order term is taken into account, so the error in the estimation is associated only with the third order term.

- A convergence analysis was performed with the confidence interval limits for each DV, and it was concluded that 4,000 to 6,000 Bootstrap replicates were required. Finally, for practical purposes, 10,000 bootstrap replicates were used to estimate the statistical parameters needed to construct the vulnerability curves for each DV. It should be noted that the calculation time of the 10,000 bootstrap replicates for these statistical parameters was approximately five minutes. The total calculation time for the NLDA was approximately six days (20 NLDA for each of the seven IM). It is evident that if one wishes to construct the vulnerability curves using classical statistical inference techniques the computation time will be considerably excessive, even if simplified nonlinear analysis theories are used to reduce the computation time (*e.g.*, concentrated plasticity). Therefore, the bootstrap statistical inference scheme is very attractive, and as demonstrated, it allows to obtain consistent results, at least from the point of view of statistical inference.

- The histogram of the sample obtained in the resilience analysis of the recovery time and percentage of usable area corresponding to the event (LS_3, IM_3) was presented and compared with the bootstrap histogram of the sample mean of both variables. The sample histogram of both DVs turned out to have a shape that does not look like the normal probability density function. This is because the sample is not large

enough for its histogram to have a normal appearance. In contrast, the bootstrap histogram of both decision variables turned out to look more like the Gaussian function. This is precisely one of the qualities of the bootstrap technique and the monotonic transformation. This transformation is an intrinsic property of the percentile method, the basis of the BC_a method, and in many cases produces a histogram very close to one with normal distribution, regardless of the shape of the histogram of the seed sample. This process was performed for each of the DVs and the results were consistent, so it can be concluded that the use of the bootstrap technique is a good option for making statistical inferences when the sample size is relatively small (greater than or equal to 20 independent and identically distributed observations).

- The results indicate that the classical method commonly used (maximum likelihood) in the practice of statistical inference, the confidence intervals are symmetric, but inconsistent. For example, with the bootstrap technique, given the seismic intensity associated with the 500-year return period, the sample mean recovery time was 47 days, and its respective confidence interval was (30, 63) days. For this DV, but using the maximum likelihood theory, the estimated mean recovery time is 47 days, and its respective confidence interval is (-28, 122) days. Evidently the negative recovery time is physically meaningless. Now, for example, analyzing the percentage of usable area, with the bootstrap technique we have an expected value of 46%, and its respective confidence interval of (29, 64)%; using the classical theory the expected value is 46%, and its respective confidence interval of (-37,130)%. For the latter case, the two confidence interval limits lack physical significance. These inconsistencies are due to the fact that the sample size is too small to use the classical theory of statistical inference; however, the bootstrap technique has been shown to give consistent results even when the sample size is small (but not smaller than 20). In this regard, it can be concluded that the bootstrap technique is suitable for statistical inference when the sample is not large enough to use the formulas of classical statistics.

- The results of the structural damage analysis for each of the study events proved to be consistent with the expectations of the NTC-DS (GCDMX, 2004a). For a random realization of event LS_1, corresponding to intensity IM_1 associated with the serviceability limit state (Tr=50 years, Sa(T1)=0.15g), of all the PGs analyzed, one interior masonry wall experienced light damage (damage configurations were reviewed for all PGs and each seismic realization of each seismic hazard level and the results were consistent in each one). The repairs corresponding to this damage level are cosmetic, so they do not really affect the performance and structural stability of the building.

  Regarding the LS_3 event, associated with a seismic realization corresponding with the limit state of collapse prevention (IM_3, Tr=250 years, Sa(T1)=0.29g), the building is expected to develop structural damage, according to the NTC-DS (GCDMX, 2004a)). However, in this particular case the building presented elastic behavior. This result is a proof of the good performance of the structural system since the

objective of avoiding partial and/or total structural collapse was achieved, thus preventing loss of life. On the other hand, the non-structural elements, mainly the interior and exterior masonry walls, as well as some stairs elements and masonry partition walls, experienced light, moderate and severe damage. Evidently, these results demonstrate that the NTC-DS (GCDMX, 2004a) do not prescribe the conditions to prevent loss of functionality at this level of seismic hazard due to damage to non-structural elements. In fact, the NTC-DS (GCDMX, 2004a) (as well as most of the seismic design regulations of other countries) at the collapse prevention intensity level accepts that the non-structural elements, and even the structural ones, develop important levels of damage, but without the collapse of the structure in order to avoid loss of life.

It can be said that seismic design codes are focused on safeguarding the lives of building occupants, and not on reducing the loss of functionality. That is, design codes are not focused on making structures resilient. In this regard, recent seismic events have shown us that damage can always be expected in a well-designed building. What must be done, then, is to plan to reduce the consequences of damage on society and the economy: creation of emergency and mitigation plans, and their execution as quickly as possible in the face of disaster. The methodology proposed in this thesis can help prevent the negative consequences experienced by a building because of potentially destructive seismic events.

- The post-seismic tagging probabilities obtained in the numerical example are congruent with the results of the damage assessment. For example, the probability that the building is structurally safe is 100% for the seismic intensity whose return period is 250 years (design earthquake). This result is consistent with the objective of the NTC-DS (GCDMX, 2004a), *i.e.*, to avoid structural collapse. Moreover, this result remains constant for seismic intensities less than or equal to those corresponding to the 1,000 year return period. Regarding the probabilities of non-structural tagging, the probability of assigning the building a red tag given that the non-structural elements are inspected at the same seismic demand is 50%. This result clearly suggests that the building has a high probability of losing functionality due to the damage experienced by this type of elements, since this event is directly associated with the usable area of the building. At intensities lower than 250 years return period, the probability that non-structural elements experience severe damage is zero. However, it is very likely that these elements will develop light damage in minor quantities.

- The numerical results suggest that irrational factors significantly influence the delay of repair initiation when damage starts to become significant. For example, in LS_4, the estimated repair initiation delay time was approximately 150 days, while the repair time was 106 days, *i.e.*, the delay time was approximately 57% of the total recovery time. The irrational factors preventing the start of repairs in this event were the post-seismic inspection, obtaining financial resources, structural design review, repair planning, bidding process, and finally the execution of repairs.

- The functionality limit states proposed in this research work are useful because

they allow knowing the probability of one or more prescribed damage configurations occurring at a given level of seismic hazard. These damage configurations allow to know roughly the vulnerability level of the building under study, and if necessary, to reinforce the building to increase its seismic resilience. That is, to increase the probability that the building will be in the limit states LS_0, LS_1 or LS_2, which, by definition, are those characterized by the lower loss of functionality.

- By definition, the LS_4 is the limit state where the building still has the capacity to be resilient, *i.e.*, it is technically possible to repair the structure. However, in this LS the magnitude of decision variables such as repair cost, recovery time and indirect economic losses can be important. For example, for the case study, the probability of LS_4 occurring given the 1,000-year return period seismic hazard level is 0.4. The expected value of the sample mean recovery time was about 260 days (approximately 9 months), while corresponding to the indirect economic losses was 1.8 MUSD, and the total repair cost was 1.1 MUSD. With this information, the owner or decision-maker will be able to decide whether it is convenient to repair the building, or it is better to demolish and rebuild it again.

- The conclusion obtained from the evaluation of the functionality limit states was that the building has the capacity to recover its initial operating condition (*i.e.*, it is technically feasible to carry out repairs) even in seismic events with an average intensity of 0.47g (Tr=1,000 years). However, from intensity 0.29g (Tr=250 years), the non-structural and furniture-type elements experience severe damage, so from this seismic hazard the building has a non-negligible probability of losing functionality and experiencing significant financial losses.

- The results of the application example indicated that the building loses 4%, 64% and 100% of usable area in the (LS_1, IM_1), (LS_3, IM_3) and (LS_4, IM_4) events. These percentages of usable area are consistent with the results of the damage analysis. In addition, as noted previously, they can be used as a weight factor to estimate the average number of components lost, either for each floor, or for the entire building. Also, these percentages of unusable area were found to be consistent with the recovery time for each event: 4.6, 78 and 260 days.

- The proposed formulation for estimating the recovery time allows optimizing only the repair time through the conditions imposed in the recursive algorithm, *e.g.*, repairing several floors within the same instant of time. The stage prior to the start of repairs (irrational factors) was not optimized for two reasons: (1) this stage is beyond the scope of engineers, and (2) there is scarce empirical information today that reveals whether irrational factors can perform in parallel, and, moreover, which of them are the ones that can be evaluated in this way. Therefore, it was established that the factors that prevent the initiation of repairs will be presented in a serial sequence, hence, the time calculated at this stage is conservative.

- It is numerically demonstrated that the repair/replacement cost corresponding to the non-structural components is higher than that of the structural elements. For

example, for the event (LS_4, IM_6), the percentage associated with the repair costs of the non-structural elements, with respect to the total repair cost, was 63.7%, the percentage corresponding to the structural elements was 35.5%, and finally, the corresponding to the replacement of the furniture was 0.80%.

- The numerical results indicate that the expected value of the sample mean of the number of injured is 0, 1 and 3, for events (LS_1, IM_1), (LS_3, IM_3) and (LS_4, IM_4), respectively. These results are consistent with the severity of damage the building experienced; however, it is desirable to verify these results with data collected in real seismic events.

- The results of the numerical example demonstrate that the economic losses associated with injuries have a non-negligible impact with respect to the losses associated with repair costs. For example, for event (LS_3, IM_3), the expected value of the sample mean of the number of people injured was 1. Its respective equivalent economic value was 0.08 MUSD, that is, 37% of the total financial losses (0.22 MUSD), which originated from the damage experienced by the exterior and interior masonry walls, as well as some stairways and partition walls. Regarding the event $(LS_4, IM4)$, the expected value of the number of injured persons was 3. Their respective equivalent economic value was 0.265 MUSD, that is, 19% of the total economic losses (1.37 MUSD), of which 0.39 MUSD correspond to structural elements, 0.7 MUSD to non-structural elements and 0.0085 MUSD to furniture. The equivalent economic value associated with the injured persons is equivalent to 68% of the cost associated with structural repairs.

12.3 Recommendations for future research

In order to complement and improve the methodology proposed in this thesis, it is recommended to continue with the following aspects that were beyond the scope of this research:

- The seismic demand considered in this research work takes into account far source earthquakes; *i.e.*, the Kohrs-Sansorny *et al.* (2005) model used is adequate only to simulate records produced by a seismic source far enough away from the site where the building is located. Therefore, the vulnerability functions obtained with the procedure developed in this thesis should be interpreted with caution. A more robust approximation of the damage and vulnerability functions of DVs used to describe seismic resilience should take into account earthquakes with a source close to the CDMX, such as the one that occurred on September 19, 2017. This event, from a nearby source, significantly affected low and medium height buildings located in the transition zone of the valley of the CDMX, therefore, developing methodologies that allow simulating earthquakes of this type to be used in the evaluation and mitigation of damage is a fundamental aspect to investigate.

- The selection of the seismic records was carried out with the imposition of two conditions. The first condition consisted of calculating the Pearson correlation coefficient between orthogonal pairs of accelerograms, and selecting those where this factor was not greater than 0.5 (in accordance with the criteria proposed by Hadjian (1981)). In this regard, the Pearson correlation coefficient value of 0.5 was estimated by Hadjian (1981), as well as that of 0.16 estimated by Newmark *et al.* (1973), using a base of seismic records produced by earthquakes in the United States. It is convenient to carry out a similar study with mexican accelerograms (recorded in firm and soft soil) for each of the types of faults that govern the seismicity of Mexico, and compare the correlation coefficients obtained for each of these sources, and determine if the value of the upper limit of the correlation coefficient proposed by Hadjian (1981) is valid when Mexican seismic records are used.

- The inference of the damage of the different *PG*s that integrate the hypothetical building under study was performed using the fragility functions developed by FEMA P-58-1 (2012a). These fragility functions were calibrated with the damage caused by earthquakes occurring in the last 30 years in the USA and from experiments also carried out in this country. Although the results of the damage inference obtained in the numerical example are consistent with the damage observed in real earthquakes, it is desirable that fragility functions be developed in Mexico with mexican data because the intensity, frequency content and duration of the accelerograms produced by mexican earthquakes are very different from those produced by earthquakes in the USA. It would even be convenient to develop fragility functions that take into account the accumulated damage generated by different earthquakes. It is worth remembering that the CDMX was affected by two potentially destructive earthquakes with a difference of occurrence of 32 years (earthquake of September 19, 1985 and 2017), and the seismic hazard curve used in the example carried out in this research work contemplated a period of 50 years. This means that it is likely that within this time frame at least two potentially destructive seismic events are probable to occur.

- In the same way, both the cost and repair time probability distributions of each performance group proposed by FEMA P-58-1 (2012a) have been calibrated with American data. In this regard, it is also convenient that in Mexico these distribution functions be developed with mexican data since labor costs and repair times are very different in Mexico.

- The behavior of furniture-type elements was modeled with a two-dimensional model of rigid rectangular blocks; therefore, strictly speaking this formulation can only be used to model bookcase or shelf-type elements. A better approach would have to be formulated using three-dimensional body dynamics (*e.g.*, Chatzis and Smyth (2012); Vassiliou *et al.* (2017)). The interaction between content-type elements was also not taken into account, *e.g.*, the interaction between a desk and a computer. As observed in recent earthquakes (Chile 2010 and Mexico 2017), this type of damage can cause loss of functionality and therefore direct and indirect economic losses, so it is worth

to be studied in more detail. It would also be convenient to study the response of the contents assuming that these can experience other types of movement, in addition to rocking and overturning, *e.g.*, slide, slide rotation, translation jump and rotation jump.

- To determine which seismic realizations at a seismic hazard level produced the damage configurations for estimating post-seismic tagging probabilities, the following criterion was used: for example, if at least one structural element experienced severe damage in a seismic realization, then the building was assigned a red tag. This is a conservative criterion. A less conservative and more refined criterion could contemplate percentage limits of damaged elements for each floor of the building, *e.g.*, at least 10% of columns with severe damage on the second floor (or in the entire building) to assign a red tag. This new criterion can be used for each of the structural, non-structural and contents post-seismic tags.

- In each of the functionality limit states, a series of events, called irrational factors, were prescribed, which delay the initiation of repairs. The prescribed sequence is based on heuristic criteria, therefore, these sequences should be used with reservation. To improve the generic sequence of each LS, the recovery process of buildings damaged by real earthquakes should be systematically documented. This, in turn, will allow the creation of more and better plans to mitigate the negative effects generated by earthquakes of low and moderate probability of occurrence. This is a complicated aspect; however, it is possible that with the systematic monitoring of the recovery of buildings, new irrational factors and the order in which they occur will be identified.

- The model developed in this research work considers as sources of functional disruption the direct damage generated by the seismic event and irrational factors. It does not take into account neighborhood effects. For example, assuming there are three buildings, and the buildings at the ends experience significant residual distortions, therefore, these buildings will have to be demolished. In order to carry out the demolition work, part of the street where these buildings are located will have to be cordoned off, even though the demolition of both buildings will not be carried out simultaneously. This will affect the functionality of the building that did not experience damage. Neighborhood effects are an aspect to be taken into account in future investigations. In fact, these effects were present in many areas of the CBD following the February 2011 Christchurch earthquake, which was cordoned off for more than two years, and construction work began approximately three years after the seismic event.

- To estimate indirect economic losses, a linear function that depends on the recovery time and the economic income of each unit of analysis was proposed. This model assumes that economic losses are experienced by the company that rents the damaged space. In this regard, if the company ceases to have income, it is possible that at some moment it will not be able to cover payroll and rent expenses, among others.

Under these circumstances, in addition to the financial losses experienced by the company, the workers and the owner also experience financial losses. On the other hand, if the company rents another space, it would experience financial losses due to moving expenses and losses associated with the stabilization of its revenues. In this respect, the owner of the damaged building would also experience the loss of rental income. The model proposed in this thesis is, therefore, quite simple, so it is advisable to investigate the subject in more depth. The branch of mathematics that allows a systematic study of this type of problem is the game theory.

- It was prescribed in which LS it is possible for structural, non-structural and contents damage to cause some type of injury on users, or even loss of life. These events are directly related to the tagging of the structural safety of the building, according to the ATC-20 (1989) post-seismic inspection criteria. It is important that in future earthquakes that cause injuries and loss of life, information be collected that specifies and relates the types of injuries experienced by users, the cost of medical treatment and, if possible, relate this data to the structural system and type of element that caused the injuries, as well as the color of the tagging that was assigned to the building after the seismic event. This will allow the creation of more robust and accurate models to estimate in probabilistic terms the injuries, loss of life and their equivalent economic value produced by mexican earthquakes, since the data used in this study, once again, come from studies carried out with the consequences of earthquakes in the USA (AAAM, 2001).

- The bootstrap technique was applied to the fourth step of the PEER framework, *i.e.*, the analysis of DVs. It would be convenient to study the effect on the vulnerability functions if the bootstrap technique is applied from the structural analysis, *i.e.*, resampling the structural response given a seismic intensity, then performing the damage and consequence analysis for that new set of structural responses. If this process is performed, for example, 1,000 times, it is feasible to construct a probability distribution for each DV given an IM. In this case the parametric bootstrap technique would be used. Obviously with this strategy the computational time would increase significantly; however, it would not compare with the time cost associated with NLDA.

- Based on the evaluation of the resilience of several buildings with the proposed methodology, post-seismic recovery strategies and mitigation plans can be developed, simulating scenarios in which the recovery of a certain number of buildings is carried out in parallel, and another quantity in series, or a combination of both. This criterion is analogous to the conditions governing the recursive process for estimating repair time, but at a different scale of analysis. These considerations must be considered when trying to estimate the seismic resilience of a community or city, since the amount of economic and human resources is limited. For example, it is possible that the repair process of several buildings depends on a single engineering firm. In such cases the repairs of the damaged buildings may be executed in series

or in parallel, depending on the number of specialized personnel contracted by the hypothetical engineering firm.

Appendix A

Limit Theorems

A.1 Strong law of large numbers

Consider the set $\mathbf{x} = (x_1, x_2, ..., x_n)$ of independent and identically distributed random variables (*iid*) with mean μ and variance σ^2. Consider the following additive function:

$$y = x_1 + x_2 + \cdots + x_n \tag{A.1}$$

Since the set of random variables are *iid*, the expected value and variance of this sample are defined as: $\mathrm{E}[y] = n\mathrm{E}[y] = n\mu$ and $Var(y) = nVar(x) = n\sigma^2$, respectively.

The strong law of large numbers states that, under certain conditions, the average of random variables $\overline{x} = y/n$ converges to the expected value $\mu = \mathrm{E}[x]$, that is, to a constant, when the population sample size n is a large value. This fact can be verified by taking the limit to the probability when effectively $y/n = \mu$. This leads us to the theorem of strong law of large numbers, developed by Émile Borel (1871-1956), a French mathematician and politician.

Theorem: If $x_1, x_2, ..., x_n$ are *iid* with expected value μ then:

$$Pr\left(\lim_{n\to\infty} \overline{x} = \mu\right) = 1 \tag{A.2}$$

A.2 Central limit theorem

The central limit theorem describes the probability distribution (continuous or discrete) that has the function y displaced to the mean value μ and normalized by the standard deviation $\sigma\sqrt{n}$.

Theorem: If $x_1, x_2, ..., x_n$ are *iid* with mean μ and variance $\sigma < \infty$, then for all $x \in \mathfrak{R}$:

$$\lim_{n\to\infty} Pr\left(\frac{\overline{x}-n\mu}{\sigma\sqrt{n}} \leq x\right) = \Phi(x,\mu,\sigma^2) \tag{A.3}$$

where $\Phi(x,\mu,\sigma)$ is the cumulative distribution function of the standard normal probability distribution. In other words, the above equation expresses the convergence of the y function to the normal probability distribution when $n \to \infty$.

In this regard, if x_i is generated by a normal distribution $\Phi(x,\mu,\sigma^2)$, then a sample taken at random, regardless of its size n, will have the properties of the normal distribution, *i.e.*, with mean μ and variance σ^2, thus fully characterizing the probability distribution. Even if the distribution of the variable x_i is moderately non-normal, its arithmetic average $\overline{x}$ will tend to be asymptotically normal. In other words, when the randomness of a natural phenomenon can be represented by the accumulation of many additive small random effects, these tend to be distributed normally, regardless of the distribution that generates the small effects (Soong, 2004). For this to happen, it is sufficient for the sample size of the random variable to be of the order of $n \geq 30$; however, if the resulting distribution has a clear tendency to non-normality, it is required that n be much larger (Kottegoda and Rosso, 2008).

In the field of seismic engineering one of the most important probability distributions is the lognormal probability distribution function. This distribution is closely related to the normal probability distribution, and therefore to the strong law of large numbers theorem and the central limit theorem. To demonstrate this, consider the following multiplicative function of a random variable *iid* which takes only values greater than zero:

$$z = x_1 \cdot x_2 \cdots x_n \tag{A.4}$$

Taking the logarithm on both sides of the previous expression results in

$$\ln(z) = \ln(x_1) + \ln(x_2) + \cdots + \ln(x_n) \tag{A.5}$$

It is easy to note the equivalence between this equation and Eq. A.1, *i.e.*, $\ln(z) \equiv y$. This means that the logarithm of the random variable z becomes normally distributed approximately when the sample size n is large enough (Benjamin and Cornell, 1970). Taking the limit of the probability of the random variable $\ln(z)$ displaced to the mean $\mu_{\ln(z)}$ and normalized to the standard deviation $\sigma_{\ln(z)}\sqrt{n}$ leads to an expression similar to Eq. A.3:

$$\lim_{n\to\infty} Pr\left(\frac{\ln(z)-n\mu_{\ln(z)}}{\sigma_{\ln(z)}\sqrt{n}} \leq \ln(x)\right) = \text{Log-}\Phi\left(\ln(x);\mu_{\ln(z)},\sigma^2_{\ln(z)}\right) \tag{A.6}$$

In other words, this limit expresses the convergence of the function $\ln(z)$ towards the lognormal distribution function when $n \to \infty$.

This probability distribution is of major importance in the calculation of several fundamental processes of the seismic performance evaluation scheme proposed by PEER. For example, in the evaluation standard FEMA P-58-1 (2012a), the processes where the lognormal probability distribution has the greatest impact is in the evaluation of the probability distribution of repair costs and repair times (positive by definition) and in the estimation of the probability distribution of structural collapse using the maximum likelihood method (Backer, 2015).

A.3 Tchebycheff's inequality

The law of large numbers presented above demonstrates from a theoretical point of view that in order to have convergence towards the normal/lognormal distribution in the estimation of the expected value of a random variable of interest μ it is required that the sample size tends to infinity, *i.e.*, $n \to \infty$. However, this conclusion lacks practical sense because $n \to \infty$ is not a number, but a concept. In general, there is no general postulate that allows us to estimate the size n of a sample so that a distribution approaches a normal distribution (Papoulis, 1990). One way to estimate the size of n is to use the Tchebycheff's inequality applied to the notion of the probability of a random experiment that may result in occurrence (success) or non-occurrence (failure), *i.e.*, a Bernoulli's trial (Papoulis, 1991).

Consider that in an experiment that is repeated n times a variable $\tilde{x}_i$ is measured along with a random error ε_i with mean zero:

$$x_i = \tilde{x}_i + \varepsilon_i \tag{A.7}$$

Tchebycheff's inequality states that the probability of the absolute difference between the arithmetic mean of a random variable $\overline{x} = y/n$ and the mathematical expectation μ is less than a certain prescribed error ε is greater than the unit minus the ratio σ^2/ε^2, when it is small enough, *i.e.*, when $\sigma \ll \varepsilon$.

Theorem: For any $\varepsilon > 0$:

$$Pr\left(|\overline{x} - \mu| < \varepsilon\right) \geq 1 - \frac{\sigma^2}{\varepsilon^2} \tag{A.8}$$

This theorem corresponds to the weak law of large numbers, attributed to Jakob Bernoulli (1655-1705), a Swiss mathematician and physicist. However, in order to arrive at the weak law it was first necessary to define the theorem of the strong law of great numbers, as it was done before.

Bernoulli's trial has the particularity that it accepts only two outcomes, the success and failure. For the first one is arbitrarily assigned number 1 when the result of a random experiment is considered a success. On the contrary, if it is considered that the trial

produced a failure, it is assigned the number 0. These two results are therefore mutually exclusive and collectively exclusive. Likewise, it is known that when a Bernoulli's trial has been performed a large number of times n, the mean $\overline{x}$ of the random variable tends to the probability of success p, *i.e.*, $\mu = p$. Under this condition it is also known that the variance of a random variable within this process is defined by $\sigma^2 = pq/n$, where $q = 1 - p$ corresponds to the probability of failure. Substituting these conditions in the above equation is obtained:

$$Pr\left(|\overline{x} - p| < \varepsilon\right) \geq 1 - \frac{pq}{n\varepsilon^2} \tag{A.9}$$

To demonstrate the applicability of this equation consider the following heuristic example. Suppose that an experiment has been performed more than 1,000 times, and that the probability of success is $p = 0.1$, and the probability of failure is $q = 1 - p = 0.9$. Likewise, consider that an error is accepted $\varepsilon = 5\%$. Performing the operation of Eq. A.9, the probability $Pr\left(|\overline{x} - p| < 0.05\right) \geq 241/250 = 0.964$. This means that if at least 1,000 Bernoulli's trials are performed, in 241 randomized realizations out of 250 the $|\overline{x} - p|$ error will be less than $\varepsilon = 5\%$. Another interpretation could be the following. If the experiment is repeated at least 1,000 times, the error $|\overline{x} - p|$ will exceed 5% only 9 times in 250 trials. That is, at least 96.4% of the trials will be successful with an error of 5%.

In the field of seismic engineering Bernoulli's trial is used with great recurrence to estimate the probability of collapse of a structure from the practical point of view of the frequentist probability. For example Vamvatsikos and Cornell (2002), Günay and Mosalam (2013), and the FEMA P-58-1 (2012a), are some of the authors who use this approach, and as mentioned above, this thesis also uses this criterion. The collapse probability $Pr(C|IM) = p$ calculated from the frequentist point of view is estimated by the number of earthquakes k that cause the structural collapse divided by the total ground motions applied in a specific seismic intensity $[N|IM] = n_s$:

$$Pr(C|IM) = \frac{k}{n_s} = p \tag{A.10}$$

Through some algebraic manipulations of the Tchebycheff's inequality, Eq. A.9, it is possible to perform some numerical experiments to determine how the parameters of this equation vary when studying the probability of an event that is treated by a Bernoulli distribution, as is the case with the probability of collapse. For example, Fig. A.1a shows the variation of the probability $Pr\left(|\overline{x} - p| < \varepsilon\right)$ as a function of the error $\varepsilon = 10\%$ for three collapse probability conditions: $p = (0.01, 0.10, 0.50)$. Setting the percentage $Pr\left(|\overline{x} - p| < \varepsilon\right) = 0.95 \rightarrow 95\%$ of the number of realizations that should be lower than the prescribed error $\varepsilon = 10\%$, requires $n \approx (20, 180, 500)$ structural analyses, *i.e.*, pairs of seismic records to satisfy each of the conditions of the probability of collapse. The 20 pairs of seismic records corresponding to the probability of collapse $p = 0.01$ can be associated to earthquakes of frequent occurrence, *e.g.*, Tr=50 years. For the most unfavorable case from the point of view of the variance, *i.e.*, $p = 0.5$ and $q = 0.5$, the number of simulations

necessary to satisfy the prescribed conditions is $n = 500$. This number of structural analyses can be attributed to earthquakes with a lower probability of occurrence, for example, those associated with a return period greater than or equal to 1,000 years. It is also possible to reduce the number of structural analyses by increasing the percentage of outputs that exceed the error ε. For example, if the number of analyses whose probability does not exceed the $\varepsilon = 10\%$ is reduced from 95% to 80%, the approximate number of simulations required is $n \approx (5, 45, 125)$, respectively. A similar example is illustrated in Fig. A.1b, only in this case the error was reduced from 10% to 5%, and the probability was kept fixed at $p = 0.1$ and $q = 0.9$. In order for at least of 95% of the analyses to be below the prescribed error, an increase in the number of simulations is required, from 180 to 720. This represents an increase of 400%.

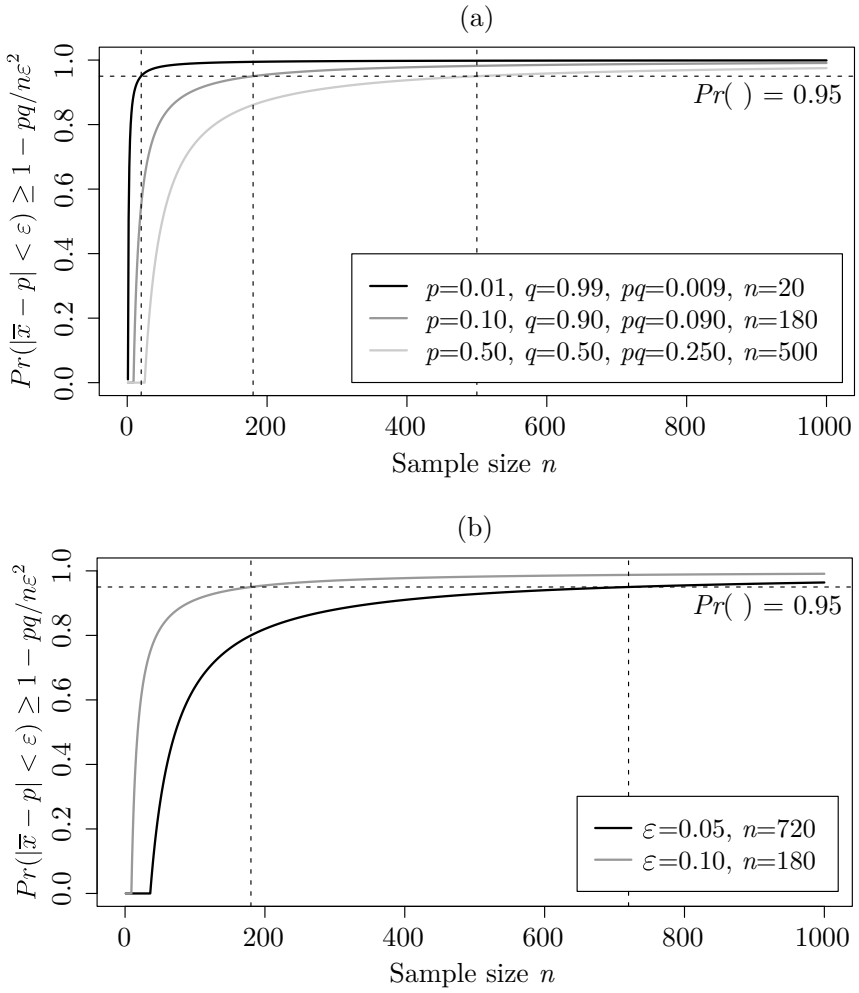

Figure A.1: (a) Estimation of the percentage of the number of structural analyses that do not exceed a certain prescribed error ε using the Tchebycheff's inequality as a function of a Bernoulli experiment to estimate the probability of structural collapse. (b) Comparison of the number of dynamic analyses required by modifying the non-exceedance error ε.

Although Tchebycheff's inequality is conservative (Papoulis, 1991), it is useful to have

an idea of the amount of minimum structural analysis (and therefore, the number of orthogonal pairs of time histories) that should be performed taking as the governing event the collapse in the probabilistic analysis of the structural seismic performance. In fact this event is very important since, as demonstrated above, this probability is used in the total probability theorem to weigh the probabilities of the consequences generated by the range of seismic intensities considered in the PEER-PBEE evaluation methodology.

In general, to make a reliable approximation from the point of view of the parametric inference of probability distributions (*e.g.*, calculation of the $\mu_{\ln(z)}$ and $\sigma_{\ln(z)}$ parameters that define the lognormal distribution function) of the DVs that constitute seismic resilience it is required a large number of structural analyses to be performed for each of the IM seismic intensities considered. However, this represents two problems. The first one, as mentioned before, is associated to the scarcity of seismic records generated by medium to high intensity earthquakes. To overcome this problem it is possible to simulate synthetic seismic records, as is done in this thesis. With this alternative it is feasible to generate the necessary amount, at least in statistical terms, of pairs of accelerograms to infer the cumulative distribution function of probabilities of a decision variable $F(DV|IM)$. The second problem lies in the high computational cost and therefore in the demand for calculation time involved in performing a large amount of NLDA in three-dimensional structural models, as in the case of this thesis. Because of this it is common to perform structural analyses in a simplified manner, as mentioned above. The following section describes the minimum amount of NLDA recommended by some design guidelines and seismic performance evaluation standards.

Appendix B

Damage description and repair activities of the damage states

Table B.1: Damage description and repair activities of the damage states of the performance groups, FEMA P-58-3 (2012b).

Performance Group *PG*	Damage States			
	DS1	DS2	DS3	DS4
Column (COL) (B1041.003b)	- Beams or joints exhibit residual crack widths > 0.06 in. No significant spalling. No fracture or buckling of reinforcing. - Remove furnishings, ceilings and mechanical, electrical and plumbing systems (as necessary) 8 feet either side of damaged area. Clean area adjacent to the damaged concrete. Prepare spalled concrete and adjacent cracks, as necessary, to be patched and to receive the epoxy injection. Patch concrete with grout. Replace and repair finishes. Replace furnishings, ceilings and mechanical, electrical and plumbing systems as necessary.	- Beams or joints exhibit residual crack widths > 0.06 in. Spalling of cover concrete exposes beam and joint transverse reinforcement but not longitudinal reinforcement. No fracture or buckling of reinforcing. - Remove furnishings, ceilings and mechanical, electrical andplumbing systems (as necessary) 15 feet either side ofdamaged area. Shore damaged member(s) a min one level below (more levels may be required). Remove damaged concrete at least 1 inch beyond the exposedreinforcing steel. Place concrete forms. Place concrete.Remove forms. Remove shores after one week. Replace andrepair finishes. Replace furnishings, ceilings and mechanical,electrical and plumbing systems (as necessary).	- Beams or joints exhibit residual crack widths > 0.06 in. Spalling of cover concrete exposes a significant length of beam longitudinal reinforcement. Crushing of core concrete may occur. Fracture or buckling of reinforcing requiring replacement may occur. - Remove furnishings, ceilings and mechanical, electrical and plumbing systems (as necessary) 15 feet either side of damaged component. Shore damaged member(s) a minimum of one level below (more levels may be required). Remove damaged component. Place and splice (as necessary) new reinforcing steel to existing, undamaged reinforcing. Place concrete forms. Place concrete. Remove forms. Remove shores after one week. Replace and repair finishes. Replace furnishings, ceilings and mechanical, electrical and plumbing systems (as necessary).	- Beams or joints exhibit residual crack widths > 0.06 in. Spalling of cover concrete exposes beam and joint transverse reinforcement but not longitudinal reinforcement. No fracture or buckling of reinforcing. - Remove furnishings, ceilings and mechanical, electrical and plumbing systems (as necessary) 15 feet either side of damaged area. Shore damaged member(s) a min one level below (more levels may be required). Remove damaged concrete at least 1 inch beyond the exposed reinforcing steel. Place concrete forms. Place concrete. Remove forms. Remove shores after one week. Replace and repair finishes. Replace furnishings, ceilings and mechanical, electrical and plumbing systems (as necessary).
Beam (BEA) (B1042.021b)	- Residual cracks no greater than 1/16 inch. Cracks are mainly at the beam to wall interface, some limited flexural cracking. - Epoxy inject cracks (200 to 240 inches in length).	- Residual cracks greater than 1/8 inch and minor spalling of concrete. - Epoxy inject cracks (600 to 720 inches) and slab (300 inches), replace spalled concrete.	- Significant strength degradation (<0.8Vn), buckling or fracture of diagonal reinforcing, crushing of concrete. - Chip away damaged concrete, attached mechanical couplers to the diagonal bars still embedded in the wall, replace damaged or fractured reinforcing. Replace damaged concrete.	

Table B.2: Damage description and repair activities of the damage states of the performance groups, FEMA P-58-3 (2012b).

Performance Group *PG*	Damage States			
	DS1	DS2	DS3	DS4
Column/Beam Connection (CB-CTN) (B1041.043b)	- Concrete cracking: beams, joints or possibly Residual concrete crack widths exceed 0.06 in. (1.5 mm). Column exhibit residual crack widths that require epoxy injection. - Remove furnishings, ceilings and mechanical, electrical and plumbing systems (as necessary) 8 feet either side of damaged area. Clean area adjacent to the damaged concrete. Prepare spalled concrete and adjacent cracks, as necessary, to be patched and to receive the epoxy injection. Patch concrete with grout. Replace and repair finishes. Replace furnishings, ceilings and mechanical, electrical and plumbing systems as necessary.	- Concrete Spalling: slabs, beams, joints or possibly columns exhibit spalling of cover concrete that exposes transverse but not longitudinal reinforcing steel. Spalling of cover concrete possibly exposing transverse reinforcement. - Remove furnishings, ceilings and mechanical, electrical andplumbing systems (as necessary) 15 feet either side ofdamaged area. Shore damaged member(s) a minimum ofone level below (more levels may be required). Remove damaged concrete at least 1 inch beyond the exposedreinforcing steel. Place concrete forms. Place concrete. Remove forms. Remove shores after one week. Replace andrepair finishes. Replace furnishings, ceilings and mechanical, electrical and plumbing systems (as necessary).	- Concrete Crushing: slabs, beams or joints. Spalling of beam, column or joint cover concrete exposes longitudinal reinforcement OR strength loss initiates in laboratory testing. exhibit concrete spalling that exposes longitudinal steel or crushing of core concrete. - Remove furnishings, ceilings and mechanical, electrical and plumbing systems (as necessary) 15 feet either side of damaged component. Shore damaged member(s) a minimum of one level below (more levels may be required). Remove damaged component. Place and splice (as necessary) new reinforcing steel to existing, undamaged reinforcing. Place concrete forms. Place concrete. Remove forms. Remove shores after one week. Replace and repair finishes. Replace furnishings, ceilings and mechanical, electrical and plumbing systems (as necessary).	
Exterior Windows (WIN-EXT) (B2022.021)	- Glass cracking - Replace cracked glass panel.	- Glass falls from frame. - Replace cracked glass panel; cover exposure in meantime.		
Ceilings (CEI) (C3032.003b)	- 5% of ceiling grid and tile damage. - Reinstall, repair, or replace 5% of the ceiling area.	- 30% of ceiling grid and tile damage. - Replace 30% of the ceiling area.	- 50% of ceiling grid and tile damage. - Replace the entire ceiling.	
Sprinklers (SPR) (D4011.021a)	- Spraying and dripping leakage at joints - 0.02 leaks per 20 ft section of pipe. - Replace leaking joints and minor water cleanup.	- Joints Break - Major Leakage - 0.02 breaks per 20 ft section of pipe - Replace 20 ft section of pipe, joints and major water cleanup at leaking joints.		
Wall Partition (GYW) (C1011.001a)	- Screw pop-out, cracking of wall board, warping or cracking of tape, slight crushing of wall panel at corners. - Retape joints, paste and repaint. May require cutting and replacing corner sections of board. Repair 5% wallboard, 10% retape, 25% repaint.	- Moderate cracking or crushing of gypsum wall boards (typically in corners). Moderate corner gap openings, bending of boundary studs. - Remove and replace 10% of wall board (both sides), retape and paste 25% of wall, paint 50% of wall. Replace boundary studs of approximately 5 intersections per 100 ft of wall length.	- Buckling of studs and tearing of tracks. Tearing or bending of top track, tearing at corners with transverse walls, large gap openings, walls displaced. - Remove and replace 50% of length of metal stud wall, 50% of both sides of the gypsum, and any embedded utilities. Retape and paste as required. Repaint 100%.	
Int/Ext Masonry Wall (MWA-INT) (B1051.013)	- A few flexural and shear cracks with hardly noticeable residual crack widths. Slight yielding of extreme vertical reinforcement. No spalling. No fracture or buckling of vertical reinforcement. No structurally significant damage. - Cosmetic repair. Patch cracks and paint each side.	- Numerous flexural and diagonal cracks with residual crack widths less than 1/64 in. Mild toe crushing with vertical cracks or light spalling at wall toes. No fracture or buckling of reinforcement. Small residual deformation. - Remove loose masonry. Patch spalls with non-shrink grout. Grout wall. Epoxy injection. Paint each side.	- Severe flexural cracks with residual crack widths greater than 1/32 in. Severe toe crushing and spalling. Fracture or buckling of vertical reinforcement. Significant residual deformation. - Shore-Demolish existing wall. - Construct new wall.	
Interior Windows (WIN-INT) (B2022.034)	- Glass cracking. - Replace cracked glass panel.	- Glass falls from frame. - Replace cracked glass panel; cover exposure in meantime.		

Table B.3: Damage description and repair activities of the damage states of the performance groups, FEMA P-58-3 (2012b).

Performance	Damage States			
Group *PG*	DS1	DS2	DS3	DS4
Concrete Stairs (STA) (C2011.011b)	- Non structural damage, local concrete cracking, localized concrete spalling, localized rebar yielding. - Patch, paint, epoxy injection. Repair finishes.	- Structural damage but live load capacity remains intact. Extensive concrete cracking, concrete crushing, buckling of rebar. - Remove damaged components, install replacement components.	- Loss of live load capacity. Extensive concrete crushing, connection failure. - Replace stair and handrail. Repair and replace affected soffits and floor finishes.	
Piping for hot/cold Drinking Water (PIP) (D2021.014a)	- Minor leakage at flange connections - 1 leak per 1000 feet of pipe. - Replace failed supports. One repair per 1000 LF.	- Pipe Break - 1 break per 1000 feet of pipe. - Replace failed supports. One repair per 1000 LF.		
Ducting HVAC (HVAC-DUC) (D3041.022c)	- Individual supports fail and duct sags - 1 failed support per 1000 feet of ducting. - Replace failed supports and repair ducting in vicinity of failed supports.	- Several adjacent supports fail and sections of ducting fall - 60 feet of ducting fail and fall per 1000 foot of ducting. - Replace sections of failed ducting and supports.		
Central Unit HVAC (HVAC-UC) (D3031.013b)	- Damaged inoperative but anchorage is OK. - Repair chiller and attached piping. Chiller removed, repaired offsite, and reinstalled.			

Appendix C

Data for the building population model

Table C.1: Recommended default fatality rates, ATC-58-1 (2011)

ATC-58 Vertical Seismic Framing System Designation & Material	Default Fatality Rate (% of Occupants) given Collapse	Fatality Rate Source
S1-Steel Moment Frame S2-Steel Braced Frame S3-Steel Eccentrically Braced Frame	10%	HAZUS default fatality rate for "Complete damage state with collapse"
S4-Steel Light Frame	5%	HAZUS default fatality rate for "Complete damage state with collapse" for light steel frame structures
S5 - Steel Moment Frame with Concrete Infill Walls	10%	HAZUS default fatality rate for "Complete damage state with collapse"
S6 - Steel Moment Frame with Unreinforced Masonry Infill Walls	19%	1999 Turkey Earthquake, Golcuk (Shoaf *et al.*, 2005; Seligson *et al.*, 2006), rate for upper floors of midrise concrete frame structures with masonry infill walls
C1-Concrete Moment Frame	11%	1999 Turkey Earthquake, Golcuk (Shoaf *et al.*, 2005; Seligson *et al.*, 2006), overall rate for all concrete frame structures.
C2-Concrete Shear Wall	10%	HAZUS default fatality rate for "Complete damage state with collapse"
C3-Concrete Frame with Unreinforced Masonry Infill Walls	19%	1999 Turkey Earthquake, Golcuk (Shoaf *et al.*, 2005; Seligson *et al.*, 2006), 2006), rate for upper floors of midrise concrete frame structures with masonry infill walls.
RM-Reinforced Masonry Bearing	10%	HAZUS default fatality rate for "Complete damage state with collapse"
URM-Unreinforced Masonry Bearing Walls	30%	1964 Tangshan Earthquake (Shiono, 1995; Nichols and Beavers, 2003)
W1-Light Wood Frame Shear Wall Light Wood Frame Diagonal Strut Bracing	1%	1995 Kobe Earthquake, Higashinada Ward (Murakami and Ohta, 2004).

Table C.2: Recommended default peak population models, FEMA P-58/BD-3.7.8 (2008).

Occupancy Population	Occupancy Description	Peak Model (Occupants per 1000 SF)	Peak Population Model-Time of Day	Default Population Model Source
1	Commercial office	4	Daytime (3 pm)	ATC (1985)
2a	Education (k-12): Elementary Schools	14	Daytime	Sample of Southern California School Data
2b	Education (k-12): Middle Schools	14	Daytime	Sample of Southern California School Data
2c	Education (k-12): High Schools	12	Daytime	Sample of Southern California School Data
3	Healthcare	5	Daytime (3 pm)	ATC (1985)
4	Hospitality	2.5	Nighttime (3 am)	ATC (1985)
5	Multi-unit residential	3.1	Nighttime (3 am)	ATC (1985)
6	Research	3	Daytime (3 pm)	ATC (1985)
7	Retail	6	Daytime (5 pm)	HAZUS CA
8	Warehouse	1	Daytime (3 pm)	ATC (1985)

Table C.3: Recommended default time of day and day of week population variations in percentage (relative to expected peak population) by occupancy class, FEMA P-58/BD-3.7.8 (2008).

Time of day	Occupancy Class									
	1-Office		2a-Elementary Schools		2b-Middle Schools		2c-High Schools		3-Healthcare	
	Weekdays	Weekends	Weekdays	Weekends	Weekdays	Weekends	Weekdays	Weekends	Weekdays	Weekends
12:00 a.m.	0	0	0	0	0	0	0	0	40	40
01:00 a.m.	0	0	0	0	0	0	0	0	40	40
02:00 a.m.	0	0	0	0	0	0	0	0	40	40
03:00 a.m.	0	0	0	0	0	0	0	0	40	40
04:00 a.m.	0	0	0	0	0	0	0	0	40	40
05:00 a.m.	0	0	0	0	0	0	0	0	40	40
06:00 a.m.	0	0	0	0	5	0	5	0	40	40
07:00 a.m.	25	0	5	0	50	0	50	0	40	40
08:00 a.m.	50	5	100	2	100	2	100	2	40	40
09:00 a.m.	75	5	100	2	100	2	100	2	60	50
10:00 a.m.	100	5	100	2	100	2	100	2	80	65
11:00 a.m.	100	5	100	2	100	2	100	2	100	80
12:00 p.m.	50	5	100	2	100	2	100	2	100	80
01:00 p.m.	50	5	100	2	100	2	100	2	100	80
02:00 p.m.	100	5	100	2	100	2	100	2	100	80
03:00 p.m.	100	5	50	2	100	2	100	2	100	80
04:00 p.m.	75	5	5	2	50	2	50	2	100	80
05:00 p.m.	50	5	5	2	25	2	25	2	100	80
06:00 p.m.	25	0	5	0	5	0	5	0	100	80
07:00 p.m.	0	0	0	0	0	0	0	0	100	80
08:00 p.m.	0	0	0	0	0	0	0	0	80	65
09:00 p.m.	0	0	0	0	0	0	0	0	60	50
10:00 p.m.	0	0	0	0	0	0	0	0	40	40
11:00 p.m.	0	0	0	0	0	0	0	0	40	40

Table C.4: Continuation. Recommended default time of day and day of week population variations in percentage (relative to expected peak population) by occupancy class, FEMA P-58/BD-3.7.8 (2008).

Time of day	Occupancy Class									
	4-Hotel		5-Multi-Unit Resid.		6-Research		7-Retail		8-Warehouse	
	Weekdays	Weekends	Weekdays	Weekends	Weekdays	Weekends	Weekdays	Weekends	Weekdays	Weekends
12:00 a.m.	100	100	100	100	10	10	0	0	0	0
01:00 a.m.	100	100	100	100	10	10	0	0	0	0
02:00 a.m.	100	100	100	100	10	10	0	0	0	0
03:00 a.m.	100	100	100	100	10	10	0	0	0	0
04:00 a.m.	100	100	100	100	10	10	0	0	0	0
05:00 a.m.	100	100	100	100	10	10	0	0	0	0
06:00 a.m.	100	100	80	100	25	25	0	0	0	0
07:00 a.m.	80	100	60	100	25	25	0	0	25	0
08:00 a.m.	70	100	40	100	50	25	5	5	50	2
09:00 a.m.	50	75	20	75	75	25	10	10	100	2
10:00 a.m.	50	50	20	50	100	25	20	25	100	2
11:00 a.m.	50	25	20	50	100	25	40	50	100	2
12:00 p.m.	50	25	20	50	50	25	60	75	100	2
01:00 p.m.	50	25	20	50	50	25	60	100	100	2
02:00 p.m.	50	25	25	50	100	25	60	100	100	2
03:00 p.m.	50	25	30	50	100	25	60	100	100	2
04:00 p.m.	50	25	35	50	75	25	60	100	100	2
05:00 p.m.	50	25	50	50	50	25	60	100	100	2
06:00 p.m.	50	25	67	50	25	25	60	75	50	0
07:00 p.m.	50	25	84	50	25	25	60	50	25	0
08:00 p.m.	50	50	100	50	10	10	40	25	0	0
09:00 p.m.	50	50	100	75	10	10	20	10	0	0
10:00 p.m.	100	100	100	100	10	10	5	5	0	0
11:00 p.m.	100	100	100	100	10	10	0	0	0	0

Table C.5: Recommended default time of day and day of week population variations in percentage (relative to expected peak population) by occupancy class, FEMA P-58/BD-3.7.8 (2008).

Occupancy Class	1-Office		2a-Elementary Schools		2b-Middle Schools		2c-High Schools		3-Healthcare	
Month	Weekdays	Weekends	Weekdays	Weekends	Weekdays	Weekends	Weekdays	Weekends	Weekdays	Weekends
Jan.	91	100	73	100	73	100	73	100	100	100
Feb.	95	100	90	100	90	100	90	100	100	100
March	100	100	100	100	100	100	100	100	100	100
April	100	100	77	100	77	100	77	100	100	100
May	95	100	95	100	95	100	95	100	100	100
June	100	100	77	100	77	100	77	100	100	100
July	95	100	0	100	0	100	0	100	100	100
Aug.	100	100	0	100	0	100	0	100	100	100
Sept.	95	100	95	100	95	100	95	100	100	100
Oct.	100	100	95	100	95	100	95	100	100	100
Nov.	95	100	81	100	81	100	81	100	100	100
Dec.	95	100	64	100	64	100	64	100	100	100

Table C.6: Continuation. Recommended default time of day and day of week population variations in percentage (relative to expected peak population) by occupancy class, FEMA P-58/BD-3.7.8 (2008).

Occupancy Class	4-Hotel		5-Multi-Unit Resid.		6-Research		7-Retail		8-Warehouse	
Time of day	Weekdays	Weekends	Weekdays	Weekends	Weekdays	Weekends	Weekdays	Weekends	Weekdays	Weekends
Jan.	100	100	100	100	91	100	95	100	91	100
Feb.	100	100	100	100	95	100	100	100	95	100
March	100	100	100	100	100	100	100	100	100	100
April	100	100	100	100	100	100	100	100	100	100
May	100	100	100	100	95	100	100	100	95	100
June	100	100	100	100	100	100	100	100	100	100
July	100	100	100	100	95	100	95	100	95	100
Aug.	100	100	100	100	100	100	100	100	100	100
Sept.	100	100	100	100	95	100	100	100	95	100
Oct.	100	100	100	100	100	100	100	100	100	100
Nov.	100	100	100	100	95	100	95	100	95	100
Dec.	100	100	100	100	95	100	95	100	95	100

References

AAAM (2001). *The abbreviated injury scale*. Association for the Advancement of Automotive Medicine, Barrington, IL, USA. 1990 Revision, Update 98.

Almufti, I. and Willford, M. (2013). *Resilience-based earthquake design initiative for the next generation of buildings, REDi Rating System*. Arup, San Francisco, CA, USA.

Almufti, I. and Willford, M. (2014). The REDi Rating System: A framework to implement resilience-based earthquake design for new buildings. In *10th U.S. National Conference on Earthquake Engineering*, Alaska, USA.

ASCE (2000). *ASCE 4-98, Seismic analysis of safety-related nuclear structures and commentary*. American Society of Civil Engineers, Reston, VA, USA.

ASCE (2005). *ASCE/SEI 43-05, Seismic design criteria for structures, systems and components in nuclear facilities*. American Society of Civil Engineers, Reston, VA, USA.

ASCE (2006). *ASCE/SEI 41-6, Seismic rehabilitation of existing buildings*. American Society of Civil Engineers, Reston, VA, USA.

ASCE (2010). *ASCE/SEI 7-10, Minimum design loads for buildings and other structures*. American Society of Civil Engineers, Reston, VA, USA.

Aslani, H. and Miranda, E. (2005). Probabilistic earthquake loss estimation and loss disaggregation in buildings. Technical report, John A. Blume Earthquake Engineering Center, Department of Civil and Environmental Engineering, Stanford University, Stanford, CA, USA.

ATC (1985). *ATC-13, Earthquake damage evaluation data for California*. Applied Technology Council, Redwood City, CA, USA.

ATC (1989). *ATC-20, Procedures for post-earthquake safety evaluation of buildings*. Applied Technology Council, Redwood City, CA, USA.

ATC (2011). *ATC-58-1, Seismic performance assessment of buildings, 90% draft*. Applied Technology Council, Redwood City, CA, USA.

Backer, J. (2015). Efficient analytical fragility function fitting using dynamic structural analysis. Technical note, Stanford University, Stanford, CA.

Beck, J., Porter, K., Shaikhutdinov, R., Au, S., Mizukoshi, K., Miyamura, M., Ishida, H., Moroi, T., Tsukada, Y., and Masuda, M. (2002). Impact of seismic risk on lifetime property values. Technical report, CUREE-Kajima Joint Research Program Phase IV.

Benjamin, J. and Cornell, C. (1970). *Probability, statistics, and decision for civil engineers*. McGraw-Hill, Inc., USA.

Bruneau, M., Chang, S., Eguchi, R., Lee, G., O'Rourke, T., Reinhorn, A., Shinozuka, M., Tierney, K., Wallace, W., and von Winterfield., D. (2003). A framework to quantitatively assess and enhance the seismic resilience of communities. *Earthquake Spectra*, 19(4):733–752.

Burton, H., Deierlein, G., Lallemant, D., and Lin, T. (2016). Framework for incorporating probabilistic building performance in the assessment of community seismic resilience. *Journal of Structural Engineering*, 142(8):C4015007–1–C4015007–11.

Chang, G. and Mander, J. (1994). Seismic energy based fatigue damage analysis of bridge columns: Part 1-Evaluation of seismic capactity. Technical Report No. NCEER-94-0006, University at Buffalo, New York, Buffalo, NY, USA.

Chatzis, M. and Smyth, A. (2012). Modeling of the 3d rocking problem. *International Journal of Non-Linear Mechanics*, 47:85–98.

Chen, C. (1975). Definition of statistically independent. *Journal of the structural division*, 101(ST2):449–451. Proceedings of the American Society of Civil Engineers, Technical Note.

Chernick, M. and LaBudde, R. (2011). *An introduction to bootstrap methods with applications to R*. John Wiley & Sons, Inc., USA.

Cimellaro, G., Reinhorn, A., and Bruneau, M. (2006). Quantification of seismic resilience. In *8th U.S. National Conference on Earthquake Engineering, EERI*, San Francisco, CA, USA.

Cimellaro, G., Reinhorn, A., and Bruneau, M. (2010a). Framework for analytical quantification of disaster resilience. *Engineering Structures*, 32(11):3639–3649.

Cimellaro, G., Reinhorn, A., and Bruneau, M. (2010b). Seismic resilience of a hospital system. *Structure and Infraestructure Engineering*, 6(1-2):127–144.

Comerio, M. (2006). Estimating downtime in loss modeling. *Earthquake Spectra*, (22):349–365.

Cornell, C. and Krawinkler, H. (2000). Progress and challenges in seismic performance assessment. Technical report, Pacific Earthquake Engineering Research (PEER), University of California, Berkeley, Berkeley, CA, USA.

Dar, A., Konstantinidis, D., and El-Dakhaknhi, W. (2016). Evaluation of ASCE 43-05 seismic design criteria for rocking objects in nuclear facilities. *Journal of Structural Engineering*, 11(142):04016110–1–04016110–13.

DiCiccio, T. and Efron, B. (1996). Bootstrap confidence intervals. *Statistical Science*, 11(3):189–228.

EERI Committee on Seismic Risk, editor (1989). *The basics of seismic risk analysis*, volume 5, chapter 4, pages 675–702. Earthquake Spectra.

Efron, B. (1979). Bootstrap methods: Another look at the jackknife. *The Annals of Statistics*, 7(1):1–26.

Efron, B. (1981). Nonparametric standard errors and confidence intervals. *The Canadian Journal of Statistics*, 9(2):139–172.

Efron, B. (1987). Better bootstrap confidence intervals. *American Statistical Association Journal of the American Statistical Association*, 82(397):171–185.

Efron, B. and Hastie, T. (2016). *Computer age statistical inference. Algorithms, evidence, and data science*. Cambridge University Press, USA.

Efron, B. and Narasimhan, B. (2018). The automatic construction of bootstrap confidence intervals. Technical Report No. 2018-07, Department of Statistics, Stanford University, Stanford, CA, USA.

Efron, B. and Tibshirani, R. (1993). *An introduction to the bootstrap*. Chapman & Hall\CRC, USA.

El Economista (2017). Impacto económico del sismo del 19 de septiembre.

Esteva, L., Díaz, O., Terán, A., and García, J. (1988). Costos probables de daños causados por temblores en construcciones. Technical Report No. 8750, Instituto de Ingeniería, UNAM, Distrito Federal, MEX.

Eurocode 8 (2004). *Eurocode 8: Design of structures for earthquake resistance-Part 1: General rules, seismic actions and rules for buildings*. European Committee for Standardization, Brussels, BE.

FEMA (2000). *FEMA 356, Prestandard and commentary for the seismic rehabilitation of buildings*. Federal Emergency Management Agency, Washington, D.C., USA.

FEMA (2008). *FEMA P-58/BD-3.7.8, Casualty consequence function and building population model development*. Applied Technology Council for the Federal Emergency Management Agency, Washington, D.C., USA.

FEMA (2012a). *FEMA P-58-1, Seismic performance assessment of buildings, Volume 1-Methodology*. Applied Technology Council for the Federal Emergency Management Agency, Washington, D.C., USA.

FEMA (2012b). *FEMA P-58-3, Seismic performance assessment of buildings, Volume 3-Fragility specification*. Applied Technology Council for the Federal Emergency Management Agency, Washington, D.C., USA.

FHWA (1994). *Technical advisory: Motor vehicle accident costs, technical advisory Num. 7570.2, U.S.* Department of Transportation, Washington, D.C., USA.

Filitrault, A. and Sullivan, T. (2014). Performance-based seismic design of nonstructural building components: The next frontier of earthquake engineering. *Earthquake Engineering and Engineering Vibration*, 13(1):17–46.

Gallagher, R. (1989). Post-earthquake safety evaluation of buildings at DOE facilities. *Second DOE Natural Phenomena Hazards Mitigation Conference*, pages 89–98.

Galvis, F., Miranda, E., Heresi, P., Dávalos, H., and Silos, J. (2017). Preliminary statistics of collapsed buildings in Mexico City in the September 19, 2017 Puebla-Morelos earthquake. Technical report, John A. Blume Earthquake Engineering Center, Department of Civil and Environmental Engineering, Stanford University, Stanford, CA, USA.

GCDMX (2004a). *Normas técnicas complementarias para diseño por sismo, Tomo II, No. 103-BIS*. Gaceta oficial del Distrito Federal, Distrito Federal, MEX. In Spanish.

GCDMX (2004b). *Normas técnicas complementarias para diseño y construcción de estructuras de concreto, Tomo I, No. 103-BIS*. Gaceta oficial del Distrito Federal, Distrito Federal, MEX. In Spanish.

GCDMX (2004c). *Normas técnicas complementarias sobre criterios y acciones para el diseño estructural de las edificaciones, Tomo II, No. 103-BIS*. Gaceta oficial del Distrito Federal, Distrito Federal, MEX. In Spanish.

GCDMX (2017). *Normas técnicas complementarias para diseño por sismo*. Gaceta oficial de la Ciudad de México, CDMX, MEX. In Spanish.

GCDMX (2020). *Normas técnicas complementarias para diseño por sismo con comentarios*. Gaceta oficial de la Ciudad de México, Ciudad de México, MEX. In Spanish.

GDF (1987). *Normas técnicas complementarias del reglamento de construcciones para el Distrito Federal*. Distrito Federal, MEX. In Spanish.

Giuffrè, A. and Pinto, P. (1970). Il comportamento del cemento armato per sollecitazioni cicliche di forte intensità. *Giornale del Genio Civile*.

Günay, S. and Mosalam, K. (2013). PEER performance-based earthquake engineering methodology, revisited. *Journal of Earthquake Engineering*, 17(6):829–858.

Goulet, C., Haselton, C., Mitrani-Reiser, J., Beck, J., Deirlein, G., Porter, K., and Stewart, J. (2007). Evaluation of the seismic performance of a code-conforming reinforced-concrete frame building–from seismic hazard to collapse safety and economic losses. *Earthquake Engineering and Structural Dynamics*, (36):1973–1997.

Gutiérrez, J., Ayala, G., and Bairán, J. (2019). Evaluación del tiempo de recuperación de edificios de concreto reforzado dañados por sismo. In *XXII Congreso Nacional de Ingeniería Sísmica*, Nuevo León, MEX.

Gutiérrez, J., Ayala, G., and Bairán, J. (2020). Assessment of earthquake-induced loss of functionality in reinforced concrete buildings. In *17th World Conference on Earthquake Engineering*, Sendai, JPN.

Hadjian, A. (1981). On the correlation of the components of strong ground motion-part 2. *Bulletin of the Seismological Society of America*, 71(4):1323–1331.

Hall, P. (1992). *The bootstrap and Edgeworth expansion*. Springer-Verlag, USA.

Hanks, T. and Kanamori, H. (1979). A moment magnitude scale. *Journal of Geophysical Research*, 84(B5):2348–2350.

Housner, G. (1963). The behaviour of inverted pendulum structures during earthquakes. *Bulletin of the Seismological Society of America*, 53(2):403–417.

Huang, Y., Whittaker, A., and Luco, N. (2010). Establishing maximum spectra for performance-based earthquake engineering: Collaborative research with the University at Buffalo and the USGS. Technical Report Award Number 08HQGR0017, USGS, Reston, VA, USA.

Huang, Y.-N., Whittaker, A., Luco, N., and Whittaker, R. (2011). Selection and scaling of earthquake ground motions in support of performance-based design. *Journal of Structural Engineering*, 137(3):311–321.

Jacques, C., McIntosh, J., Giovinazzi, S., Kirsch, T., Wilson, T., and Mitrani-Reiser, J. (2014). Resilience of the Canterbury hospital system to the 2011 Christchurch Earthquake. *Earthquake Spectra*, 30(1):533–554.

Jaimes, M. and Reinoso, E. (2013). Estimación de pérdidas por sismo de contenidos en edificios. Technical report, Serie Investigación y Desarrollo, Instituto de Ingeniería, UNAM, Ciudad de México, MEX.

Jalayer, F. (2003). *Direct probabilistic seismic analysis: Incrementing non-linear dynamic assessments*. PhD thesis, Stanford University, Stanford, United States.

Joyner, W. and Boore, D. (1986). On simulating large earthquakes by Green's function addition of smaller earthquakes. *Earthquake Source Mechanics*, 37:269–274.

Kadysiewski, S. and Mosalam, K. (2009). Modeling of unreinforced masonry infill walls considering in-plane and out-of-plane interaction. Technical Report No. 2008/102, Pacific Earthquake Engineering Research (PEER), University of California, Berkeley, Berkeley, CA, USA.

Kohrs-Sansorny, C., Courboulex, F., Bour, M., and Deschamps, A. (2005). A two-stage method for ground-motion simulation using stochastic summation of small earthquakes. *Bulletin of the Seismological Society of America*, 95(4):1387–1400.

Kottegoda, N. and Rosso, R. (2008). *Applied statistics for civil and environmental engineers*. Blackwell Publishing, UK, 2nd edition.

Krawinkler, H. (2005). Van Nuys hotel building testbed report: exercising seismic performance assessment. Technical Report No. 2005/11, Pacific Earthquake Engineering Research (PEER), University of California, Berkeley, Berkeley, CA, USA.

Krawinkler, H. and Deierlein, G. (2013). *Performance-based seismic engineering: Vision for an earthquake resilient society*, chapter 1. Springer, New York, USA.

Makris, N. and Roussos, Y. (1998). Rocking response and overturning of equipment under horizontal pulse-type motions. Technical report, Pacific Earthquake Engineering Research (PEER), University of California, Berkeley, Berkeley, CA, USA.

Mazzoni, S., McKenna, F., Scott, M. H., and Fenves, G. L. (2007). *Open System for Earthquake Engineering Simulation (OpenSees)*. Pacific Earthquake Engineering Research (PEER), Berkeley, CA, USA.

Mieler, M. and Mitrani-Reiser, J. (2017). Review of the state of the art in assessing earthquake-induced loss of functionality in buildings. *Journal of Structural Engineering*, 144(3).

Miles, S. and Chang, S. (2006). Modeling community recovery from earthquakes. *Earthquake Spectra*, 22(2):439–458.

Miranda, E. and Aslani, H. (2003). Probabilistic response assessment for building-specific loss estimation. Technical Report No. 2003/03, Pacific Earthquake Engineering Research (PEER), University of California, Berkeley, Berkeley, CA, USA.

Miranda, E., Mosqueda, G., Retamales, R., and Pekan, G. (2012). Performance of nonstructural components during the 27 Februrary 2010 Chile Earthquake. *Earthquake Spectra*, 28(S1):S453–S471.

Mitrani-Reiser, J. (2007). *An ounce of prevention: Probabilistic loss estimation for performance-based earthquake engineering*. PhD thesis, California Institute of Technology, Pasadena, CA, USA.

Mitrani-Reiser, J., Mahoney, M., Holmes, W., J.C. de la Llera, J., Bissell, R., and Kirsch, T. (2012). A functional loss assessment of a hospital system in the Bío-Bío Province. *Earthquake Spectra*, 28(S1):S473–S502.

Moehle, J. and Deierlein, G. (2004). A framework methodology for performance-based earthquake engineering. In *13th World Conference on Earthquake Engineering*, Vancouver, BC, CA.

Murakami, H. and Ohta, Y. (2004). Human entrapment in the 1995 Kobe Earthquake – comparison of urban and rural environment. Technical note.

Nazri, F. (2018). *Seismic fragility assessment for buildings due to earthquake excitation*. Springer Nature, MYS.

Newmark, N., Blume, J., and Kapur, K. (1973). Design response spectra for nuclear power plants. In *ASCE National Structural Engineering Meeting*, San Francisco, CA, USA.

Nichols, J. M. and Beavers, J. (2003). Development and calibration of an earthquake fatality function. *Earthquake Spectra*, 19(3):605–633.

NIST GCR 11-917-15 (2011). *Selecting and scaling earthquake ground motions for performing response-history analyses*. National Institute of Standards and Technology, U.S. Department of Commerce, Gaithersburg, MD, USA.

Ordaz, M., Arboleda, J., and Singh, S. (1995). A scheme of random summation of an empirical Green's function to estimate ground motions from future large earthquakes. *Bulletin of the Seismological Society of America*, 85(6):1635–1647.

Papoulis, A. (1990). *Probability and statistics*. Prentice-Hall International, Inc., USA.

Papoulis, A. (1991). *Probability, random variables, and stochastic processes*. McGraw-Hill, Inc., USA.

Polya, G. (1954). *Induction and analogy in mathematics*. Princeton University Press, USA.

Porter, K. (2000). *Assembly-based vulnerability of buildings and its uses in seismic performance evaluation and risk-management decision-making*. PhD thesis, Stanford University, Stanford, CA, USA.

Porter, K. (2003). An overview of PEER's performance-based earthquake engineering methodology. In *Proceedings of 9th international conference on applications of statistics and probability in civil engineering*, Millpress Science Publishers, San Francisco, CA, USA.

Porter, K. (2019). *A beginners's guide to fragility, vulnerability, and risk*. University of Colorado Boulder, 126 pp., Boulder, CO, USA.

Porter, K., Shoaf, K., and Seligson, H. (2006). Value of injuries in the Northridge Earthquake. *Earthquake Spectra*, 22(2):555–563. Technical Note.

Quinde, P. (2019). *Estudio de las demandas de energía sísmica en el Valle de México y su relacion con el daño estructural*. PhD thesis, Universidad Nacional Autónoma de México, Ciudad de Mexico, MEX. In Spanish.

Ramirez, C. and Miranda, E. (2012). Significance of residuals drifts in buildings earthquake loss estimation. *Earthquake Engineering and Structural Dynamics*, (41):1477–1493.

Richmond, S. (1968). *Operations research for management decisions*. John Wiley & Sons, Ltd., USA.

Rubinstein, R. and Kroese, D. (2008). *Simulation and the Monte Carlo Method*. John Wiley & Sons, Inc., CA, 2nd edition.

Scapone, E., Filippou, F., and Taucer, F. (1996). Fibre beam-column model for nonlinear analysis of r/c frames: Part I. Formulation. *Earthquake Engineering and Structural Dynamics*, 25:711–725.

SEAOC (1996). *Vision 2000, conceptual framework for performance-based seismic design*. Structural Engineers Association of California, Sacramento, CA, USA, 6th edition. Appendix B of Recommended Lateral Force Requirements.

Seligson, H. and Shoaf, K. (2003). *Human impacts of earthquakes. Earthquake engineering handbook*. CRC Press, USA.

Seligson, H., Shoaf, K. I., and Kano, M. (2006). Development of casualty models for non-ductile concrete frame structures for use in PEER's performance-based earthquake engineering framework. In *8th National Conference on Earthquake Engineering*, San Francisco, CA, USA.

Shinozuka, M., Feng, M., Lee, J., and Naganuma, T. (2000). Statistical analysis of fragility curves. *Journal of Engineering Mechanics*, 12(126):1224–1231.

Shiono, K. (1995). Interpretation of published data of the 1976 Tangshan, China Earthquake for the determination of a fatality rate function. *Japan Society of Civil Engineers Structural Engineering/Earthquake Engineering*, 11(4):155s–163s.

Shoaf, K., Seligson, H., Ramirez, M., and Kano, M. (2005). Appendix d–fatality model for nonductile concrete frame structures developed from Golcuk population survey data, in Van Nuys hotel building testbed, Report: Exercising seismic performance assessment. Technical Report No. 2005/11, Pacific Earthquake Engineering Research (PEER), University of California, Berkeley, Berkeley, CA, USA. NSF Master Contract Number BCS 90-25010.

Shoraka, M., Yang, T., and Elwood, K. (2013). Seismic loss estimation of non-ductile reinforced concrete buildings. *Earthquake Engineering and Structural Dynamics*, 42:297–310.

Soong, T. (2004). *Fundamentals of probability and statistics for engineers*. John Wiley & Sons, Ltd, UK.

Spence, R., So, E., and Scawthorn, C., editors (2011). *Human casualties in earthquakes. Progress in modelling and mitigation*, volume 29 of *Advances in Natural and Technological Hazards Research*. Springer.

Taghavi, S. and Miranda, E. (2004). Estimation of seismic acceleration demands in building components. In *13tn World Conference on Earthquake Engineering*, number 3199, Vancouver, BC, CA.

Torroja, E. (1960). *Razón y ser de los tipos estructurales*. ESP. Printed by Artes gráficas MAG, S.L., In Spanish.

Toyoda, T. (2008). Economic impacts of Kobe Earthquake: A quantitative evaluation after 13 years. In *5th International Information System for Crisis Response and Management Conference*, Washington, D.C., USA.

Urban Institute (1991). *The Costs of Highway Crashes*. Federal Highway Administration, Washington, D.C., USA. Contract DTFH61-85-C-00107.

Vamvatsikos, D. and Cornell, C. (2002). Incremental dynamic analysis. *Earthquake Engineering and Structural Dynamics*, (31):492–514.

Vassiliou, M., Burger, S., Egger, M., Bachmann, A., Broccardo, M., and Stojadinovic, B. (2017). The three-dimensional behaviour of inverted pendulum cylindrical structures during earthuakes. *Earthquake Engineering and Structural Dynamics*, 46:2261–2280.

Waller, M. (2001). Resilience in ecosystemic context: Evolution of the concept. *American Journal of Orthopsychiatry*, 71(3):290–297.

Weiser, D., Hunt, J., Jampole, E., and Gobbato, M. (2018). M7.1 Puebla, México Earthquake on September 19, 2017. Technical report, Earthquake Engineering Research Institute (EERI), Oakland, CA, USA.

Wennerberg, L. (1990). Stochastic summation of empirical Green's functions. *Bulletin of the Seismological Society of America*, 80:1418–1432.

Xue, Q., Wu, C., Chen, C., and Chen, K. (2008). The draft code for performance-based seismic design of buildings in taiwan. *Engineering and Structures*, 30:1535–1547.

Yang, T., Moehle, J., Stojadinovic, B., and Kiureghian, A. D. (2009). Seismic performance evaluation of facilities: Methodology and implementation. *Journal of Structural Engineering*, 135(10):1146–1154.

Yavari, S., Chang, S., and Elwood, K. (2010). Modeling postearthquake functionality of regional health care facilities. *Earthquake Spectra*, 26(3):869–892.

Yoo, D. (2016). Repair time model for different building sizes considering the earthquake hazard. Master's thesis, University of California, San Diego, San Diego, CA, USA.